SYNTHESIS AND CHARACTERIZATION OF NONMETALLOCENE COMPLEXES AS CATALYSTS FOR THE POLYMERIZATION OF OLEFINS

A THESIS

SUBMITTED TO THE

UNIVERSITY OF PUNE

For The Degree Of

DOCTOR OF PHILOSOPHY

In

CHEMISTRY

By

AMRITA CHAKI

DIVISION OF POLYMER SCIENCE AND ENGINEERING

NATIONAL CHEMICAL LABORATORY

PUNE - 411 008

INDIA

JULY 2007

DECLARATION BY RESEARCH GUIDE

Certified that the work incorporated in the thesis entitled **"Synthesis and characterization of nonmetallocene complexes as catalysts for the polymerization of olefins",** submitted by Ms. Amrita Chaki, for the Degree of **Doctor of Philosophy**, was carried out by the candidate, under my supervision at Polymer Science and Engineering Division, National Chemical Laboratory, Pune 411 008, India. Such material as has been obtained from other sources has been duly acknowledged in the thesis.

Dr. S. Sivaram
(Research Guide)

DECLARATION BY RESEARCH SCHOLAR

I hereby declare that the thesis entitled **"Synthesis and characterization of nonmetallocene complexes as catalysts for the polymerization of olefins",** submitted for the Degree of **Doctor of Philosophy** to the University of Pune, has been carried out by me at Polymer Science and Engineering Division, National Chemical Laboratory, Pune 411 008, India, under the supervision of Dr. S. Sivaram. The work is original and has not been submitted in part or fully by me for any other degree or diploma to this or any other University.

Amrita Chaki

(Research Scholar)

DEDICATED TO

MY PARENTS

ACKNOWLEDGEMENT

I had the privilege of associating myself with Dr. S. Sivaram, my research supervisor, whose scientific guidance and constant support helped me immensely during the course of my research work. He has given me the benefit of excellent training. His constructive criticism and enthusiasm has always been an inspiration. I am grateful to him beyond words.
I would like to express my sincere gratitude to Dr. (Smt) Rama Sivaram.

I take this opportunity to express my sincere gratitude to Dr. T. P. Mohandas for his advice and personal help. I convey my heartfelt thanks to Dr. P. K. Saxena, Shri D. H. Gholap, Mrs. Dhoble, Drs. R. P. Kamalesh Babu, C. V. Avadhani, C. Ramesh, D. Baskaran, P. R. Rajamohanan and A. M. Rajput, for useful discussions and help at various stages of work. I am also gratefull to all members of Polymer Chemistry Division, NCL, for maintaining a warm and friendly atmosphere.

I am thankful to all my lab-seniors, Drs. Saptarshi Ray, Yanjarappa, U. Subramanyam and Mr. Rajesh for their help and advice. I also wish to thank Ms. Suryakala and Mrs. Vidya Dumbre for their support. I thank all my lab-mates, Samir, Prakash, Vinu Krishnan, Samith, Yogesh, Sumesh and Javix for their help at all times of need.

I wish to thank Mr. Sheikh, Mrs. Gracy, Ms Khare and Mr. Tangade for their help in administrative matters.

I take this opportunity to thank all my friends, Sidhuda, Smritidi, Kartick, Dhananjoy, Mukul, Ashvini, Manash, Meena, Rohini, Preeti, Sreejith, Sreedhar and Jainy. My heartfelt thanks to my old friends, Samjukta, Swati, Ratna, Kamalika, Chandrachur, Abhijit, Ambika and Moloy. Their friendship has been an unforgettable experience. My thanks are due to Bhaskar, Chinmoy, Chanchal, Bibhas, Rupa, Prabhash, Gnaneshwar, Eswar, Bagh, Anuj, Mallikarjuna, Seetaram, Samrudhhi, Poorvi and Neelakshi for their help.

My friendship with Nimu, Nabanita, Ticklu and Senapati has helped me at many trying times. I am grateful to them forever for their unfailing support.

The unconditional love, support and encouragement of my parents have helped me reach this far. I do not think, I can ever repay them. My sister, though much younger, has always been my strength and my best critic. I am grateful to God, for giving me such a loving family life.

I want to place on record my deep sense of gratitude to my father and mother-in-law. I consider myself lucky to have such understanding and encouraging in-laws.

I want to express my gratefulness to my beloved husband, Ranjan. I could not have completed this thesis work without his patience and support. He plays a role not only as a loving husband, but also as a friend and guide. Thank you Ranjan, for every thing.

Finally, my thanks are due to University Grants Commission, Government of India, for the Junior and Senior Research Fellowship and Director, NCL for providing the infrastructure and facilities for successful completion of my research work, to be submitted in the form of a thesis for the award of Ph.D. degree.

July 2007 *Amrita Chaki*

CONTENTS

CHAPTER- 2

SCOPE AND OBJECTIVES OF THE PRESENT WORK

CHAPTER- 3

EXPERIMENTAL METHODS

CHAPTER- 4

OLIGOMERIZATION AND POLYMERIZATION OF ETHYLENE USING NICKEL COMPLEXES OF BIS PHOSPHINE LIGANDS

CHAPTER- 5

VINYL TYPE POLYMERIZATION OF NORBORNENE WITH NICKEL AND PALLADIUM COMPLEXES OF BIS-PHOSPHINE LIGANDS

CHAPTER- 7

POLYMERIZATION OF STYRENE WITH BIS-PHENOXY IMINE TITANIUM COMPLEXES

ABSTRACT

The thesis entitled "***Synthesis and characterization of nonmetallocene complexes as catalysts for the polymerization of olefins***" concerns the investigation of the role of a few nonmetallocene organometallic complexes for the polymerization of ethylene, norbornene and styrene.

Nickel (II) and palladium (II) complexes of novel bis-phosphines were synthesized and characterized by X-Ray crystallography. The nickel complexes oligomerize ethylene with moderate to high activities leading to butene and hexene isomers. Upon changing the steric bulk in the ligand backbone product composition could be varied from dimers and trimers to high molecular weight linear poly(ethylene)s. NMR spectroscopy revealed that the poly(ethylene)s contained exclusively ethyl branches owing to the incorporation of butene formed in the process. Absence of long chain branches confirmed the absence of "chain walking mechanism" unlike those observed for α-diimine nickel and palladium complexes.

Polymerization of norbornene was explored with the nickel (II) and palladium (II) bis-phosphine complexes. NMR spectroscopy revealed that the poly(norbornene)s obtained using the nickel complexes were amorphous and was erythrodisyndiotactic, whereas, those obtained with the palladium complexes were semicrystalline possessing erythrodiisotactic microstructure.

Bis-phenoxyimine titanium (IV) complexes were explored for the polymerization of styrene. The obtained polymers were a mixture of atactic and syndiotactic poly(styrene)s. Tacticity was found to depend on the number of fluorine substituents on the phenyl ring attached to the imine nitrogen.

Bis-phenoxyimine Ti (IV) complexes were also studied for the polymerization of ethylene in presence of silanes as chain transfer agents. Obtained poly(ethylene)s show a reduction of molecular weight with increasing silane concentration. However, the end groups of the polymers could not be analyzed by NMR. Thus the mechanism of chain transfer remains inconclusive.

LIST OF ABBREVIATIONS

acac	: acetyl acetone
AFPB	: N,N-dimethylanilinium tetrakis(pentafluoropheny1)borate
Bz	: Benzyl
Cp	: Cyclopentadiene
Cy	: Cyclohexyl
CGC	: Constrained Geometry Catalysts
DEPT	: Distortionless Enhancement by Polarization Transfer
DSC	: Differential Scanning Calorimetry
dppe	: (diphenylphosphino)ethane
dppm	: (diphenylphosphino)methane
dppp	: (diphenylphosphino)propane
DME	: ethyleneglycol dimethylether
FTIR	: Fourier Transformed Infrared
GC	: Gas Chromatography
GC-MS	: Gas Chromatography-Mass Spectroscopy
Mn	: Number average molecular weight
Mw	: Weight average molecular weight
Mv	: Viscosity average molecular weight
MWD	: Molecular weight distribution
MAO	: Methylaluminoxane
MMAO	: Modified methylaluminoxane
NMR	: Nuclear Magnetic Resonance
PDI	: Polydispersity index
PE	: Polyethylene
ODCB	: *o*-dichlorobenzene
Rac	: racemic
Tm	: Melting temperature
Tp	: Temperature of polymerization
Et_3Al	: Triethylaluminum
TIBAL	: Triisobutylaluminum
TMA	: Trimethylaluminum
TOF	: Turn over frequency

LIST OF TABLES

LIST OF FIGURES

LIST OF SCHEMES

CHAPTER 1

INTRODUCTION

1.1 Introduction

Past fifteen years have seen substantial development in the design and application of organometallic complexes as catalysts for olefin polymerization. Group 4 metallocene complexes and monocyclopentadienyl amido titanium complexes (CGC) have been widely explored. Significant understanding of the factors governing the stability of the active centers and their influence on catalyst activity as well as stereoselectivity has been gained. Steric and electronic environment around the metal centers play a critical role in determining reaction kinetics, reactivity in copolymerization and regio and stereo-selectivity. However, the search for new catalysts is far from over. The desire to discover new catalysts for olefin polymerization and copolymerization is driven by several factors. These are, search for metal catalytic centers which are more oxophilic, search for ligands which are more easily accessible, and therefore, less expensive, identification of catalytic complexes that can be used in conjunction with trialkylaluminums, rather than methyaluminoxane, and at lower Al/metal ratios and identification of metal complexes that can initiate polymerization in the absence of an activator or cocatalyst.

During the past decade, there has been a phenomenal acceleration in the research activity towards the search of novel ligand-metal complexes capable of olefin polymerization, especially, consisting of late transition metals. Late-transition metal complexes are expected to show enhanced functional group tolerance, thus, making it possible to incorporate polar comonomers into polyolefins.

Another significant discovery has been the identification of metal complexes capable of polymerizing olefinic monomers in a living fashion. Absence of chain transfer and termination processes allows access to novel polyolefinic materials, such as, block copolymers and polymers with novel topologies.

1.2 Early transition metal complexes

The first half of the transition metal series, starting from Group III (scandium) to Group VI (chromium) metals comprise of what we call the early transition metals. Group III metals are the Lanthanides and Actinide based metals which have been successfully used

in the catalysis of olefin polymerization[1]. Group V metals for e.g. vanadium and tantalum when combined with half sandwich Cp ligands show moderate activity for ethylene polymerization with MAO as the cocatalyst[2]. Group VI heterogeneous catalysts play a central role in the commercial production of polyethylene. Both the Philip's catalyst and the Union Carbide catalyst are highly active and do not need any cocatalyst for activation. There are many other chromium catalysts in combination with different ligand systems known which show moderate to very high activity for ethylene polymerization[3].

In this chapter, we will restrict ourselves to the description of Group IV transition metals titanium and zirconium, which when combined with various ligand systems apart from cyclopentadienyl ligands, give highly active non-metallocene complexes for olefin polymerization[4].

The systems discussed below are discussed in terms of five groups on the basis of their effectiveness as catalysts (in terms of activity values) [4a]. Throughout the thesis, activity values (A) are expressed as $gmmol^{-1}\ h^{-1}\ bar^{-1}$ and the ratings used in the text refer to the corresponding activity values.

Rating	**Activity ($gmmol^{-1}h^{-1}bar^{-1}$)**
Very low	<1
Low	1-10
Moderate	10-100
High	100-1000
Very high	>1000

1.2.1 Mechanisms

The mechanism of polymerization has been the subject of many experimental and theoretical investigations. Cossee's suggestions originally developed for olefin

polymerization with conventional Z-N catalysts is generally accepted to be the most plausible mechanism (**Scheme 1.1**) for metallocenes and non-metallocenes[5].

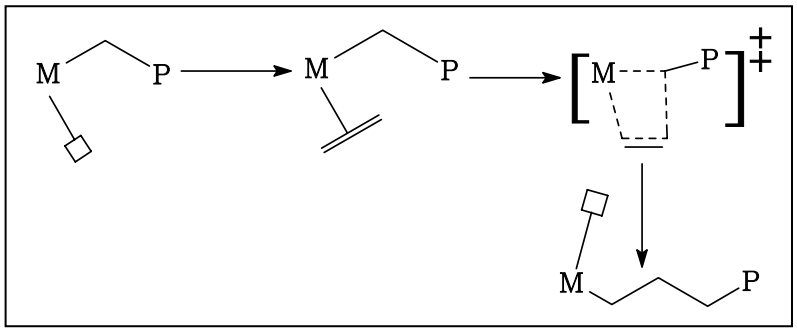

Scheme 1.1: Cossee mechanism (direct insertion)

The key features of the step insertion mechanism are: (i) that the active metal center bearing the growing alkyl chain must have an available coordination site for the incoming monomer, (ii) insertion occurs via chain migration to the closest carbon of the olefin double bond, which undergoes cis opening with formation of new metal- carbon and carbon-carbon bonds (iii) the new C-C bond is then on the site previously occupied by the coordinated monomer molecule (iv) the newly formed metal alkyl again reinserts another olefin molecule leading eventually to a polymer. During this process, shifting of growing polymer chain to position previously occupied by a coordinated monomer continues until termination of the polymer chain takes place.

1.2.2 Titanium and zirconium based catalysts

1.2.2.1 Carbon based ligands

Alkyl ligands [C^-]

Organometallic compounds of group 4 metals, such as $Cp_2Zr(CH_3)_2$, $Cp_2Ti(CH_3)_2$, $CpZrBz_3$, $TiBz_4$, $ZrBz_4$ (Cp = cyclopentadienyl, Bz = benzyl), are known to be very highly active catalysts for ethylene polymerization in combination with suitable Lewis acids of the type MAO, $[MeNHPh][B(C_6H_5)_4]$ (AFPB), $[Ph_3C][B(C_6H_5)_4]$ or $B(C_6H_5)_3$. Turner et al showed that very highly active homogeneous catalysts for ethylene

polymerization are obtained, by reacting in 1:1 mole ratio- dialkylzirconocenes, e.g. $Cp_2Zr(CH_3)_2$ with strongly acidic salts of a non-coordinating anion, e.g. N,N-dimethylanilinium tetrakis(pentafluoropheny1)borate (AFPB)[6] (**Scheme 1.2**).

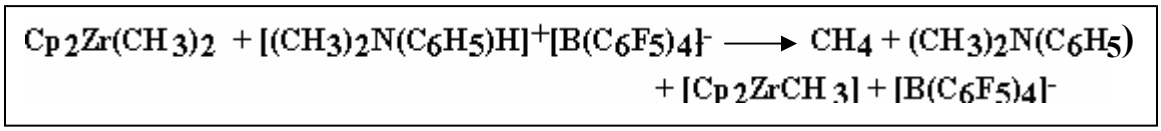

Scheme1.2: Reaction of Bronsted acidic- salt with metallocene

Hence, the true active species is believed to be basically the 14-electron cation $[Cp_2ZrCH_3]^+$. It has been found that very highly active ethylene polymerization catalysts can be also obtained by reacting monocyclopentadienyl complexes, i.e. $CpZrBz_3$ and σ-hydrocarbyls, i.e. $ZrBz_4$, instead of bis(cyclopentadieny1) derivatives with AFPB. This suggests that the role of cationic species in promoting olefin polymerization might be not limited to metallocene-based catalytic systems.

Polymerization of propylene with $TiBz_4$ and $ZrBz_4$ in the presence of $B(C_6F_5)_3$/ $Al(CH_3)_3$ afforded both stereoirregular and isotactic polypropylene with an "enantiomorphic site control" mechanism. These catalysts also promote syndiospecific polymerization of styrene when activated with MAO[7].

Allyl ligands [C_3^-]

Allyl ligands (four electron donors) are intermediate between alkyl ligands (two electron donors) and cyclopentadienyl ligands (six electron donors). Relatively less is known about such complexes in olefin polymerization. Erker and coworkers[8] have reported the reaction of [Cp(allyl)Zr(dienyl)] with tris(pentafluorophenyl)borane ($B(C_6F_5)_3$), giving a zwitterionic diallyl zirconium complex which polymerizes ethylene with moderate activity (A = 98 $gmmol^{-1}$ h^{-1} bar^{-1}), (polymerization conditions: Tp = 0°C, P_{C2H4} = 1 bar, ($B(C_6F_5)_3$) = 25 μmol, catalyst = 25 μmol). The broad molecular weight distribution of the polymer suggests presence of multiple active sites[9].

1.2.2.2 Nitrogen based ligands

Amide ligands [N⁻]

A potential advantage of the bis(amido)metal system relative to the constrained geometry half-sandwich metal amide catalyst family is a lower formal electron count [$(R_2N)_2Zr$ is formally a $10e^-$ fragment, *cf.* $12e^-$ for $CpZr(NR_2)$] which is likely to result in a more electrophilic and, therefore, potentially more active catalyst for olefin polymerization. A few reports on the use of monodentate amide ligands have appeared[10]. However, the bis(amido) complexes containing a bidentate [N^-, N^-] ligand system has received greater attention.

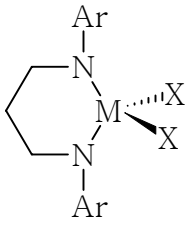

1a. Ar=2,6 *i*$Pr_2C_6H_3$,X=Me
1b. Ar=2,6 *i*$Pr_2C_6H_3$,X=Cl
1c. Ar= 2,6 *i*$Pr_2C_6H_3$, M=Zr, X=CH_2Ph
1d. Ar=2,6 $Me_2C_6H_3$, X=Cl
1e Ar= 2,6 $Me_2C_6H_3$, X=Me

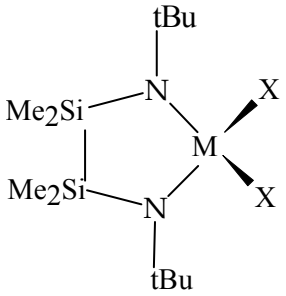

2

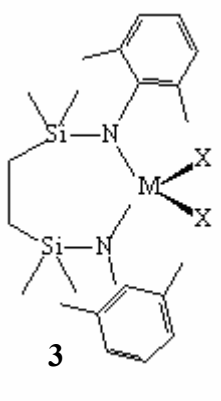

3

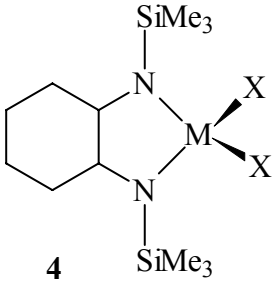

4

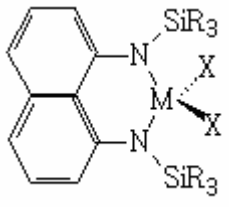

5

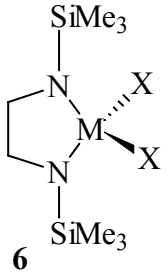

6

Various chelating bis(amido) ligands which when complexed with titanium or zirconium, form active catalysts for olefin polymerization. Chelating diamide complexes of the type **1** discovered by McConville and coworkers are active catalyst precursors for the aspecific

polymerization of hexene-1. The catalyst system generates high molecular weight polymers with narrow molecular weight distribution. Activities as high as 350 $x10^3$ $gmmol^{-1}$ Zr^{-1} h^{-1} bar^{-1} were obtained for catalyst **1a**/MAO[11]. The catalysts bearing the 2,6-$iPr_2C_6H_3$ group at nitrogen (**1a**, **1b**, A = 115 $x10^3$ $gmmol^{-1}$ Zr^{-1} h^{-1} bar^{-1}) show higher activity than the 2,6-$Me_2C_6H_3$-substituted complexes (**1d**, A = 80 $x10^3$ $gmmol^{-1}$ Zr^{-1} h^{-1} bar^{-1}; **1e,** A = 290$x10^3$ $gmmol^{-1}$ Zr^{-1} h^{-1} bar^{-1})(MAO activation) possibly, a reflection of the increased steric protection afforded by the 2,6-$iPr_2C_6H_3$ ligand. The dichloride precursors **1b, d** are about 30% less active than the dimethyl derivatives **1a,e**. Dibenzyl derivative **1c**, shows relatively low activity when activated with MAO. **1a,** upon activation by $B(C_6F_5)_3$ gives a living polymerization of hexene-1. However, the activity is greatly reduced compared to that achieved upon activation with MAO.

Polymerization of propylene has been studied with **1b,** using a combination of Al^iBu_3 and $Ph_3CB(C_6F_5)_4$ as cocatalyst. The catalyst system produced a mixture of isotactic and atactic polypropylene[12]. ^{13}C NMR analysis of the low molecular weight isotactic polypropylene proved that the propylene monomer is inserted into the metal-carbon bond via 1,2-addition and that the polymerization proceeds with an enantiomorphic-site control mechanism to produce isotactic polypropylene.

Complex **2** containing silicon in the ligand framework was found to be more active (A = 100 $gmmol^{-1}$ Zr^{-1} h^{-1} bar^{-1}) than **6** in ethylene polymerization. This may be due to the lowering of electron density around the metal center and the stabilizing effect due to "silicon effect"[13]. The dibenzyl derivative of **2** shows an activity of 500 $gmmol^{-1}$ Zr^{-1} h^{-1} bar^{-1} in ethylene oligomerization, when activated with $[CPh_3][B(C_6F_5)_4]$[14]. The silicon bridged diamide complex **3**, forms highly active ethylene polymerization catalysts (A = 990 $gmmol^{-1}$ Zr^{-1} h^{-1} bar^{-1})[15]. Zirconium complexes of type **4** have shown moderate activities for ethylene polymerization (A = 50 $gmmol^{-1}$ Zr^{-1} h^{-1} bar^{-1})[16]. However there is no report on the use of the corresponding titanium analogue. Nomura and coworkers[17] reported the synthesis of a rigidly substituted titanium diamide complex **5**, which shows significant catalytic activity for polymerization of ethylene in the presence of MAO , methyl isobutyl aluminoxane (MMAO), $AlEt_3$, Al^iBu_3 or $Ph_3CB(C_6F_5)_4$. Complex **5** polymerizes ethylene with an activity of 177 $gmmol^{-1}$ Ti^{-1} h^{-1} bar^{-1} in combination with

MMAO (heptane = 300 mL, 60°C, 1 h, P_{C2H4} = 4 bar). When the polymerization was carried out in toluene with a less bulkier cocatalyst (MAO vs MMAO or $B(C_6F_5)_3$ vs $[CPh_3][B(C_6F_5)_4]$) much lower activity was observed. The same was true for complex **1**. This is probably due to reduced cation-anion interactions in the active species. These observations suggest that amide ligands are very sensitive to polymerization conditions, especially, the solvent and the nature of activator or scavanger.

Diamide ligands with additional donors [N⁻, Y, N⁻]

The additional donor in this case may be a pyridyl, an ether or an amine donor. Interestingly, an additional pyridyl donor among the amide groups (**7, M = Zr**), affords very high activities (A = $15x10^2$ $gmmol^{-1}$ Zr^{-1} h^{-1} bar^{-1})[18]. But the corresponding titanium analogue of the same ligand shows very low activity. The ethylene bridged [N⁻, O, N⁻] ligand (**8)**, which adopts both planar (X = Me) and trigonal coordination mode (X = benzyl), does not show any activity for ethylene polymerization. But the analogous zirconium complex **9** with an aryl bridged [N⁻, O, N⁻] ligand, shows a moderate activity (A = 100 $gmmol^{-1}$ Zr^{-1} h^{-1} bar^{-1}) [19].

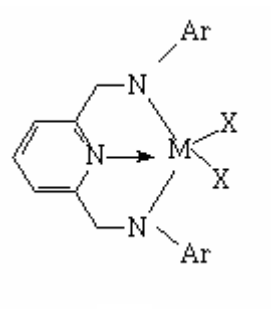

7

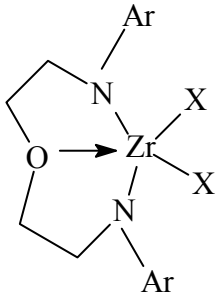

8

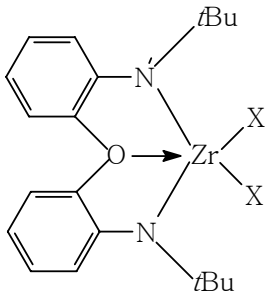

9

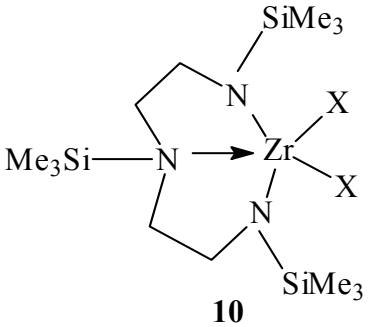

10

The zirconium dimethyl complex of the same ligand (**9**), upon activation with AFPB, produces poly(hexene-1) at 0°C with narrow polydispersity[20]. Complex **10**, polymerizes ethylene with a moderate activity (A = 46 $gmmol^{-1}$ Zr^{-1} h^{-1} bar^{-1}) [21].

Amidinate ligands [N_2^-]

Group 4 metal complexes based on amidinate ligands have been very successful in olefin polymerization catalysis. The bis(benzamidinate) dichloride group 4 complexes of the type **11**, (R'= *p*-R"C_6H_4) are obtained as a mixture of the racemic C_2-symmetry *cis*-octahedral structures. Upon activation with MAO, these complexes were found to be active catalytic precursors for the polymerization of propylene. Interestingly, when the polymerization was performed at atmospheric pressure, polypropylene was obtained as an atactic oil. However, the same complex gave a highly stereoregular solid polymer at a higher propylene pressure. This is a rare example wherein the stereoregular polymerization of an α-olefin catalyzed by early-transition-metal octahedral complexes is modulated by pressure[22].

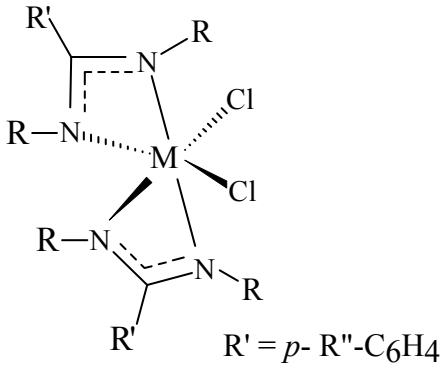

11a M = Ti, R" = Me, R = $SiMe_3$, X = Cl
11b M = Zr, R" = H, R = $CH(CH_3)$, X = C
11c M = Zr, R" = Me, R = $SiMe_3$, X = Me

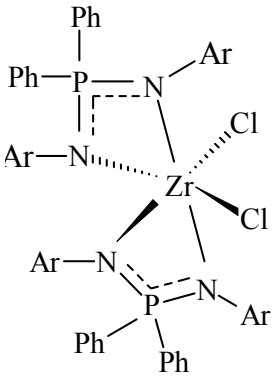

12 Ar = *p*-tolyl

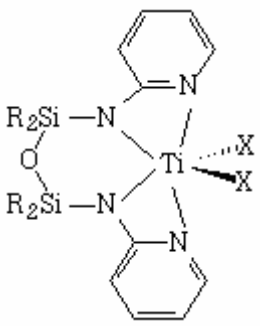

13

The related bis(iminophosphonamide)complex **12**, was reported by Collins and coworkers[23]. Complex **12** gave an ethylene polymerization activity of 1400 $gmmol^{-1}$ Zr^{-1} h^{-1} bar^{-1} which is higher than the complex of the type **11**. Ethylene polymerization using complex **12** was investigated using MAO as a cocatalyst in toluene slurry. Complex **12** (M = Zr) exhibited an activity of ca. 4-16 $x10^2$ $gmmol^{-1}$ Zr^{-1} h^{-1} bar^{-1}, the activity being higher at lower temperatures. This result suggests that the active species may have limited thermal stability. The Ti analogue was about 50-100 times less active than their Zr analogues under these conditions (50°C, P_{C2H4} = 5 bar, Al/M = 2000, [M] = $10x10^{-6}$

mol). The imine moiety of an amidinate system can be part of an aromatic system giving aminopyridinate ligands as in **13**. The complexes bearing these types of ligands, however, showed low activity[24].

β-Diketimate ligands [N_2^-]

β-diketimate or "nacnac" ligands are known to stabilize a variety of transition and main group metal complexes and can be regarded as higher homologues of amidinate ligands. A large number of early transition metal complexes bearing these ligands have been reported as catalysts for olefin polymerization. However, the activity in all cases has been moderate to low. Polymerization of ethylene using complexes **14-15** was studied in toluene slurry at 70 °C, 5 bar C_2H_4, in the presence of MAO (1000:1 Al:Zr),. Monosubstituted complexes **14** are moderately active catalysts under these conditions (A = 20 $gmmol^{-1}$ Zr^{-1} h^{-1} bar^{-1}) and produce polymers with a very broad molecular weight distribution. In fact, the polydispersity observed for both **14a** and **14b** was trimodal indicating the presence of atleast three different species.

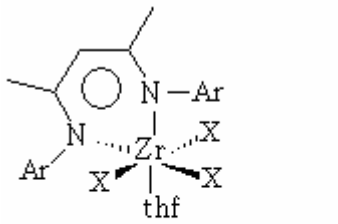

14a Ar= Ph, X=Cl
14b Ar= Ph, X=CH_2Ph

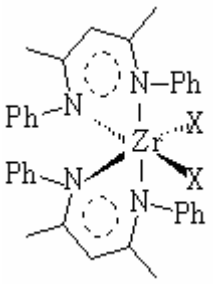

15

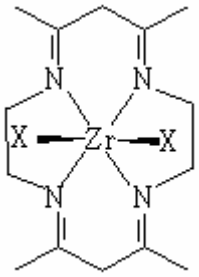

16

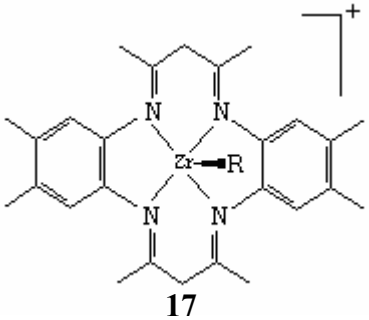

17

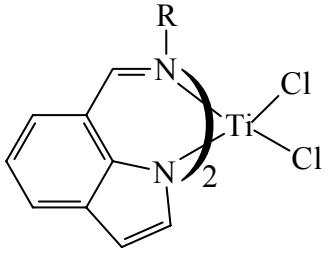

18

R =

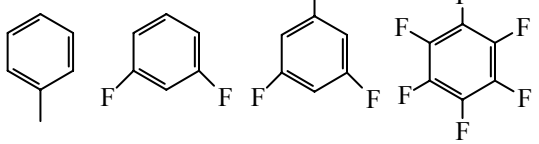

a **b** **c** **d**

In contrast, complex **15** behaves as a single-site catalysts producing poly(ethylene) with a narrower and unimodal molecular weight distribution (PDI = 2-3). Complex **15** is marginally more active than monosubstituted complex **14** (ca. A = 60 $gmmol^{-1}$ Zr^{-1} h^{-1} bar^{-1}). Zirconium complex **16** is also 30 times less active than Cp_2ZrCl_2. Complex **17** exhibits only very low activity for ethylene polymerization[25]. When one side of the β-diketimate ligand is replaced by an indole ring, the resulting complex **18** exhibits high activity for the living polymerization of ethylene at room temperature[26]. The highest activity (A = 1140 $gmmol^{-1}$ Ti^{-1} h^{-1} bar^{-1}) is observed when electron withdrawing pentafluoro phenyl groups are attached to the imino nitrogen atoms[27]. An increase in the number of fluorine atoms in the ligand resulted in enhanced catalytic activity for e.g., complex **18d** is 20 times more active than the corresponding nonfluorinated complex **18a**. These results provide a clear demonstration that the electrophilicity of the titanium center plays a dominant role in determining the catalytic activity. The activity, exhibited by complex 1**8d** is very high for a titanium complex with no Cp ligand(s) and is comparable to that displayed by the highly active titanium complex with two phosphinimide ligands reported by Stephan et al.[28] (A = 1167 $gmmol^{-1}$ Ti^{-1} h^{-1} bar^{-1}, 25°C, 1.013 bars). Complexes **18a-d** provided polyethylenes having moderate to high molecular weight values ($\overline{Mw}$: 13, 800-323, 000) and narrow polydispersity (PDI = 1.11-1.14). Complex **18d** exhibited a broader PDI of 1.93.

Iminopyrrolides and related five-membered chelate ligands

The imino-pyrollide complexes of titanium and zirconium (**19-21)** have been investigated by Fujita[29-30] and Bochmann[31] and coworkers as olefin polymerization catalysts. The X-Ray analysis of these complexes reveals a *cis* configuration of the chloride atoms. The nature of the steric bulk of the substituents on the imino nitrogen atoms decides the arrangement of the imino-pyrollide ligands around the metal center.

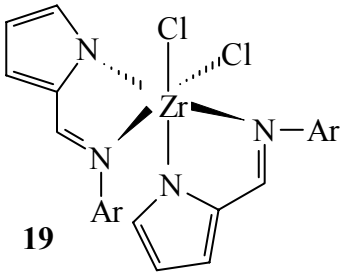

19

Ar = 2,6- $^{i}Pr_2C_6H_3$

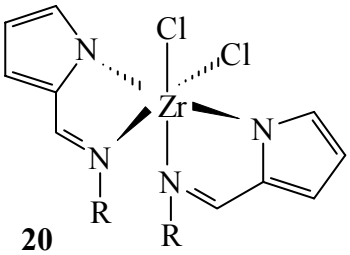

20

20a M = Zr, R = 6- $MeOC_6H_4$
20b M = Ti, R = Cy

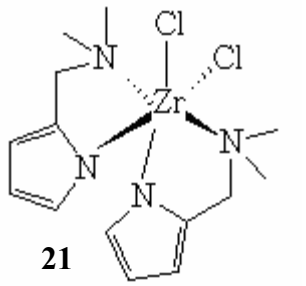

21

In **19**, **20a** and **21** both the *cis* and *trans* configuration of the pyrollide donors are observed. Titanium complex **20b** has exclusively *trans* orientation. Ethylene polymerization behavior of complexes **20a-b** was investigated in toluene at 25°C using MAO as a cocatalyst at 1.013 bars. Complex **20b** (R = cyclohexyl) showed a very high activity of 14 $x10^3$ $gmmol^{-1}$ Ti^{-1} h^{-1} bar^{-1}. The polymer had high molecular weight ($\overline{Mv}$ > 2 million). This represents one of the highest values of molecular weight reported for homogeneous titanium complexes with no Cp ligand and is comparable to those obtained with Cp_2TiCl_2 (A = 16.7 x 10^3 $gmmol^{-1}$ Ti^{-1} h^{-1} bar^{-1}). An increase in the bulk of R group on the imine nitrogen results in enhanced activity and can be attributed to the effective separation between the cationic active species and the anionic cocatalyst. Complex **20b** was also active for the copolymerization of ethylene and norbornene resulting in a copolymer of $\overline{Mn}$ value of 521 000 and a polydispersity index of 1.16. The polymer had 50 mol% comonomer content[32].

1.2.2.3 Oxygen based ligands

Alkoxide ligands

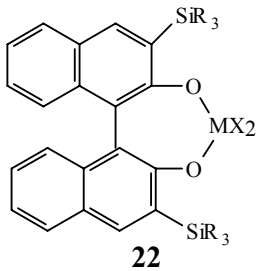

22

	SiR_3	MX_2
a	$SiMe_3$	$ZrCl_2$
b	$SiMePh_2$	$ZrCl_2$
c	$SiPh_3$	$ZrCl_2$
d	$SiMe_3$	$Ti(CH_2Ph)_2$
e	$SiMePh_2$	$Zr(CH_2Ph)_2$
f	$SiPh_3$	$ZrMe_2$
g	$SiPh_3$	$Ti(CH_2Ph)_2$
h	$SiPh_3$	$Zr(CH_2Ph)_2$
i	$SiPh_3$	$Zr(CH_2SiMe_3$

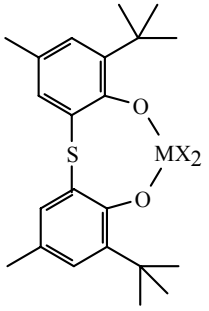

23a M=TiCl2
23b M=ZrCl2
23c M=Ti(CH2Ph)

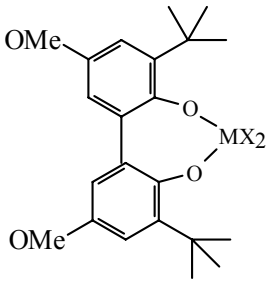

23d M=Ti(CH_2Ph)

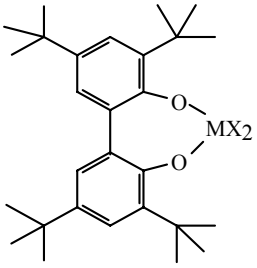

23e M=Ti(CH_2Ph)
23f M=$ZrCl_2(THF)_2$

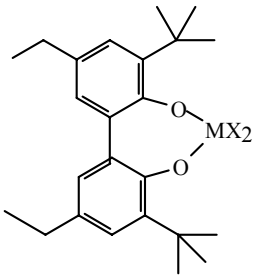

23g M=Ti(CH_2Ph)
23h M=$TiCl_2$

Terminal oxygen donors such as phenoxide ligands have been used successfully in olefin polymerization catalysis. van der Linden et al, presented a study using various sterically hindered chelating phenoxide complexes of titanium and zirconium such as **22(a-i)** and **23(a-h)**[33]. Ethylene polymerization activity of these chelating alkoxide species, with 500 molar equiv MAO as cocatalyst was studied. Activity as high as 1580 $gmmol^{-1}$ Ti^{-1} h^{-1} bar^{-1} were obtained for the polymerization of ethylene (catalyst **23a**, 20°C, P_{C2H4} = 3 bar, 5 min). Complex **22e** gave an activity of 350 $gmmol^{-1}$ Zr^{-1} h^{-1} bar^{-1}. Use of other cocatalysts, such as Et_2AlC1, resulted in much poorer activity. These activities are comparable to those obtained for various substituted $(indenyl)_2ZrC1_2$/MAO ([MAOl/[Zr] = 2000: 1, toluene, 25°C)[34a] but are much less than found for $(C_5H_5)_2$ $ZrCl_2$/MAO[34b].

Bis(alkoxides) with additional donors

Monoanionic alkoxides being isonumeral and isolobal with Cp ligands can bind to a metal atom using one σ and two π orbitals. That means, they can donate upto 6 electrons to the metal center resulting in a 14 electron cationic species like $[L_2MR]^+$. But because of the higher electronegativity of oxygen, the alkoxide ligand is normally regarded as a four electron donor. Therefore, additional donors can add to generate a cationic 14-electron species.

Bis(alkoxides) with one additional donor

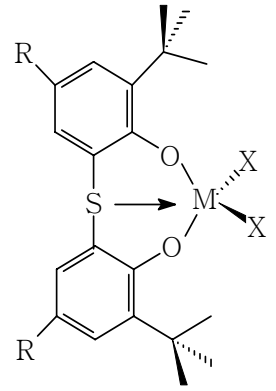

trig-[O⁻,S,O⁻]

24

The incorporation of an additional donor increases the activity of bis(alkoxide) complexes of Group 4 metals. Miyatake et al, reported a chelating phenoxide titanium complex of the type **24**[35]**.** Titanium complexes of the formula [Ti-(tbmp)X_2] derived from the sulfide-linked bis(phenol)tbmpH_2 (tbmp = 2,2´´thiobis(6-*tert*-butyl-4-methylphenolato); X = Cl, O*i*Pr) when activated with methylaluminoxane, effectively polymerize ethylene, propylene, styrene and dienes as well as copolymerize ethylene with styrene[35]. Later, Fokken et al,[36] showed the importance of the additional intramolecular sulfur donor for obtaining high catalytic activity.

Bis(alkoxides) with two additional donors

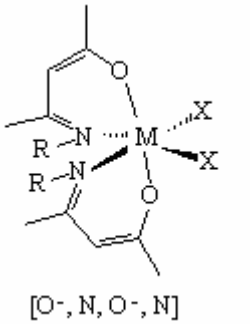

[O⁻, N, O⁻, N]

25

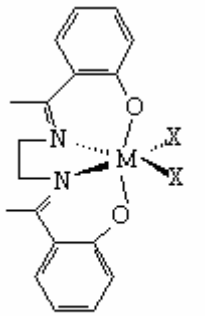

[O⁻,N,O⁻,N]

26

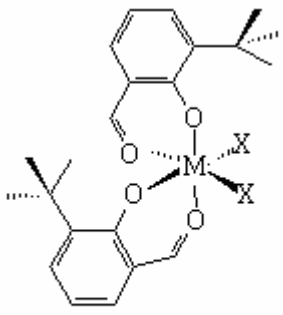

[O⁻,O,O⁻,O]

27

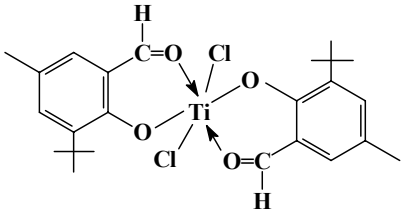

28a

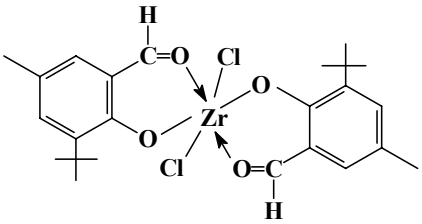

28b

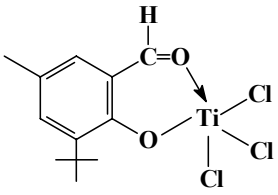

28b

Acen-type ligands (**25**) showed moderate activity for olefin polymerization[37]. These compounds can also act as highly active oligomerization catalysts[38]. Salen type complexes of the type **26**[39] **(**supported on SiO_2) showed an activity of 600 $gmmol^{-1}$ Zr^{-1} h^{-1} bar^{-1}. The use of additional oxygen donors such as in complex **27**, in combination with MAO, gave an activity of 400 $gmmol^{-1}$ Ti^{-1} h^{-1} bar^{-1} and resulted in very high molecular weight poly(ethylene)s. The polydispersity index was broad[40]. The complexation of 3-*tert*-butyl-2-hydroxy-5-methylbenzaldehyde with titanium or zirconium tetrachloride yielded two classes of complexes containing either one or two bidentate alkoxide ligands, cis-dichlorobis(3-*tert*-butyl-5-methyI-2-oxobenzoyl) titanium(IV) **28a**, cis-dichlorobis(3-*tert*-butyl-5-methyl-2-oxobenzoyl)zirconium(IV) **28b** and mer-trichloro(3-*tert*-butyl-5-methyl-2-oxobenzoyl)(tetrahydrofuran)zirconium(IV) **28c.** The titanium complex **28a** was more active (A = 80 $gmmol^{-1}$ Ti^{-1} h^{-1} bar^{-1}) than the zirconium complexes **28b** (15 $gmmol^{-1}$ Zr^{-1} h^{-1} bar^{-1}) and **28c** (A = 8 $gmmol^{-1}$ Zr^{-1} h^{-1} bar^{-1}). Poly(ethylene)s produced possess high molecular weights. Complex **28c,** containing one bidentate alkoxide ligand, results in poly(ethylene)s with higher molecular weight ($\overline{Mw}$ = $900x10^3$) than polymers produced by a complex containing two alkoxide ligands **28a** ($\overline{Mw}$ = $700x10^3$) and **28b** ($\overline{Mw}$ = $630x10^3$)**.** Molecular-weight distributions of the polymers are broad. Broad polydispersity values indicate that the complexes have more than one active site, which is surprising, since the central metal atoms are sterically crowded. Possibility of rearrangement of the ligands at the high polymerization temperature used (80°C) cannot be ruled out. Rearrangement of bidentate alkoxide ligands occurs by the torsional twist and is typical for β-diketonate complexes.

Other alkoxide and aryloxide ligands

Titanium complexes **29a** (R = H, Ar = 2,6 Me_2Ph) and **29b** (R = tBu, Ar = 2,6 Me_2Ph) were examined as potential polymerization catalyts in the presence of MAO. Polymerization was carried out at two different temperatures either with or without preactivation with trimethylaluminum (TMA). In general polymerization at room temperature afforded only low activities (12 $gmmol^{-1}$ Ti^{-1} h^{-1} bar^{-1}, Al: Zr = 4000: 1, P_{C2H4} = 1 bar, 1h). Increasing the temperature to 70°C significantly enhanced the catalyst activity (A = 1100 $gmmol^{-1}$ Ti^{-1} h^{-1} bar^{-1}).

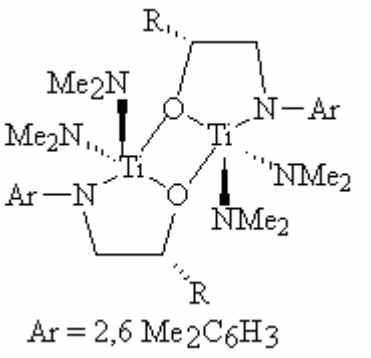

29

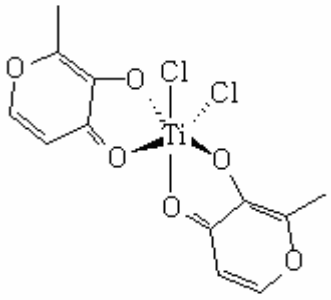

30

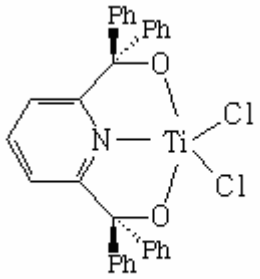

31

Apparently, these compounds are difficult to activate at ambient temperatures ie, alkylation of the titanium species is slow. In cases where the complexes were preactivated with TMA, an increase in activity was observed at room temperature (A = 1900 $gmmol^{-1}$ Ti^{-1} h^{-1} bar^{-1}). The activities are slightly lower at 70°C (A = 960 $gmmol^{-1}$ Ti^{-1} h^{-1} bar^{-1}) indicating that the methylated titanium complexes are less stable at this temperature. In all cases, catalyst activity was similar to that shown by chelating alkoxide complexes described by van der Linden et al [33]. Complex **30** is only moderately active for ethylene polymerization[41]. The pyridine alkoxide complex **31** when activated with MAO gave an activity of 58 gPE/g metal.sec[42].

Bis(phenoxy) amine ligands

Bis(phenoxy)-amino catalysts (**32-33**), exhibit very high activity for the polymerization of hexene-1 in combination with $B(C_6F_5)_3$[42]. Activities upto 50 $x10^3$ $gmmol^{-1}$ Zr^{-1} h^{-1} bar^{-1}

have been reported for the Zr derivative **32a**[43]. All precatalysts adopt a *cis*-(X-X) and *trans*-(O-O) ligand configuration. The nature of the additional donor has a pronounced effect on the activity and the molecular weight of the polymer produced. In the absence of an additional donor D, only moderate activities are obtained [42b]. In the Zr series **32**(**a-c**), activity decreases in the order **32a** (A = 50 x 10^3 gmmol^{-1} Zr^{-1} h^{-1} bar^{-1}) > **32b** (A = 21 x 10^3 gmmol^{-1} Zr^{-1} h^{-1} bar^{-1}) > **32c** (A = 9 x 10^3 gmmol^{-1} Zr^{-1} h^{-1} bar^{-1})[43].

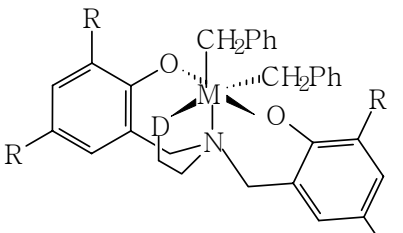

32a M= Zr, R= *t*Bu, D= OMe
32b M= Zr, R= *t*Bu D= NMe_2
32c M= Zr, R= *t*Bu, D= SMe
32d M= Ti, R= *t*Bu, D= OMe

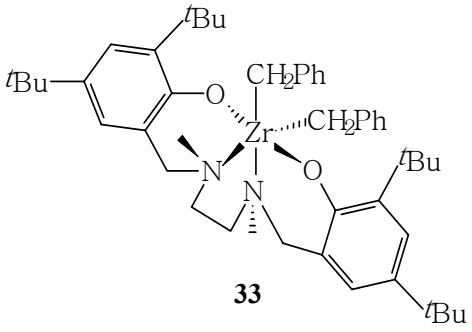

33

Reducing the size of the ortho-phenoxy substituent has little effect on catalyst activity of **32c** for the polymerization of hexene-1[44]. Though polydispersity is generally narrow, Zr complexes of the type **32**, do not polymerize hexene-1 in a living fashion. An analogous amine bis(phenolate) dibenzyl titanium complex having a methoxy donor on a side arm **32d**, upon activation with tris(pentafluorophenyl)borane, result in living properties hexene-1 polymerization. Exceptionally high molecular weight poly(hexene-1) was obtained in a living fashion. Upon activation with $B(C_6F_5)_3$, the Ti complex was found to be reactive in the polymerization of neat hexene-1, exhibiting an activity of 20-35 g mmol^{-1} Ti^{-1} h^{-1} bar^{-1}. The polymerization process was found to be living for an exceptionally long period of 31 h giving a molecular weight of 445 000 with a polydispersity index of 1.2[45b]. The related complex **33**, also polymerizes hexene-1 in a living fashion in combination with $B(C_6F_5)_3$ with a moderate activity (A = 18 gmmol^{-1} Zr^{-1} h^{-1} bar^{-1}) [46].

Salicylaldiminato ligands

Several of bis-(salicylaldiminato) complexes of titanium and zirconium (**34-37**) were reported by Fujita and coworkers for the polymerization of olefins. Titanium and zirconium complexes of the general type **34**[47-51] and **36**[52] were found to be very highly active catalysts. Activity of the catalysts and the molecular weight of the resulting polymer were dependent on the central metal atom and the size of the group (R'') attached to the imino nitrogen atoms and the ortho substituent R in **34**. It was found that for complex **34a** (R = ^{t}Bu, R' = H, R'' = Ph), activity decreases in the order M = Zr (A = 519 x 10^3 gmmol^{-1} Zr^{-1} h^{-1} bar^{-1}) >> Hf (A = 6.5 x 10^3 gmmol^{-1} Hf^{-1} h^{-1} bar^{-1}) > Ti (A = 3.3 x 10^3 gmmol^{-1} Ti^{-1} h^{-1} bar^{-1})[47d, 48a]. Increasing the size of the substituents on the imino nitrogen also has a pronounced effect on the ethylene polymerization activity. For **34b** activity decreases in the following order, R'' = Ph (A = 550 x 10^3 g mmol^{-1} Zr^{-1} h^{-1} bar^{-1}) >> 2-Me-C_6H_4 (A = 40 x 10^3 g mmol^{-1} Zr^{-1} h^{-1} bar^{-1}) = 2-^{i}Pr-C_6H_4 (A = 58 x 10^3 g mmol^{-1} Zr^{-1} h^{-1} bar^{-1}) >> 2-^{t}Bu-C_6H_4 (A = 1 x 10^2 g mmol^{-1} Zr^{-1} h^{-1} bar^{-1}) (25°C, P_{C2H4} = 1 bar, 5 min) [47c]. The molecular weight of the polymer produced increases in the same order. Increasing the steric bulk of the o-phenoxy substituent, also increases the activity. Thus for **34c** with a very bulky cumyl o-substituent R, the activity increases to 43x 10^5 gmmol^{-1} Zr^{-1} h^{-1} bar^{-1} (25°C, P_{C2H4} = 1 bar, 5 min, 0.005 μmol catalyst).

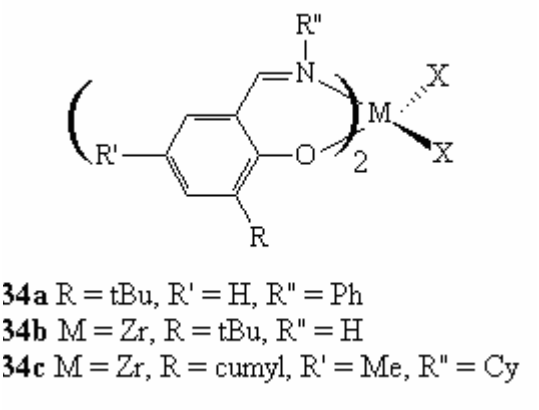

34a R = tBu, R' = H, R" = Ph
34b M = Zr, R = tBu, R" = H
34c M = Zr, R = cumyl, R' = Me, R" = Cy

34

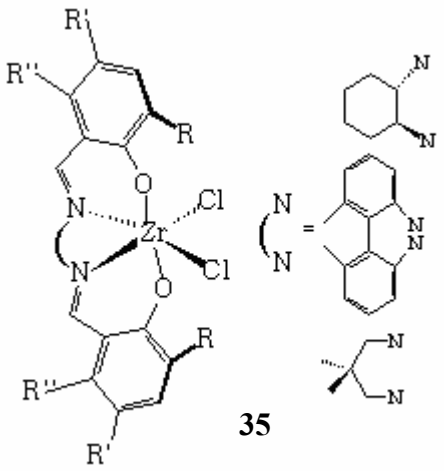

35

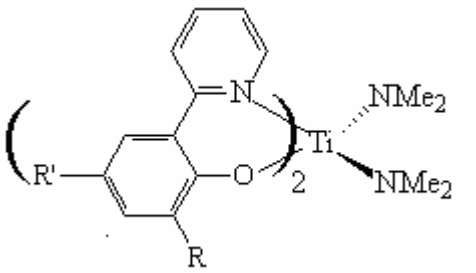

36

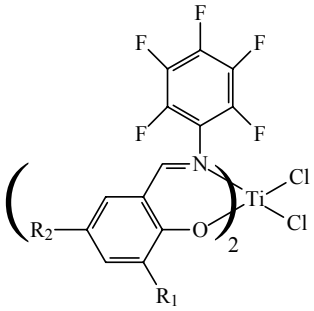

37a R_1 = $SiMe_3$, R_2 = H
37b R_1 = tBu, R_2 = H
37c R_1 = R_2 = tBu
37d R_1 = R_2 = H

37

Titanium precatalyst of the type **34a** when activated with $Al^iBu_3/[CPh_3][B(C_6F_5)_4]$, polymerizes hexene-1 to atactic, high molecular weight poly(hexene-1) with a very high activity[48c] (A = 1.12 x 10^3 gmmol^{-1} Ti^{-1} h^{-1} bar^{-1}). The resulting polymer had a $\overline{Mw}$ of 590x10^3 at 25°C. $Et(Ind)_2ZrCl_2$ and $[ArN(CH_2)_3NAr]TiCl_2$ (Ar = 2,6-$iPr_2C_6H_3$) known for giving high molecular weight poly(hexene-1)s, under the same polymerization conditions produced poly(hexene-1)s having lower $\overline{Mw}$, viz, 48x10^3 and 619x10^3 respectively. Thus, the $\overline{Mw}$ value exhibited by complex **34a** is one order of magnitude larger than $Et(Ind)_2ZrCl_2$. Moreover, this is one of the highest $\overline{Mw}$ values displayed by homogeneous olefin polymerization catalyst for hexene-1 polymerization. Poly(hexene-1) is atactic in nature with 50 mol% regioirregular units. Precatalysts of the type **36** in combination with MAO exhibit lower activity than catalysts of the type **34**. In this case, the steric bulk of the *o*-phenoxy substituent has very little effect on the polymerization activity. The related complex **35**[53] is only moderately active for the polymerization of ethylene. Complex **37** exhibited very high activities for ethylene polymerization. However in case of propylene only moderate activities were found. Furthermore, living polymerization of ethylene[49c, 50a] and propylene[50c, 51a, 54] has been achieved at room temperature with **37b**. Ethylene polymerizations with the complex **37b,** Cp_2ZrCl_2 and Cp_2TiCl_2 (for purposes of comparison), using MAO as a cocatalyst, were carried out at 25, 50 and 75°C under 1.013 bars. At 25°C the activity of the complex **37b** (A = 34 x 10^3 g mmol^{-1} Ti^{-1} h^{-1} bar^{-1}) was found to be comparable to Cp_2ZrCl_2/MAO (A = 31 x 10^3 g

$mmol^{-1}$ Zr^{-1} h^{-1} bar^{-1}) and Cp_2TiCl_2/MAO (A = 52 x 10^3 g mmol Ti^{-1} h^{-1} bar^{-1}). Polyethylenes produced with complex **37b** possess narrow polydispersity (1.13) and high molecular weight ($\overline{Mn}$ = 412 000). In addition, the $\overline{Mn}$ and polymer yield of 0.283 g obtained at 1 min polymerization is practically twice that for that obtained at 0.5 min polymerization ($\overline{Mn}$ = 191 000, yield = 0.141g). These results suggest that the ethylene polymerization catalyzed by complex **37b** catalyst system proceeds in a controlled fashion. NMR analysis of the polymers reveals a linear struture with virtually no branching. Even at higher temperatures of 50 and 70°C, the polydispersities of the polymers produced were in the range of 1.08-1.15.

Bis(salicylaldiminato) Ti complexes **34a** and **37b** were investigated by Coates and coworkers[54] to examine the effect of varying the electronic properties of the salicylaldimine ligand on polymerization behavior with propylene. **34a** exhibited low activity (A = 0.58 g $mmol^{-1}$ Zr^{-1} h^{-1} bar^{-1}, P_{C3H6} = 3 bar, 24 h, 0°C) whereas, **37b** gave moderate activities (A = 6.5 g $mmol^{-1}$ Ti^{-1} h^{-1} bar^{-1}, P_{C3H6} = 3 bar, 0.5 h, 0°C). Microstructural analysis by ^{13}C NMR revealed that a chain-end control mechanism apparently operates, producing highly syndiotactic polypropylene with an *r*-dyad content of 99% ([*rrrr*] = 0.96). The crystalline polymer exhibits a peak melting temperature of 148°C, which is among the highest reported for syndiotactic polypropylene. Microstructural analysis of polypropylene produced by **37a** reveals that the monodisperse polymer is a highly syndiotactic poly(propylene) containing 93% rr triad. Moreover, polymerization at 0°C with **37a** afforded syndiotactic poly(propylene) with an exceptionally high Tm of 156°C ([rr] 94%), which represents the highest value reported to date for a syndiotactic poly(propylene).

1.2.2.4 Mixed ligands

Cp-based precatalysts with an additional anionic donor

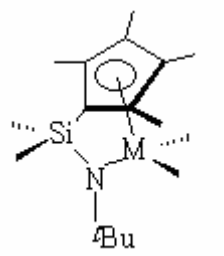

38

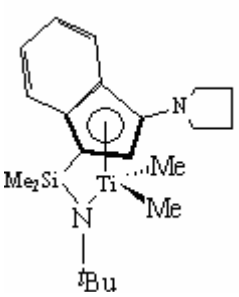

39

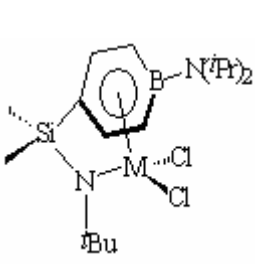

40

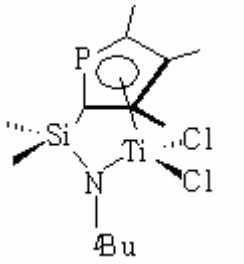

41

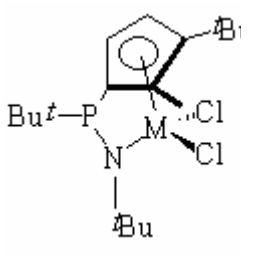

42

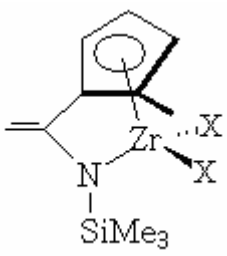

43

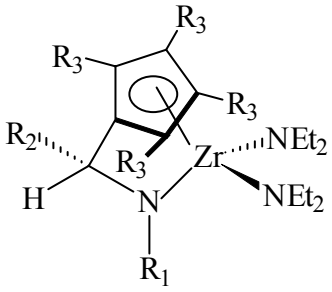

44a R_1 = p-tolyl, R_2 = CMe_3, R_3 = H
44b R_1 = CMe_3, R_2 = CMe_3, R_3 = H
44c R_1 = CMe_3, R_2 = H, R_3 = Me

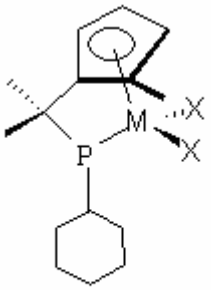

45a MX_2=$TiN(Me)_2$
45b MX_2= $ZrN(Et)_2$

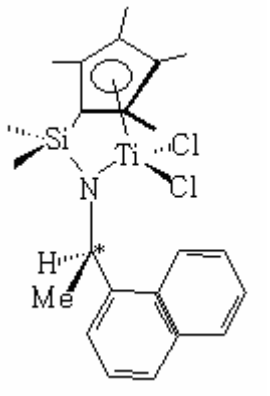

46

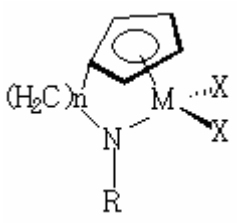

47

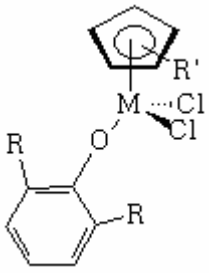

48

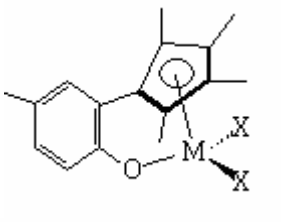

49

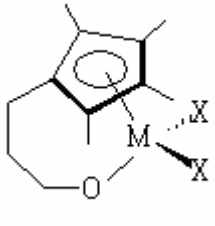

50

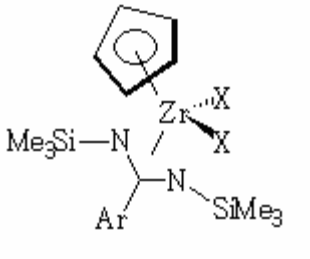

51

The linked Ti η^5:η^1-Cp-amide complexes of the type **38** are alternatively named as "constrained geometry catalysts"(CGC) and are the only non-metallocene complexes that have been commercially exploited, especially for the co-polymerization of ethylene with higher α-olefins. This area has been recently reviewed by McKnight and Waymouth [55]. The phospholyls, being readily accessible and electronically similar to cyclopentadienyl, have the greatest opportunity for yielding commercially useful catalysts. Synthesis and ethylene polymerization properties of novel *ansa*-phospholyl-amido Ti complex **41**, which is structurally similar to the well known constrained geometry catalyst **38** have been reported[56]. Polymerization of ethylene gave comparable activities for catalysts **38** (A = 300 g mmol^{-1} Ti^{-1} h^{-1} bar^{-1}) and **41** (A = 295 gmmol^{-1} Ti^{-1} h^{-1} bar^{-1}) under identical conditions. The phosphorous bridged Cp-amide Ti complex **42** shows an activity of 100 gmmol^{-1} Ti^{-1} h^{-1} bar^{-1} at Al/Ti ratio of 2000 and temperature of 80°C. 3 bars ethylene pressure was used for the polymerization reaction[57]. The product is a linear polyethylene of high molecular weight ($10^5 < \overline{Mw} < 1.4x10^6$), having melting point in the range of 123 to 132°C. C1-bridged constrained-geometry Ziegler catalysts of the type **43** (X = NEt_2), are very active catalysts for polymerization of ethylene[58]. The "CpC_1N"$M^{IV}(NR_2)_2$ (**44**) and "CpC_1P"$M^{IV}(NR_2)_2$ (**45**) complexes gave active homogeneous catalysts in conjunction with excess MAO[59]. Polymerization activity depend on the specific NR/PR group but were often found to be higher when compared to "Cp*Si_1N"Zr-derived complexes. Hetero- atom substituted complex **39**, when activated with $B(C_6F_5)_3$, shows a dramatic increase in activity for the co-polymerization of ethylene and octene-1[60] (A = 7 x10^4 gmmol^{-1} Ti^{-1} h^{-1} bar^{-1}, 140°C, P_{C2H4} = 35 bar, 15 min). The copolymer has a higher molecular weight ($\overline{Mw}$ = 280, 000) compared to a polymer derived from the dimethyl complex of **38**. Bridged boratabenzene-amido Ti and Zr complexes (**40**) have been reported. These complexes gave high activity for the co-polymerization of ethylene and octene-1, though the comonomer incorporation was much lower (1 mol%) when compared to **38** due to increased crowding at the active site[61].

The effect of the substituents on the amido nitrogen (**46**) on the stereospecific polymerization has been discussed[62]. Complex $Me_2Si[Me_4CpNCHCH_3$-naphthyl$]TiCl_2$ **46,** produces polypropylene with isotacticities as high as 56%. It was concluded that

polypropylenes with increased isotacticities can be obtained if the half-sandwich metallocene complexes contain a sterically demanding aromatic system at the amido-ligand which can interact with the active center. Carbon linkage instead of silicon in Group 4 Cp-amide complexes of the type **47** has also been studied. Ti complexes of the type **48,** have been reported[65]. Zr complex **48** (R = ^{t}Bu, R' = Me_5), shows an activity of 4260 gmmol^{-1} Zr^{-1} h^{-1} bar^{-1} for the polymerization of ethylene. Effect of ligands in a series of Cp*$TiCl_2$(OAr) –MAO catalysts [Cp* = Cp (**48a)** , ^{t}BuC_5H_4 (**48b)** , 1,3- $Me_2C_5H_3$ (**48c)** , 1,3- *t*Bu_2C5H3 (**48d)** , and C_5Me_5 (**48e)** : OAr = O-2,6- ^{i}$Pr_2C_6H_3$] was studied for polymerization of hexene-1[66].

Hexene-1 polymerization activity increased in the order: [**48e**, 728 g mmol^{-1} Ti^{-1} h^{-1} bar^{-1} >> 1,3-$Me_2C_5H_3$ (**48c**, 184 g mmol^{-1} Ti^{-1} h^{-1} bar^{-1}) ,^{t}BuC_5H_4 (**48b**, 89 g mmol^{-1} Ti^{-1} h^{-1} bar^{-1}), Cp (**48a**, 63 g mmol^{-1} Ti^{-1} h^{-1} bar^{-1}), 1,3- ^{t}Bu_2 C_5H_3 (**48d**, 26 g mmol^{-1} Ti^{-1} h^{-1} bar^{-1}). The order on **48d** was quite different from that observed in ethylene polymerization [**48e** > **48d** > **48c** > **48b** > **48a**]. $\overline{Mn}$ of the resultant poly(hexene-1)s increased in the order: **48a** (0.63 x10^4) < **48d** (2.16x10^4) < **48b** (8.0x10^4) , **48c** (8.73x10^4) < **48e** (69.4x10^4). The electron-donating substituents on cyclopentadienyl group presumably enhance the propagation rate. The resultant poly(hexene-1) was atactic in nature. 2,1- or other type of insertion were relatively small.

Combination of a Cp ligand and an aryl oxide ligand **49**, gives a highly active catalyst for the polymerization of ethylene[67]. Complex **49**, when activated with $Ph_3C^+B(C_6F_5)_4^-$ is a highly active catalyst (A = 2100 gmmol^{-1} Ti^{-1} h^{-1} bar^{-1}, 25°C, P_{C2H4} = 1 bar, 1 min) producing high molecular weight polyethylenes ($\overline{Mw}$ = 1.14x10^6, PDI >10) with Tm 142°C. Complex **49** when activated with $B(C_6F_5)_3$ gave only moderate catalytic activity (A = 15 gmmol^{-1} Ti^{-1} h^{-1} bar^{-1}). The broad polydispersities of the poly(ethylene)s may be due to rapid decomposition of the cationic species at room temperature or slow initiation compared to propagation. The difference in activity for identical cations having different counteranions further demonstrates the significant influence of the anion identity on catalytic activity[68]. Polymerization of propylene using well defined Cp-alkoxide Ti complexes of the type **50** has also been reported[69].

Combination of a Cp and an amidinate ligand **51** has been explored. Moderate activities have been obtained using the dihalide in combination with MAO[70] or the dimethyl precursor in combination with $B(C_6F_5)_3$[71] (A = 120 $gmmol^{-1}\ Zr^{-1}\ h^{-1}\ bar^{-1}$).

Monodentate trihalides

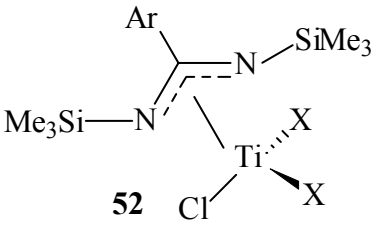

52

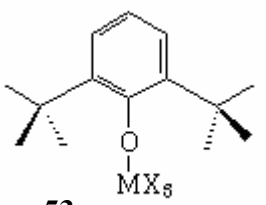

53

Monoamidinate trihalide ligands are a combination of an amidinate and a halide ligand. Titanium complexes **(52)** showed moderate activity (A = 80 $gmmol^{-1}\ Ti^{-1}\ h^{-1}\ bar^{-1}$)[72], whereas, the analogous Zr complexes gave very low activity in the polymerization of ethylene. A monoalkoxide titanium complex of the type **53**, can be regarded as a combination of an alkoxide ligand and a halide ligand [O^-, X^-]. This complex was studied for the co-polymerization of ethylene and styrene. However, only a mixture of poly(ethylene) and poly(styrene) was obtained[73].

1.3 Late transition metal complexes

Late transition metals belong to the second half of the transition metal series starting from Group 8 (Fe) and ending in Group 12 (Zn). Most of the developments in the field of olefin polymerization catalysis using the Group 8 metal Fe have been based on the bis(imino)pyridine system with bulky aryl substituents[74,75]. These catalysts show very high activities for ethylene polymerization producing linear high-molecular weight polymers. Reports on olefin polymerization catalysts based on Cu are very few. A Cu-benzamidinate[76] and a Cu- benzimidazole[77] complex have been reported to show very low activity in the polymerization of ethylene. An α-diimine Cu^{II} system, similar to Ni^{II}

and Pd^{II} diimine complexes has been reported by Gibson and coworkers[78,79]. There are no reports on group 12 metal complexes as polymerization catalysts. However, it has been shown that a Fe-bis(imino) pyridine system can promote chain growth on Zn centers affording linear alkanes or α-olefins with a Poisson distribution[80].

1.3.1 Mechanisms

Most mechanistic and theoretical work published to date has been directed at the α-diimine complexes of nickel and palladium. While details will differ for a particular metal and ligand set, all of the pertinent details are covered with these two systems[79]. It is possible to monitor ethylene chain growth at cationic α-diimine nickel and palladium centers by low-temperature NMR spectroscopy. Under these conditions, the alkyl ethylene complex (**Scheme 1.3**) is the catalyst resting state. The turnover-limiting step is the migratory insertion reaction of the alkyl ethylene complex, and as a result, the chain growth is zero-order in ethylene.

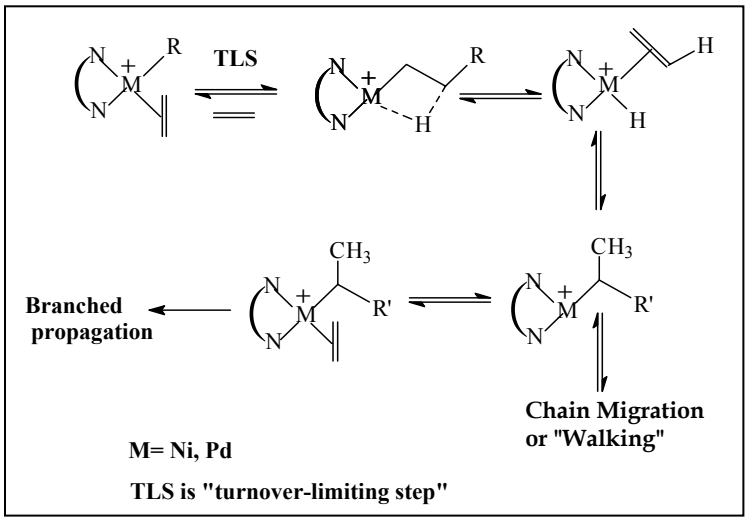

Scheme 1.3: "Chain walking" mechanism of nickel and palladium α-diimine complexes

The barriers to migratory insertions in the palladium systems lie in the range of 17-18 kcal/mol. The bulkiest ligands exhibit the lowest insertion barriers. Barriers for the insertions in the nickel complexes are substantially lower and in the range of 13-14 kcal/mol. The barrier differences ($88G^{\#}$s) of ca. 4-5 kcal/mol are due to much higher activities of the nickel complexes. The 14-electron cationic alkyl species which results from a migratory insertion have been shown to have β-agostic interactions. Trapping of this primary alkyl species by ethylene followed by insertion results in chain growth without the introduction of a branch in the polymer. If the metal alkyl species undergoes a series of β-hydride eliminations and re-additions prior to trapping and insertion, metal migration or "walking" along the polymer chain takes place. Trapping of these species with ethylene followed by insertion results in the introduction of a branch into the growing polymer chain. For example, migration one carbon down the chain followed by trapping and insertion introduces a methyl branch. If the metal migrates beyond one carbon, longer branches result. The observation of branches-on-branches indicates that palladium catalysts can migrate past tertiary carbon atoms.

1.3.2 Nickel and palladium catalysts

1.3.2.1 N, N donors

α-Diimine and related ligands

Brookhart and coworkers reported a new class of Pd(II) and Ni(II)-based catalysts which converted ethylene and α-olefins to high molecular weight polymers with unique microstructures[81]. The Pd(II) and Ni(II) initiators were cationic methyl complexes $[(ArN{=}C(R)C(R){=}NAr)M(CH_3)(OEt_2)]^+BAr'4^-$ (M = Ni, **54**; Pd, **55**; Ar′ = 3,5-$C_6H_3(CF_3)_2$) which incorporated bulky diimine ligands. Protonation of the palladium and nickel dimethyl precursors with $H(OEt_2)_2^+BAr'_4^-$ resulted in loss of methane and formation of the diethyl ether adducts. Exposure of the palladium ether adducts to ethylene, resulted in formation of high molecular weight polymers which were isolated as amorphous materials.

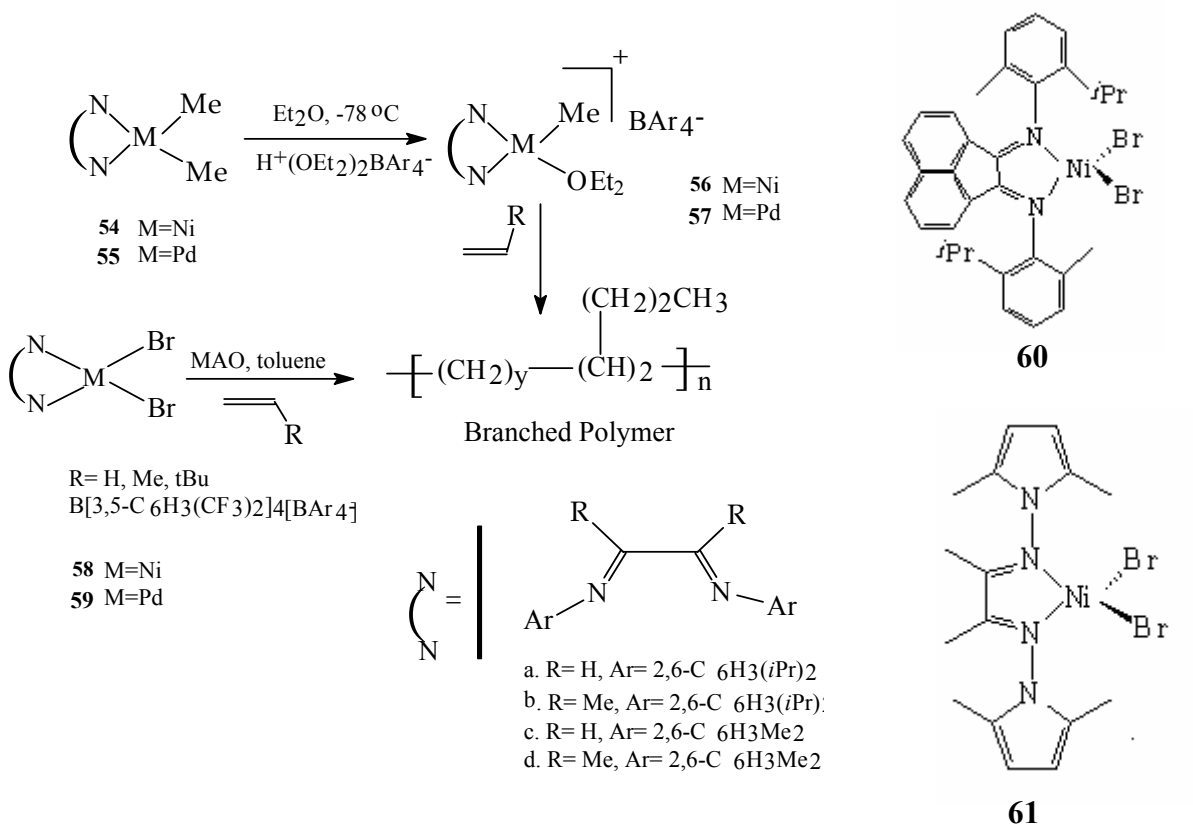

The complex ^{13}C NMR spectrum of the polyethylene produced indicated extensive branching along the main chain, with branches randomly distributed and of variable length. For example, **57b** yielded polyethylene with 103 branches/1000 carbon atoms. The amorphous polyethylene produced by these catalysts constituted a new class of polyethylene, as it was far more highly branched than low-density polyethylene. The polyethylenes produced by the Ni(II) catalysts ranged from highly linear to moderately branched, with methyl branches predominating. The extent of branching is a function of temperature, ethylene pressure, and catalyst structure. Increased branching occurs with increasing temperature, which results in lower melting temperatures of the semicrystalline polymers. The nickel catalysts exhibited very high activities which were comparable to those of metallocene catalysts. For example, the nickel bromide/MAO system **58a** exhibited an apparent turnover frequency of 3.9 x 10^5/h (A = 1 1 000 gmmol^{-1} Ni^{-1} h^{-1} bar^{-1}).

Propylene can be polymerized to a syndiotactic polymer at lower temperatures by a chain-end control mechanism[82]. Pellechia et al, reported a study concerning the effects of the coordination environment at the nickel center on the polypropylene microstructure[83]. Thus, several nickel diimine compounds having various ortho substituents on the aromatic rings were synthesized and tested in the polymerization of propylene. Complex **60a** affords a prevailingly syndiotactic polymer with a rr triad content of 75%, in agreement with previous results[84a].

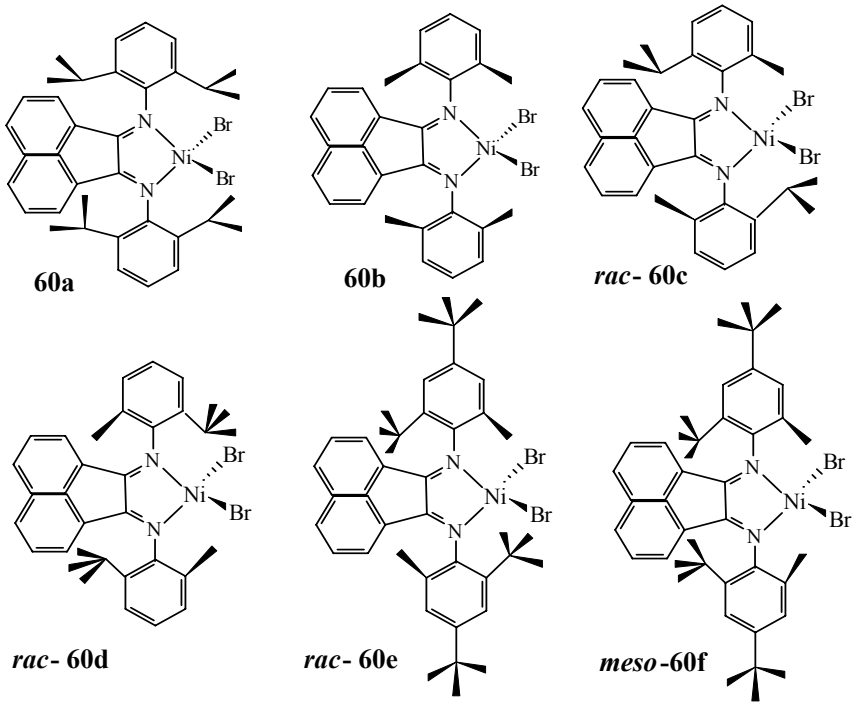

Complex **60b** also affords a prevailingly syndiotactic polymer, although with a reduced stereoselectivity (rr = 61%). In both cases, the polymers are poorly regioregular. Stereochemistry of monomer insertion is controlled by the configuration of the methine carbon of the growing chain end through 1,3-unlike asymmetric induction[84a-b]. Complex **60d** was synthesized to investigate the possible effects of the increase of steric bulk difference in the two halves of the coordination sphere of Ni. However, the microstructure of the obtained polypropylene does not show any increase of the isotactic triad content with respect to the polymer produced by **60c**, although syndiotacticity is lower when compared to **60a** and **60b**. Moreover, the polymer contains a high fraction of

1,3 inserted monomer units, apparently owing to an increased rate of "chain-running" compared to the rate of monomer insertion, the latter being slowed down by the bulky *tert*-butyl groups.

N-pyrrolyl substituents on the imino nitrogen provide a steric protection to the metal center and reduce β-hydrogen chain transfer rates. This is achieved with the nickel bromide complex **61,** which gives an activity of 5800 $gmmol^{-1}$ Ni^{-1} h^{-1} bar^{-1} for ethylene polymerization which is in the same range as imino-aryl substituted α-diimine complexes[85].

A different class of α-diimine Pd(II) complexes were reported for the living polymerization of ethylene[86].

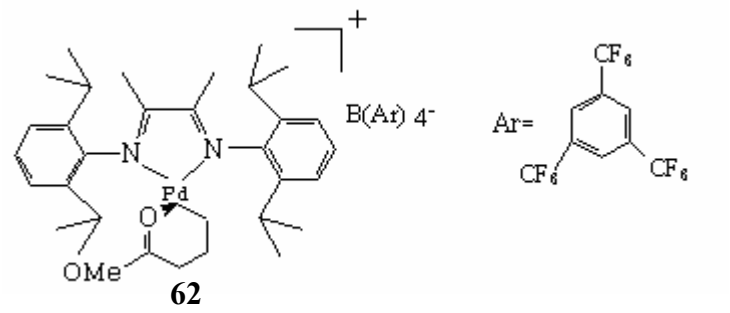

62

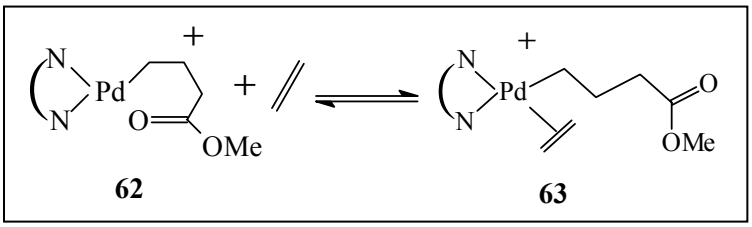

62 **63**

Scheme 1.4: Equilibrium between the chelate complex and alkyl ethylene complex

In the 7-28 bar pressure range, there is no significant change in $\overline{Mn}$ values ($57\text{-}61 \times 10^3$) or in the polydispersities (1.05-1.6) of the polymers produced with complex **62**. However, at 1.013 bars, the molecular weight distribution is substantially broadened (1.27) and the $\overline{Mn}$ is lower viz, 25×10^3. It was previously established that in the presence of ethylene, chelate complex **62** is in equilibrium with the alkyl ethylene complex **63**, and the equilibrium strongly favors the chelate at low C_2H_4 concentrations (**Scheme 1.4**). Since

initiation occurs by migratory insertion of **63**, at low ethylene pressures where **62** is highly favored, the rate of insertion will be very slow relative to the rate of propagation. Once one insertion occurs, formation of larger chelates is no longer favored. Thus, it was proposed that the broadened molecular weight distribution at 1.013 bars is due to a very slow rate of initiation relative to the rate of propagation. This was supported by observation of a low molecular weight tail in the GPC trace and a reduced polymer yield (0.044 g at 1.013 bars vs 0.151 g at 28 bars).

Neutral nitrogen based ligands

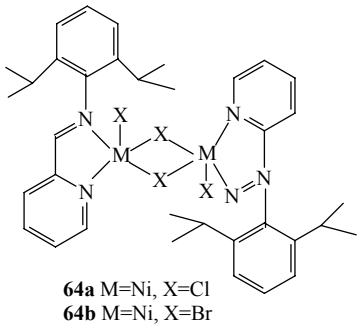

64a M=Ni, X=Cl
64b M=Ni, X=Br

64

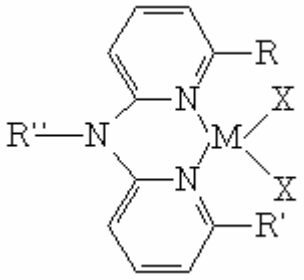

65

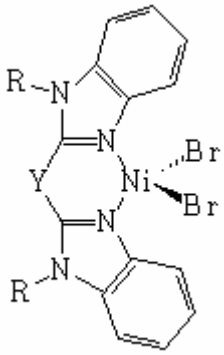

66

The presence of sterically less demanding aryl substituents on the imino nitrogen results in β-hydrogen elimination followed by fast olefin displacement leading to the formation of α-olefins[87]. Similar observations have been made for the iminopyridine ligands. Several groups have reported the use of neutral and cationic nickel complexes with unsymmetrical imino-pyridine ligands of the type (**64**) for the polymerization of ethylene. In order to study steric and electronic effects on the oligomerization–polymerization interface, Laine et al[88] synthesized nickel(II) complexes bearing the unsymmetric bidentate 2,6-bis(1-methylethyl)-*N*-(2-pyridinylmethylene)phenylamine ligand in which one side contains the pyridine ring as found in bipyridine-type alkene oligomerization catalysts and the other side consists of a 2,6-dialkylphenylimino group resembling the bulky structures of the 1,4-diazabutadiene ligands. In the nickel catalyzed reactions both the activities and product molecular weights are highly dependent on the polymerization temperature. Polymerizations at 20°C (A = 1230 $gmmol^{-1}$ Ni^{-1} h^{-1} bar^{-1}) and 40°C (A =

1240 $gmmol^{-1}$ Ni^{-1} h^{-1} bar^{-1}) provide low-melting or waxy polymers with activities comparable to the diazabutadiene systems. Lowering the temperature to 0°C leads to a sharp increase in molecular weight ($\overline{Mw}$ = 45 000) while the catalytic activity drops to 220 $gmmol^{-1}Ni^{-1}$ h^{-1} bar^{-1}. Despite this the molecular weights of the obtained polymers remain much lower than in samples produced with the corresponding diazabutadiene complexes. Besides polymer yield and chain length, degree of branching and unsaturation are also highly dependent on the polymerization conditions. The number of methyl branches varies from 9 to 71/1000 carbon atoms, the highest values being observed for samples polymerized at 40°C while polyethylene produced at 0°C is nearly linear. The absence of any significant steric protection in **65**/$Et_3Al_2Cl_3$[89] and **66**/MAO[90] systems also leads to the formation of α-olefins.

1.3.2.2 N,O donors

Grubbs and coworkers reported the synthesis of neutral Ni(II) salicylaldiminato complexes **67** and their use as catalysts for the polymerization of ethylene[91]. Introduction of bulkier substituents on the ketimine nitrogen and the phenolic ring is expected to block the axial faces of the metal center retarding the rate of associative displacement. Attempts to polymerize ethylene with **67a** with no added phosphine scavenger failed. However, in presence of a phosphine scavenger, a 5-8 min induction period was followed by rapid ethylene uptake and a rise in the reaction temperature. The induction period was attributed to the relatively slow abstraction of PPh_3 from the Ni(II) center.

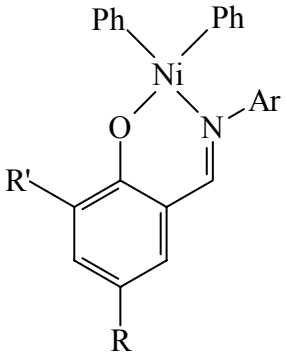

67

Ar = 2,6-$(iPr)_2C_6H_3$

67a R' = H, R = H
67b R' = tBu, R = H
67c R' = Ph, R = H
67d R' = 9-phenanthrenyl, R = H
67e R' = 9-anthracenyl, R = H
67f R' = H, R = OMe
67g R'= H, R = NO_2

The resultant polyethylene had a fairly low molecular weight ($\overline{Mn}$ = 4000, P_{C2H4} = 7 bar) and moderate branch content (45 branches/1000 carbon atoms). Increasing the pressure yielded poly(ethylene) with a higher $\overline{Mn}$ (10, 000, P_{C2H4} = 14 bar). This is consistent with the hypothesis that higher pressure reduces the rate of chain termination. The effect of various substitutents on the catalyst activity was investigated. Electron deficient systems such as **67g** were found to be the most active (A = 36 $gmmol^{-1}$ Ni^{-1} h^{-1} bar^{-1}). Electron-rich complexes such as **67f** showed lower activity (A = 2 $gmmol^{-1}$ Ni^{-1} h^{-1} bar^{-1}). Computational studies have suggested that the sterically demanding *o*-phenoxy substituents (R´) promotes the dissociation of the donor group L(PPh_3) in the initiation process. Catalyst activity, molecular weight as well as the linearity of the polymer increases in the order **67b** (A = 7 $gmmol^{-1}$ Ni^{-1} h^{-1} bar^{-1}, $\overline{Mn}$ =11 400, 55 branches/1000C) < **67c** (A = 12 $gmmol^{-1}$ Ni^{-1} h^{-1} bar^{-1}, $\overline{Mn}$ = 23,500, 40 branches/1000C) < **67d** (A = 13 $gmmol^{-1}$ Ni^{-1} h^{-1} bar^{-1}, $\overline{Mn}$ = 37,700, 30 branches/1000C) < **67e** (A = 14 $gmmol^{-1}$ Ni^{-1} h^{-1} bar^{-1}, $\overline{Mn}$ = 54,000, 30 branches/1000C)[92]. Polymerization with complex **67g** occurs with a relatively long induction period of approximately 20 min. This observation is consistent with a mechanism in which phosphine dissociation is the rate-limiting step, since an electron-withdrawing ligand strengthens the Ni-PPh_3 bond.

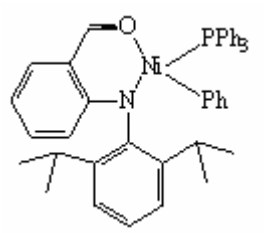

68

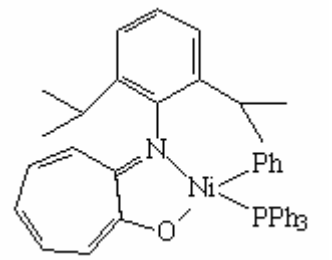

69

Nickel catalyst **68**, bearing an amido-aldehyde ligand is reported to polymerize ethylene with similar activities to **67** [93].

On the basis of a report by Keim and co-workers that homologation of a five-membered chelate Shell Higher Olefin Process-type catalyst to a six-membered one leads to an order

of magnitude loss of polymerization activity, Brookhart et al. sought to design a ligand which incorporated the key elements of the six-membered chelate salicylaldimine ligand but which lead instead to a five-membered chelate[94]. The 2-anilinotropone moiety (**69**) was chosen for this purpose because it contained the desired anionic N,O chelate, a hindered N-aryl group, and complete conjugation between the N and O. Using this ligand they described the synthesis of a highly active neutral nickel ethylene polymerization catalyst, which does not require an activator. Complex **69** produced poly(ethylene) without the addition of a cocatalyst with an activity of 314 $gmmol^{-1}$ Ni^{-1} h^{-1} bar^{-1} in a 10 min run (P_{C2H4} = 28 bar). In a series of ethylene polymerization experiments, **69** was shown to produce polyethylene of widely varying properties with changes in temperature and pressure. Polyethylene with branching numbers increasing from 8 to 67 per1000 C can be obtained by increasing temperatures from 40 to 100°C. Catalyst performance is optimal at 80°C but decreases at higher temperatures. Ethylene pressure was also been shown to have dramatic effects on the properties of the resultant poly(ethylene). Increasing the pressure from 1 bar to 28 bar at 80°C causes a decrease in the branching number from 113 to 49 branches per 1000 C.

1.3.2.3 P,O donors

Nickel and palladium catalysts with P,O donors

Group 10 metals with anionic P,O ligands are well established in the field of ethylene oligomerization and play a key role in Shell Higher Olefin Process (SHOP). It has also been reported that these catalysts can polymerize ethylene under certain conditions[95-97]. These complexes can be activated by reacting with a suitable reagent which abstracts the donor group L (e.g. $Ni(COD)_2$ or $B(C_6F_5)_3$ for L = PPh_3). Alternatively, these active catalysts can be generated in situ by treatment of a suitable Ni(0) precursor like $Ni(COD)_2$ with an α-keto-ylide ligand precursor.

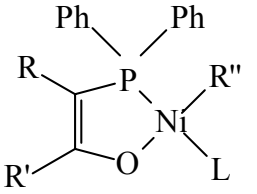

L= PPh_3, C_5H_5N

70

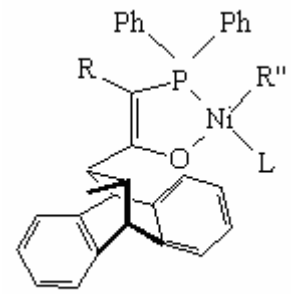

L= PPh_3, C_5H_5N

71

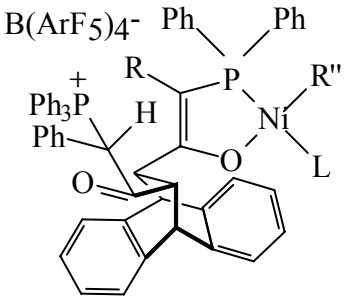

L= PPh_3, C_5H_5N

72

When L is pyridine, the complex does not require an abstracting agent. With the Ni complex **70,** activities up to 5300 $gmmol^{-1}$ Ni^{-1} h^{-1} bar^{-1} have been reported for R = COOR, R´ = CF_3, C_3F_7 or C_6F_5[98]. These complexes can also polymerize olefins in water medium. Homo and copolymerizations of ethylene and α-olefins using such complexes have been studied in aqueous emulsion and water as the reaction media[99].

Gibson and co-workers showed that a very bulky group adjacent to the oxygen donor can increase the activity dramatically[100]. Complex **71** exhibits an activity of 1730 $gmmol^{-1}$ Ni^{-1} h^{-1} bar^{-1} whereas complex **72** shows an activity of 8720 $gmmol^{-1}$ Ni^{-1} h^{-1} bar^{-1} respectively. In the case of **72**, $Ni(COD)_2$ is used as a phosphine scavanger. The polymer properties are independent of the nature of catalyst used. In all cases, linear PE with $\overline{Mn}$ in the range of 5000-10 000 and polydispersity in the range of 2.0-3.7 was obtained.

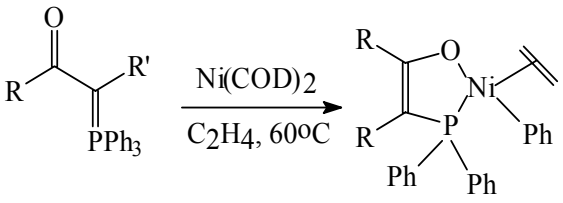

73

73a R= CF_3, R'= CO_2Et
73b R=C_3F_7, R'= CO_2Et
73c R= C_6F_5, R'= CO_2Et
73d R= C_6F_5, R'= CO_2tBu
73e R= C_6F_5, R'= CO_2Bz
73f R= C_6H_5, R'= CO_2Et

Claverie and coworkers[101] synthesized a series of nickel(II) complexes (**73 a-g**) of keto-ylide ligands exhibit high activity for ethylene polymerization. It is well known that the oxidative addition of such a keto-ylide ligand to zero valent nickel compounds (most preferably $Ni(COD)_2$) leads to an alkylated metal due to transfer of a phenyl group from the phosphorus atom to the nickel atom .Therefore, in the same step, ligand displacement and metal alkylation are effected, obviating the need for an alkylating agent such as MAO.

The influence of the ligand fluorine atoms on the activity is remarkable.**73a** is the most active (A = > 670 $gmmol^{-1}\ Ni^{-1}\ h^{-1}\ bar^{-1}$) followed by **73b** (A = 470 $gmmol^{-1}\ Ni^{-1}\ h^{-1}\ bar^{-1}$), **73d** (A = 390 $gmmol^{-1}\ Ni^{-1}\ h^{-1}\ bar^{-1}$), **73e** (A = 360 $gmmol^{-1}\ Ni^{-1}\ h^{-1}\ bar^{-1}$), **73c** (A = 200 $gmmol^{-1}\ Ni^{-1}\ h^{-1}\ bar^{-1}$) and **73f** (A = 12 $gmmol^{-1}\ Ni^{-1}\ h^{-1}\ bar^{-1}$). The pentafluoro catalysts **73c-e** are less active probably because of the decreased electrophilicity.

^{13}C and ^{1}H NMR studies showed a very low methyl branching content (less than 1 per 1000 C) and few internal double bonds due to β-H transfer followed by β-H addition on a more substituted carbon (1 per 1000 C). This indicates that the dominant mechanism for the formation of this highly linear polymer is initiation by a nickel hydride, followed by propagation and termination by β-hydride elimination.

Bulky P,O chelate phenacyldi-*tert*-butyl phosphine has been reported as a supporting ligand on Ni(II) and Pd(II) metal centers for ethylene polymerization[102]. The complexes employed for polymerization studies are the cationic nickel allyl complex **74** and the palladium methyl complexes **75a** and **75b**.

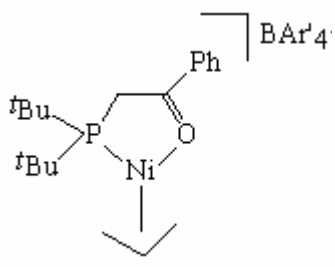

74

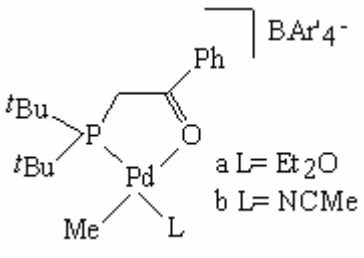

75

Polymerizations performed at 6.8-27.2 bars exhibit very high activities (A = 128-677 $x10^3$ $gmmol^{-1}$ M^{-1} h^{-1}) which are comparable to early-transition metal catalysts. Increasing the ethylene pressure results in an increase in the polymerization activity and polymer molecular weight. Polymer produced by **74** has *T*m values between 127 and 131°C. ^1H NMR analysis indicates linear polymer chains with 6-8 methyl branches per 1000 carbons. Pd catalysts **75a** and **75b** show low activities at 25°C (A = 6.8 $gmmol^{-1}$ Pd^{-1} h^{-1} bar^{-1} for **75a** and A = 0.3 $gmmol^{-1}$ Pd^{-1} h^{-1} bar^{-1} for **75b**) and moderate activities at 60°C (A = 20 $gmmol^{-1}$ Pd^{-1} h^{-1} bar^{-1} for **75a** and A = 12 $gmmol^{-1}$ Pd^{-1} h^{-1} bar^{-1} for **75b**). The Pd catalysts generate low molecular weight polyethylene oligomers with $\overline{Mn}$ = 350 as determined by $^1\overline{H}$ NMR analysis. The physical properties of the polyethylene generated by **75a** and **75b** change considerably with ethylene pressure. At 1.013 bars of ethylene pressure, the oligomeric product is a viscous oil (Tm = 5°C, 42 branches/ 1000 carbon atoms), while at higher ethylene pressures the product is an amorphous solid (Tm = 22°C, 16 branches/1000 carbons).

A neutral Ni complex can be turned into a more electrophilic cationic species by treatment with $B(C_6F_5)_3$[103]. Addition of $B(C_6F_5)_3$ to the phosphino-carboxylate Ni-complex **76**, results in the cationic species **77** via coordination of $B(C_6F_5)_3$ to the carboxyl oxygen of the carboxylate unit (**Scheme 1.5**).

This cationic derivative is much more active than its neutral counterpart. The complex promotes selective dimerization of ethylene to butene-1.

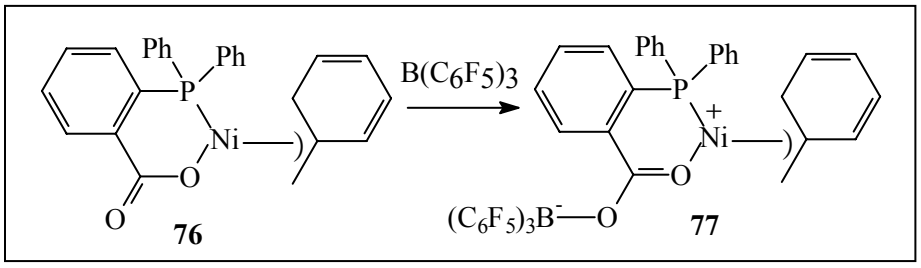

Scheme 1.5: Formation of a cationic nickel species from a neutral nickel complex upon addition of tris(pentafluorophenyl)borane

Nickel complexes bearing P,O donors for ethylene oligomerization

The first well defined nickel complex which converted ethylene in high selectivity and activity into α-olefins had the chemical composition $C_{44}H_{36}OP_2Ni$. This was obtained by reacting a phosphorus ylide Ph_3P = CHCOPh with $Ni(PPh_3)_4$ or $Ni(COD)_2Ph_3P$[96b]. The nickel atom is surrounded in a square planar arrangement by a triphenyl moiety, a σ-bonded phenyl group and a bidentate ylide ligand bonded via oxygen and phosphorus atoms. The general structural motif of the P,O chelated nickel complexes reported till then for ethylene oligomerization to give α-olefins (SHOP process) is depicted as **78**.

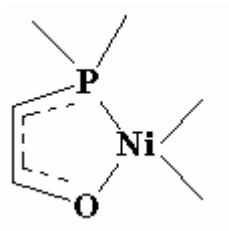

78

A study of the influence of various auxiliary phosphane ligands on the activity and selectivity of phenyl(2-diphenylphosphanylphenolato)(phosphane) nickel(II) catalysts established that high activity is seen with PPh_3, $P(4\text{-}X\text{–}C_6H_4)_3$ (X = Cl >Me > F), and PPh_2Me, whereas PCy_3 (Cy = cyclohexyl), which has a strong enhancing effect on the activity of the related phenyl(2-diphenylphosphanyl-1-phenylenolato)(phosphane) nickel(II) catalysts, induces only moderate activity. Generally, a marked tendency to produce higher oligomers, from C_{10} to C_{90}, and only minor amounts of the desired C_4 to C_{10} oligomers is observed. Exceptions are complexes with PMe_3 and $PPhMe_2$ ligands, which give α-olefins of low molecular weight (C_4 to C_{24}), although with lower catalytic activity. In view of the easy access to substituted 2-phosphanylphenols and their high tendency to form P,O chelates, Keim and coworkers turned their attention to the synthesis of catalytically active (2-phosphanylphenolato[*P*,*O*])nickel(II) complexes and tuning of their activity and selectivity by variation of substituents at the phosphorus and the phenolate group.They reported methyl(2-phosphanylphenolato) nickel complexes, which differ from cyclopentadienyl(2-phosphanylphenolato)nickel(II) complexes in that they are active oligomerization catalysts[104].

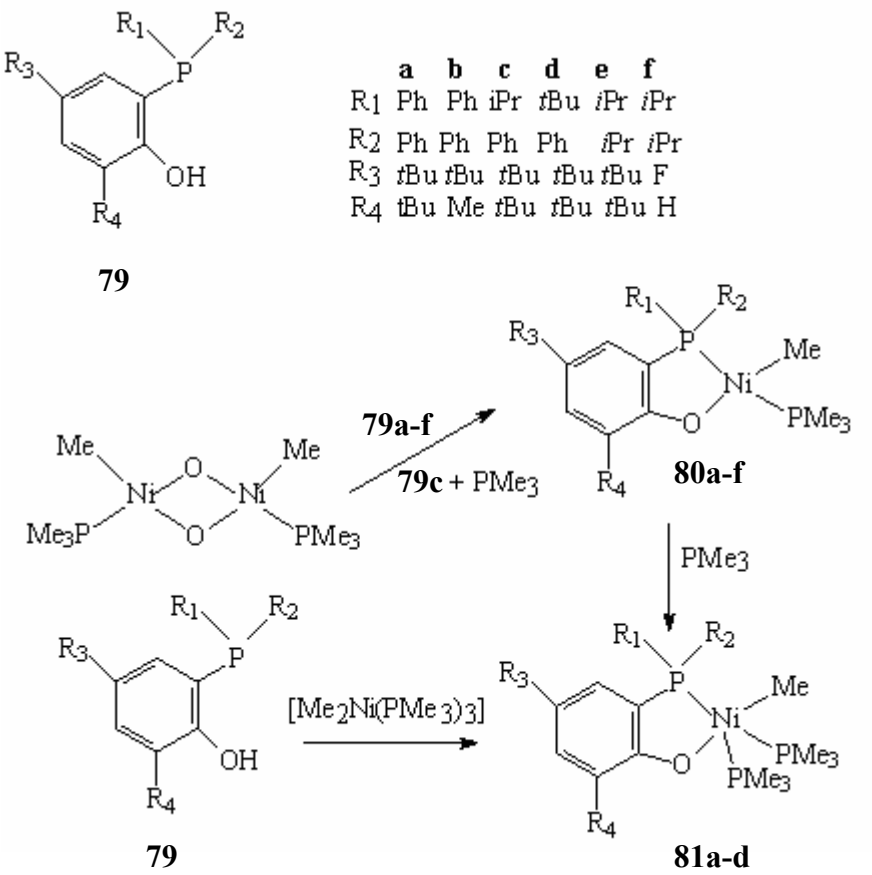

Table 1.1 Composition of ethylene oligomers from **80c, e, f** and **81d**

Catalyst	80c	80e	80f	81d
% C4 (% 1-olefin)	3.0	8.0 (100)	11.2 (100)	44.1 (100)
% C6 (% 1-olefin)	8.2 (90)	19.2 (99)	16.1 (87)	38.3 (99)
% C8 (% 1-olefin)	10.3	19.5 (99)	15.7 (94.4)	12.0 (85)
% C10 (% 1-olefin)	11.2	15.1 (85)	5.1 (91)	2.7 (79)
% C12 (% 1-olefin)	11.6	3.9 (79)	0.42	2.1 (69)
% C14	11.6	0.9	0.48	0.7
% C14+	44.1	33.3	51	

The products of the catalytic conversion of ethylene were oligomers, mainly linear α-olefins (Table 1.1). Selectivity decreased with increasing chain length, from C_4 to C_{12}, as detected by GC. Unusually high content of a hexene isomer in **79e** (11.5%) may be

attributed to a competing reaction with 1-butene. With **80d**, lower oligomers with a Schultz–Flory distribution and large amounts of 1-butene, 1-hexene, and octenes were observed. Mono-PMe_3 complexes formed longer chain oligomers with broad, flat maxima in their molecular weight distributions.

1.3.2.4 P, P donors

Nickel complexes bearing P,P donors

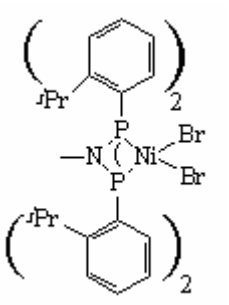

82

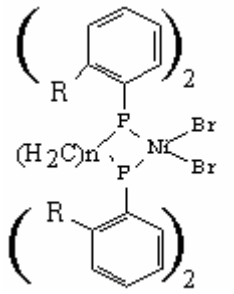

83a n = 1
83b n = 2
83c n = 3

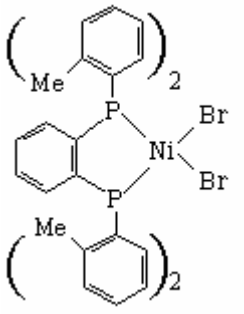

84

Strong σ donor capacity of phosphine ligands makes them more suitable for catalytic reactions requiring nucleophilic metal centers. Hence, inspite of a rich coordination chemistry of phosphine ligands with late transition metals, there is hardly any use of these ligands in olefin polymerization catalysis involving an electrophillic metal center. In cases, where these ligands have been applied in coordination with late transition metals, very low ethylene polymerization activity has been observed. One such example is a diphosphinidine Pd complex which is sterically similar to α-diimine complexes. This suggests that the polymerization activities of these Group 10 metals are very much dependent on the nature of the donor atom[105].

However, surprisingly very high activitiy of upto 2200 $gmmol^{-1}$ Ni^{-1} h^{-1} bar^{-1} has been observed for the phosphine based complex **81**. This complex gives a high molecular weight and linear PE and shows a zero order dependence on ethylene pressure[106]. Reducing the size of the aryl-phosphine substituents reduces the activity and also the

molecular weight of the polymer. When the ligand NMe backbone is substituted by a CH_2 unit (**82a**) the activity is greatly increased but a higher rate of β-hydride elimination leads to a highly branched and low molecular weight polyethylene. The less rigid ethyl (**82b**) and propyl (**82c**) bridged diphosphine complexes are unreactive towards ethylene polymerization[107]. The phenylene derivative (**83**) is also active suggesting that the backbone rigidity also has a significant influence on catalyst reactivity.

Palladium complexes bearing P,P donors

Perfectly alternating CO/ethylene copolymerization and the CO/ethylene/propene terpolymerization are efficiently carried out at moderate temperature in the presence of a catalyst system comprising as essential components, a Pd(II) salt with weakly coordinating counter anions and a 1,3-bis(diarylphosphino)propane ligand[108]. Since the discovery of the effectiveness of Pd-(diphenylphosphino)propane (dppp) catalysts in 1984 at Shell Research, various dppp like ligands have been designed and successfully employed to catalyse CO/ethylene in combination with Pd(II) salts.

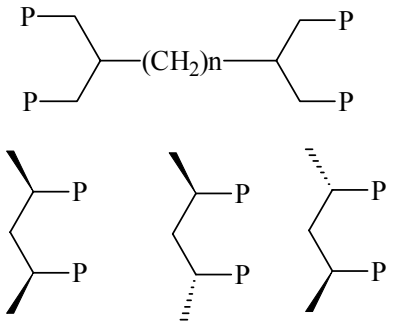

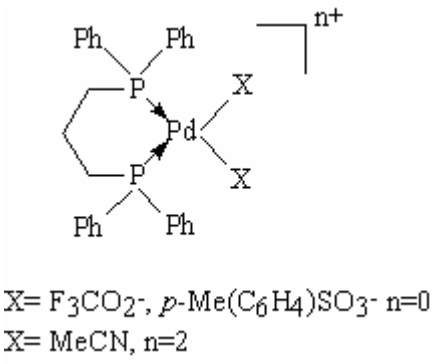

85

Variations have generally involved substitution(s) at either the phenyl rings or the saturated carbon backbone. Excellent results have been obtained with tetrakisphosphines obtained by linking two dppp units with CH_2 spacers[109]. Introduction of a methoxy substituents in the ortho position of each phenyl group as in 1,3-bis{di(2-methoxyphenyl)phosphino}propane (dmppp) or in tetrakisphosphines[110], leads to desirable characters in terms of both catalyst activity and stability.

1.4 References

1. a) Ballard, D. G. H.; Courtis, A.; Holton, J.; McMeeking, J.; Pearce, R. *J. Chem. Soc. Chem. Commun.* **1978**, 994. b) Watson, P. L. *J. Am. Chem. Soc.* **1982**, 104, 337. c) Watson, P. L.; Roe, D. C. *J. Am. Chem. Soc.* **1982**, 104, 6471. d) Watson, P. L.; Parshall, G. W. *Acc. Chem. Res.* **1985**, 18, 51.
2. a) Coles, M. P.; Gibson, V. C.; *Polym. Bull.* **1994**, 33, 529. b) Antonelli, D. M.; Leins, A.; Stryker, J. M. *Organometallics,* **1997**, 16, 2500.
3. "Recnet Advances in Chromium Catalysts for Olefin Polymerization" *Current Organic Chemistry*, **2006**, 10, 955.
4. a) Britovsek, G. J. P.; Gibson, V. C.; Wass, D. F. *Angew. Chem., Int. Ed.* **1999**, 38, 428. b) Gibson, V. C.; Spitzmesser, S. K. *Chem. Rev.* **2003**, 103, 283.
5. a) Castonguay, L. A.; Rappe, A. K. *J. Am. Chem. Soc.* **1992**, 114, 5832. b) Kawamura-Kuribayashi, H.; Koga, N.; Morokuma, K. *J. Am. Chem. Soc.* **1992**, 114, 8687.
6. a) Eur. Pat. 277004 (**1988**), Exxon Chemical Patent Inc., inv.: Turner, H. W. *Chem. Abstr.* **1989**, 110, 58290a. b) Hlatky, G. G. ; Turner, H. W. ; Eckman, R. R. *J. Am. Chem. Soc.* **1989**, 111, 2728.
7. Pellecchia, C.; Proto, A.; Longo, A.; Zambelli, A. *Macromol. Chem. Rapid. Commun.* **1992**, 13, 277.
8. Temme, B. ; Karl, J. ; Erker, G. ; Luftmann, H. ; Frohlich, R. ; Kotila, S. *Angew. Chem.* **1995**, 107, 1867; *Angew. Chem., Int. Ed. Engl.* **1995**, 34, 1755.
9. Jimenez Pindado, G.; Thornton-Pett, M.; Bouwkamp, M.; Meetsma, A.; Hessen, B.; Bochmann, M. *Angew. Chem., Int. Ed. Engl.* **1997**, 36, 2358.
10. Shah, S. A. A.; Dorn, H. ; Voigt, A. ; Roesky, H. W. ; Parisini, E. ; Schmidt, H. G. ; Noltemeyer, M. *Organometallics* **1996**, 15, 3176.
11. Scollard, J. D.; McConville, D. H.; Payne, N. C.; Vittal, J. J. *Macromolecules*, **1996**, 29, 5241.
12. Tsubaki, S.; Jin, J.; Ahn, C.-H. ; Sano, T.; Uozumi, T.; Soga, K. *Macromol. Chem. Phys.* **2001**, 202, 482.
13. Jager, F.; Roesky, H. W.; Dorn, H.; Shah, S.; Noltemeyer, M.; Schmidt, H. G. *Chem. Ber.* **1997**, 130, 399.

14. Horton, A. D.; von Hebel, K. L.; With, J. de. *Macromol. Symp.* **2001**, 173, 123.

15. Gibson, V. C. ; Kimberley, B. S. ; White, A. J. P. ; Williams, D. J. ; Howard, P. *Chem. Commun.* **1998**, 313.

16. Male, N. A. H.; Thornton-Pett, M.; Bochmann, M. *J. Chem. Soc. Dalton. Trans.* **1997**, 2487.

17. a) Nomura, K.; Naofumi, N.; Takaoki, K.; Imai, A. *J. Mol. Catal. A: Chem.* **1998**, 130, L209. b) Nomura, K.; Oya, K.; Imanishi, Y. *Polymer*. **2000**, 41, 2755.

18. Guerin, F.; McConville, D. H.; Vittal, J. J. *Organometallics,* **1996**, 15, 5586.

19. Baumann, R.; Davis, W. M.; Schrock, R. R. *J. Am. Chem. Soc.* **1997**, 119, 3830.

20. a) Baumann, R.; Schrock, R. R. *J. Organomet. Chem.* **1998**, 557, 69. b) Baumann, R.; Schrock, R. R.; Reid, S. M.; Goodman, J. T.; Stumpf, R.; Davis, W. M. *Organometallics*, **1999**, 18, 3649. c) Goodman, J.T.; Schrock, R.R. *Organometallics*, **2001**, 20, 5205.

21. Horton, A. D.; With, J. de; van der Liden, A. J.; van de Weg, H. *Organometallics*, **1996**, 15, 2672.

22. Volkis, V.; Shmulinson, M.; Averbuj, C.; Lisovskii, A.; Edelmann, F. T.; Eisen, M. S. *Organometallics*, **1998**, 17, 3155.

23. Vollmerhaus, R.; Shao, P. C.; Taylor, N. J.; Collins, S. *Organometallics*, **1999**, 18, 2731.

24. Oberthur, M.; Arndt, P.; Kempe, R. *Chem. Ber.* **1996**, 129, 1087.

25. Martin, A.; Uhrhammer, R.; Gardner, T. G.; Jordan, R. F. *Organometallics.* **1998**, 17, 382.

26. Matsugi, T.; Matsui, S.; Kojoh, S.-i.; Takagi, Y.; Inoue, Y.; Fujita, T.; Kashiwa, N. *Chem. Lett.* **2001**, 566.

27. Matsugi, T.; Matsui, S.; Kojoh, S.-i.; Takagi, Y.; Inoue, Y.; Fujita, T.; Kashiwa, N. *Macromolecules,* **2002**, 35, 4880.

28. Stephan, D. W.; Guerin, F.; Spence, R. E. V. H.; Koch, L.; Gao, X.; Brown, S. J.; Swabey, J. W.; Wang, Q.; Xu, W.; Zoricak, P.; Harrison, D. G.; *Organometallics* **1999**, 18, 2046.

29. Matsuo, Y.; Mashima, K.; Tani, K. *Chem. Lett.* **2000**, 1114.

30. Yoshida, Y.; Matsui, S.; Takagi, Y.; Mitani, M.; Nakano, T.; Tanaka, H.; Kashiwa, N.; Fujita, T. *Organometallics,* **2001**, 20, 4793.

31. Dawson, D. M.; Walker, D. A.; Thornton-Pett, M.; Bochmann, M. *J. Chem. Soc. Dalton. Trans.* **2000**, 459.

32. Yoshida, Y.; Saito, J.; Mitani, M.; Takagi, Y.; Matsui, S.; Ishii, S.; Kashiwa, N.; Fujita, T. *Chem. Commun.* **2002**, 1298.

33. van der Linden, A.; Schaverien, C. J.; Meijboom, N.; Ganter, C.; Orpen, A. G. *J. Am. Chem. Soc.* **1995**, 117, 3008.

34. a) Lee, I.-K.; Gauthier, W. J.; Ball, **J.** M.; Iyengar, B.; Collins, S. *Organometallics* **1992**,11, 2115. b) Kaminsky, W.; Steiger, R. *Polyhedron* **1988,** 7, 2375.

35. Miyatake, T.; Mizunma, K.; Seki, Y.; Kakugo, M. *Macromol. Chem. Rapid. Commun.* **1989**, 10, 34.

36. Fokken, S.; Spaniol, T. P.; Kang, H. C.; Massa, W.; Okuda, J. *Organometallics,* **1996**, 15, 5069.

37 a) Tjaden, E. B.; Swenson, D. C.; Petersen, J. L.; Jordan, R. F. *Organometallics*, **1995**, 14, 371. b) Tjaden, E. B.; Jordan, R. F. *Macromol. Symp.* **1995**, 89, 231.

38. Jones, D.; Roberts, A.; Cavell, K.; Keim, W.; Englert, U.; Skelton, B. W.; White, A. H. *J. Chem. Soc. Dalton. Trans.* **1998**, 255.

39. Repo, T.; Klinga, M.; Pietikainen, P.; Leskela, M.; Uusitalo, A. –M.; Pakkanen, T.; Hakala, K.; Aaltonen, P.; Lofgren, B. *Macromol*, **1997**, 30, 171.

40. Matilainen, L.; Klinga, M.; Leskela, M. *J. Chem. Soc. Dalton. Trans.* **1996**, 219.

41. Sobota, P.; Przybylak, K.; Utko, J.; Jerzykiewicz, L. B.; Pombeiro, A. J. L.; da Silva, M.; Szczegot, K. *Chem. Eur. J.* **2001**, 7, 951.

42 Mack, H.; Eisen, M. H. *J. Chem. Soc. Dalton. Trans.* **1998**, 917.

43. a) Tshuva, E. Y.; Versano, M.; Goldberg, I.; Kol, M.; Weitman. H.; Goldschmidt, Z. *Inorg. Chem. Commun.* **1999**, 2, 371. b) Tshuva, E. Y.; Goldberg, I.; Kol, M.; Weitman. H.; Goldschmidt, Z. *Chem. Commun.* **2000**, 379. c) Tshuva, E. Y.; Groysman, S.; Goldberg, I.; Kol, M.; Weitman. H.; Goldschmidt, Z. *Organometallics,* **2002**, 21, 662.

44. Tshuva, E. Y.; Goldberg, I.; Kol, M.; Goldschmidt, Z. *Organometallics*, **2001**, 20, 3017.

45. a) Tshuva, E. Y.; Goldberg, I.; Kol, M.; Goldschmidt, Z. *Inorg. Chem. Commun,* **2000**, 3, 611. b) Tshuva, E. Y.; Goldberg, I.; Kol, M.; Goldschmidt, Z. *Chem. Commun.* **2001**, 2120.

46. Tshuva, E. Y.; Goldberg, I.; Kol, M.; Goldschmidt, Z. *J. Am. Chem. Soc.* **2000**, 122, 10706.

47. Fujita, T. *Chem. Lett.* **1999**, 1263. b) Matsui, S.; Tohi, Y.; Mitani, M.; Saito, J.; Makio, H.; Tanaka, H.; Nitabaru, M.; Nakano, T.; Fujita, T. *Chem. Lett.* **1999,** 1065. c) Matsui, S.; Tohi, Y.; Mitani, M.; Saito, J.; Makio, H.; Tanaka, H.; Nitabaru, M.; Nakano, T.; Matsukawa, N.; Takagi, Y.; Tsuru, K.; Kashiwa, N.; Fujita, T. *J. Am. Chem. Soc.* **2001**, 123, 6847. d) Matsui, S.; Fujita, T. *Catal. Today,* **2001**, 66, 63.

48. a) Matsui, S.; Inoue, Y.; Fujita, T. *J. Synth. Org. Chem. Jpn.* **2001**, 59, 232. b) Matsui, S.; Mitani, M.; Saito, J.; Matsukawa, N.; Tanaka, H.; Nakano, T.; Fujita, T. *Chem. Lett.* **2000**, 554. c) Saito, J.; Mitani, M.; Matsui, S.; Kashiwa, N.; Fujita, T. *Macromol. Rapid. Commun.* **2000**, 21, 1333.

49 a) Kojoh, S.; Matsugi, T.; Saito, J.; Mitani, M.; Fujita, T. *Chem. Lett.* **2001,** 822. b) Matsukawa, N.; Matsui, S.; Mitani, M.; Saito, J.; Tsuru, K.; Kashiwa, N.; Fujita, T. *J. Mol. Catal. A: Chem.* **2001**, 169, 99. c) Matsui, S.; Mitani, M.; Saito, J.; Tsuru, K.; Kashiwa, N.; Mohri, J.; Fujita, T. *Angew. Chem., Int. Ed. Engl.* **2001**, 40, 2918.

50 a) Mitani, M.; Mohri, J.; Yoshida, Y.; Saito, J.; Ishii, S.; Tsuru, K.; Matsui, S.; Furuyama, R.; Nakano, T.; Tanaka, H.; Kojoh, S.; Kashiwa, N.; Fujita, T. *J Am. Chem. Soc.* **2002**, 124, 3327. b) Saito, J.; Mitani, M.; Onda, M.; Mohri, J.; Ishi, J. I.; Yoshida, Y.; Nakano, T.; Tanaka, H.; Matsugi, T.; Kojoh, S.; Kashiwa, N.; Fujita, T. *Macromol. Rapid. Commun.* **2001**, 22, 1072. c) Saito, J.; Mitani, M.; Mohri, J.; Ishii, S.; Yoshida, Y.; Matsugi, T.; Kojoh, S.; Kashiwa, N.; Fujita, T. *Chem. Lett.* **2001**, 576.

51 a) Mitani, M.; Furuyama, R.; Mohri, J.; Saito, J.; Ishii, S.; Terao, H.; Kashiwa, N.; Fujita, T. *J. Am. Chem. Soc.* **2002,** 124, 7888. b) Saito, J.; Mitani, M.; Mohri, J.; Matsui, S.; Tohi, Y.; Makio, H.; Nakano, T.; Tanaka, H.; Kashiwa, N.; Fujita, T. *Macromol. Chem. Phys.* **2002**, 203, 59. c) Ishii, S.; Saito, J.; Mitani, M.; Matsuura, S.; Kojoh, S.; Kashiwa, N.; Fujita, T. *J. Mol. Catal. A: Chem* **2002**, 179, 11. d) Ishii, S.;

Saito, J.; Mitani, M.; Matsuura, S.; Kojoh, S.; Kashiwa, N.; Fujita, T. *Chem. Lett.* **2002**, 740.

52. Inoue, Y.; Nakano, T.; Tanaka, H.; Kashiwa, N.; Fujita, T. *Chem. Lett.* **2001,** 1060.
53. Corden, J.P.; Errington, W.; Moore, P.; Wallbridge, M. G. H. *Chem. Commun.* **1999**, 323.
54. Tian, J.; Hustad, P. D.; Coates, G. W. *J. Am. Chem. Soc.* **2001**, 123, 5134.
55. McKnight, A. L.; Waymouth, R. M. *Chem. Rev.* **1998**, 98, 2587.
56. Brown, S. J.; Gao, X. L.; Harrison, D. G.; Koch, L.; Spence, R. E. V.; Yap, G. P. A. *Organometallics,* **1998**, 17, 5445.
57. Kotov, V. V.; Avtomonov, E. V.; Sundermeyer, J.; Harms, K.; Lemenovskii, D. A. *Eur. J. Inorg. Chem.* **2002**, 678.
58. Duda, L.; Erker, G.; Frohlich, R.; Zippel, F. *Eur. J. Inorg. Chem.* **1998**, 1153.
59. Kunz, K.; Erker, G.; Doring, S.; Frohlich, R.; Kehr, G. *J. Am. Chem. Soc.* **2001**, 123, 6181.
60. Klosin, J.; Kruper, W. J.; Nickias, P. N.; Roof, G. R.; De Waele, P.; Abboud, K. A. *Organometallics*, **2001**, 20, 2663.
61. Ashe, A.; Fang, X. G.; Kampf, J. W. *Organometallics*, **1999**, 18, 1363.
62. Kleinschmidt, R.; Griebenow, Y.; Fink, G. *J. Mol. Catal. A: Chem,* **2000**, 157, 83.
63. Sinnema, P. -J.; van der Veen, L.; Spek, A. L.; Veldman, N.; Teuben, J. H. *Organometallics,* **1997**, 16, 4245.
64. Gomes, P. T.; Green, M. L. H.; Martins, A. M.; Mountford, P. *J. Organomet. Chem.* **1997**, 541, 121.
65. a) Nomura, K.; Naga, N.; Miki, M.; Yanagi, K.; Imai, A. *Organometallics,* **1998**, 17, 2152. b) Antinolo, A.; Hermosilla, F. C-; Corrochano, A.; Baeza, J. F-; Sanchez, A. L-; Ribeiro, M. R.; Lanfranchi, M.; Otero, A.; Pellinghelli, M. A.; Portela, M. F.; Santos, J. V. *Organometallics,* **2000**, 19, 2837.
66. Nomura, K.; Komatsu, T.; Imanishi, Y. *J. Mol. Catal. A: Chem.* **2000**, 152, 249.
67. Chen, Y. –X.; Fu, P. –F.; Stern, C. L.; Marks, T. J. *Organometallics,* **1997**, 16, 5958.
68. a) Chen, Y. X.; Stern, C. L.; Marks, T. J. *J. Am. Chem. Soc.* **1997**, 119, 2582. b) Jia, L.; Yang, X.; Stern, C. L.; Marks, T. J. *Organometallics* **1997**, 16, 842. c) Chen, Y. X.; Stern, C. L.; Yang, S.; Marks, T. J. *J. Am. Chem. Soc.* **1996**, 118, 12451. d) Deck,

P. A.; Marks, T. J. *J. Am. Chem. Soc.* **1995**, 117, 6128. e) Giardello, M. A.; Eisen, M. S.; Stern, C. L.; Marks, T. J. *J. Am. Chem. Soc.* **1995**, 117, 12114. f) Jia, L.; Yang, X.; Ishihara, A.; Marks, T. J. *Organometallics* **1995**, 14, 3135. g) Chien, J. C. W.; Song, W.; Rausch, M. D. *J. Polym. Sci., Part A: Polym. Chem.* **1994**, 32, 2387. h) Eisch, J.; Pombrik, S. I.; Zheng, G. X. *Organometallics* **1993**, 12, 3856. i) Siedle, A. R.; Lamanna, W. M.; Newmark, R. A.; Stevens, J.; Richardson, D. E.; Ryan, M. *Makromol. Chem.Macromol. Symp.* **1993**, 66, 215.

69. Gielens, E. E. C. G.; Tienitsch, J. Y.; Hessen, B.; Teuben, J. H. *Organometallics,* **1998**, 17, 1652.
70. Chernega, A. N.; Gomez, R.; Green, M. L. H. *J. Chem. Soc. Chem. Commun.* **1993**, 1415.
71. Gomez, R.; Green, M. L. H.; Haggit, J. *J. Chem. Soc. Chem. Commun.* **1994**, 2607.
72. Flores, J. C.; Chien, J. C. W.; Rausch, M. D. *Organometallics,* **1995**, 14, 2106.
73. Aaltonen, P.; Seppala, J.; Matilainen, L.; Leskela, M. *Macromol*, **1994**, 27, 3136.
74. Small, B. L.; Brookhart, M.; Bennett, A. M. A.; *J. Am. Chem. Soc.* **1998**, 120, 4049.
75. Britovsek, G. J. P.; Gibson, V. C.; Kimberley, B. S.; Maddox, P. J.; McTavish, S. J.; Solan, G. A.; White, A. J. P.; Williams, D. J. *Chem. Commun.* **1998**, 849.
76. Shibayama, K.; Osaga, M. PCT Int Appl. WO9835996, 1998, *Chem. Abstr*. **1998**, 129, 203390.
77. Stibrany, R. T.; Patil, A. O.; Zushma, S. *PMSE-Preprints,* 223rd ACS National Meeting, Orlando, FL, April 7-11, 2002, American Chemical Society: Washington, DC, **2002**, Vol. 86, pp-323.
78. Gibson, V. C.; Tomov, A.; Wass, D. F.; White, A. J. P.; Williams, D. J. *J. Chem. Soc. Dalton. Trans.* **2002**, 2261.
79. Ittel, S. D.; Johnson, L. K.; Brookhart, M. *Chem. Rev.* **2000**, 100, 1169.
80. Britovsek, G. J. P.; Cohen, S. A.; Gibson, V. C.; Maddox, P. J.; van Meurs, M. *Angew. Chem., Int. Ed.* **2002**, 41, 489.
81. Johnson, L. K.; Killian, C. M.; Brookhart, M. *J. Am. Chem. Soc.* **1995**, 117, 6414.
82. Pellecchia, C.; Zambelli, A. *Macromol. Chem. Rapid. Commun.* **1996**, 17, 333.
83. Pappalardo, D.; Mazzeo, M.; Antinucci, S.; Pellechia, C. *Macromolecules*, **2000**, 33, 9483.

84. a) Pellechia, C.; Zambelli, A.; Oliva, L.; Pappalardo, D. *Macromolecules*, **1996**, 29, 6990. b) Pellechia, C.; Zambelli, A.; Mazzeo, M.; Pappalardo, D. *J. Mol. Catal. A*. **1998**, 128, 229.

85. Moody, L. S.; Mckenzie, P. B.; Killian, C. M.; Lavoie, G. G.; Ponasik, J. A.; Barrett, A. G. M.; Smith, T. W.; Pearson, J. C. (Eastman Chemical Co, USA) PCT Int Appl. WO0050470, 2000, *Chem Abstr.* **2000**, 133, 208316.

86. Gottfried, A. C.; Brookhart, M. *Macromolecules,* **2001**, 34, 1140.

87. Killian, C. M.; Johnson, L. K.; Brookhart, M. *Organometallics*, **1997**, 16, 2005.

88. Laine, T.V.; Lappalainen, K.; Liimatta, J.; Aitola, E.; Lofgren, B.; Leskela, M. *Macromol. Rapid. Commun.* **1999**, 20, 487.

89. Schareina, T.; Hillebrand, G.; Fuhrmann, H.; Kempe, R. *Eur. J. Inorg. Chem.* **2001**, 2421.

90. Stibrany, R. T.; Matturo, M. G.; Zushma, S.; Patil, A. O. (Exxonmobil Resarch and Engineering Co. USA). PCT Int Appl. WO0174743 1998, *Chem Abstr.* **2001**, 135, 289188.

91. Wang, C. M.; Friedrich, S.; Younkin, T. R.; Li, R. T.; Grubbs, R. H.; Bansleben, D. A.; Day, M. W. *Organometallics,* **1998**, 17, 3149.

92. Younkin, T. R.; Conner, E. F.; Henderson, J. I.; Friedrich, S.; Bansleben, D. A.; Grubbs, R. H. *Science*, **2000**, 287, 460.

93. Novak, B. M.; Tian, G.; Nodono, M.; Boyle, P. *PMSE-Preprints,* 23rd ACS National Meeting, Orlando, FL, April 7-11, 2002, American Chemical Society: Washington, DC, 2002; Vol. 86, pp-326.

94. Hicks, F. A.; Brookhart, M. *Organometallics,* **2001**, 20, 3217.

95. a) Braca, G.; Raspolli Galletti, A. M.; Di Girolamo, M.; Sbrana, G.; Silla, R.; Ferrarini, P. *J. Mol. Catal.* **1995**, 96, 203-213. b) Klabunde, U.; Ittel, S. D. *J. Mol. Catal.* **1987**, 41, 123.

96. a) Klabunde, U.; Mulhaupt, R.; Herskovitz, T.; Janowicz, A. H.; Calabrese, J.; Ittel, S. D. *J. Poly. Sci.* A. **1987**, 1989. b) Keim, W.; Kowaldt, F. H.; Goddard, R.; Kruger, C. *Angew. Chem. Int. Ed. Engl.* **1978**, 17, 466.

97. a) Keim, W.; Appel, R.; Storeck, A.; Kruger, C.; Goddard, R. *Angew. Chem., Int. Ed. Engl.* **1981**, 20, 116. b) Keim, W.; Appel, R.; Gruppe, S.; Knoch, F. *Angew. Chem.,*

Int. Ed. Engl. **1987**, 26, 1012. c) Ostoja Starzewski, K. A.; Witte, J. *Angew. Chem., Int. Ed. Engl.* **1985**, 24, 599.

98. Soula, R.; Broyer, J. P.; Llauro, M. F.; Tomov, A.; Splitz, R.; Claverie, J.; Drujon, X.; Malinge, J.; Saudemont, T. *Macromolecules*, **2001**, 34, 2438.
99. Soula, R.; Novat, C.; Tomov, A.; Spitz, R.; Claverie, J.; Drujon, X.; Malinge, J.; Saudemont, T. *Macromolecules*, **2001**, 34, 2022.
100. Gibson, V. C.; Tomov, A.; White, A. J. P.; Williams, D. J. *Chem. Commun.* **2001**, 719.
101. Soula, R.; Broyer, J. P.; Llauro, M. F.; Tomov, A.; Spitz, R.; Claverie, J.; Drujon, X.; Malinge, J.; Saudemont, T. *Macromolecules*, **2001**, 34, 2438.
102. Liu, W.; Malinoski, J. M.; Brookhart, M. *Organometallics*, **2002**, 21, 2836.
103. a) Komon, Z. J. A.; Bu, X. H.; Bazan, G. C. *J. Am. Chem. Soc.* **2000**, 122, 12379. b) Komon, Z. J. A.; Bu, X. H.; Bazan, G. C. *J. Am. Chem. Soc.* **2000**, 122, 1830.
104. Heinicke, J.; He, M. Z.; Dal, A.; Klein, H. F.; Hetche, O.; Keim, W.; Florke, U.; Haupt, H. *Eur. J. Inorg. Chem.* **2000**, 431.
105. Ikeda, S.; Ohhata, F.; Miyoshi, M.; Tanaka, R.; Minami, T.; Ozawa, F.; Yoshifuji, M. *Angew. Chem., Int. Ed.* **2000**, 39, 4512.
106. Cooley, N. A.; Green, S. M.; Wass, D. F.; Heslop, K.; Orpen, A. G.; Pringle, P. G. *Organometallics,* **2001**, 20, 4769.
107. Carter, A.; Cooley, N. A.; Pringle, P. G.; Scutt, J.; Wass, D. F. *PMSE-Preprints,* 23rd ACS National Meeting, Orlando, FL, April 7-11, 2002, American Chemical Society: Washington, DC, 2002; Vol. 86, pp-314.
108. a) Sen, A.; *Acc. Chem. Res.* **1993,** 303. b) Drent, E.; Budzelaar, P. H. M.; *Chem. Rev.* **1996**, 96, 663. c) Sommazzi, A.; Garbassi, F.; *Prog. Polym. Sci.* **1997**, 22, 1547.
109. Wong P. K.; Keijsper, J. J.; van der Made, A. W.; Eur. Pat. Appl. 408155A2, **1990**.
110. Drent, E.; Wife, L.; Eur. Pat. Appl. B222454, **1987**.

CHAPTER 2

SCOPE AND OBJECTIVES

2.1 Objective in undertaking the present work

The nature of legends plays a key role in the design of efficient catalysts for olefin polymerization[1]. Selective dimerization and oligomerization of olefins are also of significant importance. These are typically carried out using homogeneous late-transition metal catalysts, particularly nickel based catalysts, because of their strong propensity to undergo β-H elimination[2].

Most of the late transition metal catalysts are based on hard oxygen and nitrogen donors. Strong σ donor capacity of phosphine ligands makes them more suitable for catalytic reactions requiring nucleophilic metal centers. Hence, in spite of a rich coordination chemistry of phosphine ligands with late transition metals, there is hardly any use of these ligands in olefin polymerization catalysis which require an electrophilic metal center. In cases, where these ligands have been applied in coordination with late transition metals, very low ethylene polymerization activity has been observed[3]. Isolated reports mention the use of phosphine ligands of the type $R_2PCH_2PR_2$ (R = ^{t}Bu) in combination with $Ni(acac)_2$/MMAO leading to amorphous poly(ethylene)s with low activity of 1.0 gPE/mmol^{-1}Ni h^{-1}bar^{-1} (0.10 mmol Ni, P_{C2H4} = 6.9 bar, 18.5 h)[3b]. Another example is a diphosphinidine palladium complex which is sterically similar to α-diimine complexes[4]. This complex exhibited an activity of 50-130 gPE/mmol^{-1} Pd^{-1} h^{-1} (P_{C2H4} = 5-30 bar). These reports suggest that the polymerization activities of these Group 10 metals are very much dependent on the nature of the donor atom.

An exception to this trend is the nickel (II) complexes of bulky bis(diarylphosphino)methyl amines $(PAr_2)_2NMe$ [Ar = 2-C_6H_4 (^{i}Pr), 2-C_6H_4 (Et) , 2-C_6H_4 (Me)][5]. High catalyst activity (A = 2200 g/mmol^{-1} Ni^{-1} h^{-1} bar^{-1}) has been observed for this complex resulting in high molecular weight linear poly(ethylene)s. Chromium catalysts with P-N-P type ligands of the formula $(PAr_2)_2NR$ (Ar = *o*-substituted phenyl group) are also reported to be active catalysts for the trimerization[6a] and tetramerization[6b] of ethylene to produce hexene-1 and octene-1 respectively. It has been found that the substitution of ligand NMe backbone by a CH_2 unit as in bis(diarylphosphino)methane (dppm) greatly increases the activity for ethylene polymerization, but a higher rate of β-

hydride elimination leads to a highly branched and low molecular weight polyethylene[7]. When the study was extended to five and six membered chelates formed by bis(diarylphosphino)ethane (dppe) and bis(diarylphosphino)propane (dppp) respectively, no activity for ethylene polymerization was observed[7].

The larger bite angle and correspondingly smaller space available for substrate binding in the latter two cases in comparison to the four-membered chelate as in dppm was the most plausible explanation for the reduction in activity. On the contrary, Drent et al.[8] have shown that the CO/C_2H_4 copolymerization catalytic activity of palladium(II) complexes of diphosphines of the type $Ar_2P(CH_2)nPAr_2$ is a sensitive function of the backbone chain length, n, and the aryl group, Ar. Six-membered chelates are an order of magnitude more active than the five-membered analogues, whereas, the four-membered chelates are essentially inactive. However, by introducing bulky *o*-substituents on the aryl groups, highly active palladium catalysts for the copolymerization reactions could also be achieved with four-membered chelates[9]. Precise reasons for this difference in behavior still remain ambiguous.

One of the objectives of the present investigation was to examine novel bisphosphine ligands which had structural resemblance to both the bis(diarylphosphino) methyl amines and the bis(diarylphosphino)propane (dppm) ligands. It was proposed to study a C-N-C ligand backbone which when complexed to Ni (II) salts can form a six-membered chelate. Such a chelate is expected to have a larger bite angle. This ligand framework will also enable the study of the influence of nitrogen on polymerization behavior[5]. Though the activity is expected to be low as compared to four-membered chelates, introduction of steric bulk on the nitrogen could lead to interesting changes in product composition, from dimers to high molecular weight linear poly(ethylene)s.

The nickel chloride (**1a-c**) and nickel bromide (**2a-c**) complexes of bis-phosphine ligands synthesized, have the general structural motif as shown below:

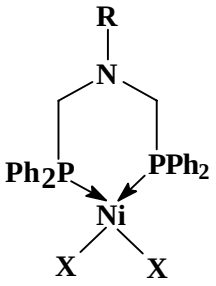

a. R= *tert*-butyl
b. R= 3,5-(Me $_2$)C_6H_4
c. R= 2,6-(^{i}Pr$_2$)C_6H_4

1. X= Cl
2. X= Br

Single crystal X-Ray diffraction studies on the Ni (II) complexes were carried out to define the solid state structure of the complexes **1**(**a-c**) and **2**(**a-c**). Complexes **1**(**a-c**) and **2**(**a-c**) were employed as catalysts for ethylene polymerization. Differential scanning calorimetry (DSC) and high temperature ^{13}C NMR spectroscopy were used to determine thermal properties and branching characteristics of the polymer.

Vinyl addition polymerization of norbornene using late transition metal catalysts continues to be of interest. Polynorbornene is a speciality polymer having good mechanical strength, heat resistivity and optical transparency. Catalysts most frequently described in the literature for vinyl addition polymerization of norbornene are the cationic palladium (II) system $[Pd(CH_3CN)_4](BF_4)_2$[10]. Nickel complexes for vinyl addition polymerization of norbornene were described in 1990's in combination with MAO as a cocatalyst[11]. Use of $B(C_6F_5)_3/Et_3Al$ in the polymerization of norbornene has been described with Ni (II) and Pd (II) complexes of bis(diarylphosphino)ethane (dppe) and bis(diarylphosphino)propane (dppp)[12-14].

Another objective of the present investigation was to study the effect of ligand structure on catalyst activity for the vinyl polymerization of norbornene in combination with $B(C_6F_5)_3/Et_3Al$. Palladium (II) complexes of bis(diphenylphosphinomethyl)alkyl/aryl amines of the formula $(PPh_2CH_2)_2NR$ (R = ^{t}Bu, 3,5-$C_6H_4Me_2$, 2,6-$C_6H_4(^iPr)_2$) were synthesized which unlike C_2 and C_3 ligand backbone in dppe and dppp respectively have a C-N-C framework. These Pd (II) complexes along with their Ni (II) counterpart were explored for norbornene polymerization. Effect of reaction parameters, such as, catalyst structure, nature of metal, catalyst concentration, Al/M ratio and temperature were explored. The obtained polymers were analyzed using high temperature ^{13}C NMR

spectroscopy, gel permeation chromatography (GPC), infra-red spectroscopy (IR) and thermogravimetric analysis (TGA).

In-situ introduction of versatile functional groups into nonpolar polyolefins, especially, at chain ends offer a means of constructing a variety of polymer architechtures such as block and graft polymers[15]. Controlled chain transfer processes to organometalloids[16-17] offer an excellent means to achieve this objective. Silanes are reported to be promising candidates for organometalloid chain transfer processes[16]. Marks and coworkers reported the use of $PhSiH_3$, n-$BuSiH_3$ and $C_6H_5CH_2SiH_3$ as efficient and selective chain transfer agents in organolanthanide catalyzed alpha-olefin polymerizations and copolymerizations yielding families of new silapolyolefins[16b]. Organolanthanides are efficient hydrosilylation catalysts and their work demonstrated that hydrosilylation and polymerization could be coupled to afford silyl-capped polyolefins. Homogeneous organotitanium catalysts showed a lower propensity to undergo silanolytic chain transfer[16]. A variety of zirconium metallocene complexes and quasi-metallocene complexes upon silanolytic chain transfer process, resulted in predominantly or exclusively polyolefins devoid of silyl end groups together with dehydrogenative silane coupling products[18] ($PhSiH_2$-SiH_2Ph, etc).

Polymerization of ethylene using bis-phenoxyimine titanium complexes are characterized by high catalyst activity (34000 $gmmol^{-1}$ Ti^{-1} h^{-1} bar^{-1}), narrow molecular weight distribution (< 1.15) and high molecular weights. A linear relationship between $\overline{Mn}$ and polymerization time has been observed. These features have led to the conclusion that the polymerization shows some characteristics of "living" behavior[19]. However, there is no report in the literature concerning the ability of the chain ends derived from such a catalyst to undergo silanolytic chain transfer. Therefore, an objective of this work was to study the feasibility of chain transfer with silanes ($PhSiH_3$ and $MePhSiH_2$) in presence of bis-phenoxyimine titanium complexes in ethylene polymerization.

The polymers thus produced were characterized by gel permeation chromatography (GPC) and high temperature ^{13}C NMR spectroscopy to gain insight into polymer properties and structure.

Schiff-base ligands have played a key role in the development of coordination chemistry since the late nineteenth century. Metal complexes of Schiff-base ligands are easily prepared with diverse structural features. However, till recently, there have been no reports of styrene polymerization with Schiff-base titanium complexes. Kim and coworkers[20] reported a series of titanium salen complexes as catalysts for the syndiospecific polymerization of styrene. Recently, Fujita and coworkers reported the polymerization of styrene using bis-phenoxy imine complexes of group 4 metals[21].

Another objective of the study was to examine the role of fluorine atoms on the aromatic ring attached to the imine nitrogen of Schiff-base complexes of titanium on the polymerization of styrene. Four different bis-phenoxyimine titanium complexes viz, bis [N(3-*tert*-butyl salicylidene)anilinato]Ti(IV) dichloride, bis[N(3-*tert*-butyl salicylidene)2,6-difluoroanilinato]Ti(IV) dichloride, bis[N(3-*tert*-butyl salicylidene)2,4,6-trifluoroanilinato]Ti(IV) dichloride and bis[N(3-*tert*-butyl salicylidene)2,3,4,5,6-pentafluoroanilinato]Ti(IV) were employed in the polymerization of styrene at 70^{o}C using MAO as cocatalyst. Reaction conditions, such as, catalyst concentration, Al/Ti ratio, reaction temperature and reaction time were studied. The syndiotactic fractions as well as the whole polymer containing both syndiotactic and atactic fractions were analyzed by high temperature ^{13}C NMR spectroscopy and differential scanning calorimetry (DSC).

2.2 References

1. a) Parshall, G. W.; Ittel, S. D. In *Homogeneous Catalysis*: *The Applications and Chemistry of Catalysis by Soluble Transition Metal Complexes*; Wiley: New York, **1992**; pp 68. b) Vogt, D. In *Applied Homogeneous Catalysis with Organometallic compounds*; Cornils, B., Hermann, W. A.; Eds.; VCH: Weinheim, Germany, **1996**; Vol. 1, pp 245. c) Chauvin, Y.; Olivier, H. In *Applied Homogeneous Catalysis with Organometallic compounds*; Cornils, B., Hermann, W. A.; Eds.; VCH: Weinheim, Germany, 1996; Vol. 1, pp 258. d) Small, B. L. *Organometallics* **2003**, 22, 3178.
2. a) Muthukumaru Pillai, S.; Ravindranathan, M.; Sivaram, S. *Chem. Rev*. **1986**, 86, 353. (b) Keim, W. *Angew. Chem., Int. Ed. Engl*. **1990**, 29, 235.
3. a) Mui, H. D.; Riehl, M. E.; Wilson, S. R.; Girolami, G. S. *ACS Abstracts* **1994**, 208, 530-INOR. b) Hoehn, A.; Lippert, F.; Schauss, E. (to BASF) WO 96/37522 c) Brookhart, M. S.; Feldman, J.; Hauptman, E.; McCord, E. F. (to Dupont) WO 98/47934, *Chem. Abstr*. **1998**, 129(25)331169D.
4. Ikeda, S.; Ohhata, F.; Miyoshi, M.; Tanaka, R.; Minami, T.; Ozawa, F.; Yoshifuji, M. *Angew. Chem., Int. Ed. Engl.* **2000**, 39, 4512.
5. Cooley, N. A.; Green, S. M.; Wass, D. F. *Organometallics* **2001**, 20, 4769.
6. a) Agapie, A.; Day, M. W.; Henling, L. M.; Labinger, J. A.; Bercaw, J. E. *Organometallics* **2006**, 25, 2733. b) Bollmann, A.; Blann, K.; Dixon, J. T.; Hess, F. M.; Killian, E.; Maumela, H.; McGuinness, D. S.; Morgan, D. H.; Neveling, A.; Otto, S.; Overett, M.; Slawin, A. M. Z.; Wasserscheid, P.; Kuhlmann, S. *J. Am. Chem. Soc.* **2004**, 126, 14712.
7. Dennett, J. N. L.; Gillon, A. L.; Heslop, K.; Hyett, D. J.; Fleming, J. S.; Emma Lloyd-Jones, C.; Guy Orpen, A.; Pringle, P. G.; Wass, D. F. *Organometallics* **2004**, 23, 6077.
8. a) Drent. E.; Budzelaar, P. H. M. *Chem. Rev.*, **1996**, 96, 663 and references therein. b) Drent, E.; vanBroekhoven, J. A. M.; Budzelaar, P. H. M. *Recl. Trav. Chim.*, **1996**, 115, 263. c) Mul, W. P.; Oosterbeek, H.; Beitel, G. A.; Kramer, G. J.; Drent, E. *Angew. Chem., Int. Ed.*, **2000**, 39, 1848. d) Drent, E. *Eur. Pat. Appl.*, 1984, EP121965 (to Shell).
9. Dossett, S. J.; Gillon, A.; Guy Orpen, A.; Fleming, J. S.; Pringle, P. G.; Wass, D. F.;

Jones, M. D. *Chem Commun.* **2001**, 699.

10. (a) Sen, A.; Lai, T.-W. *J. Am. Chem. Soc*. **1981**, 103, 4627-4629. (b) Sen, A.; Lai, T.-W. *Organometallics*, **1982**, 1, 415.
11. a) Peruch, F.; Cramail, H.; Deffieux, A. *Macromol. Chem.Phys*. **1998**, 199, 2221–2227. b) Arndt, M.; Gosmann, M. *Polym. Bull*. **1998**, 41, 433.
12. US 5912313 (1999), B.F. Goodrich Company, USA, invs.; McIntosh, L. H.; Goodall, B. L.; Shick, R. A.; Jayaraman, S. *Chem. Abstr*. **1997**, 127, 110414m.
13. Lassahn, P. G.; Janiak, C.; Oh, J. S. *Macromol. Rapid. Commun.* **2002**, 23, 16.
14. a) Jang, Y.; Sung, H-K.; Lee, S.; Bae, C. *Polymer* **2005**, 46, 11301. b) Lassahn, P-G.; Lozan, V.; Wu, B.; Weller, A. S.; Janiak, C. *Dalton Trans.* **2003,** 4437. c) Jang , Y.; Sung, H-K.; Kwag, H. *European. Polymer. Journal.* **2006**, 42, 1250.
15. Reviews of functionalized polymers: a) Ittel, S. D.; Johnson, L. K.; Brookhart, M. *Chem. Rev.* **2000**, 100, 1169. b) Boffa, L. S.; Novak, B. M. *Chem. Rev.* **2000**, 100, 1479.
16. Chain transfer to silanes: a) Koo, K.; Marks, T. J. *CHEMTECH* **1999**, 13-19. b) Koo, K.; Fu, P.-F.; Marks, T. J. *Macromolecules* **1999**, 32, 981. c) Koo, K.; Fu, P. -F.; Marks, T. J. *J. Am. Chem. Soc.* **1999**, 121, 8791. d) Koo, K.; Fu, P. -F.; Marks, T. J. *J. Am. Chem. Soc.* **1998**, 120, 4019. e) Fu, P. -F.; Marks, T. J. *J. Am. Chem. Soc.* **1995**, 117, 10747.
17. Chain transfer to boranes: a) Xu, G.; Chung, T. C. *Macromolecules* **1999**, 32, 8689-8692. b) Xu, G.; Chung, T. C. *J. Am. Chem. Soc.* **1999**, 121, 6763.
18. a) Harrod, J. F.; Dioumaev, V. K. *J. Organomet. Chem.* **1996**, 521, 133. b) Tilley, T. D. *Acc. Chem. Res.* **1993**, 26, 22-29 and references therein. c) Corey, J. Y.; Huhmann, J. L.; Zhu, X. -H. *Organometallics* **1993**, 12, 1121 and references therein. d) Fu, P.-F.; Brard, L.; Li, Y.; Marks, T. J. *J. Am. Chem. Soc.* **1995**, 117, 7157.
19. Fujita, T. *Angew. Chem., Int. Ed.* **2001,** 40, 15, 2918.
20. Kim, H.; Ha, Y. S.; Zhang, D. F.; Ha, C.-S.; Lee. U. *Macromol. Rapid. Commun.* **2004**, 1319.
21. Michiue, K.; Onda, M.; Tanaka, H.; Mitani, M.; Fujita, T. *PMSE Preprints*. **2006**, 94, 236.

CHAPTER 3

EXPERIMENTAL METHODS

3.1 Introduction

Synthesis of transition metal complexes and polymerization of olefins require scrupulous purification of all the ingredients involved in catalyst preparation and polymerization reactions. The solvents and other reagents have to be purified and dried in multiple steps to remove traces of impurities as well as moisture. All manipulations involving air and/or moisture sensitive compounds were performed using high vacuum Schlenk techniques or within an inert atmosphere glove box (M. Braun/ labmaster 100) continuously purged with high purity nitrogen. Argon and nitrogen were purified by passage through columns of 4 Å and 3 Å molecular sieves.

In this chapter, materials used, purification and drying of reagents and chemicals, and analytical techniques used for the characterization of catalysts and polymers are discussed.

3.2 Materials

Chemicals used for the work

Name of chemical	Grade/Purity	Source
Acetone	AR	S.d. Fine. Chemicals, Mumbai, India
Aluminium oxide	Active neutral	S.d. Fine. Chemicals, Mumbai, India
Aniline	99 %	Aldrich, USA
Benzene-d6	99 atom % D	Aldrich USA
BF_3. Et_2O		Fluka chemika
Bromo-pentafluoro benzene	99 %	Aldrich, USA
Butyllithium	2.5 M in hexanes	Aldrich, USA
Calcium hydride	-40 mesh, 90-95 %	Aldrich USA
o-dichlorobenzene (ODCB)	99 %	Aldrich USA
Dichloromethane	LR	Merck, India
Diethyl ether	LR	S.d. Fine. Chemicals, Mumbai, India

Name of chemical	Grade/Purity	Source
2,6-Difluoroaniline	≥ 97 %	Aldrich, USA
2,6-Diisopropyl aniline	Technical grade, 90 %	Aldrich, USA
3,5-Dimethyl aniline	98 %	Aldrich, USA
Ethylene	Polymerization grade	Gas Cracker plant, Indian Petrochemical Corporation Ltd., Nagothane, Maharashtra, India
Ethyleneglycol dimethylether (DME)	99+ %	Aldrich, USA
Formalin	37-41 % w/v for synthesis	S.d. Fine. Chemicals, Mumbai, India
n-hexane	For synthesis	Merck, India
Li rods	99.9 %	Aldrich, USA
Magnesium turnings	98 %	Aldrich, USA
Methanol	AR	S.d. Fine. Chemicals, Mumbai, India
Methylaluminoxane	10 wt % solution in toluene	Witco GmbH, Germany
Methyl phenyl silane	98 %	Aldrich, USA
Nickel chloride (anhydrous)	99.99 %	Aldrich, USA
Norbornene	99 %	Aldrich, USA
Palladium (II) chloride	99.9+ %	Aldrich, USA
2,3,4,5,6-pentafluoroaniline	99 %	Aldrich, USA
Phenyl silane	97 %	Aldrich, USA
Sodium hydride	95 % dry	Aldrich, USA
Sodium metal	LR	S.d. Fine. Chemicals, Mumbai, India
Styrene	99 %	Aldrich, USA
Tertiary butyl amine	For synthesis	Loba chemicals, Mumbai, India
3-*tert*-butyl-2-hydroxy benzaldehyde	98%	Aldrich, USA

Name of chemical	Grade/Purity	Source
1,1,2,2-tetrachloroethane-D2	99.5 atom % D	Aldrich, USA
Tetrahydrofuran (THF)	AR	Merck, India
Titanium tetrachloride	99.9 %	Aldrich, USA
1,2,4-trichlorobenzene (TCB)	Spectrophotometric grade	Aldrich, USA
Triethylaluminum	Neat	Witco GmbH, Germany
Triethyl amine	LR for synthesis	Loba Chemicals, Mumbai, India
Triethyl ortho formate	Anhydrous, 98 %	Aldrich, USA
2,4,6-trifluoroaniline	≥ 97 %	Aldrich, USA
Triphenyl phosphine	Puriss for synthesis	Spectrochem, Mumbai, India
Toluene	Sulfur free, LR	S.d. Fine. Chemicals, Mumbai, India

3.3 Purification and drying

All solvents and reagents were purified and dried under dry nitrogen atmosphere using standard procedures[1]. Toluene (sulfur free), diethyl ether and tetrahydrofuran were purified by refluxing over sodium wire and subsequent distillation under nitrogen. Dichloromethane was stirred over CaH_2 and n-hexane over NaH for 24 h and subsequently distilled under a nitrogen atmosphere. Methanol, water, dichloromethane and the amines/anilines were degassed by using freeze-pump-thaw technique. Tertiary butyl amine, 2,6-diisopropyl aniline and 3,5-dimethyl aniline were distilled freshly just before use. Norbornene was distilled over sodium before use. $TiCl_4$ was refluxed over Cu turnings and distilled just before use. Styrene was washed with 5% NaOH solution 2-3 times followed by a water wash. The organic layer was separated and stored over $MgSO_4$ for 12 h. Thereafter, it was stirred over CaH_2 for 24 h and vacuum distilled before use.

3.4 Analysis and characterization

3.4.1 Gel permeation chromatography (GPC)

Molecular weights of poly(ethylene)s were measured by GPC in 1,2,4-trichlorobenzene at 135°C. For these measurements, a Polymer Laboratories 220 high temperature GPC was used. This instrument was equipped with polystyrene gel columns (PL Gel- 3 x Mixed B, Particle size- 10 μ) along with refractive index, viscosity and light scattering triple detector system. The mass constant (2750) and viscosity constant (1.000) for RI and viscosity detector were determined using a 0.08 wt% solution (in 1,2,4-TCB) of polystyrene standard of $\overline{Mn}$ = 1,86,000 supplied by Polymer Laboratories. The absolute molecular weights of poly(ethylene)s were calculated using Trisec Triple Detector GPC software supplied by Viscotek using a dn/dC value of 0.097 mL/g. The sample was prepared by dissolving a known weight of polymer in 10 mL 1,2,4-TCB at 135^{o}C. This polymer solution in TCB was then filtered through a filtration unit (Schleicher& Schuell, Rezist 30/0, 45 PTFE, 0.45 lm, Grünrand) maintained at 135^{o}C, and the filtrate was used for analysis.

In case of poly(norbornene)s, the dn/dC values for were calculated from the mass constant (k) of RI detector and the actual weight of the sample injected (C) using the following equation:

$$\text{Area under the peak (RI)} = k.\ dn/dC.\ C$$

Where, area under the concentration trace is directly related to the mass [Concentration x Injection volume (200 μL)] of the sample injected.

3.4.2 Gas chromatography

The dimers and trimers of ethylene were analyzed using an Agilent Technologies (6820) gas chromatograph using a Porapak-P column (6 metres, 1/8 inches inner diameter)) and a flame ionization detector (FID). The oven temperature was held at 40^{o}C for 3 min followed by a ramp rate of 15^{o}C/min up to 150^{o}C and hold for 42 min. The flame ionization detector (FID) was maintained at 250^{o}C. The carrier gas was helium and flow rate was 30 mL /min.

3.4.3 Differential scanning calorimetry (DSC)

Thermal properties of polymer samples were measured on a Perkin Elmer DSC-7 instrument. The sample was equilibriated at 0°C and then heated to 150°C with a ramp rate of 10°C/min in the first cycle. The temperature was kept on hold for 1 min (isothermal condition) and then cooled from 150°C to 0°C with a ramp rate of 10°C /min in the second cycle. Isothermal condition was maintained for 1 min and finally the third cycle consisted of reheating the sample to 150°C with the same ramp rate. The second heating scan was used to calculate melting and crystallization temperatures of poly(ethylene)s. In case of poly(styrene)s, the samples were heated to 300^{o}C instead of 150^{o}C.

3.4.4 Thermogravimetric analysis (TGA)

Thermal properties of poly(norbornene)s were investigated by TGA studies using a Perkin Elmer TGA 7 instrument. The polymer sample was heated at a rate of 10^{o}C/min, from 50^{o}C to 500^{o}C under a nitrogen atmosphere.

3.4.5 Nuclear magnetic resonance spectroscopy (NMR) techniques

High Temperature ^{1}H and ^{13}C NMR spectra were recorded on a Bruker DRX 500 MHz NMR Spectrometer in TCB containing 3% (v/v) C_6D_6 at 130°C (unless otherwise mentioned). Typically 10 wt% (w/v) solutions of the polymers were used for high temperature measurements. The high temperature measurements were carried out on a dedicated 10 mm high temperature probe.

a) The measurement conditions for quantitative ^{13}C measurements of poly(ethylene) samples are as follows: using 45°, spectral width of 20.66 kHz, a relaxation delay of 10 s, an acquisition time of 0.81 s and number of acquisitions ~3200. Spectra are referenced to the highest field solvent resonance at 127.9 ppm. For high temperature ^{1}H NMR measurements, the conditions are as follows: spectral width = 5.0 kHz, relaxation delay = 2 s, acquisition time = 1.64 s and number of acquisitions ~100.

b) For end group analysis of poly(ethylene) samples, the conditions for ^{1}H NMR measurements are as follows: spectral width = 7.5 kHz, relaxation delay = 2 s, acquisition time = 2.2 s and number of acquisitions ~2000-4000, solvent = $C_2D_2Cl_4$, spectra are referenced to the solvent resonance at 6.0 ppm.

c) For poly(norbornene) samples, the conditions for qualitative ^{13}C measurements are : using 45°, spectral width of 20.66 kHz, a relaxation delay of 1.7 s, an acquisition time of 0.81 s and number of acquisitions ~6000.

d) For poly(styrene) samples, the conditions for qualitative ^{13}C measurements are : using 45°, spectral width of 22.5 kHz, a relaxation delay of 3.5 s, an acquisition time of 1.45 s and number of acquisitions ~6000-8000, solvent $C_2D_2Cl_4$, spectra are referenced to the solvent resonance at 75.06 ppm.

3.4.6 Infrared (IR) spectroscopy

Fourier transform infrared (FTIR) spectra (KBr pellets) were measured using Perkin Elmer PC-16 instrument.

3.4.7 Single crystal X-Ray crystallography

Single-crystal diffraction data were collected on a Bruker AXS Smart Apex CCD diffractometer at 297(2) K. The X-ray generator was operated at 50 kV and 30 mA using MoK_α radiation. Data were collected with ω scan width of 0.3° and with three different settings of φ (0°, 90°, 180° and 270°) keeping the sample-to-detector distance fixed at 6.145 cm and the detector position (2θ) fixed at -28°. The X-ray data collection was monitored by Bruker's SMART program (Bruker (1998). SMART. Version 5.0. Bruker AXS Inc., Madison, Wisconsin, USA). All the data were corrected for Lorentzian polarization and absorption effects using Bruker's SAINT and SADABS programs (Bruker *SMART* (V5.628), *SAINT* (V6.45a), Bruker AXS Inc. Madison.Wisconsin, USA, 2004). XPREP was used to determine the space group. SHELX-97 was used for structure solution and full matrix least-squares refinement on F^2 (Sheldrick, G. M. *SHELXS97, SHELXL97*: University of Göttingen, Germany. 1997). Molecular diagrams were

generated using XShell program embedded in SHELXTL. Geometrical calculations were done using SHELX-97. All the hydrogen atoms were treated as riding model and refined isotropically.

3.5 References

1. Armarego, W. L. F.; Perrin, D. D.; Heinemann, B. "*Purification of laboratory chemicals*", 4th Edition. **1996**.

CHAPTER 4

OLIGOMERIZATION AND POLYMERIZATION OF ETHYLENE USING NICKEL COMPLEXES OF BIS PHOSPHINE LIGANDS

4.1 Introduction

Nonmetallocene late transition metal single-site olefin polymerization catalysts have attracted significant attention[1]. The discovery of highly active nickel and palladium catalysts by Brookhart and coworkers is considered to be a water shed in the development of late transition metal polymerization catalyst systems[2]. More recently the focus of research has shifted to the exploration of novel metal-ligand frameworks[3].

Most of the late transition metal catalysts are based on hard oxygen and nitrogen donors. The ‘’softer’’ phosphorus ligand is relatively less known in the chemistry of olefin polymerization[4], although the coordination chemistry of these ligands has been widely reported[5]. Hydroformylation of alkenes, alternating copolymerization of alkenes and CO, cross-coupling reactions and allylic alkylation are some of the most important applications of transition metal complexes bearing phosphorus based ligands.

Rhodium catalyzed hydroformylation is one of the most prominent applications of homogeneous catalysis. High selectivities of terminal alkenes have been reported using both diphosphine and diphosphite based catalysts[6-9]. Rhodium catalysts containing diphosphine ligands exhibiting very high selectivity for straight chain aldehyde formation were reported by Devon et al[6c]. The bidentate ligand **1** gave excellent results in the hydroformylation of propylene at 125^{o}C and 18 bar pressure of synthesis gas (turn over frequency of 3000-4000 mol. mol catalyst^{-1} h^{-1}).

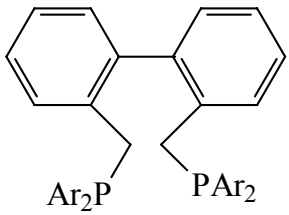

1a Ar= Ph
1b Ar= 3,5-diCF$_3$C$_6$H$_3$

Drent discovered cationic palladium complexes containing chelating bidentate diphosphine ligands which resulted in alternating copolymers of ethylene and CO with

100% selectivity, high molecular weights and activity up to several kolograms per gram metal per hour[10]. Suitable ligands are bis(diphenylphosphino)ethane (dppe), bis(diphenylphosphino)propane (dppp) and bis(diphenylphospino)butane (dppb). The nature of the bidentate ligand has a strong influence on the rate of the reaction and the molecular weight of the polymer. Increasing the bite angle, generally, increases the rate of the reaction, though for the three widest bite angles (bridge length n = 4, 5, 6), the rate decreases again. The observed trend in rates and bridge lengths have been confirmed in a series of ligands **2a-c**, with polymerization rates for C2, C3 and C4 bridges amounting to 0, 5100 and 46 300 g polymer.$mol^{-1}.h^{-1}$ [11].

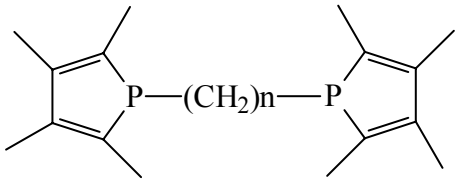

2a n= 1
2b n= 2
2c n= 3

Transition metal catalyzed carbon-carbon bond formation is a challenging area of research. Development of efficient catalysts has expanded the scope of this reaction[12]. One of the first examples of metal-mediated cross-coupling of two functionalized organic molecules is the Grignard cross-coupling. Hayashi et al showed, that dppf (diphenyl phosphino ferrocene), a diphosphine with a large P-Pd-P bite angle of 96^o in $(dppf)PdCl_2$ (**3**), induced the highest activity and selectivity of a range of diphosphine ligands (dppe, dppp, dppb and dppf)[13].

Strong σ donor capacity of phosphine ligands makes them more suitable for catalytic reactions requiring nucleophilic metal centers. Consequently, there is hardly any use of these ligands in olefin polymerization catalysis which involves an electrophilic metal center. Hence only very low ethylene polymerization activity has been observed[4].

A phosphine ligand of the type $R_2PCH_2PR_2$ (R= ^{t}Bu) in combination with $Ni(acac)_2$/MMAO gave an amorphous polyethylene with activity as low as 1.0 $gmmol^{-1}$

Ni^{-1} h^{-1} bar^{-1} (0.10 mmol Ni, P_{C2H4} = 6.9 bar, 18.5 h)[14b]. A diphosphinidine palladium complex which is sterically similar to α-diimine complexes exhibited an activity of 50-130 $gmmol^{-1}Pd^{-1}h^{-1}$ (P_{C2H4}= 5-30 bar)[14].

Synthesis of ligands containing P-N-P donors was reported in the early sixties[15]. Polydentate phosphine ligands with methylene spacers between the donor atoms are useful backbones for the construction of polynuclear transition metal complexes. Methylene group provides proper separation and flexibility between the donor atoms. The chemistry of phosphines of the type Ph_2PCH_2XH (X= O, NR) containing an active hydrogen has been examined with the aim of using this functionality to construct homo- and hetero-bimetallic complexes. Reaction of $[Mo(CO)_4(piperidine)_2]$ or $[Mo(CO)_4$ (norbornadiene)] with 2.0 equivalents of the phosphines Ph_2PCH_2NHR gave the complex *cis*-$[Mo(CO)_4(Ph_2PCH_2NHR)_2]$ (**4**). The reaction of the bisphosphines $(Ph_2PCH_2)_2NR$ with $[Mo(CO)_4(piperidine)_2]$ or $[Mo(CO)_4(norbornadiene)]$ was found to give complexes **5a** (R = t-Bu) and **5b** (R = C_6H_4Me-4).

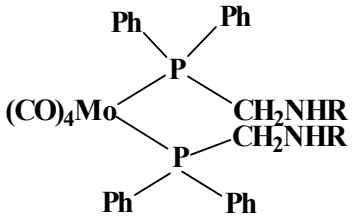

4 R=t-Bu

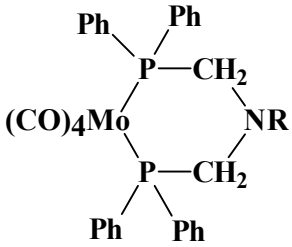

5a, R=tBu 5b, R=C_6H_4Me-4

The corresponding palladium (**6**) and platinum (**7**) complexes have been reported[16]. Such complexes have not been widely explored as polymerization catalysts barring a few patents[17].

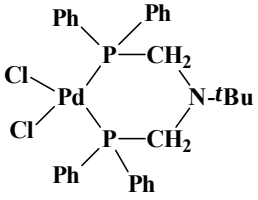

6

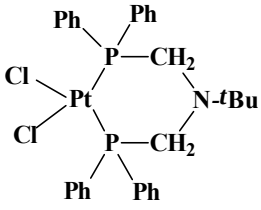

7

On the contrary, nickel (II) complexes of bulky bis(diarylphosphino)methyl amines (**8a-c**) $(PAr_2)_2NMe$ [Ar = 2-C_6H_4 (iPr), 2-C_6H_4 (Et), 2-C_6H_4 (Me)], exhibited an activity of 2200 $gmmol^{-1}$ Ni^{-1} h^{-1} bar^{-1} leading to high molecular weight poly(ethylene)s[18] and low levels of branching consistent with a chain walking mechanism[19].

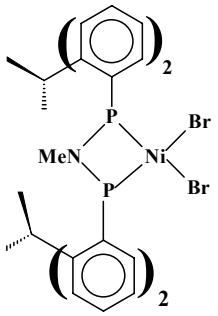

8a Ar= 2-C_6H_4(ipr), 8b Ar= 2C_6H_4(Et), 8c Ar= 2-C_6H_4(Me)

Chromium complexes with P-N-P type ligands of the formula $(PAr_2)_2NR$ (Ar = *o*-substituted phenyl group) have shown to be exceptionally active catalysts for the trimerization[20a] and tetramerization[20a] of ethylene and produce hexene-1 and octene-1. These catalysts also are useful for the cotrimerization of ethylene and styrenic monomers[20b].

It has been found that the substitution of ligand NMe backbone by a CH_2 unit as in nickel (II) complexes of bis(diarylphosphino)methane (dppm) (**9a-d**) significantly increases the activity of the catalyst for ethylene polymerization. A higher rate of β-hydride elimination results in a highly branched and low molecular weight polyethylene[21]. When the study was extended to five and six membered chelates formed by dppe (**10a-d**) and dppp (**11a-d**) respectively, no activity for ethylene polymerization was observed[21]. The larger bite angle and the correspondingly smaller space available for substrate binding in the latter two cases in comparison with a four-membered chelate (dppm), is likely responsible for the reduction in activity.

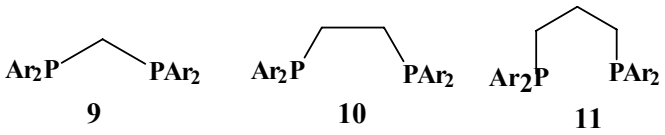

9 **10** **11**

a. Ar= Ph
b. Ar= 2-(Me)C_6H_4
c. Ar= 2-(iPr)C_6H_4
d. Ar= 2-(CF_3)C_6H_4

Olefin oligomerization as well as selective dimerization of ethylene to 1 and 2-butenes has been accomplished using Ni catalysts[22-23]. By varying the steric bulk of the ligand the product composition could be controlled from lower oligomers to polymers. Late transition metal based catalysts show a great propensity to undergo β-H elimination and hence are useful for the dimerization or oligomerization process[24].

The objective of the present investigation was to explore novel bisphosphine ligands which had a structural resemblance to both the bis(diarylphosphino) methyl amines and the bis(diarylphosphino)propane (dppm) ligands. With this in view, ligands with a C-N-C framework were identified which can complex with Ni(II) and form a six-membered chelate. Such complexes are expected to lead to a larger bite angle. This ligand framework will also enable the study of the influence of nitrogen on polymerization behavior.

The basic framework of the ligands chosen for the study is shown below:

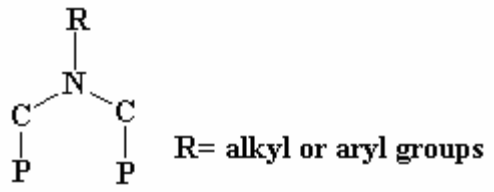

R= alkyl or aryl groups

4.2 Experimental Methods

Materials used and their methods of purification have been described in Chapter 3 under Section 3.2 and 3.3

4.2.1 Synthesis of ligands and complexes

4.2.1.1 Synthesis of the phosphonium Salt: $Ph_2P(CH_2OH)_2^+Cl^-$

Diphenyl phosphine (**12**) and the phosphonium salt **(13)** were synthesized according to literature procedure[5].

$$(C_6H_5)_3P + 2\,Li \xrightarrow[RT]{THF} (C_6H_5)_2PLi + C_6H_5Li \qquad \textbf{(eqn-1.1)}$$

$$(C_6H_5)_2PLi + H_2O \longrightarrow \underset{\textbf{12}}{(C_6H_5)_2PH} + LiOH \qquad \textbf{(eqn- 1.2)}$$

In a 500 mL round-bottom flask cooled under nitrogen, 200 mL of dry THF was added through a cannula. To this, triphenylphosphine (50 g, 0.191 mol) and Li metal (3 g, 0.43 mol) were added under N_2. The mixture was stirred for a few minutes when the whole solution turned deep red confirming the formation of Ph_2PLi. The flask was then fitted with a reflux condensor and the deep red solution was hydrolyzed under stirring with deoxygenated water to form the lithium diphenyl phosphide. This reaction was highly exothermic. After hydrolysis, a pale yellow clear solution resulted and LiOH precipitated partially. The THF layer containing the phosphine was decanted using a cannula into another round-bottom flask. THF was evaporated under vacuum to obtain a yellow colored oily liquid **12** which was further purified by vacuum distillation to a clear colorless oily liquid. ^{31}P NMR ($CDCl_3$): δ -41.8 ppm.

$$(C_6H_5)_2PH + 2\,HCHO + HCl \longrightarrow \underset{\textbf{13}}{\left[Ph_2P(CH_2OH)_2\right]^+Cl^-} \qquad \textbf{(eqn-1.3)}$$

Into a round-bottom flask 10 mL (10.7 g, 0.057 mol) diphenyl phosphine, 10 mL of HCHO (40 % aqueous solution, 0.13 moles) and 5 mL concentrated HCl (0.05 mol) were added and stirred for 1 h. An exothermic reaction was observed. Upon cooling the solution, a white crystalline solid was obtained. ^{31}P NMR ($CDCl_3$): δ +16.0 ppm.

4.2.1.2 Synthesis of *N*(diphenylphosphinomethyl) *tert*-butyl amine

The synthesis of *N*(diphenylphosphinomethyl)-*tert*-butyl amine is shown in **Scheme 4.1**.

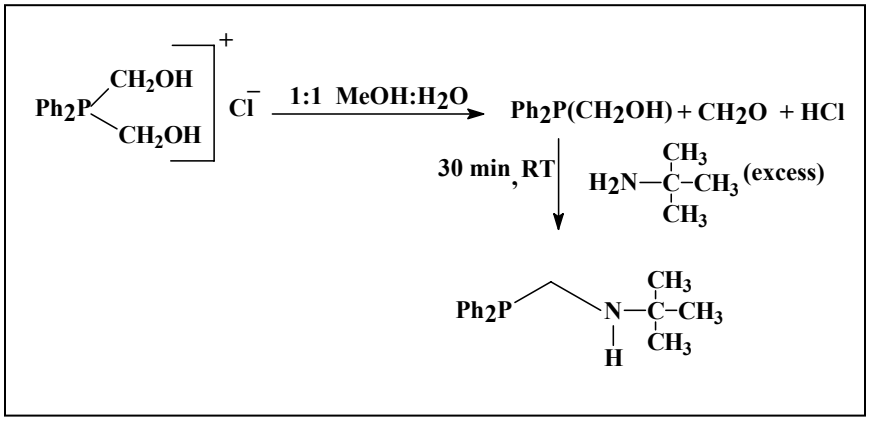

Scheme 4.1: Synthesis of (Ph_2PCH_2)NH(*tert*-butyl) (**14a**)

In a round bottom flask equipped with a magnetic stiring bar, 3.0 g (10.62 mmol, 1 eqv.) of phosphonium salt **(13)** was taken and methanol (30 mL, degassed) was added. To this solution was added, 7.8 mL (74.35 mmol, 7 eqv.) of *tert*-butylamine. The mixture was stirred for a period of 30 min. A 1:1 v/v mixture of dichloromethane and water was added and the organic layer separated and concentrated under reduced pressure. A creamish-white oil (**14a)** was isolated. ^{1}H NMR (C_6D_6, 200 MHz, 25^{o}C): δ 0.73 (s, $C(CH_3)_3$, 9H), 3.10 (dd, -CH_2, 2H), 6.91 (m, Ph, 6H), 7.40 (m, Ph, 4H) ppm. ^{13}C (DEPT) NMR (C6D6, 200 MHz, 25^{o}C): δ 28.14, 31.59, 42.44, 128.19, 132.53, 132.90 ppm. ^{31}P NMR (C_6D_6, 200 MHz, 25^{o}C): δ -15.46 ppm.

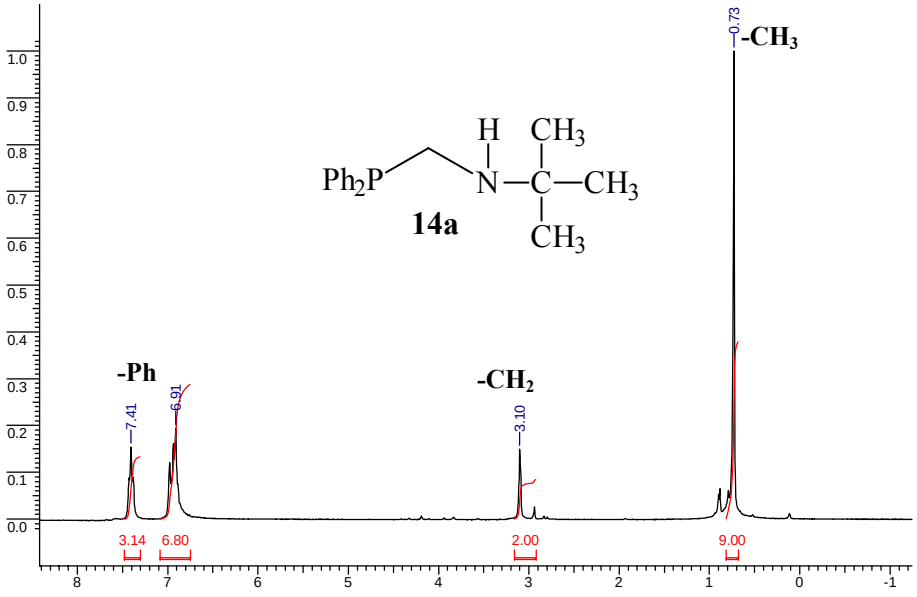

Figure 4.1: ^{1}H NMR spectrum (C_6D_6, 200 MHz, 25^{o}C) of **14a**

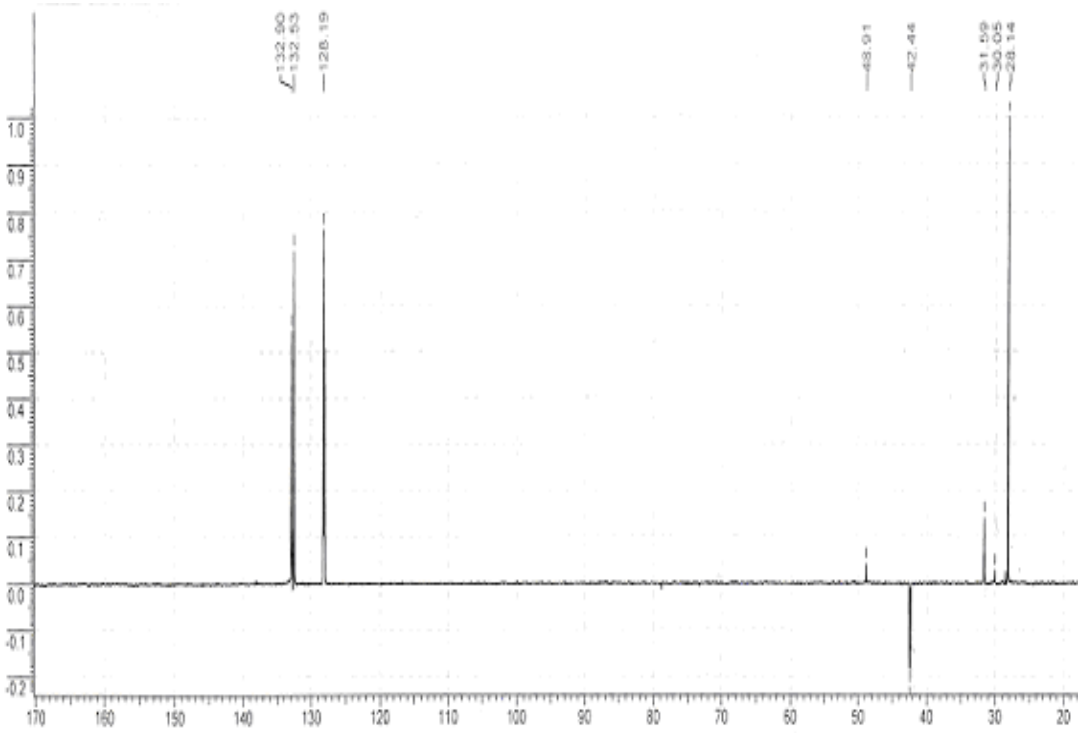

Figure 4.2: ^{13}C (DEPT) NMR spectrum (C_6D_6, 200 MHz, 25^{o}C) of **14a**

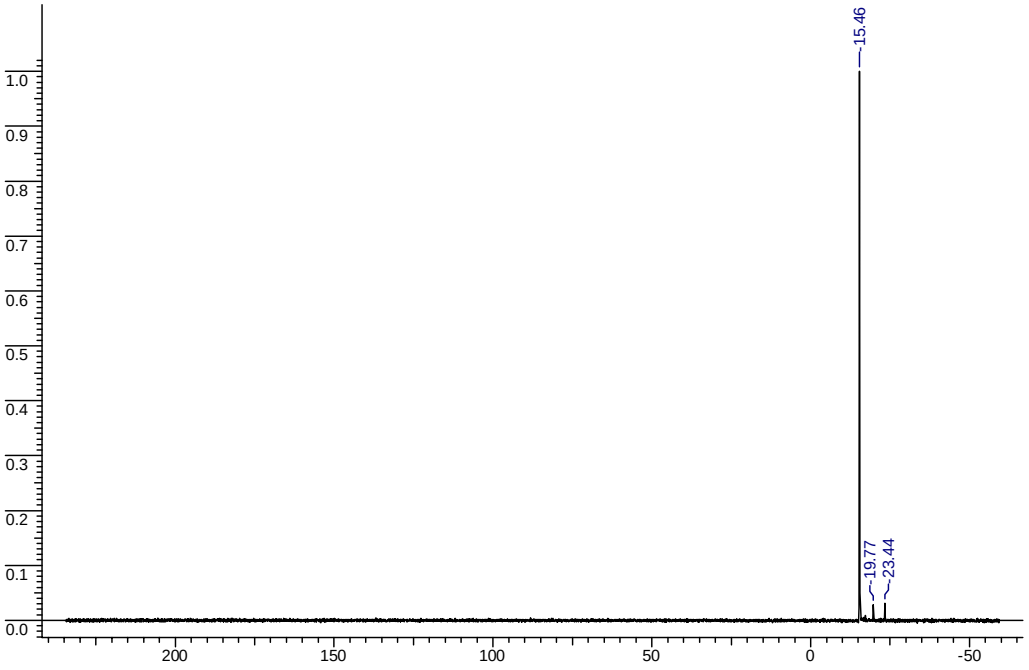

Figure 4.3: ^{31}P NMR spectrum (C_6D_6, 200 MHz, 25°C) of **14a**

4.2.1.3 Synthesis of bis-[*N*,*N*(diphenylphosphinomethyl)]-3,5-dimethyl aniline

The synthesis of bis-[*N*,*N*(diphenylphosphinomethyl)]-3,5-dimethyl aniline is shown in **Scheme 4.2**.

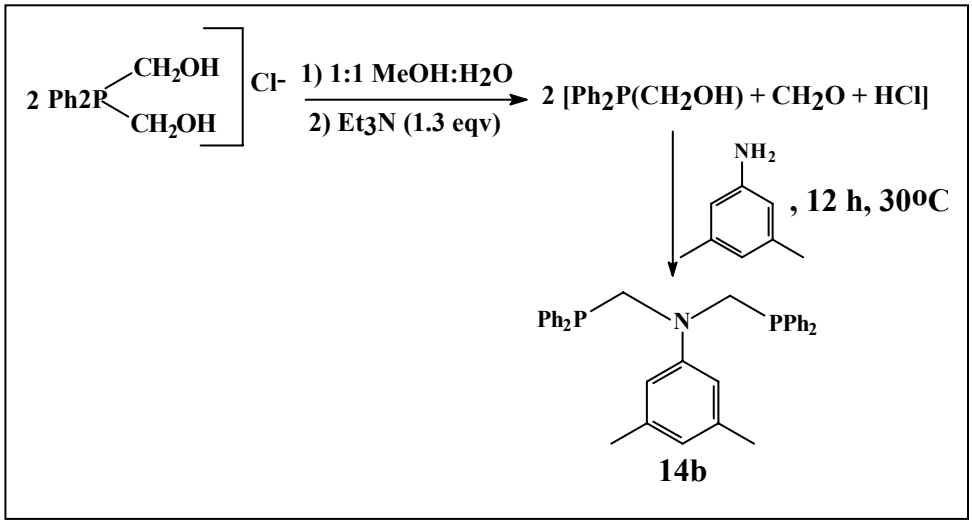

Scheme 4.2: Synthesis of $(Ph_2PCH_2)_2N$-3,5-$(Me)_2C_6H_4$ (**14b**)

In a round bottom flask equipped with a magnetic stirring bar, 5.0 g (17.7 mmol) of the phosphonium salt (**13**) was taken and dissolved in 30 mL of degassed methanol. To this was added 3.2 mL (23.01 mmol, 1.3 eqv.) of triethylamine and stirred for 15 min. This was followed by addition of 1.1 mL (8.85 mmol, 0.5 eqv.) of freshly distilled 3,5-dimethylaniline and the reaction mixture was stirred at 30°C for 12 h. Degassed dichloromethane and water (1:1 v/v) were added to the reaction mixture and the organic layer was extracted and concentrated to obtain a creamish-white oil which was re-dissolved in methanol at 60°C, cooled to room temperature and stored at –20°C for 3 days. A white solid precipitated out. $^{31}P\{^{1}H\}$ NMR (C_6D_6, 200 MHz, 25°C) spectrum of the white solid revealed a sharp peak at –25.7 ppm. Besides, there were 2 unidentified peaks of very small intensities at – 23.85 and – 18.65 ppm. ^{1}H NMR (C_6D_6 , 200 MHz, 25°C): δ 2.305 (s, 6 H, -CH_3), 3.109, 4.393 (s, 4 H, -CH_2), 6.56-7.59 ppm (aromatic-H, 23 H). $^{13}C\{^{1}H\}$ NMR (C_6D_6, 200 MHz, 25°C): δ 21.2, 54.36, 113.24, 119.85, 126.88, 127.36, 128.09, 128.15, 132.99, 133.18, 137.76, 138.10, 148.47, 149.54. An attempt to purify the ligand by column chromatography was not successful as it was oxidized to the corresponding phosphine oxide upon exposure to air and moisture.

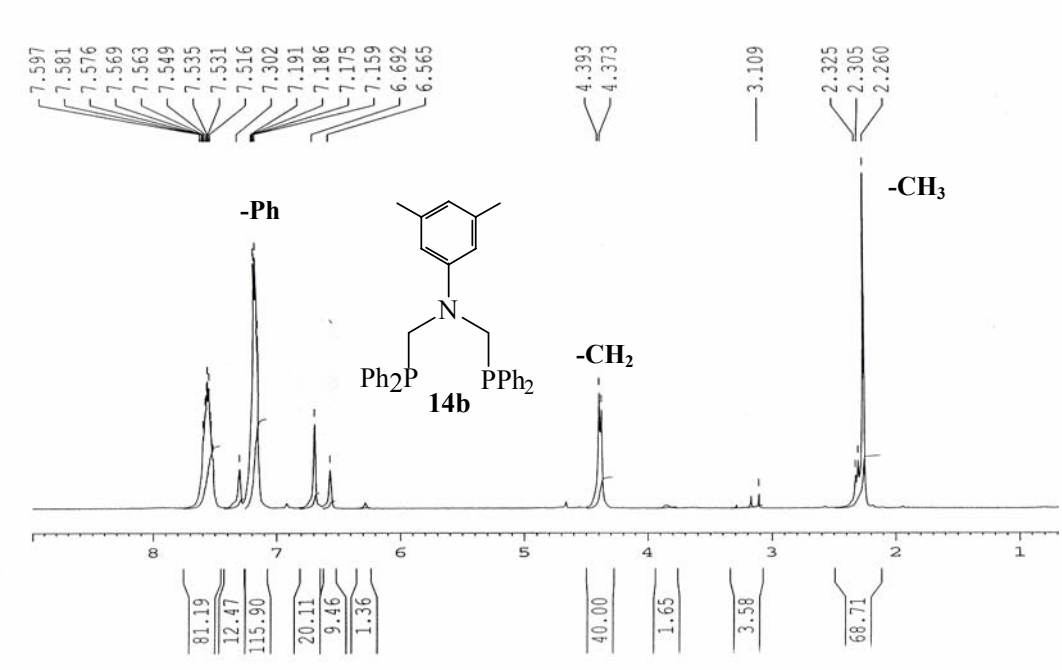

Figure 4.4: ^{1}H NMR spectrum (C_6D_6, 200 MHz, 25°C) of **14b**

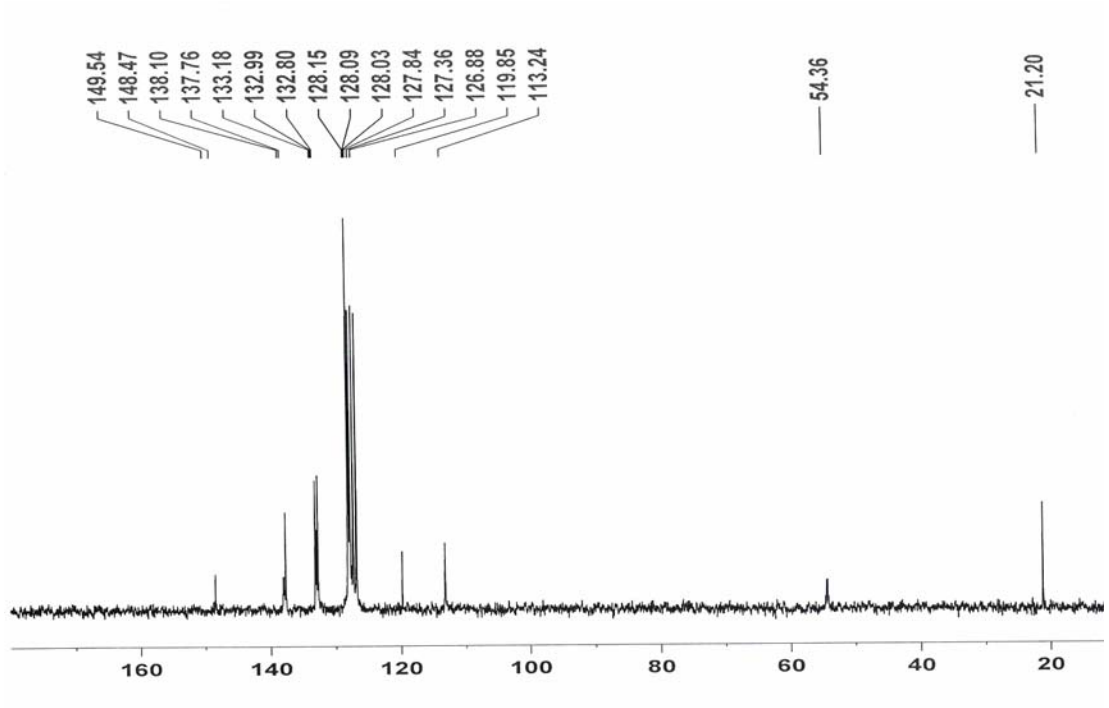

Figure 4.5: ^{13}C NMR spectrum (C_6D_6, 200 MHz, 25°C) of **14b**

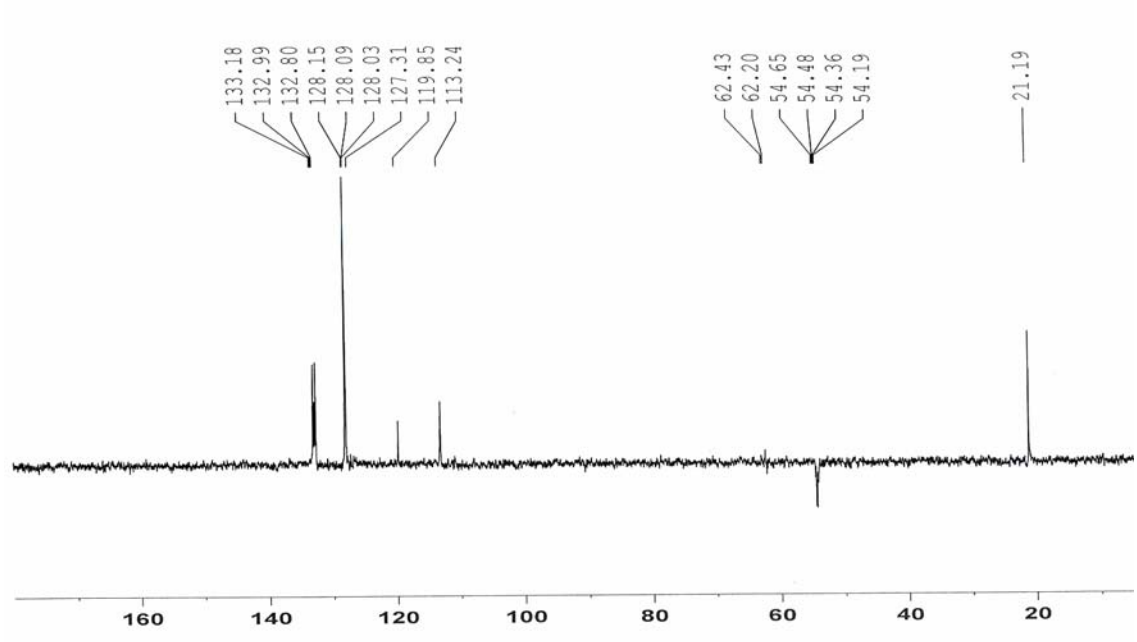

Figure 4.6: ^{13}C (DEPT) NMR spectrum (C_6D_6, 200 MHz, 25°C) of **14b**

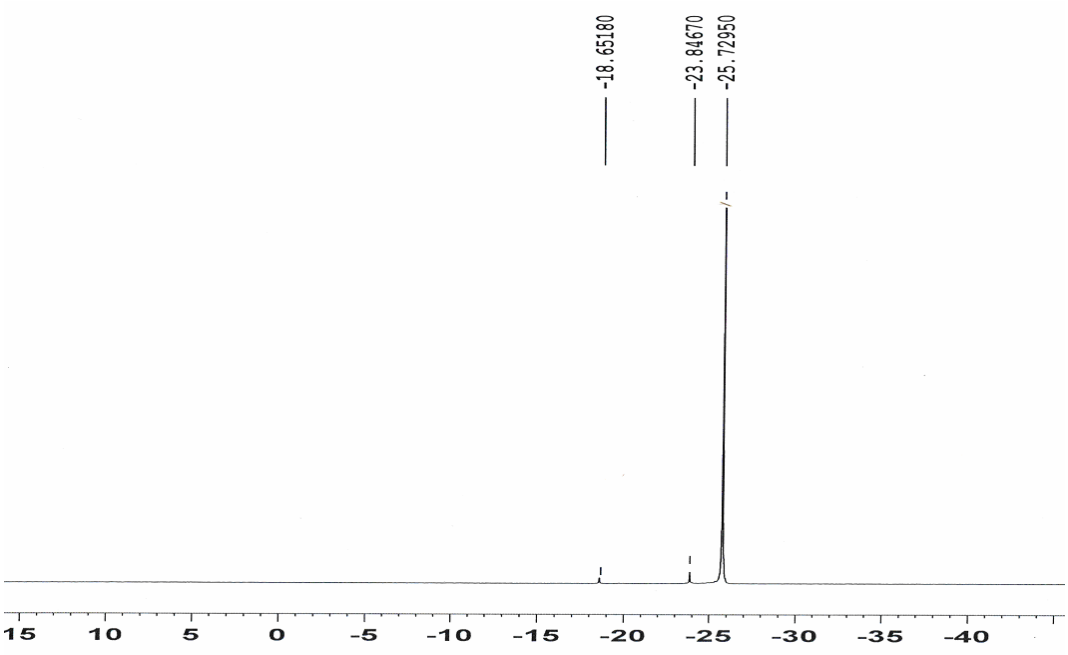

Figure 4.7: ^{31}P NMR spectrum (C_6D_6, 200 MHz, 25°C) of **14b**

4.2.1.4 Synthesis of bis-[*N*,*N*(diphenylphosphinomethyl)]-2,6-diisopropyl aniline

The synthesis of bis-[*N*,*N*(diphenylphosphinomethyl)]-2,6-diisopropyl aniline is shown in **Scheme 4.3**.

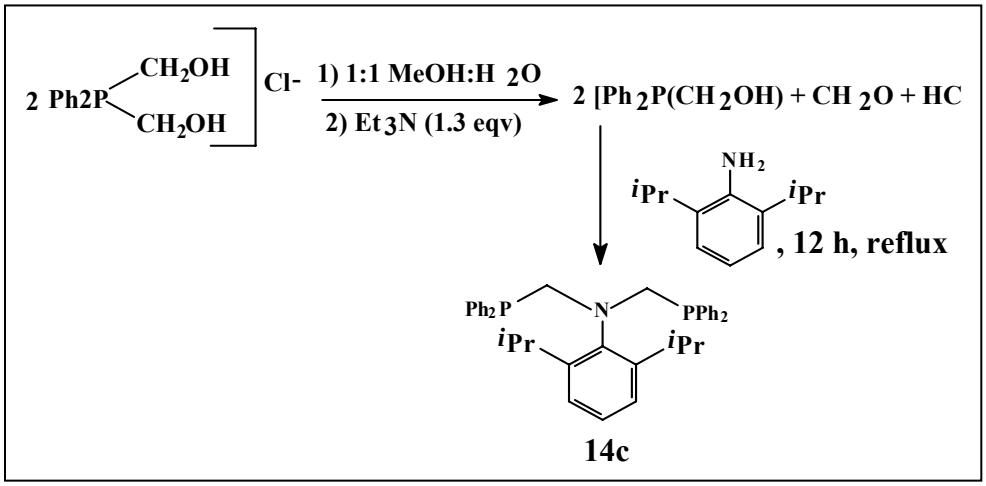

Scheme 4.3: Synthesis of $(Ph_2PCH_2)_2N$-2,6 $(^{i}Pr)_2C_6H_4$ (**14c**)

Into a round bottom flask equipped with a magnetic stirring bar, 5.0 g (17.7 mmol) of the phosphonium salt (**13**) was placed and dissolved in 30 mL of methanol. To this was added 3.2 mL (23.01 mmol, 1.3 eqv.) of triethylamine followed by 1.7 mL (8.85 mmol, 0.5 eqv.) of freshly distilled 2,6-diisopropylaniline.The reaction mixture was refluxed for 12 h. A mixture of dichloromethane and water (1:1 v/v) was added, the organic layer separated and concentrated in vacuo to obtain a creamish-white oil. The oil was re-dissolved in methanol at 60°C, cooled to room temperature and stored at –20°C for 3 days. A white solid precipitated out. The precipitate was decanted and dried under vacuo. ^{1}H NMR (C_6D_6, 200 MHz, 25°C): δ 1.24 (s, 12H, -CH(CH_3)$_2$), 3.22, 3.69 (m, 2H, -CH-), 4.60 (dd, 4H, -CH_2), 7.15, 7.22, 7.30, 7.57, 7.70 (m, 23H, aromatic H). ^{13}C NMR (C_6D_6, 200 MHz, 25°C): δ 24.20, 28.12, 59.46, 124.30, 126.87, 127.35, 127.99, 132.60, 132.98, 138.05, 138.36, 145.24, 147.63. ^{31}P{^{1}H} NMR (C_6D_6, 200 MHz, 25°C) revealed a sharp peak at –23.98 ppm. Besides, there were many unidentified peaks of very small intensities at – 15.70, -21.49, - 24.88 and – 27.27 ppm.

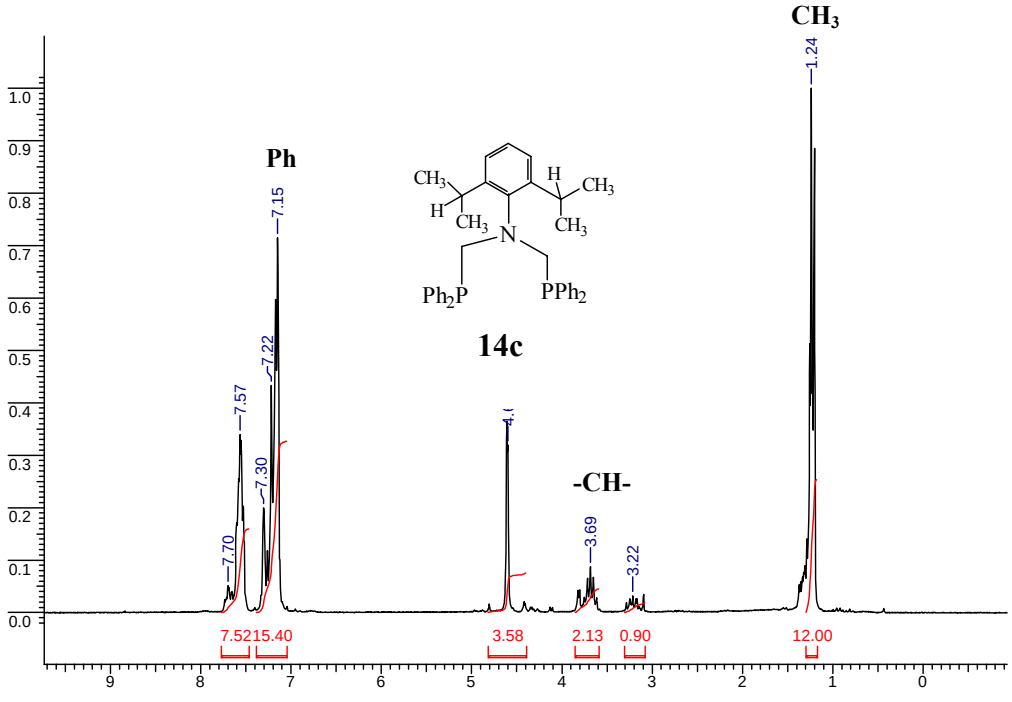

Figure 4.8: ^{1}H NMR spectrum (C_6D_6, 200 MHz, 25°C) of **14c**

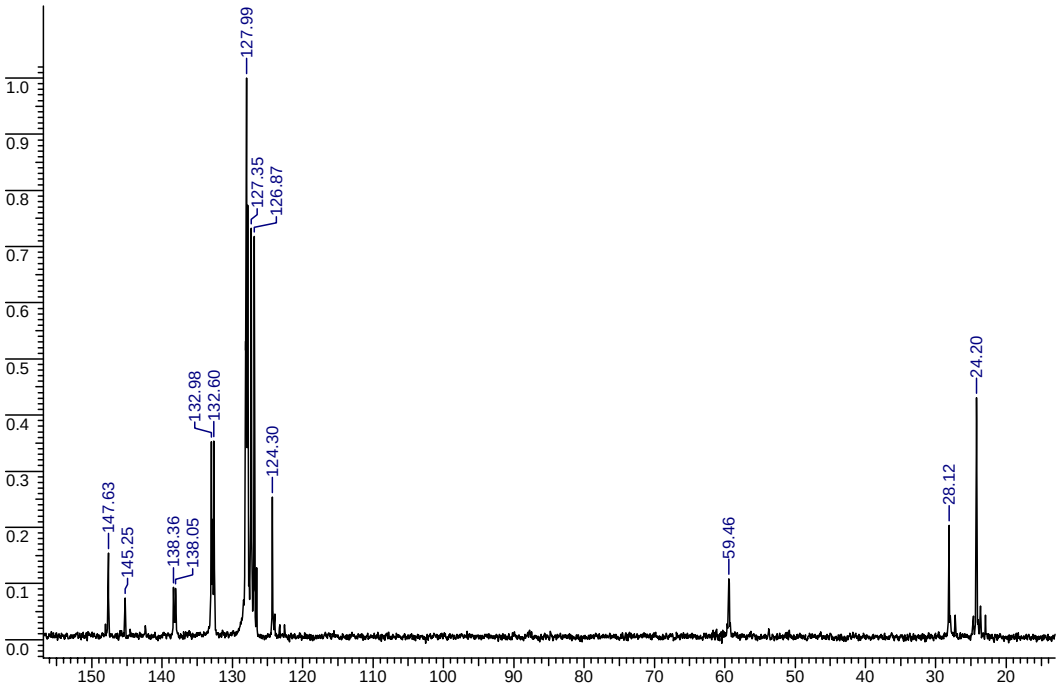

Figure 4.9: ^{13}CNMR spectrum (C_6D_6, 200 MHz, 25^{o}C) of **14c**

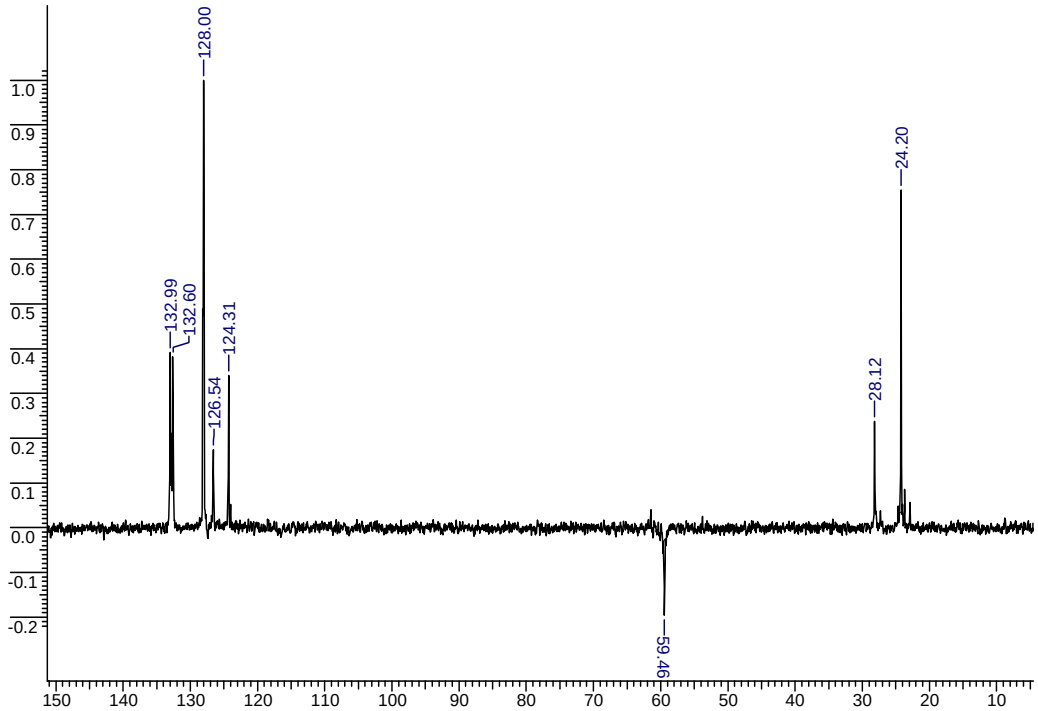

Figure 4.10: ^{13}C (DEPT) NMR spectrum (C_6D_6, 200 MHz, 25^{o}C) of **14c**

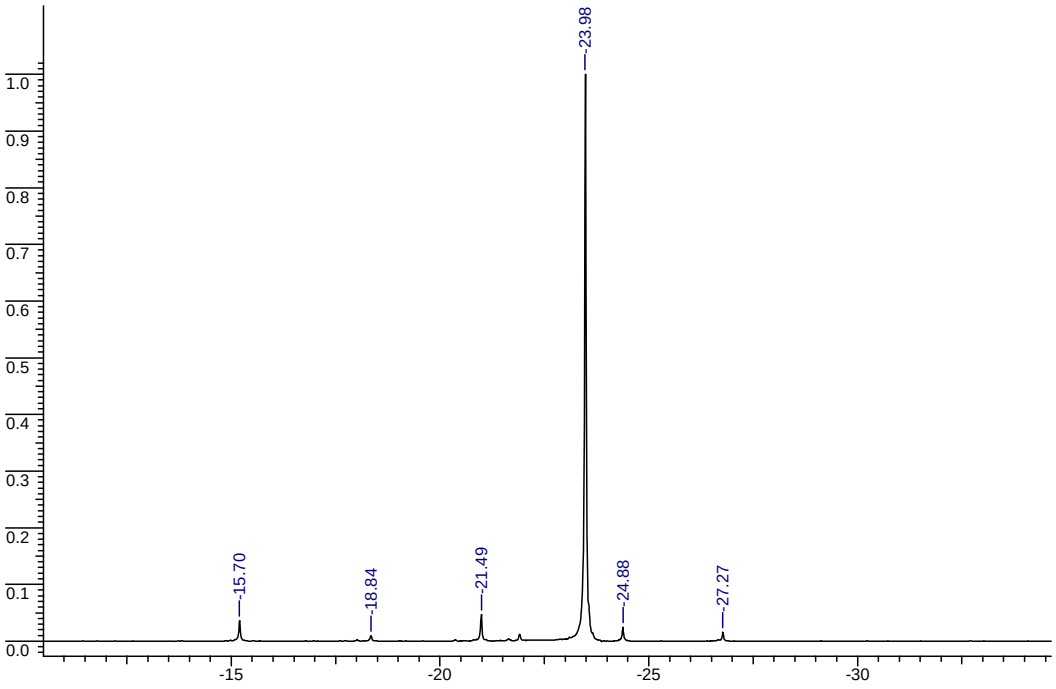

Figure 4.11: ^{31}P NMR spectrum (C_6D_6, 200 MHz, 25°C) of **14c**

4.2.1.5 Preparation of $NiCl_2$ complex of bis-[*N*,*N*(diphenylphosphinomethyl)]-*tert*-butyl amine: [$NiCl_2${$(Ph_2PCH_2)_2N$-^{t}Bu}] (15a)

The synthesis of [$NiCl_2${$(Ph_2PCH_2)_2N$-^{t}Bu}] is shown in **Scheme 4.4**.

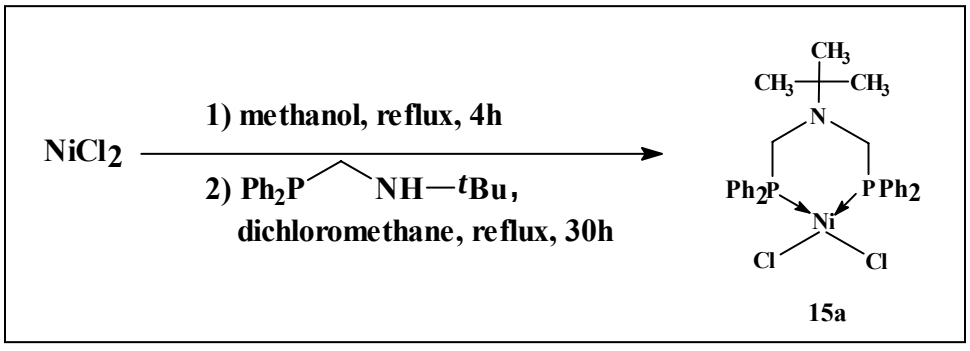

Scheme 4.4: Synthesis of [$NiCl_2${$(Ph_2PCH_2)_2N$-^{t}Bu}] **(15a)**

In a round bottom flask, 0.480 g (3.69 mmol) of $NiCl_2$ was taken and 25 mL of dry methanol was added to it. The reaction mixture was refluxed under nitrogen atmosphere for 4 h. A pale green solution was formed. The solution was cooled to room temperature. Ligand **14a** (1.0 g, 3.69 mmol) dissolved in a minimum volume of dichloromethane was added to the $NiCl_2$ solution in methanol. The mixture was refluxed under a nitrogen atmosphere for 30 h. A dark reddish brown colored solution was formed. This solution was filtered and added to a large volume of n-hexane (4 times its volume) resulting in the formation of an orange solid. This solid was redissolved in dichloromethane and reprecipitated from hexane. The procedure was repeated 2-3 times. Finally, the complex was recrystallised from dichloromethane. Needle shaped orange-red colored crystals of **15a** was obtained. (0.735 g, 58 % yield). Anal Calcd for $C_{30}H_{33}P_2NNiCl_2.CH_2Cl_2$: C, 54.4: H, 5.119; N, 2.047. Found: C, 54.5; H, 5.27; N, 2.30.

4.2.1.6 Preparation of $NiCl_2$ complex of bis-[*N*,*N*(diphenylphosphinomethyl)]-3,5-dimethyl aniline (15b)

The synthesis of $[NiCl_2\{(Ph_2PCH_2)_2N\text{-}3,5\text{-}(Me)_2C_6H_4\}]$ is shown in **Scheme 4.5**.

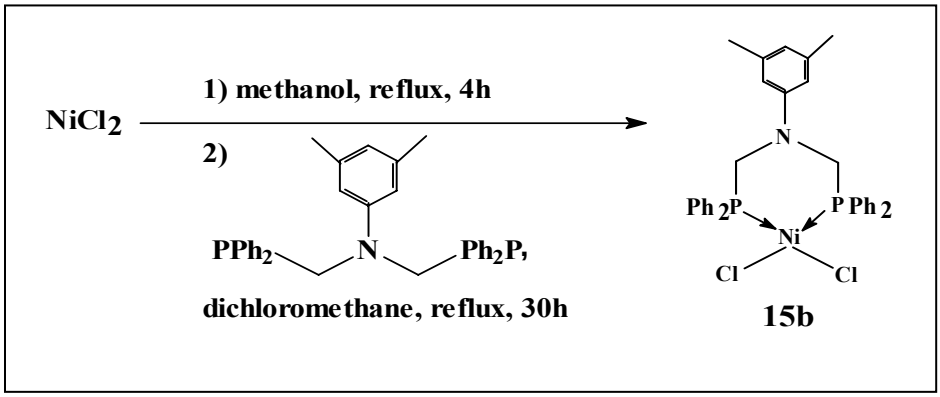

Scheme 4.5: Synthesis of $[NiCl_2\{(Ph_2PCH_2)_2N\text{-}3,5\text{-}(Me)_2C_6H_4\}]$ (**15b**)

In a round bottom flask, 0.176 g (1.35 mmol) of $NiCl_2$ was taken and 25 mL of dry methanol was added to it. The reaction mixture was refluxed under nitrogen atmosphere

for 4 h. A pale green solution was formed. The solution was cooled to room temperature. Ligand **14b** (0.70 g, 1.35 mmol) dissolved in a minimum volume of dichloromethane was added to the $NiCl_2$ solution in methanol. The mixture was refluxed under a nitrogen atmosphere for 30 h. A dark reddish brown colored solution was formed. This solution was filtered and added to a large volume of n-hexane (4 times its volume) resulting in the formation of an orange solid. This solid was redissolved in dichloromethane and reprecipitated from hexane. The procedure was repeated 2-3 times. Finally, the complex was recrystallised from dichloromethane. Needle shaped orange-red colored crystals of **15b** was obtained. (0.45 g, 45 % yield). Anal Calcd for $C_{34}H_{33}P_2NNiCl_2.CH_2Cl_2$: C, 57.38; H, 4.78; N, 1.91. Found: C, 57.66; H, 4.91; N, 2.00.

4.2.1.7 Preparation of $NiCl_2$ complex of bis-[*N*,*N*(diphenylphosphinomethyl)]-2,6-diisopropyl aniline (15c)

The synthesis of $[NiCl_2\{(Ph_2PCH_2)_2N\text{-}2,6\text{-}(^iPr)_2C_6H_4\}]$ is shown in **Scheme 4.6**.

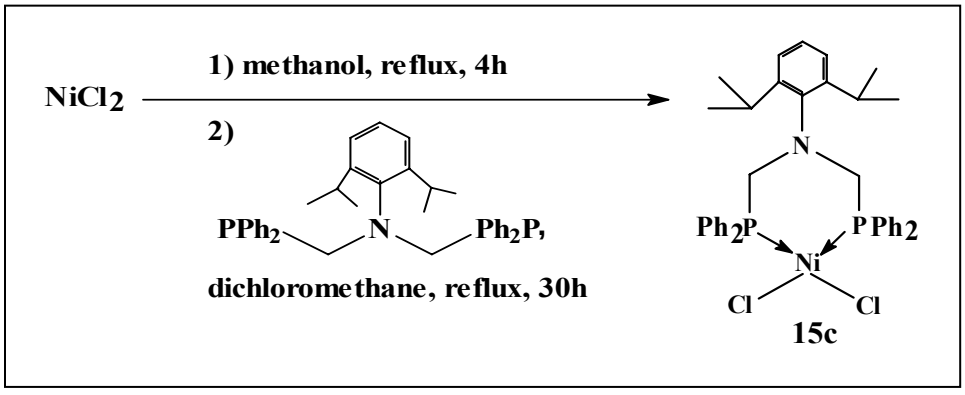

Scheme 4.6: Synthesis of $[NiCl_2\{(Ph_2PCH_2)_2N\text{-}2,6\text{-}(^iPr)_2C_6H_4\}]$ (**15c**)

In a round bottom flask, 0.355 g (2.736 mmol) of $NiCl_2$ was taken and 25 mL of dry methanol was added to it. The reaction mixture was refluxed under nitrogen atmosphere for 4 h. A pale green solution was formed. The solution was cooled to room temperature. Ligand **14c** (1.568 g, 2.736 mmol) dissolved in a minimum volume of dichloromethane was added to the $NiCl_2$ solution in methanol. The mixture was refluxed under a nitrogen atmosphere for 30 h. A dark reddish brown colored solution was formed. This solution

was filtered and added to a large volume of n-hexane (4 times its volume) resulting in the formation of an orange solid. This solid was redissolved in dichloromethane and reprecipitated from hexane. The procedure was repeated 2-3 times. Finally, the complex was recrystallised from dichloromethane. Needle shaped orange-red colored crystals **15c** was obtained. (0.75 g, 39 % yield). Anal Calcd for $C_{38}H_{41}P_2NNiCl_2$: C, 64.87; H, 5.83; N, 1.99. Found: C, 64.32; H, 5.95; N, 2.27.

4.2.1.8 Preparation of $NiBr_2$ complex of bis-[*N*,*N*(diphenylphosphinomethyl)]-*tert*-butyl amine: [$NiBr_2${$(Ph_2PCH_2)_2N$-^{t}Bu}] (16a)

The synthesis of [$NiBr_2${$(Ph_2PCH_2)_2N$-^{t}Bu}] is given in **Scheme 4.7**.

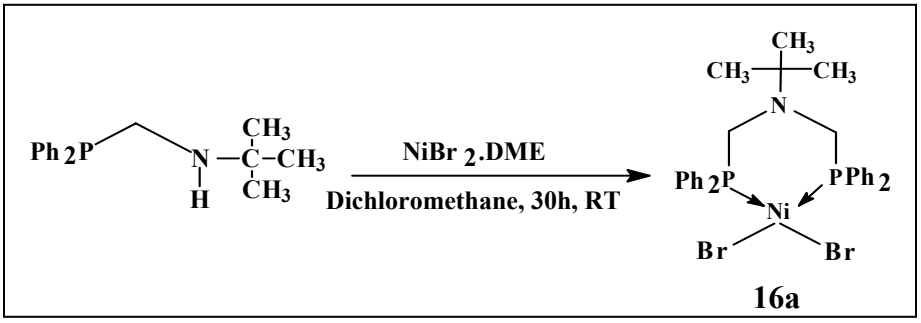

Scheme 4.7: Synthesis of [$NiBr_2${$(Ph_2PCH_2)_2N$-^{t}Bu}] (**16a**)

In a round bottom flask 1.0 g (3.69 mmol) of N-(diphenylphosphinomethyl)tert-butylamine (**14a**) was placed and dissolved in dry dichloromethane. $NiBr_2$.DME (1.139 g, 3.69 mmol) was added to this solution. Immediate appearance of dark reddish-brown color was noticed. The reaction mixture was stirred at room temperature for 30 h. This solution was filtered and added to a large volume of n-hexane (4 times its volume). The resulting red- brown solid was redissolved in dichloromethane and reprecipitated from n-hexane. This procedure was repeated 2-3 times. Finally, the complex was recrystallised from dichloromethane. Needle shaped reddish brown colored crystals of **16a** was obtained. (0.85 g, 60% yield). Anal Calcd for $C_{30}H_{33}P_2NNiBr_2.CH_2Cl_2$: C, 48.14; H, 4.53; N, 1.81. Found: C, 48.25; H, 4.31; N, 1.94

4.2.1.9 Preparation of $NiBr_2$ complex of bis-[*N*,*N*(diphenylphosphinomethyl)]-3,5-dimethyl aniline: [$NiBr_2${$(Ph_2PCH_2)_2$N-Ar}] (Ar= 3,5-dimethyl phenyl, (16b)

The synthesis of is [$NiBr_2${$(Ph_2PCH_2)_2$N-3,5-$(Me)_2C_6H_4$}] given in **Scheme 4.8**.

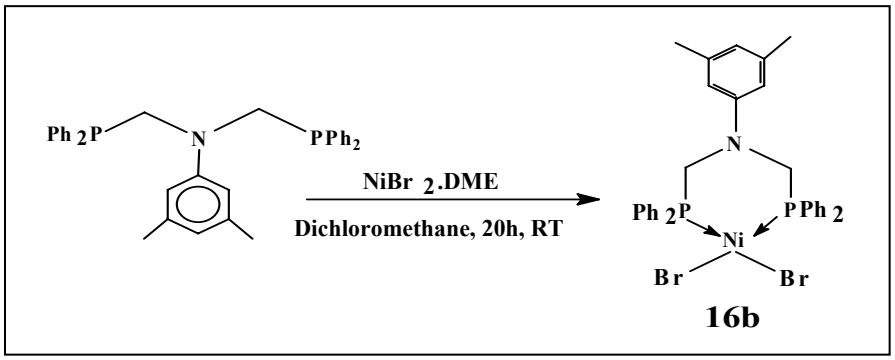

Scheme 4.8: Synthesis of [$NiBr_2${$(Ph_2PCH_2)_2$N-3,5-$(Me)_2C_6H_4$}] (**16b**)

In a round bottom flask 1.0996 g (2.127 mmol) of bis-[N,N(diphenylphosphinomethyl)]3,5-dimethyl aniline (**14b**) was placed and dissolved in dry dichloromethane. $NiBr_2$.DME (0.656 g, 2.127 mmol) was added to this solution. Immediate appearance of dark reddish-brown color was noticed. The reaction mixture was stirred at room temperature for 20 h. This solution was filtered and added to a large volume of n-hexane (4 times its volume). The resulting red- brown solid was redissolved in dichloromethane and reprecipitated from n-hexane. This procedure was repeated 2-3 times. Finally, the complex was dried under vacuum

and a pure reddish brown solid (**16b**) was isolated. (1.12 g, 64% yield). Anal Calcd for $C_{34}H_{33}P_2NNiBr_2.CH_2Cl_2$: C, 51.17; H, 4.26; N, 1.70. Found: C, 51.50; H, 4.23; N, 2.07.

4.2.1.10 Preparation of $NiBr_2$ complex of bis-[*N*,*N*(diphenylphosphinomethyl)]-2,6-diisopropyl aniline: [$NiBr_2${$(Ph_2PCH_2)_2$N-Ar}] (Ar= 2,6-diisopropyl phenyl, (16c)

The synthesis of [$NiBr_2${$(Ph_2PCH_2)_2$N-2,6-(^{i}Pr)$_2C_6H_4$}] is given in **Scheme 4.9**.

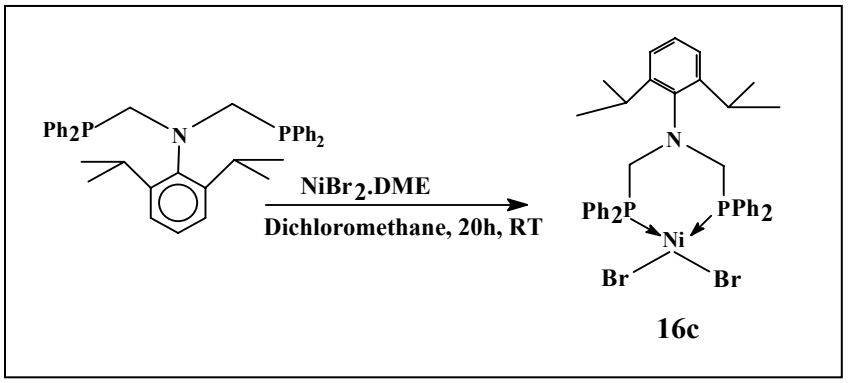

Scheme 4.9: Synthesis of [$NiBr_2${$(Ph_2PCH_2)_2$N-2,6-(^{i}Pr)$_2C_6H_4$}] (**16c**)

In a round bottom flask 1.266 g (2.21 mmol) of bis-[N,N(diphenylphosphinomethyl)]2,6-diisopropyl aniline (**14c**) was placed and dissolved in dry dichloromethane. $NiBr_2$.DME (0.687 g, 2.21 mmol) was added to this solution. Immediate appearance of dark reddish-brown color was noticed. The reaction mixture was stirred at room temperature for 20 h. This solution was filtered and added to a large volume of n-hexane (4 times its volume). The resulting red- brown solid was redissolved in dichloromethane and reprecipitated from n-hexane. This procedure was repeated 2-3 times. Finally, the complex was dried under vacuum and a pure reddish brown solid (**16c**) was isolated. (1.225g, 70% yield). Anal Calcd for $C_{38}H_{41}P_2NNiBr_2$: C, 57.59; H, 5.18; N, 1.77. Found: C, 56.95; H, 5.91; N, 1.87.

4.2.2 Polymerization

4.2.2.1 Oligomerization of ethylene using nickel complexes at 1.013 bar

A three-neck jacketed glass reactor equipped with a magnetic stirrer was baked overnight in an oven at 180°C. The reactor was cooled to room temperature by flushing with nitrogen. It was then connected to an ethylene supply system (**Figure 4.12**). The ethylene

set up consisted of an ethylene source, the glass reactor and a 100 c.m long graduated burette (containing paraffin oil) as the reservoir for ethylene gas. The whole system was flushed with ethylene and the burette volume above the level of paraffin oil was filled with ethylene gas. Dry toluene (30 mL) was added to the reactor followed by the required quantity of MAO. The temperature was maintained at 28°C using a thermostat for circulating water through the jacket. The solution was stirred for 5 min. Polymerization was initiated by the addition of 3 mL of catalyst solution **15** (**a-c**) and **16** (**a-c**) in ortho-dichlorobenzene. Thereafter, the ethylene source was cut off from the rest of the system. Ethylene from the gas burette was consumed due to the onset of polymerization. Ethylene uptake was noted as a function of time by the rise in oil level in the graduated burette. After the desired time interval, the connection of the burette to the reactor was cut off and the reactor cooled to -20°C. An aliquot of the reaction mixture was taken out with the help of a gas-tight syringe and stored over a thin bed of neutral alumina in a sure-seal glass vial at -20°C. Aluminum alkyl was adsorbed on the neutral alumina bed and the supernatant liquid was used directly for GC analysis. In the case of complexes **15b** and **16b**, the activity was extremely high and within a period of 90 minutes, ethylene contained in whole of the burette length (100 cm = 2748 mL of C_2H_4 at 28°C) was consumed. Hence, the experimental runs were restricted to 90 minutes.

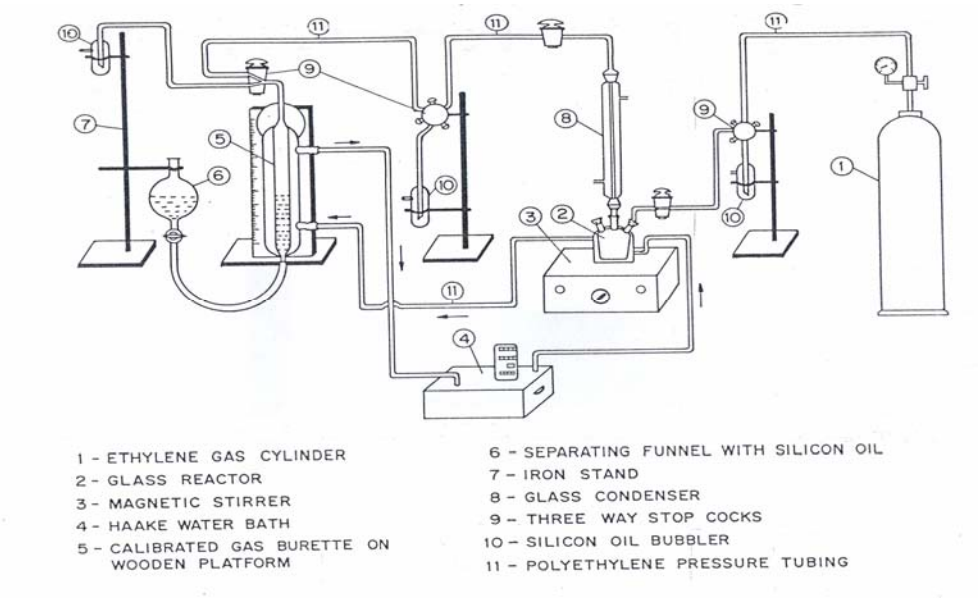

Figure 4.12: Apparatus for ethylene polymerization at one atmosphere pressure

4.2.2.2 Polymerization of ethylene using nickel complexes at 5 bar

Polymerization at 5 bar pressure was carried out in a Buchi AG miniclave (**Figure 4.13**). The reactor, equipped with a magnetic stirring bar was heated at 180°C overnight and then cooled to room temperature by flushing with nitrogen. The cooled miniclave was taken inside the glove box. Required amount of catalyst was transferred into the reactor inside the glove box. The miniclave was taken out and flushed with ethylene for a few minutes. Toluene (30 mL) was added using a syringe and the catalyst slurry in toluene was stirred for 10 minutes. The reaction temperature was maintained at 60°C by keeping the reactor over an oil bath maintained at 60^{o}C. Polymerization was initiated by adding MAO using a syringe. The reactor was pressurized to 5 bar of ethylene and a continuous flow of ethylene was maintained through out the run. The reaction was quenched after the desired time interval by venting out the volatiles and adding 200 mL of a mixture of methanol and HCl (10% by volume). Finally 100 mL of acetone was added to precipitate the polymer. The polymer was then filtered, washed with methanol and acetone and dried in vacuo at 60°C for 10 h.

Figure 4.13: Buchi miniclave

4.2.3 Analytical and characterization

The Ni (II) complexes and the poly(ethylene)s obtained were characterized by GPC, GC, DSC, NMR and X-Ray crystallography. The procedures have been described in Chapter 3, sections 3.4.1, 3.4.2, 3.4.3, 3.4.5 and 3.4.7, respectively.

Full crystallographic data of complexes **15** (**a-c**) and **16a** are given in Appendix 1.

4.3 Results and discussions

4.3.1 Structure of the complexes

The Ni(1)-Cl(1) bond distance in **15a** is 2.2098 Å where as the Ni(1)-Br(1) bond distance in **16a** is 2.3333 Å . The bite angles P(1)-Ni(1)-Pl(1) in **15a** and P(1)-Ni(1)-P(1) in **16a** are similar (≈ 96^{o}). The closer the value of bite angle to 90°, stabler is the complex[25]. If the two phosphorus atoms, the nickel atom and the two chlorine atoms in **15a** are considered to lie on one plane, the metal being at the center of the square plane, the four phenyl rings attached to the two P atoms block the axial sites of the coordination plane to a large extent (**Fig. 4.14**). The ^{t}Bu substituent on the nitrogen is oriented in such a manner that it is capable of blocking the access of the monomer unit to the metal center. The angle between the two phenyl rings C(11)-P(1)-C(5) is 108.24^{o} in **16a** whereas in **15a** the angle is 108.45^{o}. If we take into consideration the same square planar arrangement around the nickel center in **16a**, it is seen from the molecular structure that the ^{t}Bu substituent on the nitrogen atom does not block the lower half of the coordination plane as much as in **15a** though it blocks the upper half to some extent (**Fig. 4.15**). So by changing the halogen atom from chlorine to bromine, the steric environment appears to change substantially.

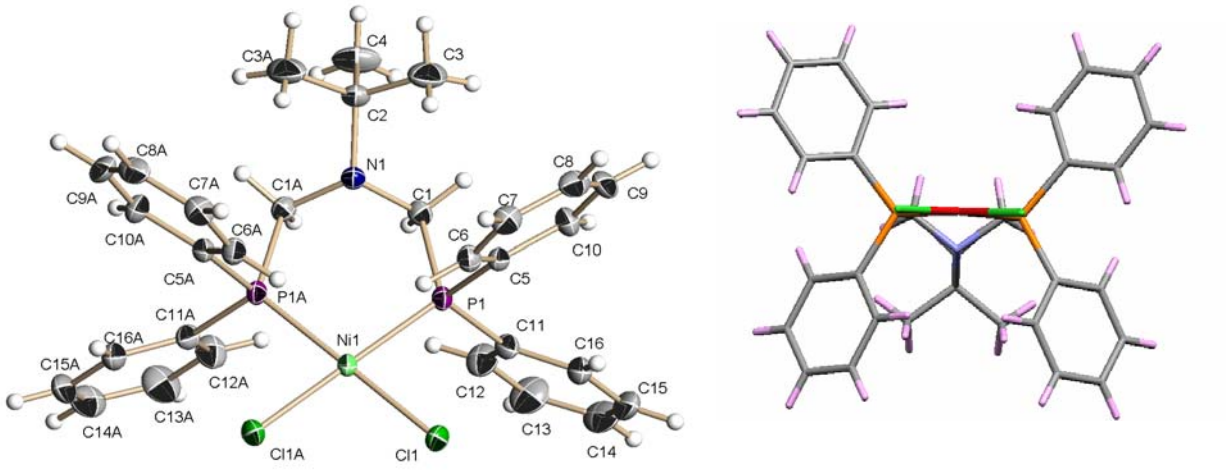

Figure 4.14: Molecular structure and numbering scheme for $[NiCl_2\{(Ph_2PCH_2)_2N\text{-}^tBu\}]$ (**15a**)

Table 4.1: Selected bond distances (Å) and angles (deg) in **15a**

Ni(1)-Cl(1)#1	2.2098(9)
Ni(1)-Cl(1)	2.2099(9)
Ni(1)-P(1)	2.1716(9)
P(1)#1-Ni(1)-Cl(1)	177.38(4)
P(1)-Ni(1)-Cl(1)	85.45(4)
Cl(1)#1-Ni(1)-P(1)-C(11)	114.5(9)
Cl(1)-Ni(1)-P(1)-C(11)	58.63(13)
P(1)#1-Ni(1)-P(1)	95.94(5)

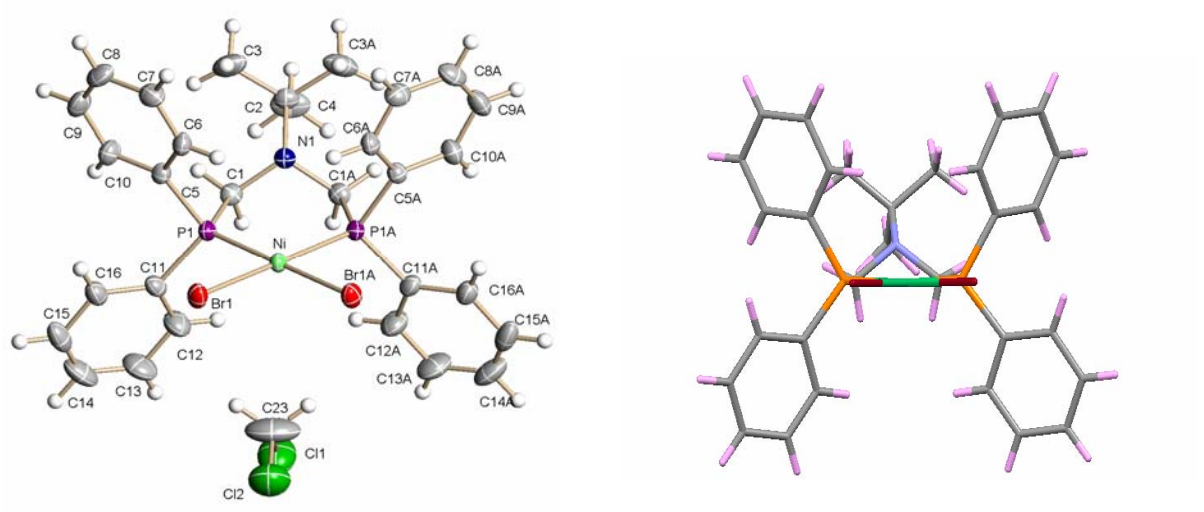

Figure 4.15: Molecular structure and numbering scheme for $[NiBr_2\{(Ph_2PCH_2)_2N\text{-}^tBu\}]$ **16a**

Table 4.2: Selected bond distances (Å) and angles (deg) in **16a**

Br(1)-Ni	2.3333(7)
Ni-P(1)	2.1678(11)
P(1)-Ni-Br(1)	86.00(4)
Br(1)#1-Ni-P(1)-C(11)	104.3(8)
Br(1)-Ni-P(1)-C(11)	58.81(16)
P(1)-Ni-P(1)#1	96.01(6)

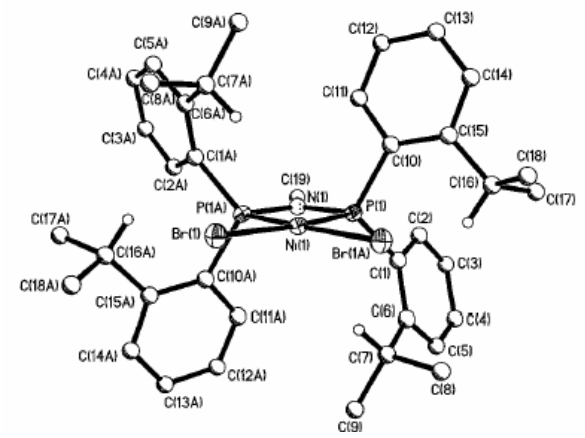

Figure 4.16: Molecular structure and numbering scheme for **8a**. Important molecular dimensions: bond lengths (Å): Ni(1)-P(1) 2.1611(6), Ni(1)-Br(1) 2.3276(4); bond angles (deg) P(1)-Ni(1)-P(1a) 74.07(3), P(1)-N(1)-P(1a) 92.49(7).

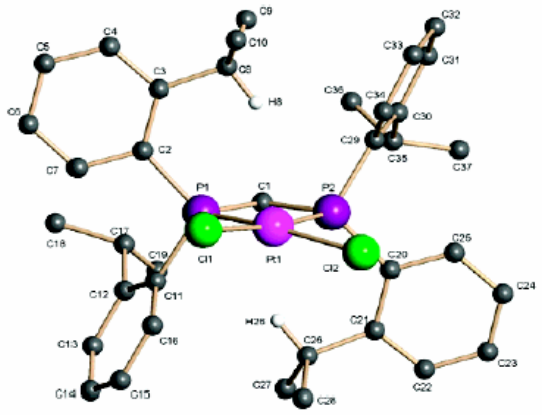

Figure 4.17: Molecular structure and numbering scheme for **17** $[PtCl_2\{CH_2(PAr_2)_2\}]$ (Ar = 2-(iPr)C_6H_4).
Important molecular dimensions include the following bond lengths (Å), bond angles (deg): Pt(1)-P(1)) 2.2301(9), Pt(1)-P(2)) 2.2202(9), Pt(1)-Cl(1)) 2.3627(9), Pt(1)-Cl(2))2.3465(9); P(1)-Pt(1)-P(2)) 75.96(3), Cl(1)-Pt(1)-Cl(2) 91.99(3).

The principle difference between the complexes **15-16** (**a-c**) and **8a**[18] and **17**[21] is the "bite angle" (<P-M-P), which plays an important role in phosphine based systems. The latter two systems have much smaller bite angles (74.07^o and 75.96^o respectively) than **15-16** (**a-c**) (close to 90^o). Electronic changes in the metal-ligand interaction that follow from the change in bite angle may also be important for catalyst reactivity.

Moving along the series, it is seen that though the 3,5-dimethyl phenyl ring is bulkier than the corresponding *tert*-butyl substituent, the orientation of the meta- substituted phenyl ring is such that, the metal center in **15b** is much more accessible for the monomer unit from both sides of the coordination plane. The bite angle (P(1)#-Ni(1)-Pl(1)) is 89.72^{o} in **15b** (**Fig. 4.18**).

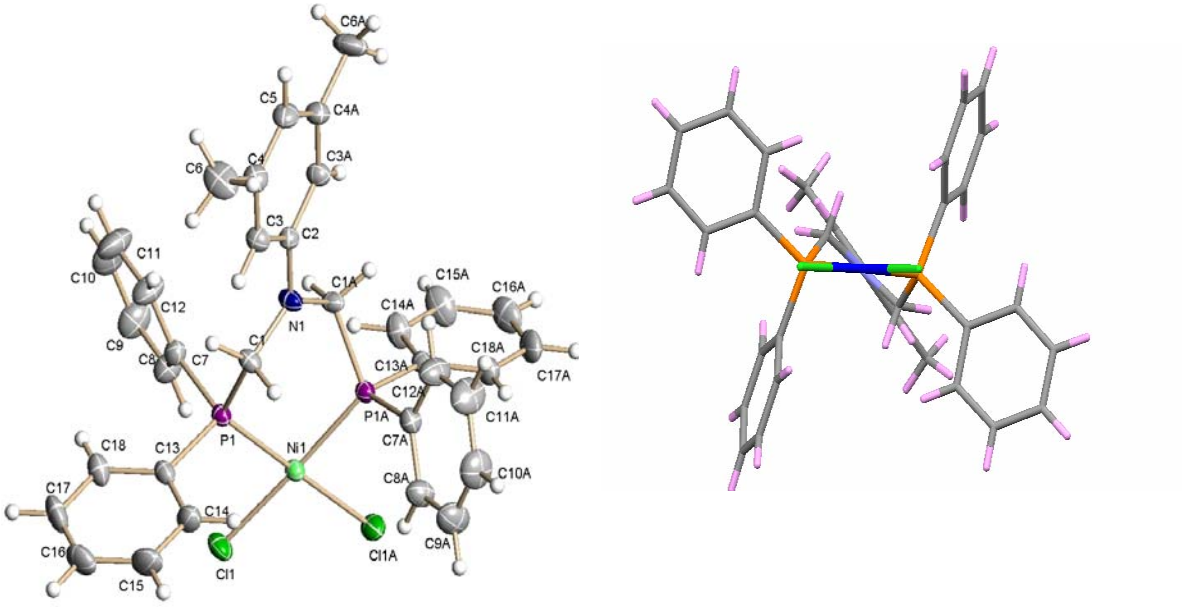

Figure 4.18: Molecular structure and numbering scheme for [$NiCl_2${$(Ph_2PCH_2)_2$N-3,5-$(Me)_2C_6H_4$}] **15b**

Table 4.3: Selected bond distances (Å) and angles (deg) in **15b**

Ni(1)-P(1)#1	2.1523(9)	
Ni(1)-P(1)	2.1523(9)	
Ni(1)-Cl(1)#1	2.1967(9)	
Ni(1)-Cl(1)	2.1967(9) 1)-Ni(1)-Cl(1)	88.67(4)
Cl(1)#1-Ni(1)-P(1)-C(13)	83.7(6)	
Cl(1)-Ni(1)-P(1)-C(13)	42.76(12	
P(1)#1-Ni(1)-P(1)	89.72(5)	

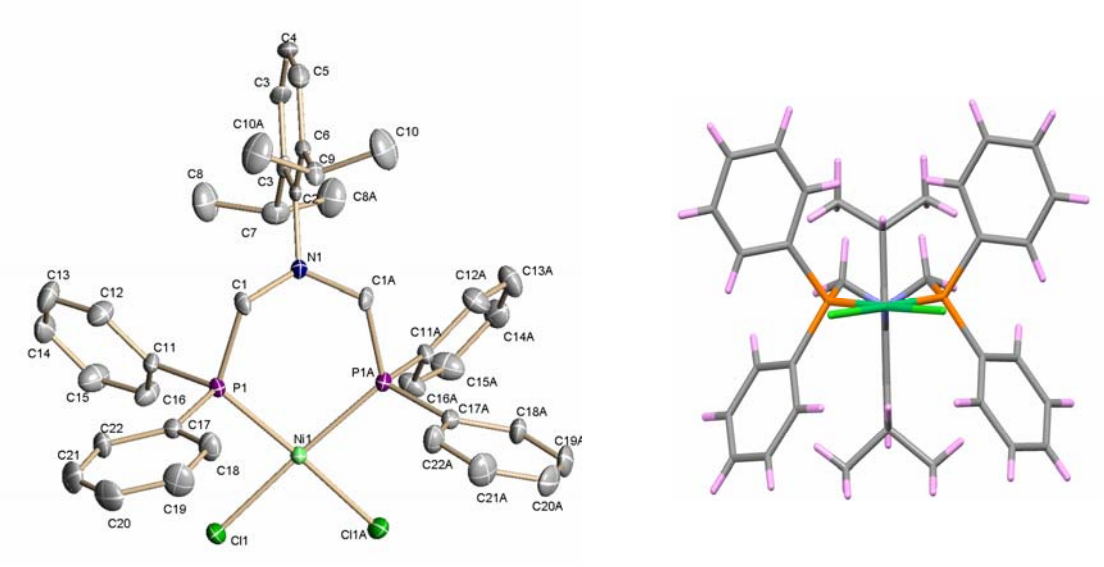

Figure 4.19: Molecular structure and numbering scheme for $[NiCl_2\{(Ph_2PCH_2)_2N\text{-}2,6\text{-}(^iPr)_2C_6H_4\}]$ **15c**

The X-Ray crystal structure of **15c** reveals that the 2,6-diisopropyl phenyl ring on the nitrogen blocks the coordination sites of the complex completely from both the sides. **15c** has the largest bite angle of 97°.

Table 4.4: Selected bond distances (Å) and angles (deg) in **15c**

Ni(1)-P(1)	2.163(2)
Ni(1)-Cl(1)	2.188(2)
P(1)-Ni(1)-P(1)#1	97.16(11)
P(1)-Ni(1)-Cl(1)	85.14(7)

4.3.2 Oligomerization and polymerization of ethylene

4.3.2.1 Oligomerization of Ethylene using nickel complexes at 1.013 bar

4.3.2.1.a Effect of catalyst structure

All the six nickel chloride and nickel bromide complexes **15-16** (**a-c**) were explored for oligomerization of ethylene at 1.013 bar using MAO as cocatalyst. Both **15a** and **16a** show an appreciable induction period of more than 1 h (**Fig. 4.20**) Ethylene consumption

increases rapidly thereafter and continues for about 3 h. The nickel bromide complex **16a** is more active than the nickel chloride complex **15a**. The products of the reaction are predominantly C4 and C6 isomers.

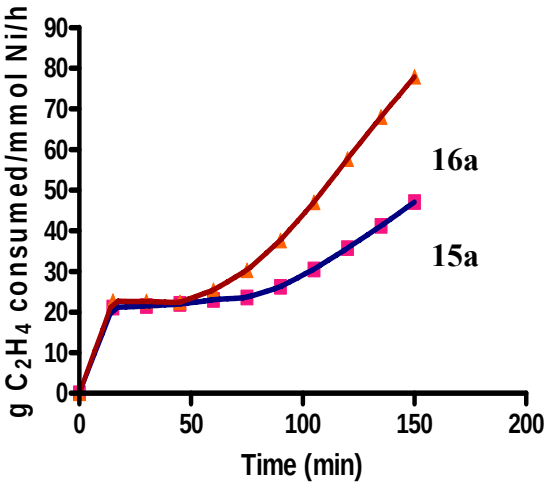

Figure 4.20: Catalyst activity as a function of reaction time (**entries 1 and 3, Table 4.5**) (catalyst = 15 µmol, Al/Ni = 1000, Temp = 28°C, Solvent = Toluene = 30 mL, catalyst dissolved in 3 mL ODCB)

The nickel chloride and nickel bromide complexes **15b** and **16b** exhibited similar behavior in the oligomerization process. They were more active (A = 105-135 $gmmol^{-1}$ Ni^{-1} h^{-1}) than their respective tertiary butyl derivatives **15a** and **16a** (A = 60-65 $gmmol^{-1}Ni^{-1}h^{-1}$). However, **15b** and **16b** showed no induction period (**Fig. 4.21**). Major products of oligomerization are 1- and 2-butenes in all cases. In case of **15b** and **16b**, hexene isomers were also detected (**Table 4.5**).

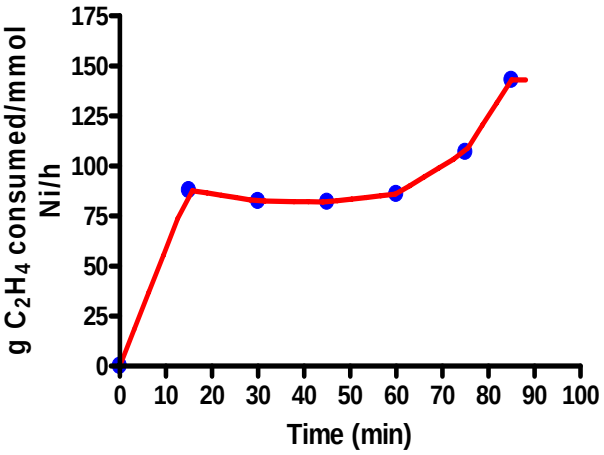

Figure 4.21: Catalyst activity as a function of reaction time for **16b** (**entry 4, Table 4.5**)
(catalyst = 15 µmol, Al/Ni = 1000, Temp = 28°C, Toluene = 30 mL, catalyst dissolved in 3 mL ODCB)

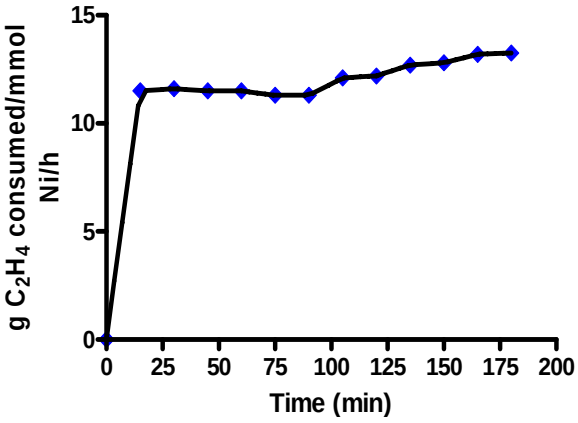

Figure 4.22: Catalyst activity as a function of reaction time for **16c** (**entry 5, Table 4.5**)
(catalyst = 15 µmol, Al/Ni = 1000, Temp = 28°C, Toluene= 30 mL, catalyst dissolved in 3 mL ODCB)

The nickel chloride complex **15c** and nickel bromide complex **16c** (**Fig. 4.22**) showed poor activity (A ≈ 10-12 $gmmol^{-1}\,Ni^{-1}\,h^{-1}$).

Table 4.5: Oligomerization of ethylene with **15(a-b)** and **16(a-c)**

Entry	Catalyst	Time (min)	Yield (g)	ToF mol C_2H_4/mol Ni.h	[a]C_4 wt%	[a]C_6 wt%
1	15a	180	2.74	2177	91	9
2	15b	90	2.17	3699	71	29
3	16a	150	2.92	2781	89	11
4	16b	90	3.04	4823	70	30
5	16c	180	0.52	410	94	6

Reaction conditions: [Ni] = 15µmol, Al/Ni: 1000, Toluene = 30 mL, P_{C2H4} = 1 atm, Catalyst dissolved in ODCB (3 mL), Cocatalyst = MAO. Temp = 28°C. [a]Relative percentage of C4 and C6 fractions.

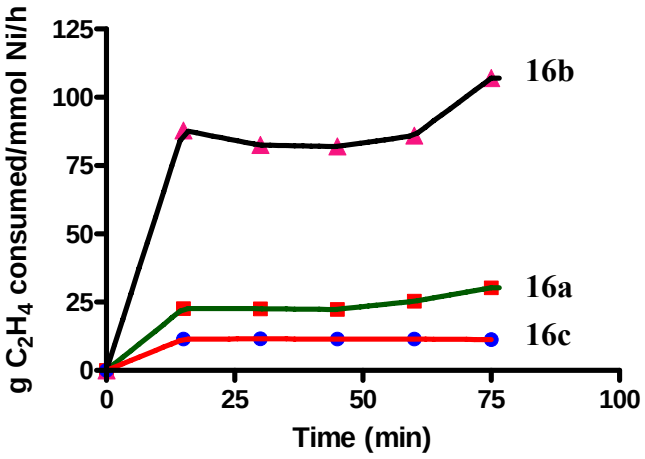

Figure 4.23: Catalyst activity as a function of reaction time (entries 3-5, Table 4.5) (catalyst = 15 μmol, Al/Ni = 1000, Temp = 28°C, Toluene = 30 mL, catalyst dissolved in 3 mL ODCB)

4.3.2.1.b Effect of catalyst pretreatment and the nature of solvent

Complex **15a** dissolved in ODCB, when pretreated with MAO for 1 h prior to initiating the oligomerization run (Tp = 28°C) showed no induction period (**Fig. 4.24**). Similar behavior was noted for oligomerization conducted at 60°C with **15a** (without catalyst pretreatment) (**Fig. 4.25**). Much lower activities were observed for oligomerization runs (Tp = 28°C and 60°C) with **15a** when the complex was dissolved in toluene. The catalyst activity died down with time, the decrease in activity being more pronounced at 60°C (**Fig. 4.26 – Fig. 4.27**). Pretreatment of **15a** (dissolved in toluene) with MAO for 1 h, followed by initiation of reaction did not result in ethylene consumption.

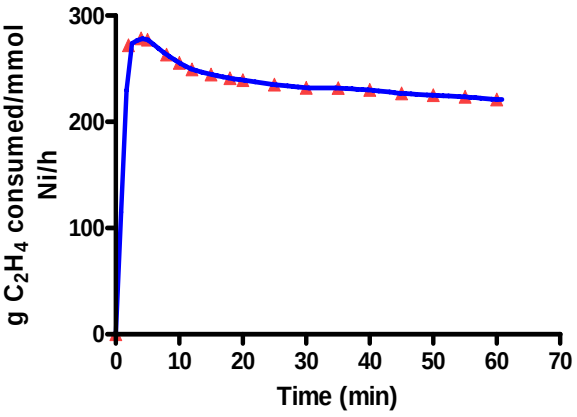

Figure 4.24: Catalyst activity as a function of reaction time for **15a** (Al/Ni = 1000, Temp = 28°C, Toluene = 30 mL, catalyst dissolved in 3 mL ODCB and pretreated with MAO for 1 h)

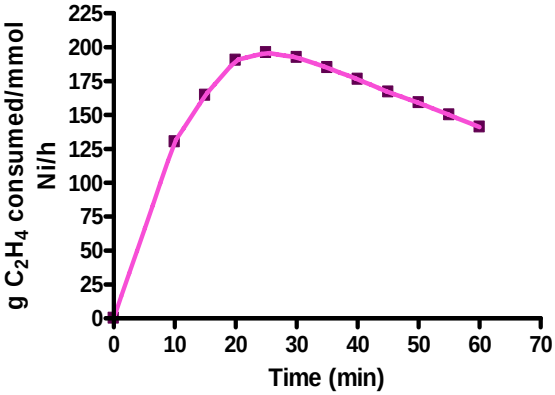

Figure 4.25: Catalyst activity as a function of reaction time for **15a** (Al/Ni = 1000, Temp = 60°C, Toluene = 30 mL, catalyst dissolved in 3 mL ODCB)

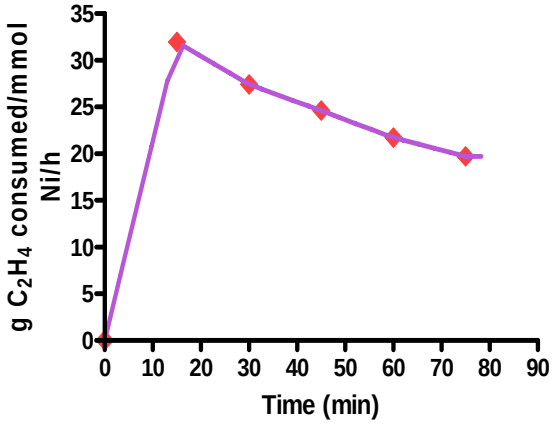

Figure 4.26: Catalyst activity as a function of reaction time for **15a** (Al/Ni = 1000, Temp = 28°C, Toluene = 30 mL, catalyst dissolved in 3 mL toluene at 60°C)

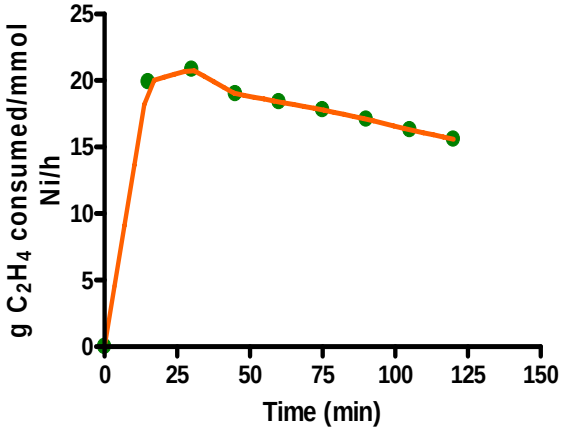

Figure 4.27: Catalyst activity as a function of reaction time for **15a** (Al/Ni = 1000, Temp = 60°C, Toluene = 30 mL, catalyst dissolved in 3 mL toluene at 60°C)

4.3.2.1.c Effect of Al/Ni ratio on catalyst performance

The effect of Al/Ni ratio was studied. Increasing the ratio from 1000 to 1500, resulted in decrease of activity (**Fig. 4.28**). However when Al/Ni ratio of 1500 was used, selectivity to butenes decreased dramatically.

Table 4.6: Oligomerization of ethylene with **15a** at different Al/Ni ratio

Entry	Al/Ni	Yield (g)	ToF mol C_2H_4/mol Ni.h	[a]C_4 (wt%)	[a]C_6 (wt%)
1	1000	2.74	2177	91	9
2	1500	1.91	1519	24	76

Reaction conditions: [Ni] = 15µmol, Toluene = 30 mL, P_{C2H4} = 1 atm, Catalyst dissolved in ODCB (3 mL), Cocatalyst = MAO. Temp = 28°C, Time = 3 h. [a]Relative percentage of C4 and C6 fractions.

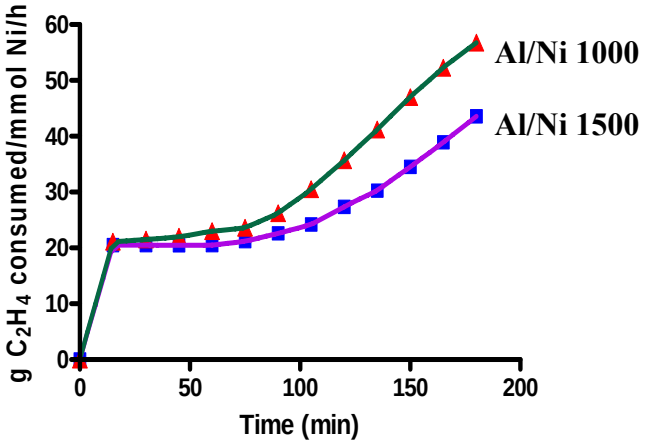

Figure 4.28: Catalyst activity as a function of reaction time at different Al/Ni ratios for **15a** (entries 1-2, Table 4.6)
Catalyst = 15 µmol, Temp = 28°C, Toluene = 30 mL, catalyst dissolved in 3 mL ODCB), Time = 3 h

4.3.2.1.d Effect of catalyst concentration

The effect of catalyst concentration on reactivity was studied for the complex **15a.** It was observed that higher concentration of catalyst resulted in increase of activity (**Fig. 4.29**). The product composition though remained unchanged.

Table 4.7: Oligomerization of ethylene with **15a** at different [Ni]

Entry	[Ni]x10^{-6} mol	Time (min)	Yield (g)	ToF mol C_2H_4/mol Ni.h	$^aC_4$ wt%	$^aC_6$ wt%
1	15	180	2.74	2177	91	9
3	30	150	4.85	2311	92	8

Reaction conditions: Al/Ni: 1000, Toluene = 30 mL, P_{C2H4} = 1 atm, Catalyst dissolved in ODCB (3 mL), Cocatalyst = MAO. Temp = 28°C. [a]Relative percentage of C4 and C6 fractions.

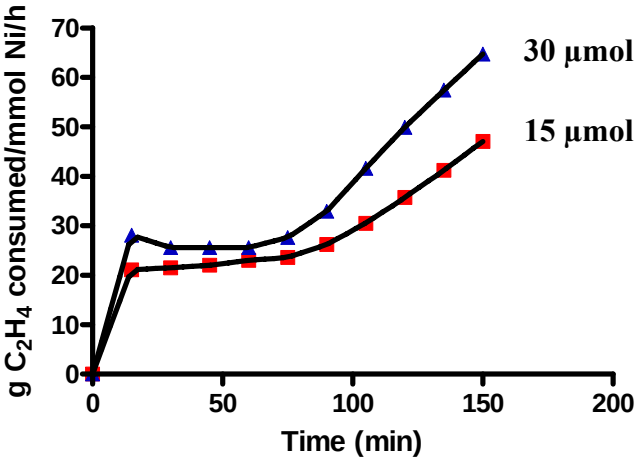

Figure 4.29: Catalyst activity as a function of reaction time at different [Ni] for **15a** (entries 1-2, Table 4.7). Catalyst = 15 µmol, Temp = 28°C, Toluene = 30 mL, catalyst dissolved in 3 mL ODCB)

4.3.2.2 Polymerization of ethylene using complexes 15-16 (a-c) at 5 bar pressure

4.3.2.2.a Effect of catalyst structure

The nickel complexes **15-16** (**a-c**) were explored for the polymerization of ethylene at 5 bar pressure in combination with MAO. Best results were achieved at a temperature of 60^{o}C and an Al:Ni ratio of 1000. Catalyst **15a** produced solid poly(ethylene)s, whereas, **15b** and **16b** gave mainly dimers.

Table 4.8: Polymerization of ethylene with **15(a-c)** and **16(a-c)**

Entry	catalyst	[Ni]x 10^6 mol	Yield (g)	Activity $gmmol^{-1}Ni^{-1}\ h^{-1}bar^{-1}$ [a]	Tm (°C)	[b] $\overline{Mw}$ x10^{-5}	[b] $\overline{Mn}$ x10^{-5}	PDI
1	15a	18.43	2.800	30	129	1.93	1.14	1.71
2	15b	16.7	0.180	2	118	1.55	0.90	1.72
3	15c	16.4	traces	-	-	-	-	-
4	16a	13.2	0.060	1	129	2.35	1.00	2.35
5	16b	12.23	0.055	1	120	1.23	0.60	2.05
6	16c	15.9	0.085	1	131	Bimodal	Bimodal	-

Reaction conditions: Toluene = 30 mL, Cocatalyst = MAO, Al/Ni = 1000, Temp = 60^{o}C, Time = 1 h, PC_2H_4 = 5 bar. Catalysts dissolved in toluene at 60^{o}C. [a]The activities are calculated based on the solid product obtained. [b]GPC values in TCB at 135^{o}C.

4.3.2.2.b Effect of temperature and Al/Ni ratio

The activity of **15a** increased with increasing the polymerization temperature from 40 to 60°C and then dropped with further increase in temperature to 80^{o}C. Catalyst activity also decreased with increasing the Al/Ni ratio. These observations are similar to that observed for the oligomerization reactions with **15a**.

Table 4.9: Polymerization of ethylene with **15a** at different temperatures and Al/Ni ratios

entry	[Ni]x 10^6 mol	Al/Ni	Temp °C	Time (h)	Yield (g)	Activity $gmmol^{-1}$ Ni^{-1} $h^{-1}bar^{-1}$	Tm (°C)	$\overline{Mw}$ $x10^{-5}$	$\overline{Mn}$ x 10^{-5}	PDI
1	14.63	1000	40	3	0.05	<1	129	2.54	1.00	2.5
2	15.20	1500	40	3	0.01	<1	-	-	-	-
3	18.43	1000	60	1	2.80	30	129	1.93	1.14	1.7
4	14.50	1500	60	1	0.15	2	130	3.25	1.81	1.8
5	15.80	1000	80	1	0.08	1	124	1.92	1.07	1.8

Reaction conditions: Catalyst **15a**, Toluene = 30 mL, Cocatalyst = MAO, PC_2H_4 = 5 bar. Catalyst dissolved in toluene at 60°C. [a]The activities are calculated based on the solid product obtained. [b]GPC values in TCB at 135°C.

4.3.3 Polymer structure and properties

4.3.3.1 Polymer molecular weights

Weight and number average molecular weights and polydispersities of the poly(ethylene)s produced by complexes **15-16** (**a-c**) were determined using gel permeation chromatography (**Fig. 4.30**). The polydispersity indices of all the poly(ethylene)s were close to the value of 2.0 indicating single-site catalysis. The Mw values of poly(ethylene)s synthesized by **15a** and **16a** were higher than that produced by **15b** and **16b** (**Table 4.8, entries 1**& **4** and **2** & **5**).

The polyethylene produced by **15a** at 40°C had a molecular weight (Mw) of $2.54x10^5$ (Table 4.9, entry 1) and that produced at 80°C had a Mw value of $1.92x10^5$ (Table 4.9, entry 5).

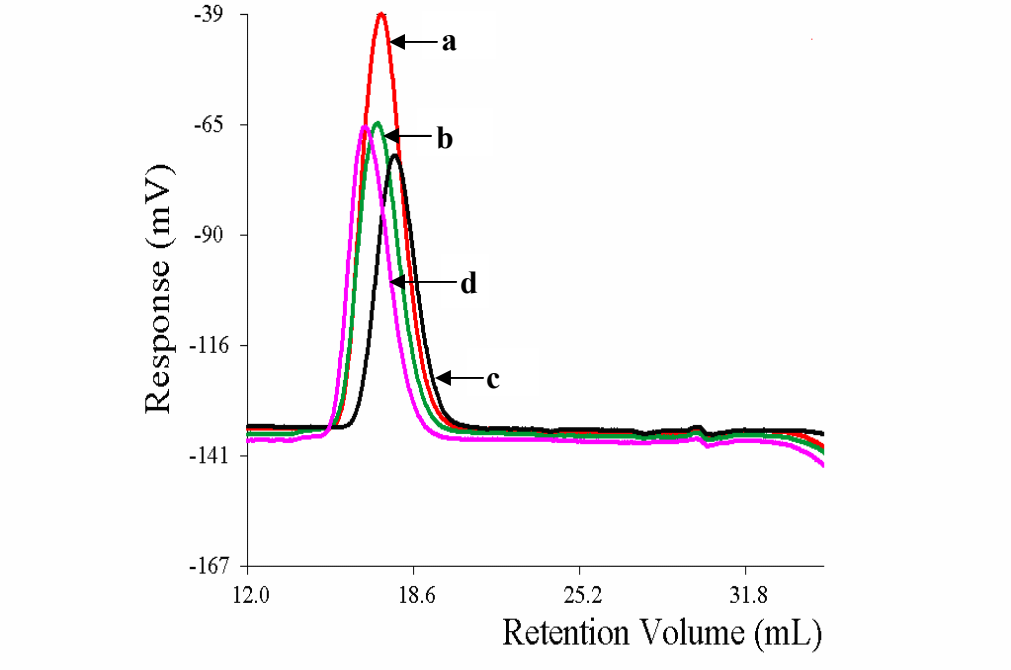

Figure 4.30: GPC of poly(ethylene)s produced by catalysts: a) **15a**, Al/Ni:1000, Tp = 60°C (Table 4.8, entry 1) b) **16a**, Al/Ni: 1000, Tp = 60°C (Table 4.8, entry 4) c) **16b**, Al/Ni: 1000, Tp = 60°C (Table 4.8, entry 5) d) **15a**, Al/Ni: 1500, Tp = 60°C (Table 4.9, entry 4)

4.3.3.2 Melting behavior of poly(ethylenes)

The poly(ethylene)s produced by **15a** and **16a** had a high Tm value (≈ 129°C) (**Table 4.8, entries 1 & 4**; **Fig. 4.31** and **Fig. 4.33**) compared to those produced by **15b** and **16b** (118°C and 120°C respectively, **Table 4.8, entries 2 and 5**; **Fig. 4.34 – Fig. 4.35**). The highly sterically crowded complex **16c**, gave a polyethylene with a Tm value of 131°C (**Table 4.8, entry 6**, **Fig. 4.32**). **15a** produced a polyethylene with a Tm value of 124°C at a polymerization temperature of 80°C (**Table 4.9, entry 5**).

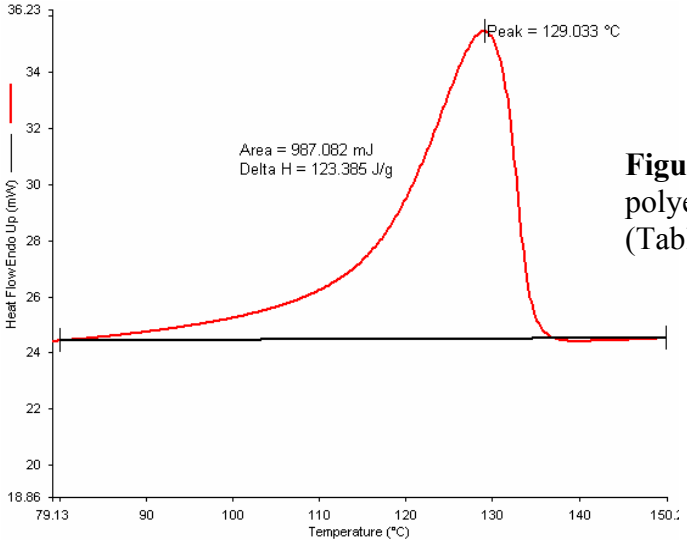

Figure 4.31: DSC thermogram of polyethylene produced by **15a** (Table 4.8, entry 1)

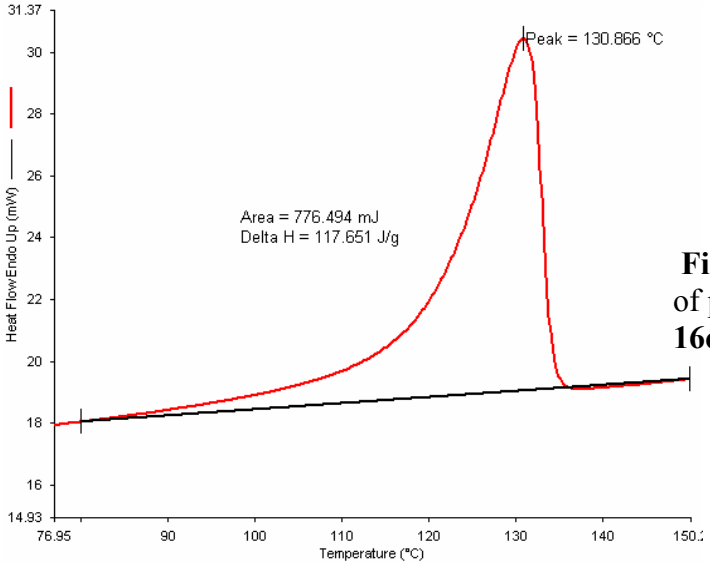

Figure 4.32: DSC thermogram of polyethylene produced by **16c** (Table 4.8, entry 6)

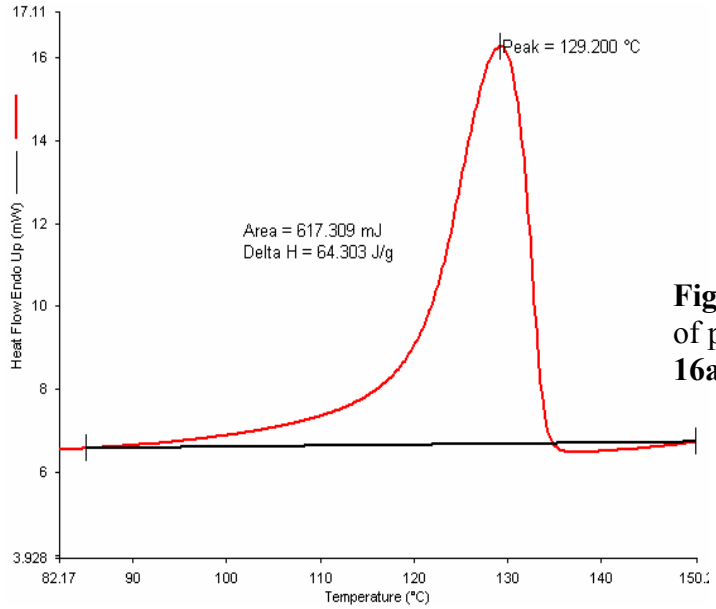

Figure 4.33: DSC thermogram of polyethylene produced by **16a** (Table 4.8, entry 4)

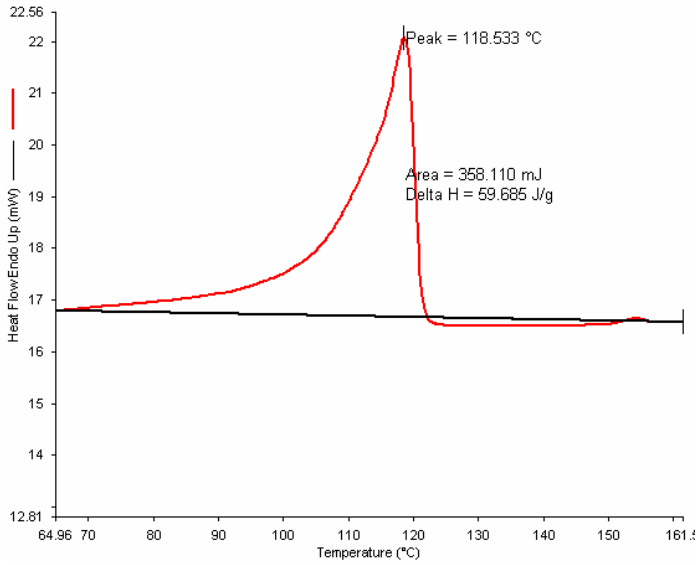

Figure 4.34: DSC thermogram of polyethylene produced by **15b**, (Table 4.8, entry 2)

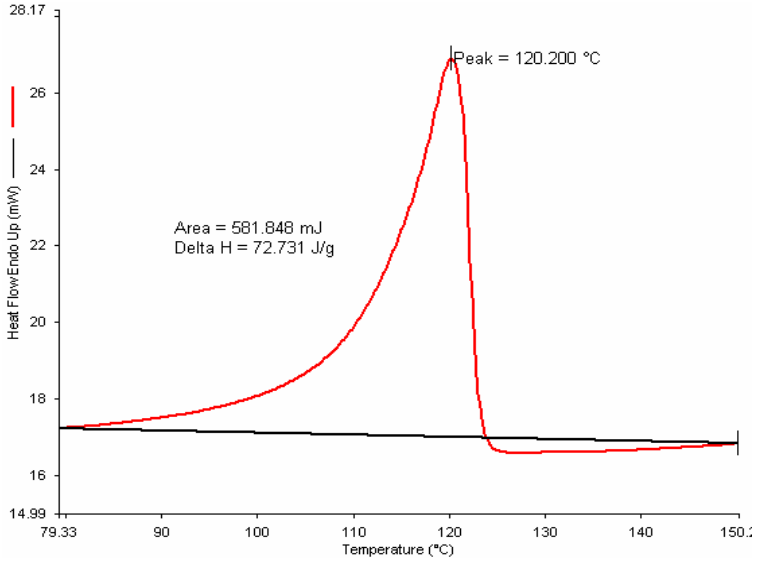

Figure 4.35: DSC thermogram of polyethylene produced by **16b** (Table 4.8, entry 5)

4.3.3.3 Nature and degree of branching

The nature and degree of branching was established using quantitative ^{13}C nmr spectroscopy. ^{13}C NMR spectra of poly(ethylene)s synthesized using complex **15b**/**15a** are shown in **Fig. 4.36** and **Fig 4.38**.

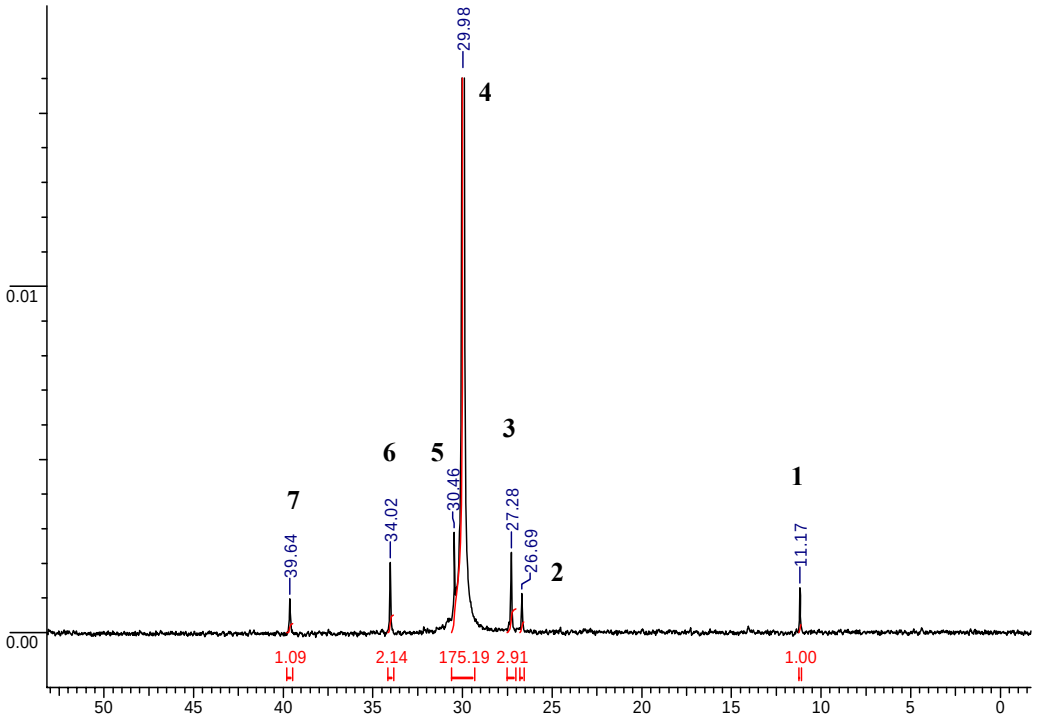

Figure 4.36: Quantitative 125.77 MHz ^{13}C NMR spectrum of a polyethylene synthesized by using **15b** in trichlorobenzene (135^{o}C)

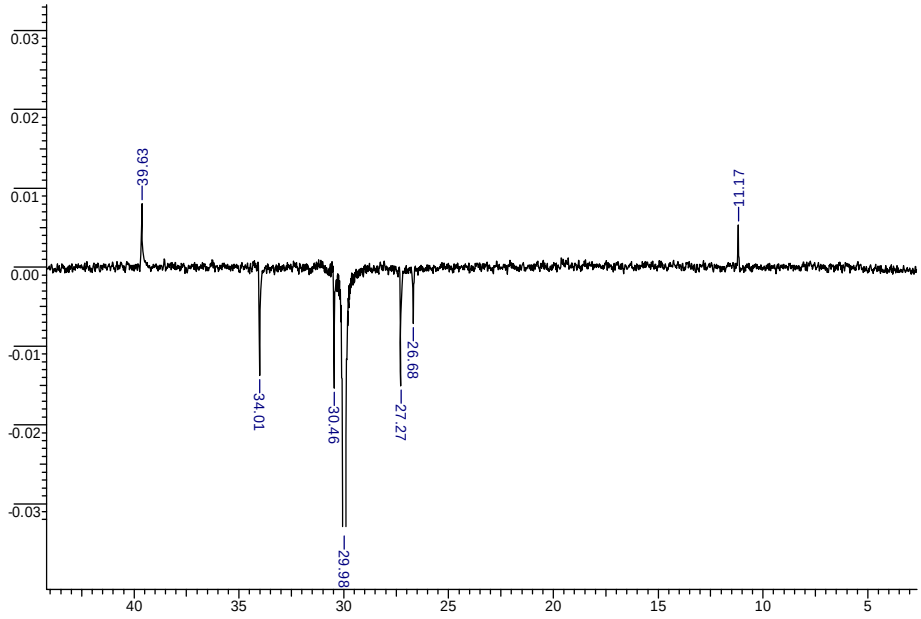

Figure 4.37: Quantative 125.77 MHz ^{13}C (DEPT) NMR spectrum of a polyethylene synthesized by using **15b** in trichlorobenzene

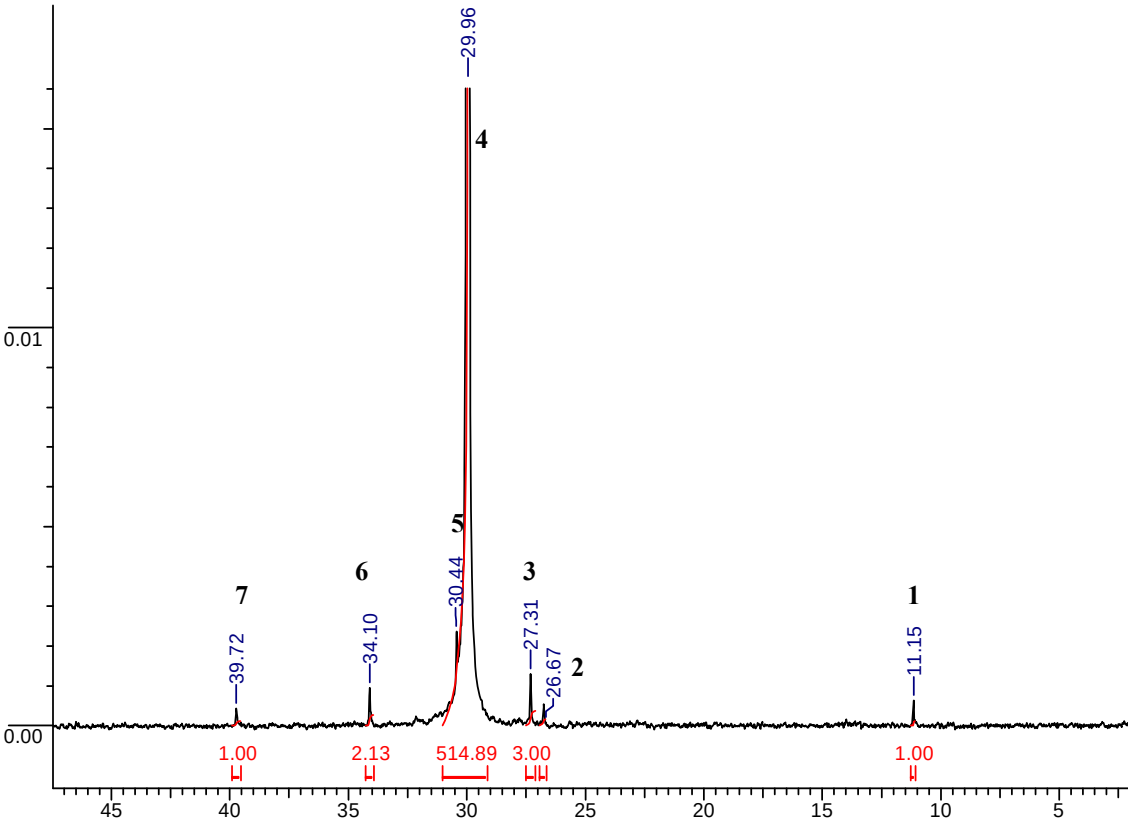

Figure 4.38: Quantitative 125.77 MHz ^{13}C NMR spectrum of a polyethylene synthesized by using **15a** in trichlorobenzene (135^{o}C)

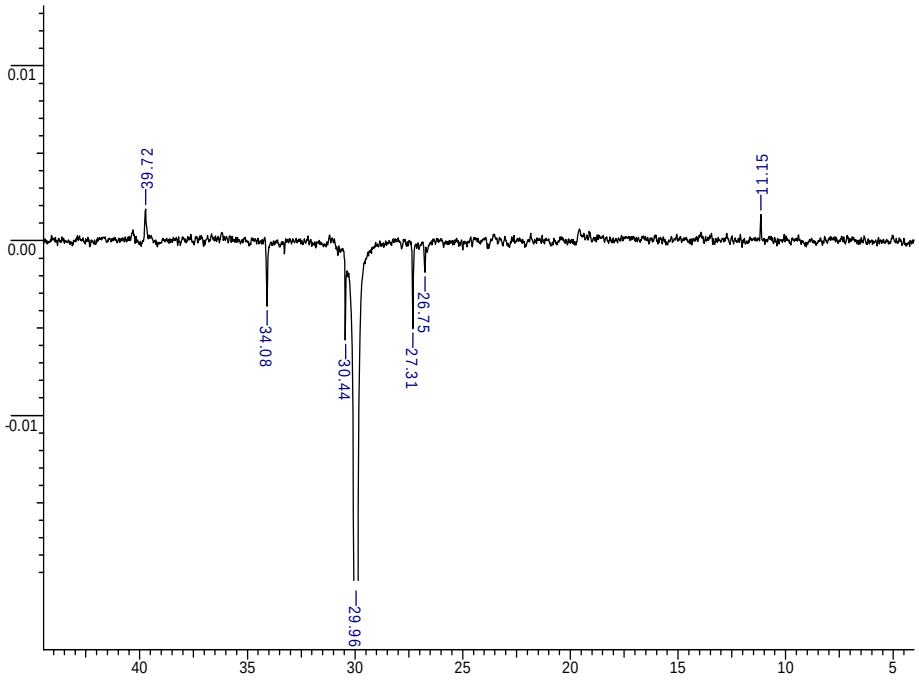

Figure 4.39: Quantative 125.77 MHz ^{13}C (DEPT) NMR spectrum of a polyethylene synthesized by using **15a** in trichlorobenzene

These spectra are obtained in 1,2,4-TCB at 135^{o}C. The methyl, methylene and methine carbons were differentiated with the help of DEPT spectra. The nomenclatures for carbons are according to that suggested by Usami and Takayama for isolated branches[26]. Branches are named by xB_n, where n is the length of the branch and x is the carbon number starting with the methyl group as 1. For the backbone carbons, Greek letters and "br" are used instead of x for the methylenes and a branch point respectively. For example, $1B_1$ designates the methyl in a methyl branch, $2B_2$ the methylene carbon in an ethyl branch, and γB2 the back bone carbon in the γ-position from an ethyl branch.

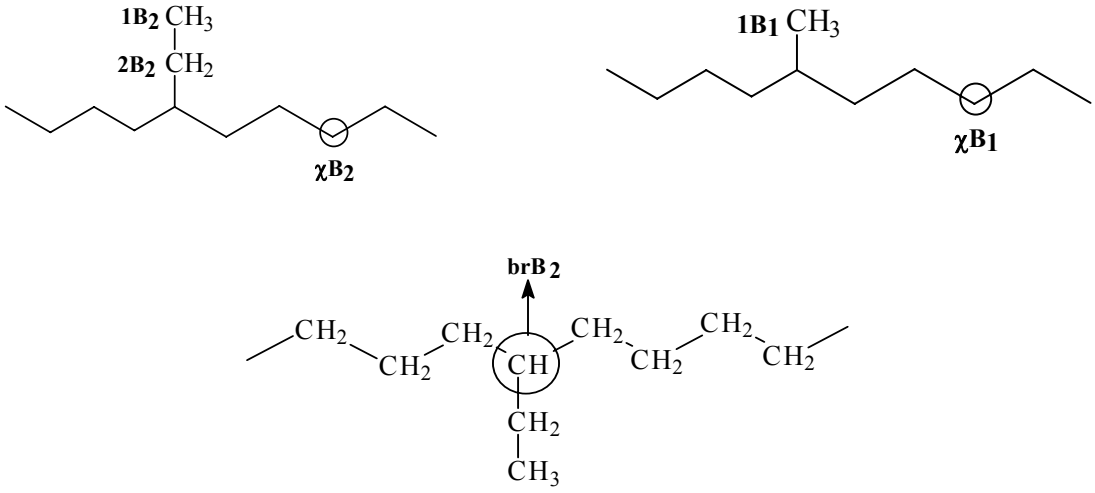

An alternative nomenclature as has been proposed by Randall which identifies a backbone carbon (CH_2) as follows[27]: Greek letters α, β, γ, δ are used to refer to branching points 1, 2, 3, 4 carbons away from a CH_2 carbon. When a branching point is more than 4 carbons away, it is referred to as δ^+. For eg, $\beta\delta^+$ refers to a CH_2 carbon atom of a polyethylene backbone, which has a branching point two carbons away on one side and a branching point more than 4 carbons away on the other side.

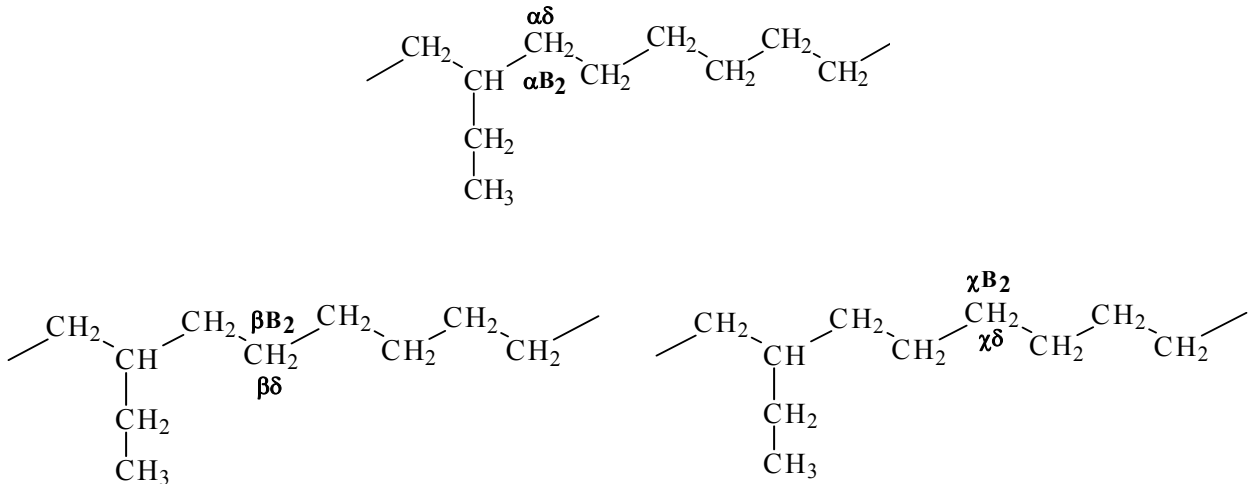

Table 4.10: Chemical shift assignments of poly(ethylene)s synthesized using **15a**

Peak No	Chemical shift (ppm)			Assignments		Sequence Assignments (Randall)
	Usami	Randall	Exptl	Usami	Randall	
1	11.21	11.18	11.15	$1B_2$	$1B_2$	EBE
2	26.79	26.68	26.76	$2B_2$	$2B_2$	EBE
3	27.35	27.27	27.31	βB_2	$S_{\beta\delta+}$	EBEE+EEBE
4		29.98	29.96		$S_{\delta\delta+}$	(EEE)n
5	30.50	30.47	30.44	γB_2	$S_{\gamma\delta+}$	BEEE + EEEB
6	34.13	34.01	34.10	αB_2	$S_{\alpha\delta+}$	BBEE + EEBB
7	39.75	39.61	39.73	brB_2	-CH-	EBE

E = ethylene, B = butene

Table 4.11: Chemical shift assignments of poly(ethylene)s synthesized using **15b**

Peak No	Chemical shift (ppm)			Assignments		Sequence Assignments (Randall)
	Usami	Randall	Exptl	Usami	Randall	
1	11.21	11.18	11.17	$1B_2$	$1B_2$	EBE
2	26.79	26.68	26.69	$2B_2$	$2B_2$	EBE
3	27.35	27.27	27.28	βB_2	$S_{\beta\delta+}$	EBEE + EEBE
4		29.98	29.98		$S_{\delta\delta+}$	(EEE)n
5	30.50	30.47	30.46	γB_2	$S_{\gamma\delta+}$	BEEE + EEEB
6	34.13	34.01	34.02	αB_2	$S_{\alpha\delta+}$	BBEE + EEBB
7	39.75	39.61	39.64	brB_2	-CH-	EBE

E= ethylene, B= butene

The peaks at δ 39.64 and 39.73 ppm in both the ^{13}C NMR spectra of the polymers synthesized by using **15b** (**Fig. 4.36**) and **15a** (**Fig. 4.38**) respectively are due to the presence of a branching point (-CH-, brB_2), which has been further confirmed by the ^{13}C (DEPT) NMR spectra of the polymer samples (**Fig. 4.37** and **Fig. 4.39**). The peaks at δ 11.17 and 11.15 ppm respectively are due to methyl resonances of ethyl branches ($1B_2$), whereas the out of phase orientation of other peaks in the DEPT NMR spectra is attributed to methylene resonances of ethyl branches ($2B_2$). The highly intense peak around δ 29.98 ppm is assigned to the $–CH_2-$ resonance of the main ethylene backbone ($S_{\delta\delta+}$). Only ethyl branches are present through out the polymer chain in both the samples.

Ethyl branches are introduced in to the polymer chain by insertion of butene units formed in the process, which act as comonomer.

The degree of branching was calculated in the following way: The resonance at 11.15 ppm for a polymer sample prepared by **15a** is considered to be a methyl resonance (CH_3) and given an integral value of 1 (one). Areas under the peaks for other chemical shift resonances are integrated with reference to this peak at 11.15 ppm and the total of these values is calculated. The peak at 39.73 is due to a branching point (-CH-) and the integral area under this peak is 0.92 (which is close to 1).

So the degree of branching = integral value of the area for a single branching point/ (Total of the integral values of area for all the peaks) x 1000

Degree of branching for a polymer sample prepared by **15a:** {1.00/(1.00+2.13+514.89+3.00+1.34+1.00)} x 1000 = 1.9 branches/1000 carbon atoms. Similarly, the degree of branching for a polymer sample prepared by **15b** was calculated to be 5.9 branches/1000 carbon atoms.

A typical cationic α-diimine nickel catalyst produces poly(ethylene)s with 100-300 branches/1000 carbon atoms[28]. On the contrary nickel(II) complexes of bulky bis(diarylphosphino)methyl amines (**8a-c**) $(PAr_2)_2NMe$ [Ar= 2-C_6H_4 (iPr), 2-C_6H_4 (Et) , 2-C_6H_4 (Me)] produce poly(ethylene)s with low levels of branching (2-36 branches/1000 carbon atoms)[18].

Key results from the foregoing study are summarized in **Table 4.12**

Table 4.12: Summary of results of oligomerization and polymerization with complexes **15**(**a-c**) and **16**(**a-c**)

Complex	Bite angle (^{o})	Oligomerization activity (g mmol^{-1} Ni^{-1} h^{-1} bar^{-1})[a]	Polymerization activity (g mmol^{-1} Ni^{-1} h^{-1} bar^{-1})[b]	Tm (^{o}C)	Branch/ 1000C
15a	96	60	30	129	2 (ethyl)
15b	89	[c]100	2	118	6 (ethyl)
15c	97	10	-	-	-
16a	96	65	1	129	-
16b	-	[c]135	1	120	-
16c	-	12	1	130	-

[a]P_{C2H4} = 1.013 bar, Temp = 25^{o}C, Al/Ni = 1000, Time = 3 h; [b]P_{C2H4} = 5 bar, Temp = 60^{o}C, Al/Ni = 1000, Time = 3 h; [c]Time = 1.5 h

The above results are indicative of the significant influence of steric blocking of active sites in complexes **15** (**a-c**) and **16** (**a-c**). The N-^{t}Bu substituent in **15a** and **16a** is oriented in such a manner (**Fig. 4.14** and **Fig. 4.15**) that it effectively blocks monomer access to the active site from both sides of the square planar complex. This effect is even more severe in the case of N-2,6-diisopropyl phenyl substituent (**15c** and **16c**) (**Fig. 4.19**). On the contrary, with N-3,5-dimethyl phenyl substituent, the active center at the metal atom is relatively open (**15b** and **16b**) (**Fig. 4.18**).

These structural features influence monomer insertion reaction in two ways. One, at 1.013 bar ethylene pressure all the complexes (**15a-c**, **16a-c**) yield only oligomers. Apparently the rate of propagation is much slower relative to the rate of β-hydrogen transfer under these conditions. Furthermore the oligomerization activity decreases in the order **16b**/**15b** > **16a**/**15a** > **16c**/**15c**, which is also the order of increasing steric crowding at the metal atom. Additionally, the induction time for initiation of oligomerization increases with increasing steric crowding at the metal atom. The more

sterically crowded complex (**15a**/**16a**) produces predominantly butenes, whereas, the less sterically crowded complex (**15b**/**16b**) yields significant amounts of hexenes. Successive monomer addition is inhibited by the nature of N-substituents.

The extent of induction period observed with complex **15a** can be reduced, if complex **15a** is pretreated with MAO in *o*-dichlorobenzene. This observation implies that the alkylation of Ni-X bond by MAO may be the rate limiting step causing the induction period.

Upon increasing the ethylene pressure to 5 bar, complex **15a** is active for the polymerization of ethylene. This is a consequence of increased monomer concentration which enhances the rate of polymerization relative to β-H transfer. The poly(ethylene)s obtained have high molecular weights ($\overline{Mw}$ = 1.93-2.35 x 10^5). They are substantially linear with a Tm ~129^{o}C. **15b**/**c** and **16b**/**c** show insignificant activity for polymerization. For **15c**/**16c**, this can be attributed to excessive steric crowding at the active center, the same cannot hold true for **15b**/**16b**. The possible reason for low polymerization activity for **15b**/**16b** could be due to competitive oligomerization of ethylene occurring under the same conditions. This is supported by the fact that the obtained polymer shows presence of 6 ethyl branches/ 1000 C atoms, arising as a result of copolymerization of ethylene with the dimer formed for oligomerization reaction.

Since branches other than ethyl branch are not observed in the poly(ethylene)s synthesized using both **15a** and **15b**, it is evident that " chain walking" process is absent in these systems. Based on the extensive mechanistic work published on α-diimine complexes of nickel, one can assume that the resting state of the catalyst is the alkyl ethylene complex. The turnover limiting state is the migratory insertion reaction of the alkyl ethylene complex leading to cationic (primary) alkyl species stabilized by β-agostic interactions. Whether, the cationic alkyl species will insert ethylene, resulting in chain growth (without branching) or will undergo a series of β-hydride eliminations and re-additions, resulting in "chain walking" along the polymer chain will depend on the steric environment around the metal center. Complex **15a** apparently is far more open to ethylene coordination than the α-diimine ligands containing bulky substituents on the

aryl ring. Consequently chain growth occurs by normal insertion without chain walking". Complexes **15** (**a-c**) and **16** (**a-c**) show significant oligomerization activity. Thus in these complexes chain transfer is faster relative to chain propagation. Unlike α-diimine complexes of nickel, complexes **15** (**a-c**) and **16** (**a-c**) lack large steric bulk in the axial sites of the square plane. Thus chain transfer by an associative displacement mechanism[19] becomes more facile, leading to products of dimerization and trimerization. Even at higher pressures, only **15a** resulted in polymerization of ethylene. Apparently, the N-^{t}Bu substituent, partially, retards the rate of chain transfer relative to rate of chain propagation.

The higher activity for ethylene oligomerization and polymerization observed for the six-membered chelates bearing a C-N-C ligand backbone (**15-16 a-c**) in comparison to six-membered chelates bearing C-C-C ligand framework may be attributed to the difference in steric crowding around the metal activation site**.** The bite angle in a $NiCl_2$(dppp) complex (C-C-C) has a value of 91^o [29]. The bite angles in the nickel chloride C-N-C systems have values of 89^o, 96^o and 97^o for N-3,5- dimethyl phenyl substituted, N-2,6-diisopropyl phenyl substituted and N-*tert*-butyl substituted complexes, respectively. In view of above, the lower activities observed for the C-C-C systems seems anomalous.

4.4 Conclusions

A new class of P-N-P ligands based $Ni^{II}Cl_2$ and $Ni^{II}Br_2$ complexes were prepared and their solid state structures established by X-ray crystallography. The Ni (II) complexes exhibit moderate to high activities in ethylene oligomerization yielding predominantly C4 and C6 olefins. The corresponding Ni (II) complexes bearing ligands of the type $Ar_2P(CH_2)_3PAr_2$ (C-C-C ligand framework) are inactive for the oligomerization and polymerization of ethylene. The four-membered complexes formed by the ligand $Ar_2P(CH_2)_2PAr_2$ show moderate activity. Incorporating a nitrogen atom in the C3 ligand framework provides easier access to the monomer for coordination at the active center. Steric protection of the axial coordination sites was found to have beneficial effect on the ability of the complex to promote polymerization to high molecular weight linear poly(ethylene)s.

4.5 References

1. a) McConville, D. H.*Organometallics* **1995**,14, 5478. b) McConville, D. H. *J. Am. Chem. Soc.* **1996**, 118, 10008. c) R. R. Schrock. *Organometallics*. **1998**, 17, 308. d) Cloke, F. G. N.; Geldach, T. J.; Hitchcock, P. B. *Organomet. Chem.* **1996**, 506, 343. e) Nomura, K. *Organometallics.* **1998,** 17, 2152. f) Jordan, R. F. *Organometallics.* **1997**, 16, 3303. g) Schaverien, C. J. *J. Am. Chem. Soc.* **1995**, 117, 3008. h) Bazan, G. C. *J. Am. Chem. Soc.* **1996**, 118, 2291. h) Bazan, G. C. *Organometallics.* **1997**, 16, 2492. i) Dehnicke, K. Z. *Anorg. Allg. Chem.* **1998**, 624, 159. j) Dehnicke, K. Z. *Anorg. Allg. Chem.* **1995**, 621, 953. k) L. K. Johnson, C. M. Killian, M. Brookhart, *J. Am. Chem. Soc.* **1995**, 117, 6414. l) G. J. P. Britovsek, V. C. Gibson, B. S. Kimberley, P. J. Maddox, S. J. McTavish, G. A. Solan, A. J. P. White, D. J. Williams, *Chem. Commun.* **1998**, 849.

2. a) Johnson, L. K.; Killian, C. M.; Brookhart, M. *J. Am. Chem. Soc.* **1995**, 117, 6414. b) Gates, D. P.; Svejda, S. A.; Onate, E.; Killian, C. M.; Johnson, L. K.; White, P. S.; Brookhart, M. *Macromolecules*. **2000**, 33, 2320. c) Johnson, L. K.; Killian, C. M.; Arthur, S. D.; Feldman, J.; McCord, E. F.; McLain, S. J.; Kreutzer, K. A.; Bennett, A. M. A.; Coughlin, E. B.; Ittel, S. D.; Parthasarathy, A.; Tempel, D. J.; Brookhart, M. WO 96/23010 (to Dupont) **1996** [*Chem. Abstr:* **1996**, 125, 222773t].

3. a) McConville, D. H.; *Organometallics* **1995**,14, 5478. b) McConville, D. H. *J. Am. Chem. Soc.* **1996**, 118, 10008. (c) Schrock, R. R. *Organometallics*. **1998**, 17, 308. d) Cloke, F. G. N.; Geldach, T. J.; Hitchcock, P. B. *Organomet. Chem.* **1996**, 506, 343. e) Nomura, K. *Organometallics.* **1998**, 17, 2152. f) Jordan, R. F. *Organometallics.* **1997**, 16, 3303. g) Schaverien, C. J. *J. Am. Chem. Soc.* **1995**, 117, 3008. h) Bazan, G. C. *J. Am. Chem. Soc.* **1996**, 118, 2291. i) Dehnicke, K. Z. *Anorg. Allg. Chem.* **1998**, 624, 159. j) Britovsek, G. J. P.; Gibson, V. C.; Kimberley, B. S.; Maddox, P. J.; McTavish, S. J.; Solan, G. A.; White, A. J. P.; Williams, D. J. *Chem. Commun*. **1998**, 849.

4. a) Mui, H. D.; Riehl, M. E.; Wilson, S. R.; Girolami, G. S. *ACS abstracts* **1994**, Vol. 208 (part 1), pp 530-INOR. b) Hoehn, A.; Lippert, F.; Schauss, E. (to BASF) WO 96/37522 c) Brookhart, M.; Feldman, J.; Hauptman, E.; McCord, E. F. (to Dupont) WO 98/47934, *Chem. Abstr*. **1998**, 129(25)331169D.

5. a) Khan, M.M.T.; Rao, E.R., *Polyhedron*, **1987**, 6, 1727 b) Khan, M.M.T.; Bajaj, H.C.; Siddiqui, M.R.H.; Khan, B.T.; Reddy, M.S., *J. Chem. Soc. Dalton Trans.*, **1985**, 2603. c) Khan, M.M.T.; Rao, E.R., *Polyhedron*, **1987**, 6, 1727 d) Khan, M.M.T.; Bajaj, H.C.; Siddiqui, M.R.H.; Khan, B.T.; Reddy, M.S., *J. Chem. Soc. Dalton Trans.*, **1985**, 2603.

6. a) Unruh, J. D.; Christenson, J. R. *J. Mol. Catal.* **1982**, 14, 19. b) Hughes, O. R.; Young, D. A. *J. Am. Chem. Soc.* **1981**, 103, 6636. c) Devon, T. J.; Phillips, G. W.; Puckette, T. A.; Stavinoha, J. L.; Vanderbilt, J. J. U. S. Pat. 4,694,109, **1987** (to Eastman Kodak); *Chem. Abstr.* **1988**, 108, 7890. d) Casey, C. P.; Whiteker, G. T.; Melville, M. G.; Petrovich, L. M.; Gavney, J. A., Jr.; Powell, D. R. *J. Am. Chem. Soc.* **1992**, 114, 5535.

7. a) Kranenburg, M.; van der Burgt, Y. E. M.; Kamer, P. C. J.; van Leeuwen, P. W. N. M. *Organometallics* **1995**, 14, 3081. b) Billig, E.; Abatjoglou, A. G.; Bryant, D. R. (to Union Carbide) U.S. Pat. 4,769,498) EP 214622 U.S. 4668651; Eur. Pat. 213,-639) U.S. 4748261, 1987; *Chem. Abstr.* **1987**, 107, 7392r.

8. a) van Rooy, A.; Kamer, P. C. J.; van Leeuwen, P. W. N. M.; Goubitz, K.; Fraanje, J.; Veldman, N.; Spek, A. L. *Organometallics* **1996**, 15, 835. b) Buisman, G. J. H.; Vos, E. J.; Kamer, P. C. J.; van Leeuwen, P. W. N. M. *J. Chem. Soc., Dalton Trans.* **1995**, 409. c) Buisman, G. J. H.; van der Veen, L. A.; Kamer, P.C. J.; van Leeuwen, P. W. N. M. *Organometallics* **1997**, 16, 5681. d) Cuny, G. D.; Buchwald, S. L. *J. Am. Chem. Soc.* **1993**, 115, 2066.

9. a) Burke, P. M.; Garner, J. M.; Tam, W.; Kreutzer, K. A.; Teunissen, A. J. J. MWO 97/33854, 1997 (to DSM/Du Pont); *Chem. Abstr.* **1997**, 127, 294939. b) Yamamoto, K.; Momose, S.; Funahashi, M.; Ebata, S.; Ohmura, H.; Komatsu, H.; Miyazawa, M. *Chem. Lett.* **1994**, 2, 189.

10. a) Drent, E. Eur. Pat. Appl. 121,965, 1984 (to Shell); *Chem. Abstr.* **1985**, 102, 46423. b) Drent, E. *Pure Appl. Chem.* **1990**, 62, 661. c) Drent, E. Eur. Pat. Appl. 229408, 1986; *Chem. Abstr.* **1988**, 108, 6617. d) Drent, E. Eur. Pat. Appl. 399617, 1990; *Chem. Abstr.* **1991**, 114, 165108. e) Drent, E.; van Broekhoven, J. A. M.; Doyle, M. J. *J. Organomet. Chem.* **1991**, 417, 235. f) Drent, E.; Budzelaar, P. H. M. *Chem. Rev.* **1996**, 96, 663.

11. Doherty, S.; Eastham, G. R.; Tooze, R. P.; Scanlan, T. H.; Williams, D.; Elsegood, M. R. J.; Clegg, W. *Organometallics* **1999**, 18, 3558.

12. a) Kumada, M. *Pure Appl. Chem.* **1980**, 52, 669. b) Negishi, E.-i. *Acc. Chem. Res.* **1982**, 15, 340.

13. a) Hayashi, T.; Konishi, M.; Kumada, M. *Tetrahedron Lett.* **1979**, 21, 1871. b) Hayashi, T.; Konishi, M.; Kobori, Y.; Kumada, M.; Higuchi, T.; Hirotsu, K. *J. Am. Chem. Soc.* **1984**, 106, 158.

14. Ikeda, S.; Ohhata, F.; Miyoshi, M.; Tanaka, R.; Minami, T.; Ozawa, F.; Yoshifuji, M. *Angew. Chem. Int. Ed. Engl.* **2000**, 39, 4512.

15. Sacconi, L., *J. Chem. Soc. A.* **1971**, 492.

16. David, L.D.; Neild, J.; Prouse, L. J. S.; Russell, D. R. *Polyhedron*, **1993**, 12, 2121.

17. WO 9825939, EP 965606.

18. Cooley, N. A.; Green, S. M.; Wass, D. F. *Organometallics* **2001**, 20, 4769.

19. Ittel, S. D.; Johnson, L. K.; Brookhart, M. *Chem. Rev.* **2000**, 100, 1169.

20. a) Agapie, A.; Day, M. W.; Henling, L. M.; Labinger, J. A.; Bercaw, J. E. *Organometallics* **2006**, 25, 2733. b) Bollmann, A.; Blann, K.; Dixon, J. T.; Hess, F. M.; Killian, E.; Maumela, H.: McGuinness, D. S.; Morgan, D. H.; Neveling, A.; Otto, S.; Overett, M.; Slawin, A. M. Z.; Wasserscheid, P.; Kuhlmann, S. *J. Am. Chem. Soc.* **2004**, 126, 14712.

21. Dennett, J. N. L.; Gillon, A. L.; Heslop, K.; Hyett, D. J.; Fleming, J. S.; Emma Lloyd-Jones, C.; Guy Orpen, A.; Pringle, P. G.; Wass, D. F. *Organometallics* **2004**, 23, 6077.

22. a) Parshall, G. W.; Ittel, S. D. In *Homogeneous Catalysis: The Applications and Chemistry of Catalysis by Soluble Transition Metal Complexes;* Wiley: New York, **1992**; pp- 68. b) Vogt, D. In *Applied Homogeneous Catalysis with Organometallic Compounds;* Cornils, B.; Herrmann, W. A.; Eds.; VCH Weinheim, Germany, **1996**; Vol. 1, pp-245.

23. a) Chauvin, Y.; Oliver, H. In *Applied Homogeneous Catalysis with Organometallic Compounds;* Cornils, B.; Herrmann, W. A.; Eds.; VCH Weinheim, Germany, **1996**; Vol. 1, pp-258-268. b) Small, B. L. *Organometallics* **2003**, 22, 3178.

24**.** a) Wilke, G. *Angew. Chem. Int. Ed. Engl.* **1998**, 27, 185. b) Keim, W.; Behr, A.; Limbacker, B.; Kruger, C. *Angew. Chem. Int. Ed. Engl.* **1983**, 22, 503. c) Peuckert, M.; Keim, W. *Organometallics* **1983**, 2, 594. d) Cavell, K. J.; Masters, A. F. *Aust. J. Chem.* **1986**, 39, 1129. e) Rix, F. C.; Brookhart, M. *J. Am. Chem. Soc.* **1995**, 117, 1137. f) Svedja, S. A.; White, A. H.; Keim, W. *J. Organomet. Chem.* **1997**, 544, 163. g) Pillai, M.; Ravindranathan, M.; Sivaram, S. *Chem Rev.* **1986**, 86, 353. h) Skupinska, J. *Chem. Rev.* **1991**, 91, 613.

25. van Leeuwen, P. W. N. M.; Kamer, P. C. J.; Reek, J. N. H.; Dierkes, P. *Chem. Rev.* **2000,** *100,* 2741.

26. Usami, T.; Takayama, S. *Macromolecules,* **1984**, 17, 1756.

27. Randall, J.C. *JMS-Rev. Macromol. Chem. Phys.,* **1989**, C29(2 & 3), 201.

28. Johnson, L. K.; Killian, C. M.; Brookhart, M. *J. Am. Chem. Soc.* **1995**, 117, 6414.

29. Bomfim, J. A. S.; de Souza. F. P.; Filgueiras, C. A. L.; de Sousa, A. G.; Gambardella, M. T. P. *Polyhedron,* **2003**, 22, 1567.

CHAPTER 5

VINYL TYPE POLYMERIZATION OF NORBORNENE WITH Ni (II) AND Pd (II) COMPLEXES OF BIS-PHOSPHINE LIGANDS

5.1 Introduction

Bicyclo[2.2.1]hept+--2-ene, better known by its trivial name norbornene (**1**) and its derivatives can be polymerized in three different ways (**Scheme 5.1**).

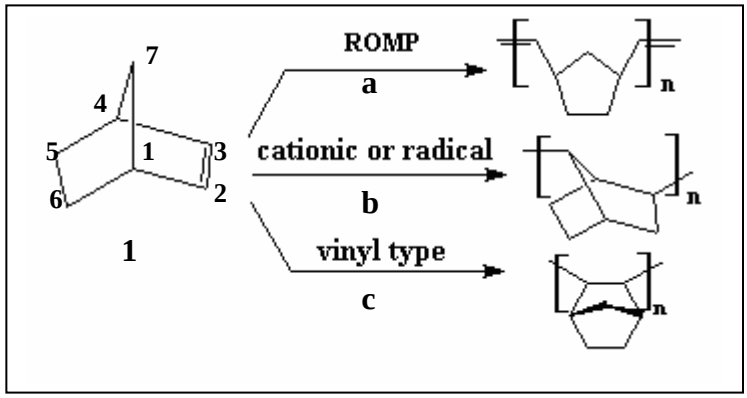

Scheme 5.1: Polymerization of norbornene

The best known polymerization of norborne is the ring-opening metathesis polymerization (ROMP)[1]. The polymer, thus, obtained is a polyalkenamer which has the double bonds intact in the polymer backbone.

Little is known about the cationic (or radical) polymerization of norbornene. This route was first described in 1967[2-4]. The product is a low molecular weight oligomer with 2,7-connectivity of the monomer. Azoisobutyronitrile (AIBN), tert-butyl peracetate or tert-butyl perpivalate are used as radical initiators. Cationic polymerization is initiated using $EtAlCl_2$[2].

Norbornene can also be polymerized via the 2,3-double bond which leaves the bicyclic structural unit intact. Such a polymerization, which is akin to the classical olefin polymerization, is termed a vinyl addition polymerization (**c**). The resulting product does not contain any unsaturation. The homopolymer, poly(norbornene), is a specialty polymer with excellent mechanical properties, high Tg, heat resistivity, good solubility in organic solvents, and desirable optical properties. Films made from this polymer possess excellent transparency and heat resistance and have unchanged viscoelastic and electric properties at markedly high temperatures. Such films are suitable for condensors

or insulators. Homopolymer poly(norbornene) films have been employed as cover layers for liquid-crystal displays.

Titanium, zirconium, cobalt, chromium, nickel and palladium catalysts are described in the literature for the vinyl addition homopolymerization of norbornene and strained cyclic olefins[5]. Titanium and cobalt catalysts are interesting cases because both pathways (**a** and **c**) become possible depending on the cocatalyst ratio[6-8] or the type of cocatalyst employed[9].

Catalysts for vinyl addition polymerization of norbornene can be divided into three groups[10]: (a) early transition metals, especially metallocene complexes of zirconium; (b) late transition metal palladium (II) and nickel (II) catalysts and (c) transition metal complexes containing chromium (III) and cobalt (II).

The first example of vinyl polymers of norbornene were reported with a $TiCl_4$/Al(iso-Bu)$_3$ catalyst with an Al:Ti ratio of 1:2 in the early sixties[7]. With $TiCl_4$/$AlEt_3$ it was shown that an increase in the Al:Ti ratio resulted in a mixture of metathesis polymer and vinyl addition polymer[8].

Metallocene catalysts promoted facile polymerization of cyclic olefins without ring opening. Kaminsky described the polymerization of cyclobutene, cyclopentene and norbornene with chiral metallocenes viz, Et(indenyl)$_2$$ZrCl_2$ (**2**) and Me_2Si(indenyl)$_2$$ZrCl_2$ (**3**) in combination with MAO[11].

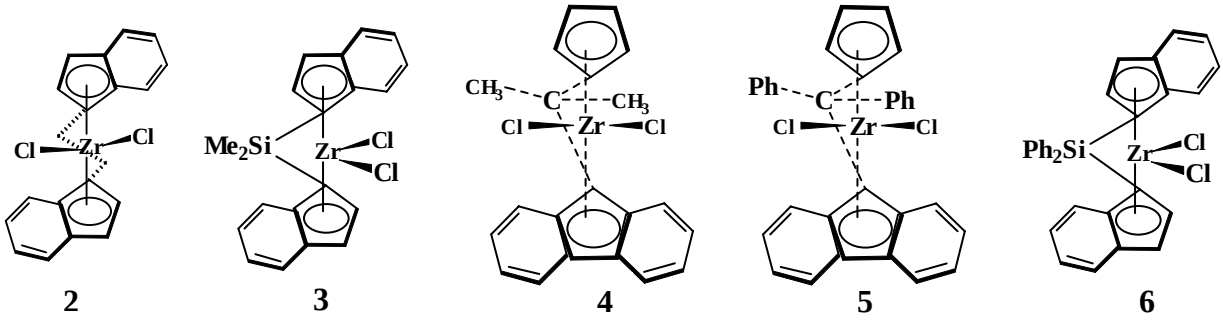

2 **3** **4** **5** **6**

In a series of experiments it was shown that the catalytic systems **2** /MAO or **3** /MAO exhibit a considerably higher polymerization activity towards cyclobutene and cyclopentene relative to norbornene. The copolymerization of norbornene and ethylene

was investigated. The copolymerization was strongly influenced by relative monomer ratios and reaction temperature. Catalyst **2**/MAO showed maximum activity at a molar ratio of ethylene: norbornene of 1:1.

In another study the copolymerization of norbornene and ethylene was investigated in more detail using complexes **3-6**[12]. It became clear that the polymerization rates were quite different for the two types of catalysts. The C_2-symmetrical catalysts **3** and **6**/MAO were highly active for copolymerization. In both cases the activities dropped rapidly with increasing norbornene/ethylene ratio. *Cs*-symmetrical complexes **4** and **5** showed different copolymerization behavior. Both complexes in conjunction with MAO showed a slight maximum in activity as a function of norbornene/ethylene monomer ratio. For complex **4** this maxiumum was at norbornene:ethylene = 3 and for **5** at norbornene:ethylene = 0.6. At higher monomer ratios both the catalysts showed similar activity (A = 2200 for **4** and 2400 g copolymer $mmol^{-1}$ Zr^{-1} $bar^{-1}h^{-1}$ for **5**, respectively). This behavior clearly indicates greater propensity of *Cs*-symmetrical complexes viz, **4** and **5** towards insertion of bulky olefins. The shorter bridge of the ansa-catalysts results in a wider opening angle of the ring ligands around zirconium, thus, creating a larger coordination gap.

The first vinyl addition polymerization of norbornene and substituted norbornenes with a palladium catalyst was reported in 1966 using $PdCl_2$[13] and in the late seventies using $Pd(C_6H_5CN)_2Cl_2$[14] and also $Pd(Ph_3P)_2Cl_2$[14]. Eventually, cationic palladium(II) system, $[Pd(CH_3CN)_4](BF_4)_2$ (**7**) became the best studied catalyst system for norbornene

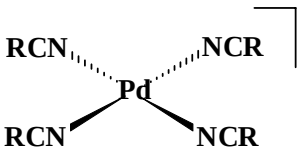

7. R= CH_3
8. R= $CH_3(CH_2)_2$
9. R= $CH_3(CH_3)_2$
10. R= $(CH_3)_2CH$
11. R= $(CH_3)_3C$
12. R= C_6H_5

13 R= 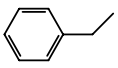

14. R= 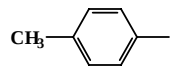

15. R= 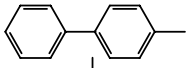

16. R= 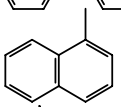

17. R= 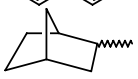

polymerization[15]. Complex **7** with weakly bound acetonitrile ligands was catalytically

active for norbornene polymerization. The vinyl polymerization of norbornene was carried out by adding 100 equivalents of monomer to a solution of **7** in nitromethane at 25°C. After 5 min, polymer was obtained in >90% yield. Heitz and Wendorff showed that all nitriles (**7–17)** exhibited very similar behavior[16].

Nickel complexes (**18-20**) for vinyl polymerization of norbornene were reported in the nineties[17].

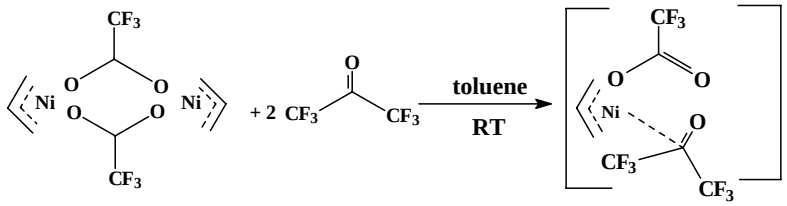

18 **19**

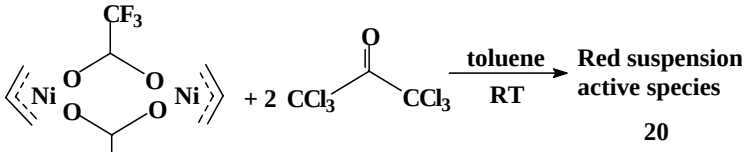

20

18

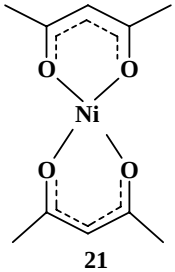

21

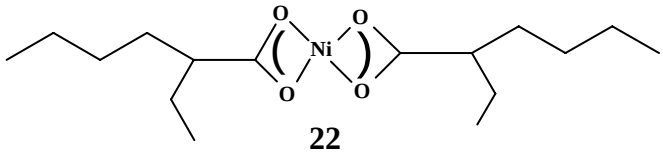

22

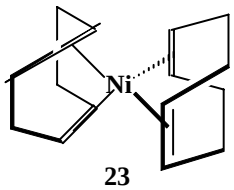

23

Complexes **19** and **20** are very active catalysts for the polymerization of norbornene without any added cocatalyst. $Ni(acac)_2$ (**21**), Ni(2-ethylhexanoate)$_2$ (**22**), and $(COD)_2Ni^o$(**23**) (COD = cyclooctadiene) in combination with MAO catalyze the polymerization of norbornene in toluene[18]. Complex $[BrNi(NPMe_3)]_4$ (**24**) in combination with MAO exhibited catalyst activities up to 20.5 x 10^3 $gmmol^{-1}$ Ni^{-1} h^{-1} and polymer molecular weight up to 3.46 x 10^6 g[19].

The use of the organic Lewis acid, tris(pentafluorophenyl)borane ($B(C_6F_5)_3$), in combination with or without Et_3Al as an activator for late transition metal complexes in

olefin polymerization is well known[20]. However, the use of this activator for norbornene polymerization is rare. A patent issued to BF Goodrich Company (USA) describes the use of $(B(C_6F_5)_3)/Et_3Al$ for norbornene polymerization[21]. Nickel and palladium complexes (**25-28**) have been employed for the polymerization of norbornene using $(B(C_6F_5)_3)/ Et_3Al$ as activator[22].

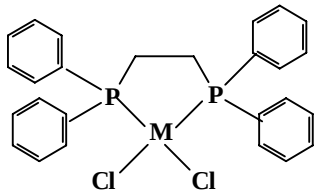

M= Ni (**25**)
M= Pd (**27**)

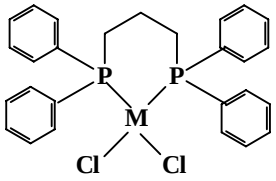

M=Ni (**26**)
M=Pd (**28**)

These complexes showed moderate to high activity when used in combination with $B(C_6F_5)_3/Et_3Al$ or MAO**.**

Synthesis of $Ni^{II}Cl_2$ and $Ni^{II}Br_2$ complexes of Bis-[N,N(diphenylphosphinomethyl)]alkyl/aryl amines **(29-34)** and their use in the oligomerization and polymerization of ethylene has been previously described in Chapter 4. These bis-phosphine donor ligands are different from diphenyl-phosphino propane (dppp) ligands in one respect. The latter has a C_3 ligand backbone while the former has a C-N-C backbone.

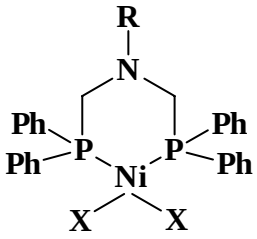

29 R = *t*Bu, X = Cl
30 R = 3,5-$Me_2C_6H_3$, X = Cl
31 R = 2,6-*i*$Pr_2C_6H_3$, X = Cl
32 R = *t*Bu, X = Br
33 R = 3,5-$Me_2C_6H_3$, X = Br
34 R = 2,6-*i*$Pr_2C_6H_3$, X = Br

In this Chapter, studies have been extended to the synthesis of palladium(II) complexes of bis-[N, N(diphenylphosphinomethyl)]-3,5-dimethyl aniline (**35**) and bis-[N, N(diphenylphosphinomethyl)]-2,6-diisopropyl aniline (**36**) and use of these complexes along with the nickel(II) analouges (**29-34**) for the vinyl addition polymerization of norbornene.

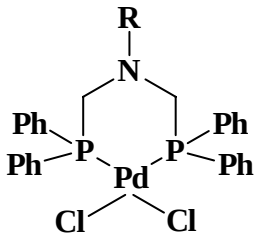

35 R = 3,5-$Me_2C_6H_3$

36 R = 2,6-$^iPr_2C_6H_3$

5.2 Experimental Methods

Materials used and their purification methods are described in Chapter 3 under Section 3.2.2, 3.2.5 and 3.3

5.2.1 Synthesis of ligands and complexes

Synthesis of the $Ni^{II}Cl_2$ complexes (**29-31**) and $Ni^{II}Br_2$ (**32-34**) complexes are described in Chapter 4 (Section 4.2.1.5 to 4.2.1.10).

5.2.1.1 Preparation of $PdCl_2$ complex of bis-[N,N(diphenylphosphinomethyl)]-3,5-dimethyl aniline [$PdCl_2\{(Ph_2PCH_2)_2N$-Ar}] (Ar= 3,5-$Me_2C_6H_3$, (35))

Synthesis of bis-[N,N(diphenylphosphinomethyl)]3,5-dimethyl aniline has been described in Chapter 4 (Section 4.2.1.3).

In a round bottom flask equipped with a magnetic stirring bar, 0.345 g (1.934 mmol) of $PdCl_2$ was taken and dry dichloromethane was added to it. To this was added, bis-

[N,N(diphenylphosphinomethyl)]3,5-dimethyl aniline, 1.0 g (1.93 mmol) under nitrogen atmosphere. An orange colored slurry was obtained. The reaction mixture was refluxed under nitrogen for 12 h. The orange colored solution changed to yellow upon refluxing. Solvent dichloromethane was removed in vacuo to obtain a yellow solid. The solid was dissolved in a minimum quantity dichloromethane and stored. Some black solid particles of Pd(0) separated out. The solution was filtered and diluted with n-hexane. After two days at -20^{o}C, yellow needle shaped crystals of the complex **35** separated out (0.6 g, 40%). Anal. Calcd for $C_{34}H_{33}P_2NPdCl_2.CH_2Cl_2$: C, 53.89; H, 4.49; N, 1.80. Found: C, 53.57; H, 4.36; N, 1.74.

5.2.1.2 Preparation of $PdCl_2$ complex of bis-[N,N(diphenylphosphinomethyl)]-2,6-diisopropyl aniline [$PdCl_2\{(Ph_2PCH_2)_2N$-Ar}] (Ar= 2,6-$^{i}Pr_2C_6H_3$, (36))

Synthesis of bis-[N,N(diphenylphosphinomethyl)]2,6-diisopropyl aniline has been described in Chapter 4 (Section 4.2.1.4).

In a round bottom flask equipped with a magnetic stirring bar, 1.138 g (1.986 mmol) of bis-[N,N(diphenylphosphinomethyl)]2,6-diisopropyl aniline was taken and dissolved in dry degassed dichloromethane. To this, 0.362 g (1.986 mmol) of $PdCl_2$ was added. A brown-red slurry was obtained. The reaction mixture was refluxed under nitrogen for 12 h to obtain an orange yellow color solution. Solvent dichloromethane was removed in vacuo to obtain a yellow solid. This solid was dissolved in a minimum quantity dichloromethane and diluted with a large volume of n-hexane. A yellow precipitate was obtained. This solid was redissolved in dichloromethane and reprecipitated from n-hexane. This procedure was repeated 2-3 times resulting in a pure yellow solid of **36** (0.670 g, 45 %). Anal Calcd for $C_{38}H_{41}P_2NPdCl_2$: C, 60.76; H, 5.46; N, 1.87. Found: C, 60.32; H, 5.99; N, 1.78.

5.2.1.3 Preparation of Tris-(pentafluorophenyl)borane[23]

In a round bottom flask equipped with a magnetic stirring bar, 1.44 g (0.06 mol) of magnesium turnings was taken and 100 mL of dry ether added along with a pinch of

iodine. The round bottom flask was kept over a water bath at 25°C. A dropping funnel was fitted to the flask and bromo-pentafluoro benzene (7.48 ml, 0.06 mol) was added drop wise till a grey turbid solution appeared. The round bottom flask was cooled to 0°C and the addition of bromo-pentafluoro benzene was completed. The reaction was stirred at 0°C for 1 h.

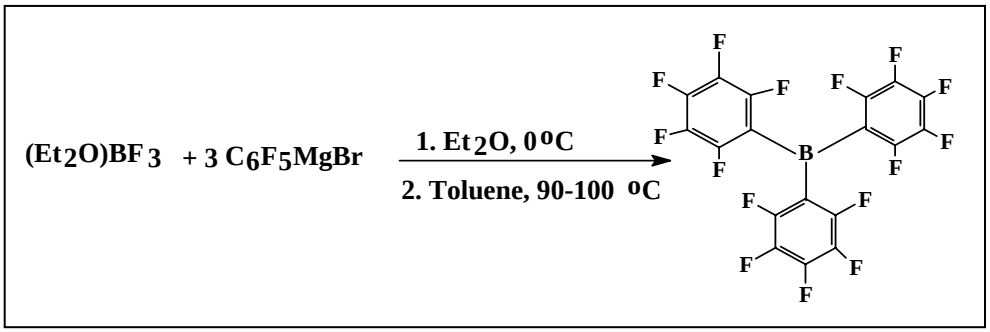

Scheme 5.2: Synthesis of tris(pentafluorophenyl)borane

In another round bottom flask, 40 mL toluene was taken and 2.5 mL (0.02 mol) BF_3. Et_2O was added. The flask was cooled to 0°C. The contents of the first round bottom flask were added via a cannula to the second round bottom flask with vigorous stirring. A dark brownish black solution appeared. The reaction mixture was concentrated by evaporating approximately 100 mL of solvent in vacuo. The reaction mixture was refluxed for 1 h at 100°C over a boiling water bath. Thereafter, the solvent was completely removed to obtain a dry brown cake. The crude product was extracted with 150 mL of warm hexane (45°C) and the extracts collected in a flask containing around 10 mL of dry ether. Cubic crystals of $(Et_2O)B(C_6F_5)_3$ appeared upon cooling to -20°C. The crystals were separated and purified by sublimation twice at 100°C for 2-3 h at 0.2 mbar to obtain feathery white crystals of $B(C_6F_5)_3$. Anal. Calcd for $B(C_6F_5)_3$: C, 42.2 . Found: C, 42.9.

5.2.2 Polymerization of norbornene

5.2.2.1 Polymerization of norbornene with nickel complexes (29-34) using $B(C_6F_5)_3/Et_3Al$ as cocatalyst

A jacketed glass reactor equipped with a magnetic stirring bar was assembled hot and cooled under nitrogen. Norbornene (2.834 g, 30.1 mmol) was dissolved in 13 mL toluene and added to the reactor. A solution of the nickel complex (**29-34**, 30.1 μmol) in dichloromethane (9 mL) was added. A toluene solution (14 mL) of $B(C_6F_5)_3$ (0.139 g, 270.9 μmol) was added to the reaction mixture and stirred for 5 min. The polymerization temperature (25^oC-45^oC) was maintained using a thermostat for circulating water through the jacket. Polymerization was initiated by adding a toluene solution of Et_3Al (0.04 mL, 301 μmol) into the reactor using a syringe. After 1 h, the polymerization was quenched by addition of acidified methanol (10%). The polymer was filtered and washed several times with methanol and acetone and dried in vacuo at 60°C for 10 h.

5.2.2.2 Polymerization of norbornene with palladium complexes (35-36) using $B(C_6F_5)_3/Et_3Al$ as cocatalyst

The polymerization procedure was identical to that described above (5.2.4.1).

5.2.2.3 Polymerization of norbornene with nickel complexes (30 and 33) using MAO as cocatalyst

A jacketed glass reactor equipped with a magnetic stirring bar was assembled hot and cooled under nitrogen. Norbornene (0.996 g, 10.6 mmol) was dissolved in 6 mL toluene and added to the reactor using a syringe. The required amount of MAO was added and the reaction mixture stirred for 5 min. Polymerization temperature was maintained at 35^oC using a thermostat for circulating water through the jacket. Polymerization was initiated by adding 4 mL dichloromethane solution of the complex (10.6 μmol, **30** and **33**) using a syringe. After 1 h, the polymerization was quenched by addition of acidified methanol (10%). The polymer was filtered and washed several times with methanol and acetone and dried in vacuo at 60°C for 10 h.

5.2.3 Analysis and characterization

The obtained poly(norbornene)s were characterized by G.P.C, TGA, NMR and IR. The procedures have been described in Chapter 3, sections 3.4.1, 3.4.4, 3.4.5 and 3.4.6, respectively.

Full crystallographic data of complex **35** is given in Appendix 2.

5.3 Results and discussions

5.3.1 Structure of the palladium complex 35

The $Pd^{II}Cl_2$ complex **35**, with a 3,5-dimethyl phenyl moiety as a substituent on the nitrogen atom was crystallized from a mixture of dichloromethane and hexane. A dichloromethane molecule is bound to the crystal lattice to stabilize the complex. Complex **36**, could not be crystallized and was obtained as an amorphous solid. Similar to the $Ni^{II}Cl_2$ complex **30**, $Pd^{II}Cl_2$ complex **35** has a square planar structure. The Pd-P (2.2299 Å) and the Pd-Cl (2.3413 Å) bond lengths are longer than the Ni-P (2.1523 Å) and Ni-Cl (2.1967 Å) bond lengths for obvious reasons. The P-Pd-P bite angle of 89.05^o is very close to the theoretical value of 90^o, which enhances the stability of the complex.

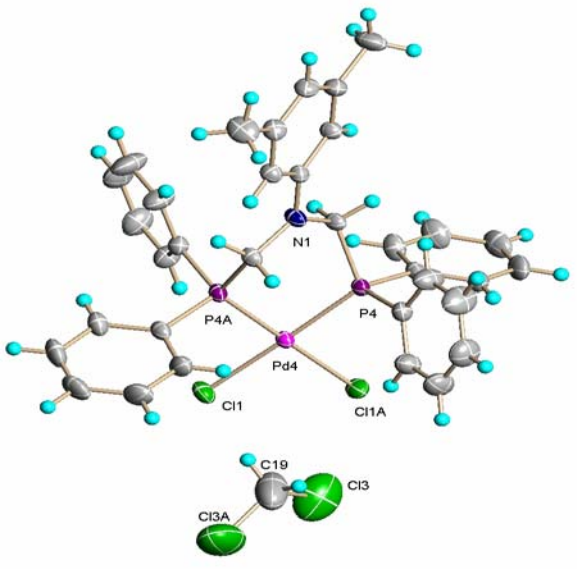

Figure 5.1: Molecular structure and numbering scheme for $[PdCl_2\{(Ph_2PCH_2)_2N\text{-}C_6H_3(CH_3)_2\}]\ .CH_2Cl_2$ **(35)**

Table 5.1: Selected bond distances (Å) and angles (deg) in (**35**)

Pd(4)-P(4)	2.2299(6)
Pd(4)-Cl(1)	2.3413(6)
P(4)-Pd(4)-Cl(1)	178.25(2)
P(4)-Pd(4)-Cl(1)#1	89.76(2)
Cl(1)-Pd(4)-Cl(1)#1	91.46(3)
P(4)#1-Pd(4)-P(4)	89.05(3)

5.3.2 Polymerization of norbornene with nickel complexes (29-34)

5.3.2.1 Effect of catalyst structure

The effect of the structure of nickel complexes (**29-34**) on norbornene polymerization activity was studied.

Table 5.2: Norbornene polymerization with nickel complexes **29-34**[a]

Entry	Catalyst	Yield(g)	Conversion (%)	Activity $gmmol^{-1} Ni^{-1} h^{-1}$	$\overline{Mn}$[b] $x10^{-5}$	$\overline{Mw}$[b] $x10^{-5}$	PDI[b]
1	29	1.22	43	40.5	7.74	12.23	1.6
2	30	1.99	70	66	4.96	8.34	1.7
3	31	traces	-	-	-	-	-
4	32	1.90	67	63	4.14	6.83	1.7
5	33	2.03	72	67	4.04	7.38	1.8
6	34	0.84	30	28	5.76	9.39	1.6
[c]7	26	traces	9	8.6	-	8.10	2.4

[a]Conditions: Catalyst = 30.1 μmol, Norbornene = 30.1 mmol (2.834 g), Cat: $B(C_6F_5)_3$: Et_3Al = 1:9:10, $B(C_6F_5)_3$ = 270.9 μmol (0.139 g), Et_3Al = 301 μmol (0.04 mL). Toluene: Dichloromethane = 3:1, Total volume = 36 mL, Temp = 25°C, Time = 1 h; [b]By G.P.C. measurements in trichlorobenzene at 135°C; [c]Nickel chloride complex of bis(diphenylphosphino)propane[22].

The nickel chloride complex **30** and the nickel bromide complex **33** with a 3,5-dimethyl phenyl substituent on nitrogen atom, exhibited similar activities (66-67 $gmmol^{-1} Ni^{-1} h^{-1}$). The $NiBr_2$ complex **32** with a *tert*-butyl substituent was more active than its $NiCl_2$ counterpart **29**. The highly sterically crowded nickel bromide complex **34** with a 2,6-

diisopropyl phenyl substituent on the nitrogen atom, shows the lowest activity of 28 gmmol^{-1} Ni^{-1} h^{-1}. A nickel complex **26** with a C-C-C ligand framework exhibited much lower activity[22].

5.3.2.2 Effect of temperature

The effect of temperature on catalyst activity and polymer molecular weight was studied for the nickel complexes **29-34**.

Table 5.3: Polymerization of norbornene with nickel complexes **29-34** at variable temperatures[a]

Entry	Catalyst	Temp (°C)	Yield (g)	Conversion (%)	Activity gmmol^{-1} Ni^{-1} h^{-1}	$\overline{Mn}^{b}$ x10^{-5}	$\overline{Mw}^{b}$ x10^{-5}	PDI[b]
1	29	25	1.22	43	40	7.74	12.23	1.6
2	29	35	2.10	74	70	5.87	9.38	1.6
3	29	45	2.50	88	83	2.29	4.20	1.8
4	30	25	1.99	70	66	4.96	8.34	1.7
5	30	35	2.25	79	75	4.91	7.90	1.6
6	30	45	2.19	77	73	1.42	2.56	1.8
7	32	25	0.91	32	30	4.14	6.83	1.7
8	32	35	1.56	55	52	5.09	8.50	1.7
9	32	45	1.68	59	56	5.26	8.56	1.6
10	33	25	2.03	72	67	4.04	7.38	1.8
11	33	35	2.15	76	71	4.49	7.76	1.7
12	33	45	2.56	90	85	2.45	5.19	2.0
13	34	25	0.84	30	28	5.76	9.39	1.6
14	34	35	1.20	42	40	6.07	9.78	1.6
15	34	45	2.43	86	81	3.01	4.83	1.6

[a]Conditions: Catalyst = 30.1 μmol, Norbornene = 30.1 mmol (2.834 g), Cat: $B(C_6F_5)_3$: Et_3Al = 1:9:10, $B(C_6F_5)_3$ = 270.9 μmol, Et_3Al = 301 μmol. Toluene: Dichloromethane = 3:1, Total volume = 36 mL, Time = 1 h; [b]By G.P.C. measurements in trichlorobenzene at 135°C.

From Table 5.3, it is evident that with increasing temperature, the monomer conversion increases. The highest activity is seen for the $NiBr_2$ complex **33** at 45°C, with a monomer conversion of 90% (**Table 5.3, entry 12**). The molecular weight of the polymers synthesized using **31-34** increase from 25°C to 35°C and then drop down at 45°C (**Table**

5.3, entries 7-15). In the case of **29** and **30**, there is a gradual decrease of polymer molecular weight with increasing temperature (**Table 5.3, entries 1-6**).

5.3.2.3 Effect of catalyst concentration and cocatalyst

Effect of catalyst concentration and the nature of the cocatalyst have been studied for the two catalyst systems **30** and **33**. The results reveal that with increasing catalyst concentration from 10.6 μmol to 30.1 μmol, monomer conversion increases from 70% to 80% in case of **30** (**Table 5.4, entries 1** and **3**) and from 68% to 76% in case of **33** (**Table 5.4, entries 4** and **6**) when $B(C_6F_5)_3/Et_3Al$ is used as cocatalyst.

Table 5.4: Norbornene polymerization with nickel complexes **30** and **33** at variable catalyst concentration and cocatalyst

Entry	Catalyst	[M]x10^6 mol	Cocatalyst	Yield (g)	Conversion (%)	$\overline{Mn}$ x10^{-5}	$\overline{Mw}$ x10^{-5}	PDI
1[a]	30	10.6	$B(C_6F_5)_3/Et_3Al$	0.700	70.	5.12	8.70	1.7
2[b]	30	10.6	MAO	0.647	65	4.16	7.78	1.9
3[a]	30	30.1	$B(C_6F_5)_3/Et_3Al$	2.25	79	4.91	7.90	1.6
4[a]	33	10.6	$B(C_6F_5)_3/Et_3Al$	0.681	68	4.76	8.09	1.7
5[b]	33	10.6	MAO	0.276	28	5.97	10.6	1.8
6[a]	33	30.1	$B(C_6F_5)_3/Et_3Al$	2.15	76	4.49	7.76	1.7
7[b]	33	30.1	MAO	0.54	19	1.27	2.68	2.0
[c]8	26	10.6	MAO	-	2.5		26	1.9

[a]Conditions: Catalyst: Norbornene = 1:1000, Norbornene = 10.6 mmol (0.998g), Norbornene = 30.1 mmol (2.834 g), Cat: $B(C_6F_5)_3$: Et_3Al = 1: 9: 10, Et_3Al = 301 μmol, Toluene: Dichloromethane = 3:1, Total volume = 36 mL, Temp = 35°C, Time = 1 h; [b]Conditions: Catalyst: Norbornene = 1:1000, Al/Ni = 100, Dichloromethane = 4 mL, Toluene = 6 mL, Total volume = 10 mL, Temp = 35°C, Time = 1 h. [c]Nickel chloride complex of bis(diphenylphosphino)propane, Time = 5 min, Temp = 25°C, Al/Ni = 100, Catalyst: Norbornene = 1: 1000, Total volume = 10 mL[22].

Use of MAO as a cocatalyst with complex **33** resulted in lower conversions relative to tris-(pentafluorophenyl)borane (**Table 5.4, entries 5** and **7**). However, in the case of

complex **30**, no change in conversion was observed when $B(C_6F_5)_3/Et_3Al$ was replaced with MAO (**Table 5.4, entries 1-2**). This difference in behavior for the otherwise structurally similar nickel complexes (**30** and **33**) is not clearly understood at this time.

5.3.2.4 Effect of Al/Ni on catalyst performance

The effect of Al/Ni ratio was studied. For complex **30**, the highest monomer conversion (65%) is achieved at an Al/Ni ratio of 100 (**Table 5.5, entry 1**). With an increase in Al/Ni ratio to 200, the conversion drops to 46% (**Table 5.5, entry 2**). Further increase has a negligible effect (**Table 5.5, entry 5**). However, the molecular weights of poly(norbornene)s decrease gradually with increase in Al/Ni ratio (**Table 5.5, entries 1-5**).

Table 5.5: Effect of Al/Ni on catalyst activity[a]

Entry	Al/Ni	Yield (g)	Conversion (%)	$\overline{Mv} \times 10^{-5}$
1	100	0.65	65	7.9
2	200	0.46	46	7.7
3	500	0.43	43	7.3
4	800	0.42	42	6.8
5	1000	0.41	42	6.7

[a]Conditions: Catalyst = **30**, Cocatalyst = MAO, [Ni] = 10.6 μmol, Norbornene = 10.6 mmol, Toluene = 6 mL, DCM = 4 mL, Total volume = 10 mL, Temp = 35°C, Time = 1 h.

5.3.3 Polymerization of norbornene with palladium complexes (35-36)

5.3.3.1 Effect of catalyst structure

Effect of the structure of palladium complexes (**35-36**) on norbornene polymerization activity was studied.

Table 5.6: Polymerization of norbornene with palladium complexes **35** and **36**[a]

Entry	Catalyst	Yield (g)	Conversion %	Activity $gmmol^{-1}\,Pd^{-1}\,h^{-1}$	[b]$\overline{Mn}$	[b]$\overline{Mw}$	[b]PDI
1	36	1.12	39	37	-	-	-
2	37	1.20	42	40	-	-	-
[c]3	28	-	3.1	3.0	-	-	-

[a]Conditions: Catalyst = 30.1 μmol, Norbornene = 30.1mmol (2.834 g), Cat: $B(C_6F_5)_3$: Et_3Al = 1: 9: 10, $B(C_6F_5)_3$ = 270.9 μmol (0.139 g), Et_3Al = 301 μmol (0.04 mL), Toluene: Dichloromethane = 3:1, Total volume = 36 mL, Temp = 25°C, Time = 1 h; [b]polymers insoluble in 1,2,4-TCB at 135°C; [c]Palladium chloride complex of bis(diphenylphosphino)propane[22].

Performance of the palladium (II) complexes is less affected by the steric bulk of the nitrogen substituent and both the complexes **35** and **36** show similar activities (**Table 5.6, entries 1** and **2**). The poly(norbornene)s synthesized using **35** and **36** are insoluble in chlorinated organic solvents (ODCB and 1,2,4-TCB) even at high temperatures and hence could not be characterized. I.R of poly(norbornene)s synthesized using **35** and **36** show absence of peaks at 735 and 960 cm^{-1}, indicating that the polymerization had occurred via 2,3-double bond.

Palladium complex **28**, with a C-C-C ligand framework, showed much less activity under similar conditions[22]. However, the polynorbornene obtained in this case was also insoluble in organic solvents (ODCB and 1,2,4-TCB).

5.3.3.2 Effect of temperature

The effect of temperature on catalyst activity was studied for the palladium complexes **35-36**.

Table 5.7: Polymerization of norbornene with **35** and **36** at variable temperatures[a]

Entry	Catalyst	Temp (°C)	Yield (g)	Conversion (%)	Activity $gmmol^{-1}\,Ni^{-1}\,h^{-1}$	$\overline{Mn}^{b}$ $x10^{-5}$	$\overline{Mw}^{b}$ $x10^{-5}$	PDI[b]
1	35	25	1.12	39.5	3.72	-	-	-
2	35	35	1.82	64	6.05	-	-	-
3	35	45	1.35	48	4.49	-	-	-
4	36	25	1.20	42	3.99	-	-	-
5	36	35	2.08	73	6.91	-	-	-
6	36	45	2.37	84	7.87	-	-	-

[a]Conditions: Catalyst = 30.1 μmol, Norbornene = 30.1 mmol (2.834 g), Cat: $B(C_6F_5)_3$: Et_3Al=1:9:10, $B(C_6F_5)_3$ = 270.9 μmol, Et_3Al = 301 μmol. Toluene:Dichloromethane = 3:1, Total volume = 36 mL, Time = 1 h; [b]Polymers insoluble in 1,2,4-TCB at 135°C.

Table 5.7 shows that upon increasing the polymerization temperature from 25°C to 35°C the catalyst activity also increases for both **35** and **36** (**entries 1-2**, **4-5**). Further increase in polymerization temperature to 45°C has different effects for these two palladium complexes. While there is a rise in catalyst activity for **36**, palladium complex **35**, exhibits a marginal drop in activity.

5.3.4 Polymer structure and properties

5.3.4.1 Polymer molecular weights

Weight and number average molecular weights and polydispersities of the poly(norbornene)s produced by Ni (II) complexes **29-34** were determined using gel permeation chromatography (**Fig. 5.2 - 5.4**).

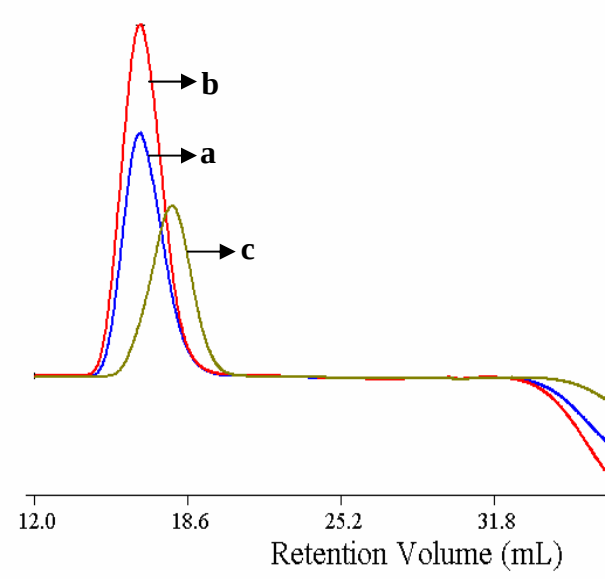

Figure 5.2: GPC of poly(norbornene)s synthesized using catalyst **30**: a) 25°C, (Table 5.3, entry 4) b) 35°C, (Table 5.3, entry 5) c) 45°C (Table 5.3, entry 6)

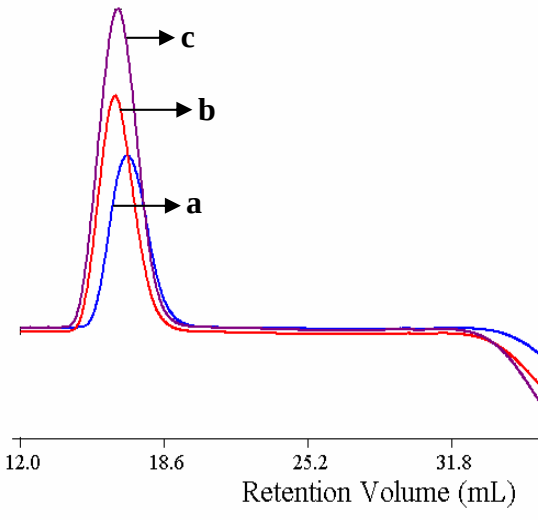

Figure 5.3: GPC of poly(norbornene)s synthesized using catalyst **32**: a) 25°C, (Table 5.3, entry 7) b) 35°C, (Table 5.3, entry 8) c) 45°C (Table 5.3, entry 9)

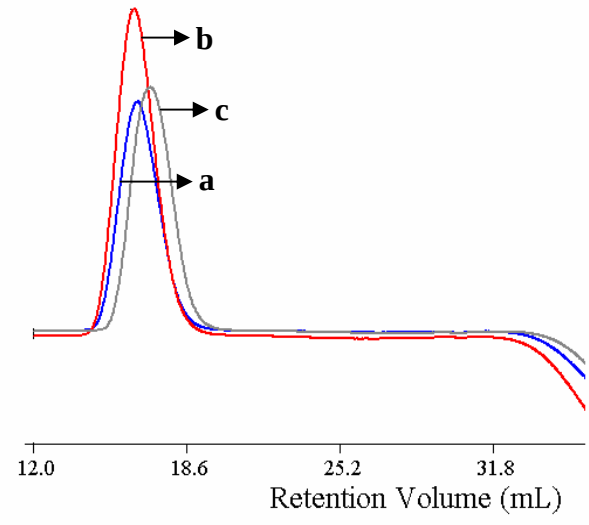

Figure 5.4: GPC of poly(norbornene)s synthesized using catalyst **34**: a) 25°C, (Table 5.3, entry 13) b) 35°C, (Table 5.3, entry 14) c) 45°C (Table 5.3, entry 15)

5.3.4.2 Thermal behavior

Thermal property of poly(norbornene)s synthesized using $NiBr_2$ complex **33** was investigated by thermo gravimetric analysis (TGA). The polymer was stable up to a temperature of 430^oC.

5.3.4.3 Infrared spectroscopy

The FTIR spectra of the poly(norbornene)s prepared by the nickel (**29-34**) and palladium (**35-36**) complexes have confirmed the absence of double bonds (**Fig 5.5 – Fig 5.6**). The spectra show characteristic absorption peaks at 2946 (s), 2866 (s), 1475 (s), 1454 (s), 1339 (m), 1297 (s), 1259 (s), 1225 (s), 1188 (s), 1144 (m), 1110 (s), 1031(m), 985 (s), 938 (m), 890 (m), 853 (s), and 749 (s) and are identical to that reported in the literature[24-25]. Bands at 735 and 960 cm^{-1}, attributed to double bonds following ROMP are absent. Thus, the polymer obtained was a vinyl-type addition product. Unlike earlier reports[10], even at high Al/Ni ratio, poly(norbornene)s prepared by **30**/MAO did not show any evidence of ring opening mode of polymerization (**Fig. 5.6**)

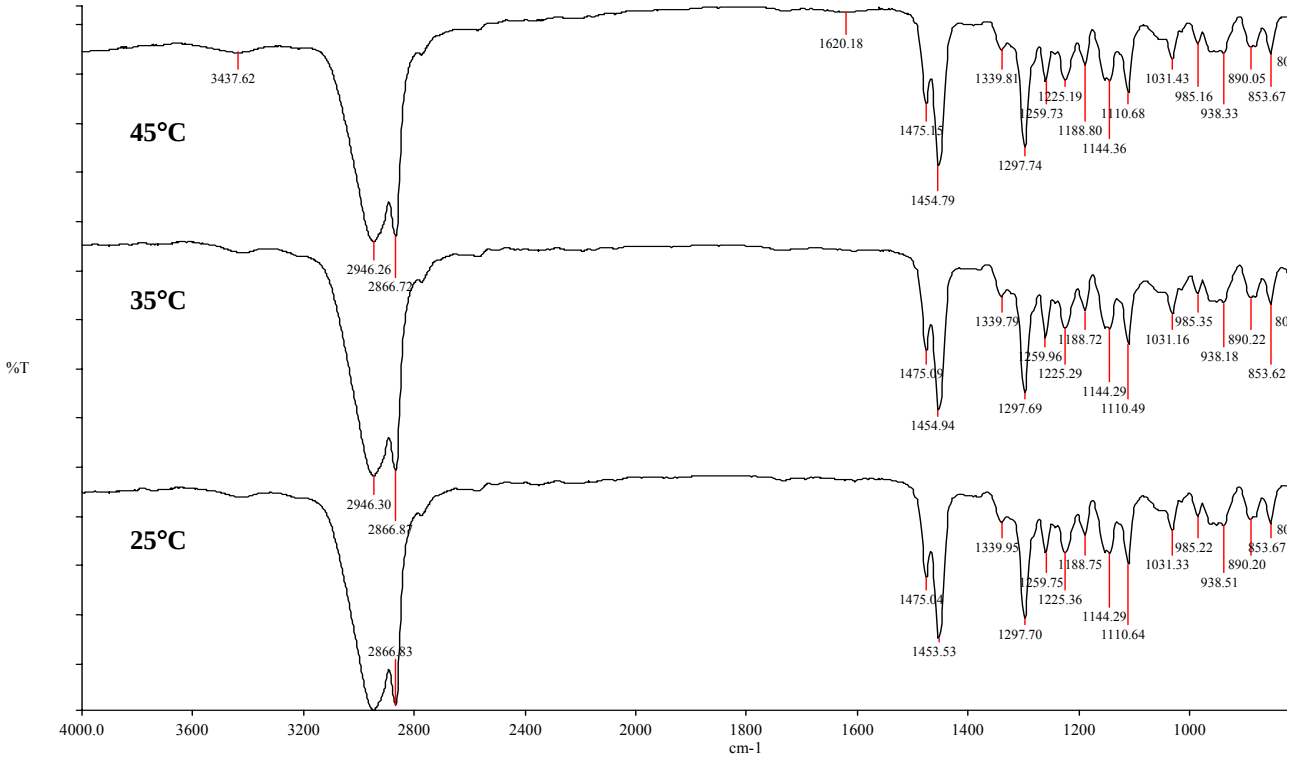

Figure 5.5: I.R spectra of poly(norbornene)s prepared by **35** at: (a) 45^{o}C, (Table 5.7, entry 3) (b) 35^{o}C, (Table 5.7, entry 2) (c) 25^{o}C, (Table 5.7, entry 1)

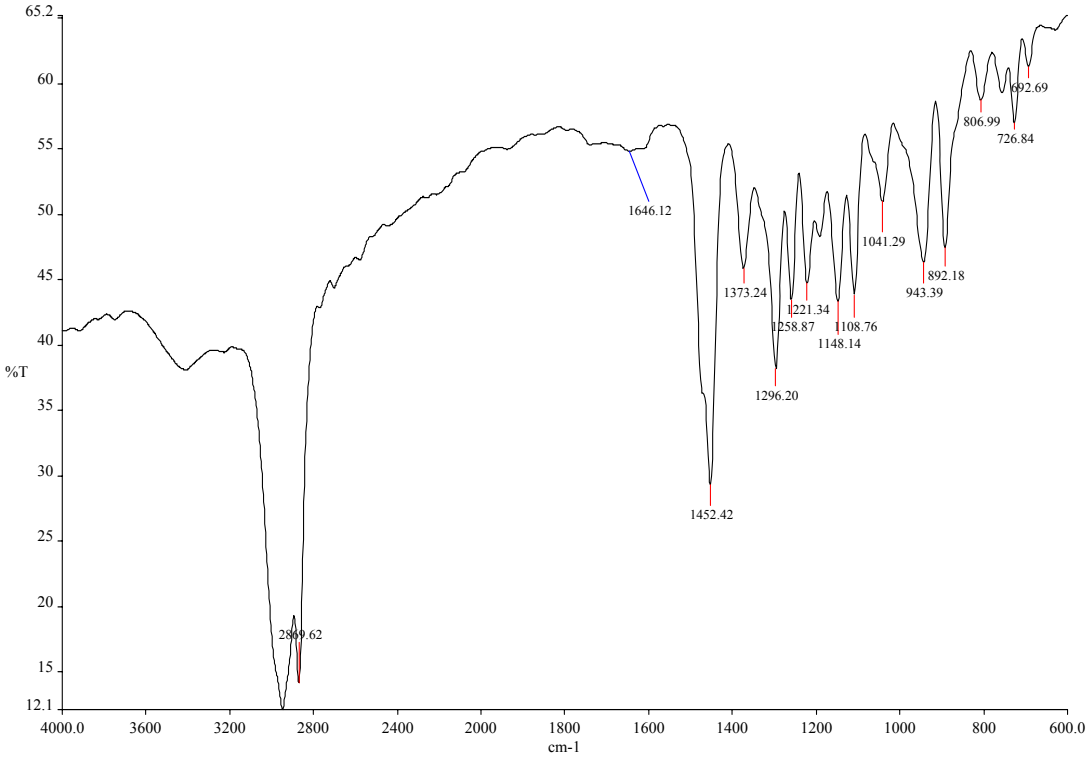

Figure 5.6: I.R spectrum of poly(norbornene) prepared using **30**/MAO (Table 5.5, entry 5)

5.3.4.4 NMR spectroscopy

High temperature ^{13}C NMR spectra of poly(norbornene)s synthesized using **32-34**, in 1,2,4-trichlorobenzene revealed peaks in the region of 29.53- 32.31 ppm, which appear due to methylene resonances of carbon-5 and carbon-6. Peaks at 35.26-37.47 ppm appear for carbon-7, 38.47-39.90 ppm for carbon-1 and carbon-4 and at 47.19- 54.06 for carbon-2 and carbon-3 (**Fig 5.7 – Fig 5.9**). These spectra are similar to that reported by Greiner et al[19] and Wu et al[24-25].

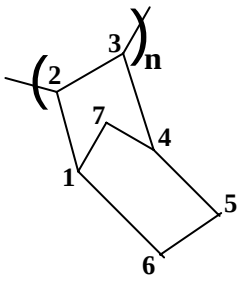

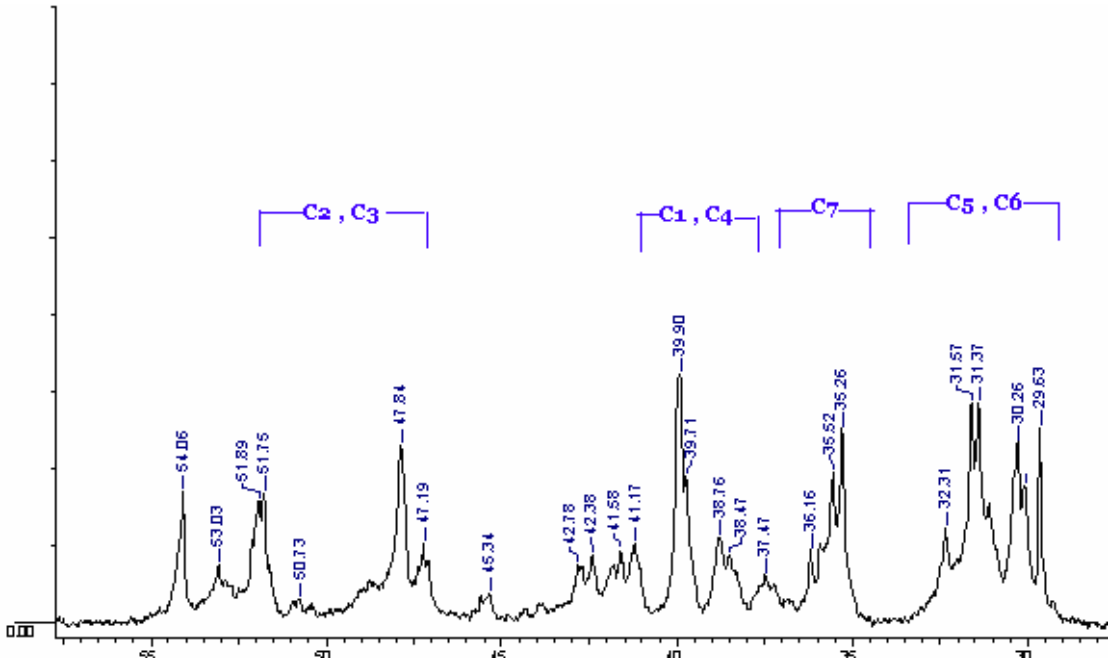

Figure 5.7: ^{13}C NMR spectrum of poly(norbornene)s prepared using **33** at 35^{o}C (Table 5.3, entry 11)

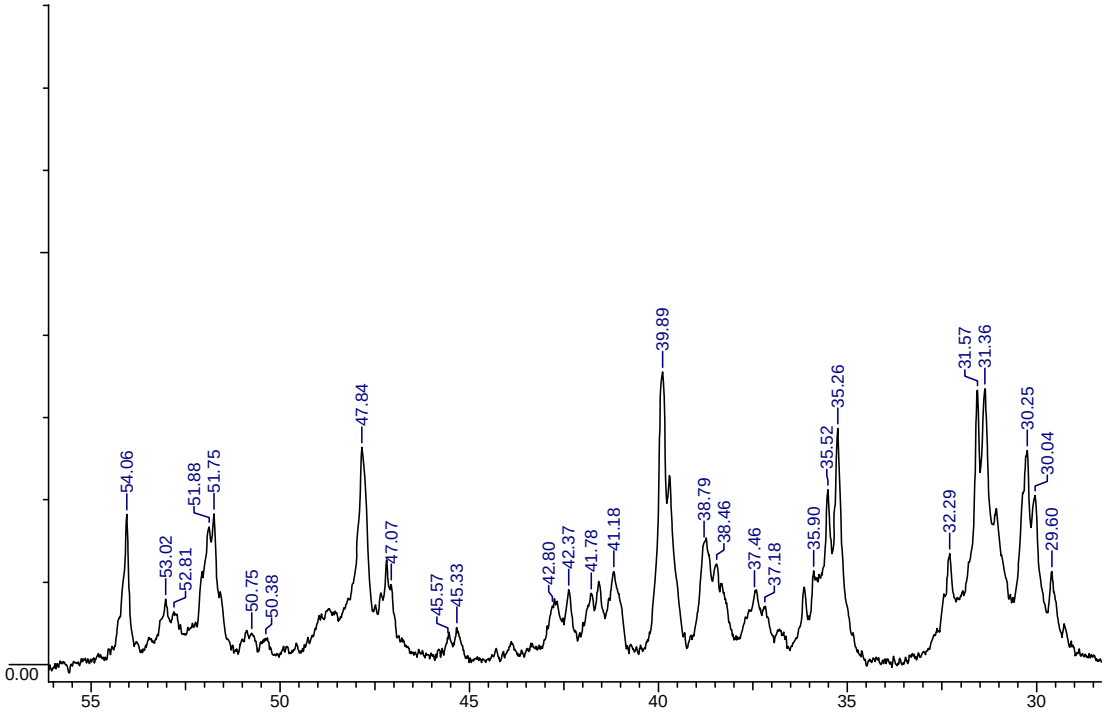

Figure 5.8: ^{13}C NMR spectrum of poly(norbornene)s prepared using **32** at 35^{o}C (Table 5.3, entry 8)

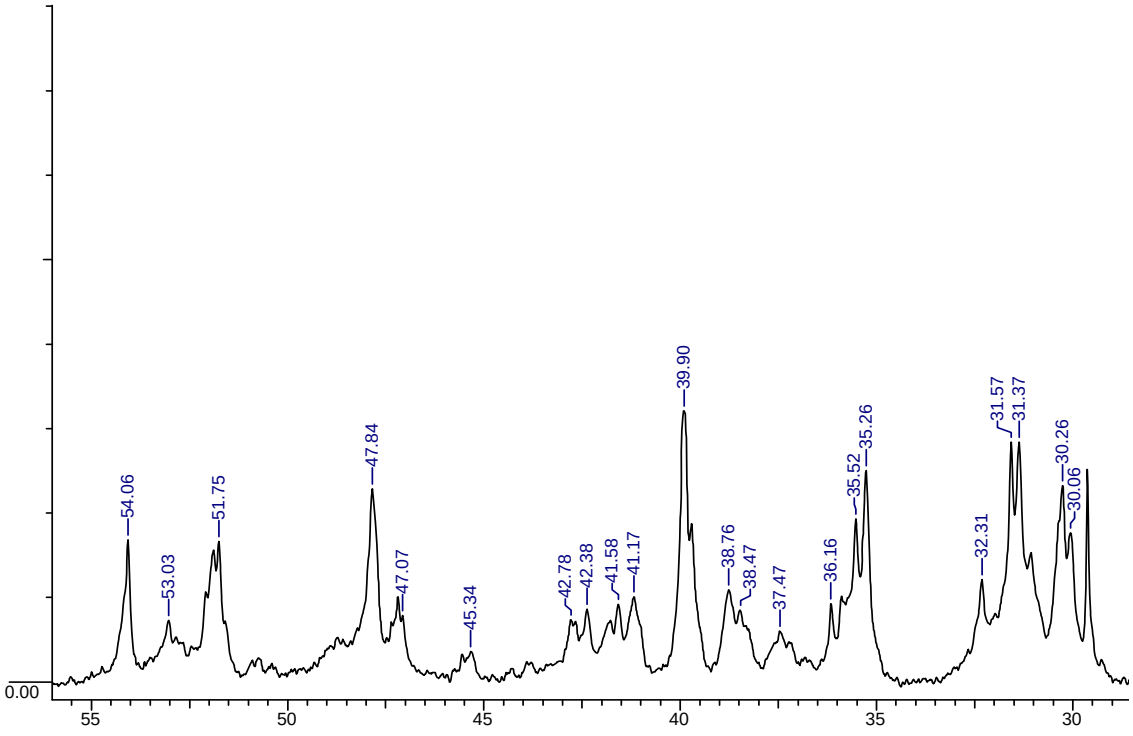

Figure 5.9: ^{13}C NMR spectrum of poly(norbornene)s prepared using **34** at 35°C (Table 5.3, entry 14)

The key observations from this study are summarized below:

The $Pd^{II}Cl_2$ complex (**35)** has a structure similar to the corresponding $Ni^{II}Cl_2$ analog (**30)** (Chapter 4, Fig 4.18). The substituted phenyl ring attached to nitrogen is oriented away from the coordination square plane. A dichloromethane molecule is bound to the crystal lattice offering additional stability to the complexes. $Ni^{II}Cl_2$ and $Ni^{II}Br_2$ complexes (**29-34**) are both active catalysts for the polymerization of norbornene. Highly sterically crowded $Ni^{II}Br_2$ complex with a 2,6-diisopropyl phenyl ring attached to nitrogen exhibits the lowest activity. The analogous $Ni^{II}Cl_2$ complex (**31**) also shows negligible activity. The reactivities of $Pd^{II}Cl_2$ complexes (**35-36**) for norbornene polymerization are independent of the nature of nitrogen substituent and exhibit similar activities which are lower than those exhibited by the nickel (II) chloride analogues. $B(C_6F_5)_3/Et_3Al$ is a

better cocatalyst compared to MAO in case of $Ni^{II}Br_2$ complex (**33)**. The nature of cocatalyst has negligible effect on the $Ni^{II}Cl_2$ complex (**30)**. Poly(norbornene)s synthesized using the Ni (II) and Pd (II) complexes are exclusively vinyl addition products. No evidence of any other mode of polymerization was found.

The order of activity of the $NiCl_2$ and $NiBr_2$ complexes for homopolymerization of norbornene is as follows: **33-30** > **32** > **29** > **34** > **31**. The 3,5-dimethyl phenyl substituted $NiCl_2$ and $NiBr_2$ complexes (**30** and **33**) have more open structure due to relatively smaller bite angles (89^o) which makes the approach of the monomer to the metal coordination site easier. The highly sterically crowded complexes with 2,6-diisopropyl substituent on nitrogen (**31** and **34**) with the highest bite angles of 97^o exhibit the least activity. The substituent on nitrogen is oriented in a manner as to completely block both planes of the coordination complex. Complexes with N-tBu substituents (**29** and **32**) exhibit a polymerization activity in between the above two cases. Both the complexes have a bite angle ~96^o. The nickel bromide complexes are more active than the nickel chloride complexes as alkylation of Ni-Br is more facile.

The obtained poly(norbornene)s, in general, have high molecular weights indicative of the absence of one of the modes of chain transfer ie, β-H elimination. Bredt's rule prevents loss of β-hydrogen in such bicyclic monomers.

The poly(norbornene)s produced by the Ni (II) complexes (**29-34**) readily dissolve in chlorinated organic solvents, presumably, because of their amorphous structure. The polymers synthesized using nickel complexes are known to be erythrodisyndiotactic[18]. Poly(norbornene)s produced by Pd (II) complexes (**35-36**) were found to be insoluble in chlorinated aromatic solvents at 135^oC. Insolubility in poly(norbornene)s have been frequently observed with Pd catalysts[22,26]. Insolubility arises owing to cross-linked structures. These polymers have erythrodiisotactic microstructures[18].

$NiCl_2$(dppp) (**26**) and $PdCl_2$(dppp) (**28**) are less active than the Ni(II) and Pd(II) systems presently studied (**29-36**). Though both types of ligands form six-membered chelates, The C3 ligand back bone in **26** and **28** possibly induces such a geometry around the metal center which makes the metal center less accessible to the monomer. The bite angle in a

$NiCl_2$(dppp) complex (C-C-C) has a value of 91°. The bite angles in the nickel chloride C-N-C systems have values of 89°, 96° and 97° for N-3,5- dimethyl phenyl substituted, N-2,6-diisopropyl phenyl substituted and N-*tert*-butyl substituted complexes, respectively. In view of the above, the lower activities observed for the C-C-C systems remains unexplained.

5.4 Conclusions

A significant improvement in catalyst productivity is observed for vinyl addition polymerization of norbornene when a C3 ligand framework was replaced by a C-N-C ligand framework. This observation is similar to what was observed in the case of ethylene polymerization. Pd (II) complexes showed marginally lower reactivity than their Ni (II) analogues. Best results were obtained with $Ni^{II}Br_2$ complex with a 3,5-dimethyl phenyl substituent on nitrogen. $B(C_6F_5)_3$/TEAL was a better cocatalyst compared to MAO. Poly(norbornene)s produced are 2,3-linked vinyl addition products. There is no evidence of ring-opened products even at higher temperatures of polymerization and higher Al/M ratios.

5.5 References

1. Ivin, K. J.; Mol, J. C. Olefin Metathesis and Metathesis Polymerization, Academic Press, London, **1997**.
2. Kennedy, J. P.; Makowski, H. S. *J. Macromol. Sci., Chem*.**1967**, A1, 345.
3. Gaylord, N. G.; Mandal, B. M.; Martan, M. *J. Polym. Sci., Polym. Lett. Ed.* **1976**, 14, 555.
4. a) Gaylord, N. G.; Deshpande, A. B.; Mandal, B. M.; Martan, M. *J. Macromol. Sci., Chem.* **1977**, A11(5), 1053. b) Gaylord, N. G.; Deshpande, A. B. *J. Polym. Sci., Polym. Lett. Ed.* **1976,** 14, 613.
5. Rush, S.; Reinmuth, A.; Risse, W. *Macromolecules* **1997**, 30, 7375.
6. Seehof, N.; Mehler, C.; Breunig, S.; Risse, W. *J. Mol. Catal*.**1992**, 76, 219.
7. Sartori, G.; Ciampelli, F. C.; Cameli, N.; *Chim. Ind. (Milano*) **1963**, 45, 1478.

8. Tsujino, T.; Saegusa, T.; Furukawa, J. *Makromol. Chem*.**1965**, 85, 71.

9. Goodall, B. L.; McIntosh III, L. H.; Rhodes, L. F. *Makromol.Chem., Macromol. Symp*. **1995**, 89, 421.

10. Lassahn, P. G.; Janiak, C. *Macromol. Rapid. Commun.* **2001**, 22, 479.

11. Kaminsky, W.; Bark, A.; Arndt, M. *Makromol. Chem.,Macromol. Symp*. **1991**, 47, 83.

12. Kaminsky, W.; Noll, A. *Polym. Bull*. **1993,** 31, 175.

13. a) Schultz, R. G. *Polym. Lett*. **1966**, 4, 541. b) US 3330815 (**1967**), Union Carbide Corp. (US), invs.: Mckeon, J. E.; Starcher, P. S. *Chem. Abstr*. **1967**, 67, 64884g.

14. Tanie´lian, C.; Kiennemann, A.; Osparpucu, T. *Can. J. Chem*. **1979**, 57, 2022.

15. a) Sen, A.; Lai, T.-W. *J. Am. Chem. Soc*. **1981**, 103, 4627. b) Sen, A.; Lai, T.-W. *Organometallics*, **1982**, 1, 415.

16. Haselwander, T. F. A.; Heitz, W.; Kru¨gel, S. A.; Wendorff, J. H. *Macromol. Chem. Phys.* **1996**, 197, 3435.

17. Deming, T. J.; Novak, B. M. *Macromolecules* **1993**, 26, 7089.

18. Arndt, M.; Gosmann, M. *Polym. Bull*. **1998**, 41, 433.

19. a) Mast, C.; Krieger, M.; Dehnicke, K.; Greiner, A. *Macromol. Rapid Commun*. **1999**, 20, 232. b) Mast, C.; Krieger, M.; Dehnicke, K.; Greiner, A. *Polym. Mater. Sci. Eng.* **1999**, 80, 423.

20. Janiak, C.; Braun, L.; Scharmann, T. G.; Girgsdies, F. *Acta Crystallogr. C.* **1998**, 54, 1722.

21. US 5912313 (1999), B.F. Goodrich Company, USA, invs.: McIntosh III, L. H.; Goodall, B. L.; Shick, R. A.; Jayaraman; S. *Chem. Abstr*. **1997**, 127, 110414m.

22. Lassahn, P. G.; Janiak, C.; Oh, J. S. *Macromol. Rapid. Commun***. 2002**, 23, 16.

23. a) Massey, A. G.; Park, A. J.; Stone, F. G. A. *Proc. Chem. Soc.* **1963**, 212. b) Massey, A. G.; Park, A. J. *J. Organomet. Chem.* **1964**, 2, 245.

24. Wu, Q.; Lu, Y. *J. Polym Sci Part A: Polym Chem*. **2002**, 40, 1421.

25. Wu, Q.; Lu, Y.; Lu, Z. *Polym Mater Sci Eng*. **1999**, 80, 483.

26. Abu-Surrah, A. S.; Thewalt, U.; Rieger, B. *J. Organomet. Chem.* **1999**, 587, 58.

CHAPTER 6

SILANOLYTIC CHAIN TRANSFER IN ETHYLENE POLYMERIZATION USING bis[N(3-*tert*-butyl salicylidene) 2,3,4,5,6-pentafluoroanilinato]Ti (IV) Dichloride

6.1 Introduction

In-situ introduction of versatile functional groups into nonpolar poly(olefin)s, especially, at chain ends offer a means of constructing a variety of polymer architechtures such as block, and graft multi-arm star polymers[1]. Chain transfer process to organometalloids[2-3] provides an excellent means to achieve this objective since they introduce functionality at chain ends along with control of molecular weight. Silanes are promising candidates for organometalloid chain transfer processes[2]. Marks and coworkers demonstrated that hydrosilylation and polymerization could be coupled to afford silyl-capped polyolefins. The mechanism involves rapid irreversible insertion of olefin into Ln-H bond followed by Ln-C/Si-H transposition[4] (**Scheme 6.1 and 6.2**).

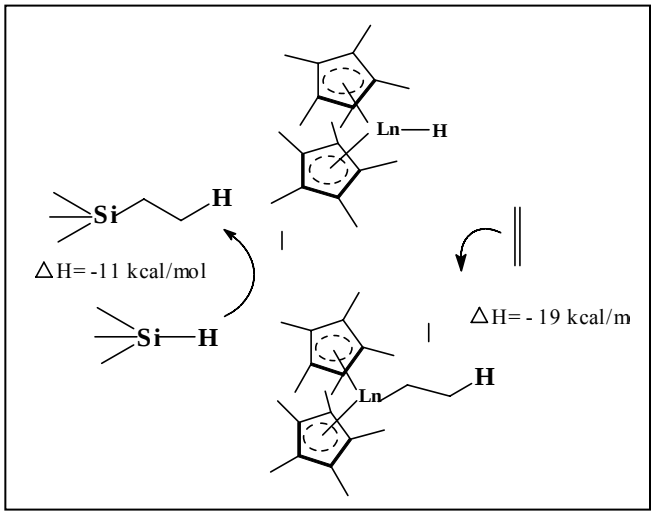

Scheme 6.1: Proposed mechanism for organolanthanide catalyzed olefin hydrosilylation

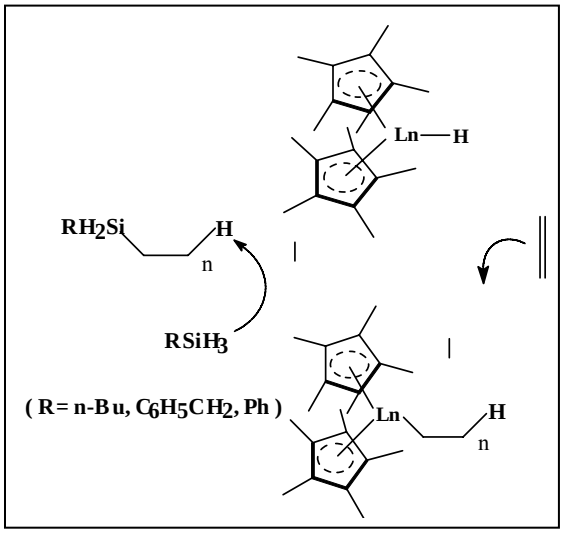

Scheme 6.2: Proposed mechanism for the formation of silyl-capped poly-olefins

Use of $PhSiH_3$, n-$BuSiH_3$ and $C_6H_5CH_2SiH_3$ as chain transfer agents in organolanthanide catalyzed alpha-olefin polymerizations and copolymerizations have been reported to yield families of new silapolyolefins[2b]. The reaction of $Me_2Si(Me_4C_5)_2LnCH(SiMe_3)_2$ (**1a-d**) (Ln= Sm, Lu, Y, La) with $PhSiH_3$ gives the active polymerization/hydrosilylation catalyst $[Me_2Si(Me_4C_5)_2LnH]_2$ *via* Ln-C/Si-H transposition.

$$Me_2Si(Me_4C_5)_2LnCH(SiMe_3)_2 + PhSiH_3 \longrightarrow \tfrac{1}{2}\,[Me_2Si(Me_4C_5)_2LnH]_2 + PhH_2SiCH(SiMe_3)_2 \quad \text{...(eqn 6.1)}$$

The rate of ethylene polymerization in presence of $PhSiH_3$ was lower than observed with lanthanide metallocene alone. An ideal chain transfer agent, however, should not affect the rate of polymerization. This observation was therefore, attributed to competitive coordination of weakly basic silanes at the Lewis acidic lanthanide olefin activation sites[4].

A variety of zirconium metallocene and quasi-metallocene with a variety of cocatalysts were explored with $PhSiH_3$ as chain transfer agent. However, the reaction led to poly(olefin)s devoid of silyl end caps. Products of dehydrogenative silane coupling were also observed[5,6] (**Scheme 6.3** and **Scheme 6.4**). Supported metallocenes, namely $Cp_2ZrCl_2/SiO_2/MAO$, however resulted in a mixture of silyl-capped (53%) and uncapped (47%) polyethylene with n-hexyl-SiH_3 as a chain transfer agent[7].

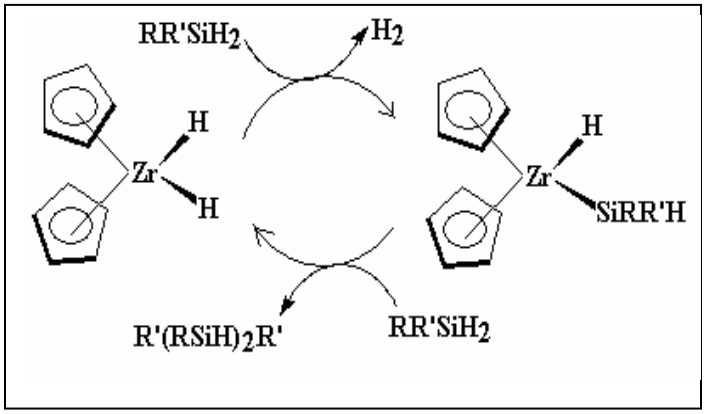

Scheme 6.3: Sigma-bond metathesis mechanism for silane dehydropolymerization

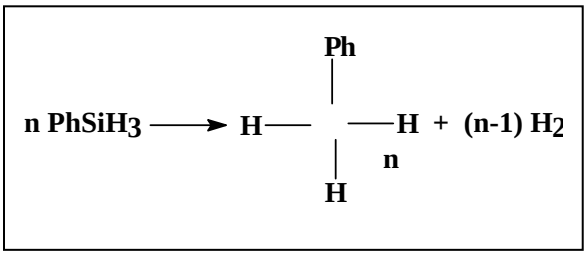

Scheme 6.4: Dehydrogenative silyl coupling

A "constrained geometry catalyst" of the type $[Me_2Si(Me_4C_5)^tBuN]TiMe^+B(C_6F_5)_4^-$, showed high sensitivity to $PhSiH_3$ as chain transfer agent leading to linear, stereoregular and unusual branched silapoly(olefin)s[2d].

$$[Me_2Si(Me_4C_5)^tBuN]TiMe^+B(C_6F_5)_4^- + PhSiH_3 \longrightarrow [Me_2Si(Me_4C_5)^tBuN]TiH^+B(C_6F_5)_4^- + PhMeSiH_2 \quad \text{….(eqn 6.2)}$$

This suggests that coordinatively more open catalysts more readily accommodate incoming chain transfer agents and facilitate the formation of four centered sigma bond metathesis transition state (**2**).

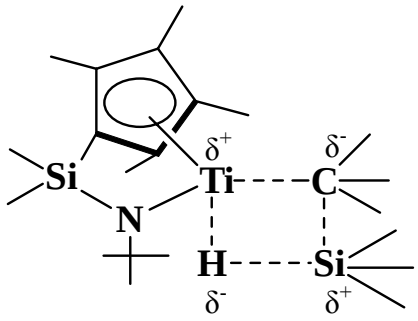

2

The "constrained geometry" $[Me_2Si(Me_4C_5)^tBuN]TiMe^+B(C_6F_5)_4^-$ catalyst mediates rapid polymerization of propylene with efficient silanolytic chain transfer with no detectable silane dehydrocoupling products. Secondary silanes like $PhMeSiH_2$ were also examined for silanolytic chain transfer in organotitanium mediated polymerization of propylene. Highest yield of silapoly(propylene)s were formed at relatively high concentration of the secondary silane. At lower $PhMeSiH_2$ concentrations, β-H elimination is competitive resulting in the formation of a mixture of silyl-capped and uncapped polypropylene. This catalyst also underwent silanolytic chain transfer in the course of hexene-1 polymerization. However, silanolytic chain transfer was not observed during the course of ethylene polymerization[2d]. Vinyl terminated polyethylene was formed by β-H elimination process. Interestingly, ethylene-hexene-1 and ethylene-styrene copolymerizations with high degree of comonomer incorporation was observed in the presence of $PhSiH_3$ with the silicon functionality located predominantly adjacent to 1,2-inserted comonomer units. Sila(polyethylene)s were formed only at -25°C.

Polymerization of propylene with $[Me_2Si(Me_4C_5)^tBuN]TiMe^+B(C_6F_5)_4^-$ in the presence of polyfuncntional silanes like, 1,4-disilabenzene and 1,3,5-trisilabenzene resulted in chain extended and branched poly(propylene)s (**3** and **4**).

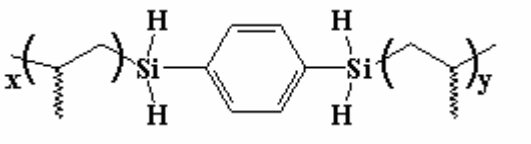

3

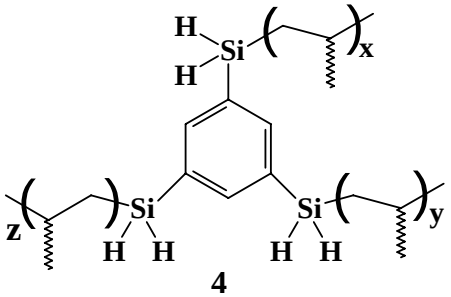

4

Bis-phenoxyimine titanium complexes are an interesting class of organometallic compounds, which exhibit high activity (A = 34000 $gmmol^{-1}$ Ti^{-1} h^{-1} bar^{-1}) for the homopolymerization of ethylene. Furthermore, evidence is available in the literature which indicates that such polymerization may be "living" in nature[8].

However, there are no reports in the literature concerning silanolytic chain transfer with a bis-phenoxyimine Ti (IV) complex. Therefore, a study was undertaken to explore chain transfer reactions with silanes ($PhSiH_3$ and $MePhSiH_2$) using bis[N(3-tert butyl salicylidene)2,3,4,5,6-pentafluoroanilinato]Ti(IV) dichloride (**8**), in conjunction with MAO for the polymerization of ethylene.

6.2 Experimental Methods

Materials used and their methods of purification are described in Chapter 3 under Section 3.2.3, 3.2.5 and 3.3

6.2.1 Synthesis of ligands and complexes

6.2.1.1 Preparation of [N(3-*tert*-butyl salicylidene)]2,3,4,5,6-pentafluoroaniline (6)

Synthesis of the Schiff's base ligand [N(3-*tert* butyl salicylidene)]2,3,4,5,6-pentafluoroaniline was performed according to reported procedures[8].

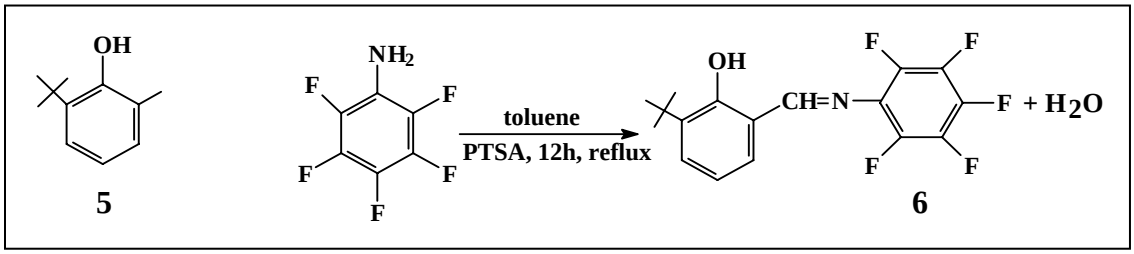

Scheme 6.5: Synthesis of [N(3-*tert* butyl salicylidene)]2,3,4,5,6-pentafluoroaniline (**6**)

In a 100 mL round bottom flask, 1.993g (11.2 mmol) of 3-tertiary butyl salicylaldehyde (**5**) was placed along with 25mLof toluene. 2,3,4,5,6-pentafluoroaniline, 3.00 g (1.5eqv) was added to the flask with a pinch of *p*-toluene sulphonic acid (PTSA). The mixture was refluxed for 12 h and the water of reaction separated using a Dean Stark apparatus. At the end of the reaction toluene was evaporated in vacuo to obtain an orange colored oil. The residue was washed with 5% $NaHCO_3$ solution and purified by column chromatography (basic alumina, 100% pet-ether). The pure compound (**6**) was a crystalline yellow solid (yield: 3.06 g, 80%). ^{1}H NMR spectrum (200 MHz, $CDCl_3$): ∂ 1.46 ppm (9H, s, $C(CH_3)_3$), 6.91, 7.26 and 7.49 ppm (m, 3H, aromatic-H), 8.82 ppm (s, 1H, CH=N), 12.90 ppm (s, 1H, -OH). The spectral data was in agreement with the values reported in the literature[8].

6.2.1.2 Synthesis of bis[N(3-*tert*-butylsalicylidene)2,3,4,5,6-pentafluoroanilinato]Ti(IV) dichloride (8)

Synthesis of bis[N(3-tertbutylsalicylidene)2,3,4,5,6-pentafluoroanilinato]Ti(IV) dichloride (8) was performed according to reported procedures[7].

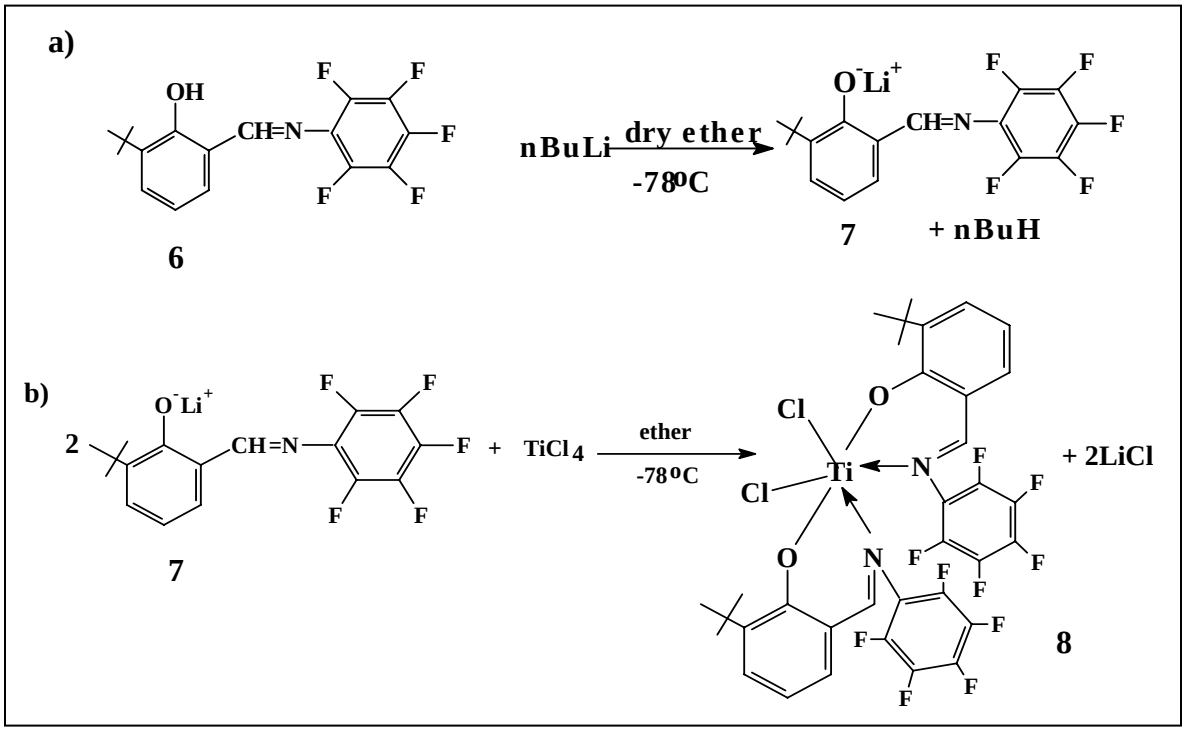

Scheme 6.6: Synthesis of bis [N(3-*tert* butyl salicylidene)2,3,4,5,6-pentafluoroanilinato] Ti(IV) dichloride (**8**)

In a 250 mL round bottom flask equipped with a magnetic stirring bar was placed 4.12 g (16.29 mmol) of the aldimine ligand (**6**) and 30 mL of dry ether. n-BuLi (1.6 M in hexane, 16.29 mmol, 10.2 mL) was added dropwise over a period of 10 min at -78°C. The flask was slowly brought to room temperature and stirred for 2 h. Freshly distilled $TiCl_4$ (0.5 eqv) was taken in a round bottom flask and dissolved in 40 mL of dry ether. The lithiated aldimine solution was added dropwise over 30 min at -78°C to the ether solution of $TiCl_4$. The flask was warmed to 25°C and stirred for 17 h. A dark red colored turbid solution was obtained. A white precipitate of LiCl settled down upon storage. Ether was evaporated in vacuo and the product redissolved in dichloromethane and stirred for 1 h. Precipitated LiCl was filtered through a celite bed and the filtrate was

concentrated in vacuo. Thereafter, dry ether (20 mL) and dry n-hexane (80 mL) were added and the mixture stirred for 90 min. The reddish brown solid thus obtained was separated and washed with n-hexane thrice and dried in vacuo (yield: 3.26 g, 50%). Anal Calcd for $C_{34}H_{26}O_2N_2F_{10}TiCl_2$. 1/3 Et_2O: C, 51.25; H, 3.57; N, 3.38. Found: C, 50.46; H, 3.06; N, 3.20. ^{1}H NMR (200 MHz, $CDCl_3$): δ 1.36 ppm (s, 18H, -$C(CH_3)_3$); 3.47 ppm (1/3 Et_2O); 7.04, 7.30, 7.64 ppm (m, 6 H, aromatic-H) and 8.24 (s, 2H, CH=N) ppm. The spectral data was in agreement with the values reported in the literature[8].

6.2.2 Ethylene Polymerization

The procedure for polymerization of ethylene is described in Chapter 4, Section 4.2.2.1.

6.2.3 Analysis and Characterization

Detailed procedures for performing GPC and ^{1}H NMR spectroscopy have been described in Chapter 3, Section 3.4.1 and 3.4.5

6.3 Results and Discussions

6.3.1 Phenyl silane and methyl phenyl silane as chain transfer agents

The $\overline{Mn}$ of poly(ethylene)s decreased with increasing concentration of phenyl silane (Tp = 25^{o}C) (**Table 6.1**, **entries 1-7, Fig. 6.1**). Similar observation was also made when the polymerization was performed at 0^{o}C (**Table 6.1, entries 8-12, Fig. 6.3**) and at -10^{o}C (**Table 6.1, entries 13-17, Fig. 6.5**). The catalyst activity also showed a decrease with increasing concentration of phenyl silane (**Fig. 6.2**). Phenyl silane concentration in excess of 0.2 M caused complete deactivation of the catalyst at 25^{o}C. Deactivation was also observed for polymerization below room temperature, but at much higher silane concentrations.

Table 6.1: Polymerization of ethylene using **8/MAO** in presence of phenyl silane [a]

Entry	$PhSiH_3$ M	Temp (^oC)	Yield(g)	[b]Activity X 10^{-3}	[c]$\overline{Mn}x10^{-6}$	[c]$\overline{Mw}x10^{-6}$	[c]PDI
1	0	25	0.520	20.8	1.10	1.84	1.7
2	0.03	25	0.494	19.8	1.06	1.69	1.6
3	0.05	25	0.460	18.4	0.99	1.83	1.8
4	0.08	25	0.120	4.8	0.96	1.78	1.8
5	0.10	25	0.232	9.3	0.95	1.92	2.0
6	0.20	25	0.080	3.2	0.61	1.21	2.0
7	0.30	25	-	-	-	-	-
8	0	0	0.240	9.6	0.61	1.10	1.8
9	0.10	0	0.171	6.8	0.54	1.01	1.9
10	0.20	0	0.180	7.2	0.49	0.95	1.9
11	0.30	0	0.136	5.4	0.43	0.81	1.9
12	0.40	0	0.074	3.0	0.42	0.79	1.9
13	0	-10	0.203	8.1	0.57	1.14	2.0
14	0.08	-10	0.120	4.8	0.53	1.00	1.9
15	0.10	-10	0.106	4.2	0.50	0.95	1.9
16	0.20	-10	0.175	7.0	0.48	0.94	2.0
17	0.30	-10	0.080	3.2	0.45	0.93	2.1

[a]Conditions: Toluene = 50 mL , Chain transfer agent = phenyl silane, Cocatalyst = MAO, P_{C2H4}= 1.013 bar, time = 3 min, [Ti] = 0.5 µmol, Al/Ti = 2500, Temperature = 25°C
[b]gPE $mmol^{-1}$ Ti^{-1} h^{-1} bar^{-1} [c]GPC studies in trichlorobenzene at 135°C

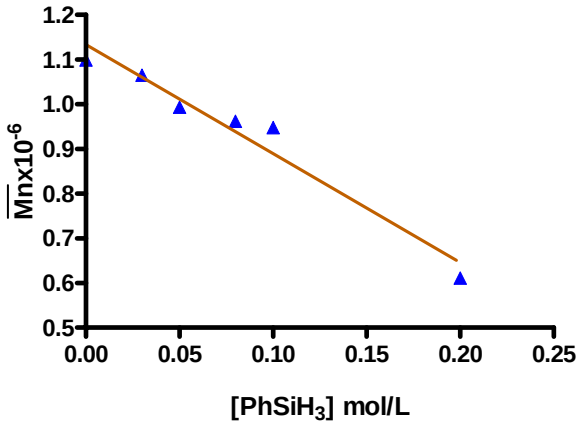

Figure 6.1: Relationship of $\overline{Mn}$ of poly(ethylene)s to concentration of phenyl silane at 25°C

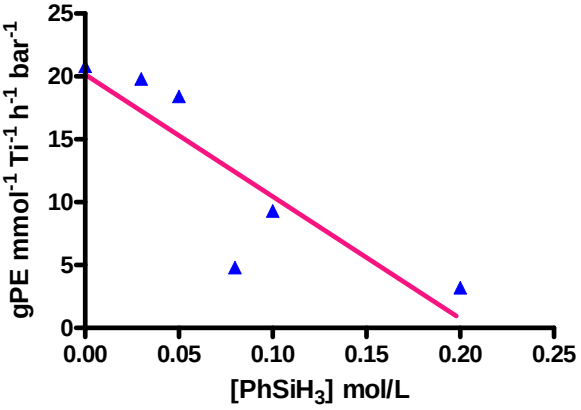

Figure 6.2: Catalyst activity as a function of molar concentration of $PhSiH_3$ at 25°C

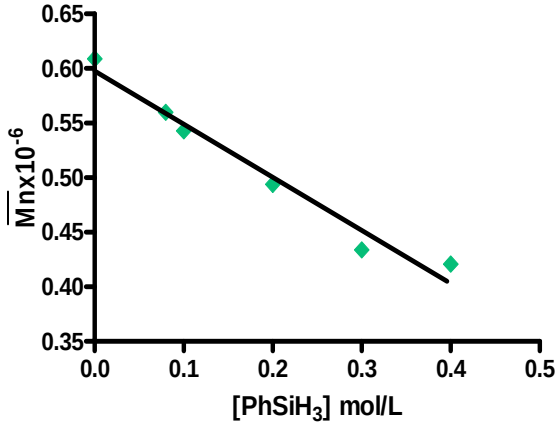

Figure 6.3: Relationship of $\overline{Mn}$ of poly(ethylene)s to concentration of phenyl silane at 0^{o}C

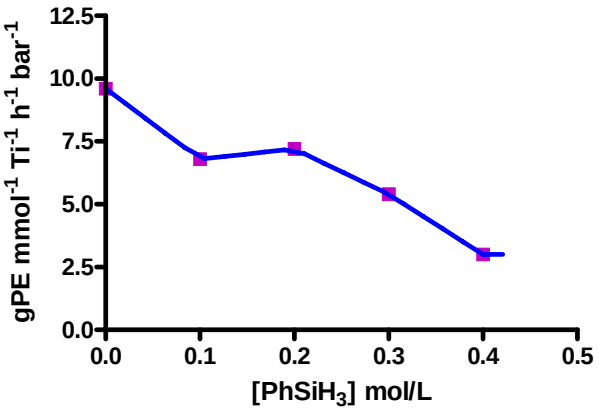

Figure 6.4: Catalyst activity as a function of molar concentration of $PhSiH_3$ at 0^{o}C

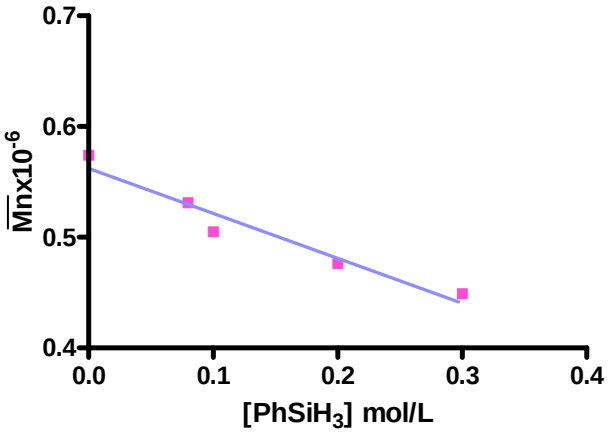

Figure 6.5: Relationship of $\overline{Mn}$ of poly(ethylene)s to concentration of phenyl silane at -10^{o}C

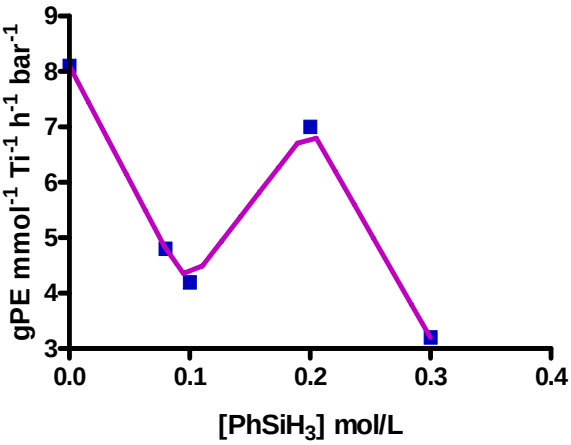

Figure 6.6: Catalyst activity as a function of molar concentration of $PhSiH_3$ at -10^{o}C

Use of a secondary silane like $MePhSiH_2$ also depressed the number average molecular weight and catalyst activity for ethylene polymerization. **Table 6.2** gives the results of polymerization of ethylene using $MePhSiH_2$ as chain transfer agent at 0^{o}C.

Table 6.2: Polymerization of ethylene using **8/MAO** in presence of methyl phenyl silane[a]

Entry	$MePhSiH_2$ M	Yield (g)	[b]Activity X 10^{-3}	[c]$\overline{Mn}$ x 10^{-6}	[c]$\overline{Mw}$ x 10^{-6}	[c]PDI
1	0	0.240	9.6	0.60	1.10	1.8
2	0.075	0.160	6.4	0.57	1.08	1.9
3	0.15	0.175	7.0	0.54	0.97	1.8
4	0.20	0.255	10.2	0.52	0.93	1.8
5	0.30	0.073	2.9	0.47	0.87	1.8

[a]Conditions: Toluene = 50 mL , Chain transfer agent = methyl phenyl silane, Cocatalyst = MAO, P_{C2H4} = 1.013 bar, time = 3 min, [Ti] = 0.5 µmol, Al/Ti = 2500, Temp = 0°C [b]gPE $mmol^{-1}$ Ti^{-1} h^{-1} bar^{-1} [c]GPC studies in trichlorobenzene at 135°C

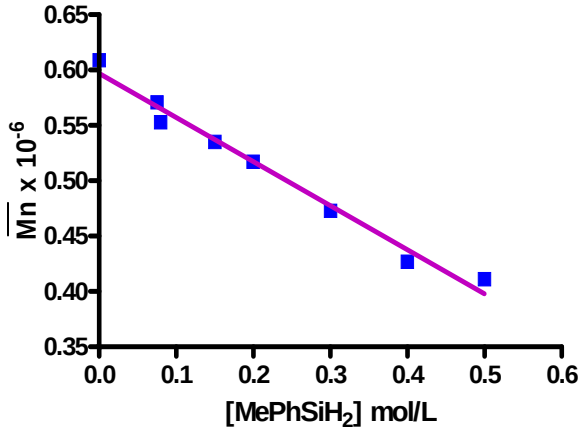

Figure 6.7: Relationship of $\overline{Mn}$ of poly(ethylene)s to concentration of methyl phenyl silane at 0°C

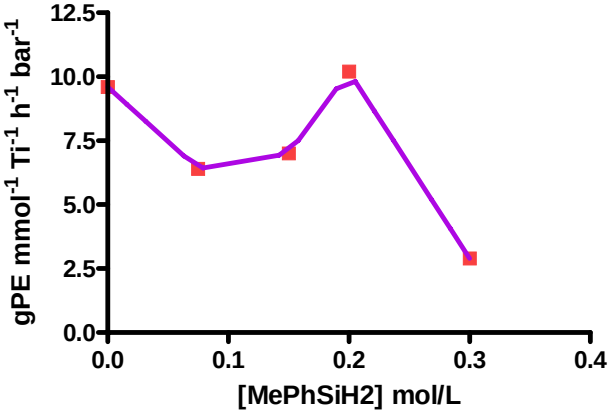

Figure 6.8: Catalyst activity as a function of molar concentration of $MePhSiH_2$ at 0°C

In principle, catalyst activity should show no dependence on silane concentration. Interestingly, at a silane concentration of 0.2 M, and at lower temperatures (0°C, -10°C) a peak in catalyst activity is observed both with $PhSiH_3$ and $MePhSiH_2$ (**Fig. 6.4**, **6.6** and **6.8**). Similar observations have been made with organolanthanide and Ti-CGC mediated silanolytic chain transfer processes[2b, 2d]. The reason for this observation is not apparent at present.

6.3.2 Effect of chain transfer agent ($PhSiH_3$ and $MePhSiH_2$) on overall rate of polymerizations (Rp)

The kinetic profiles of catalyst **8/MAO** for the polymerization of ethylene in the presence and absence of chain transfer agents are shown in **Fig. 6.9**.

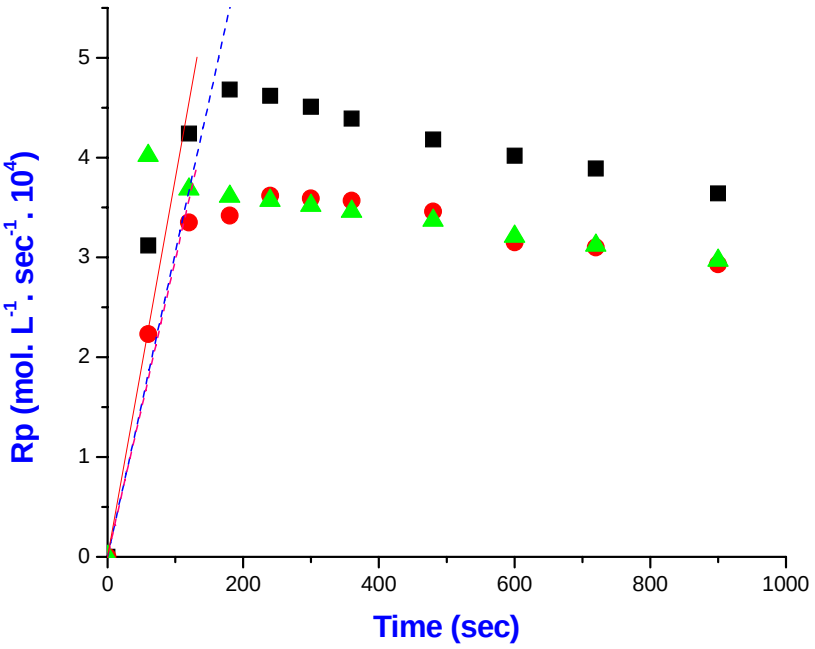

Figure 6.9: Catalyst activity as a function of reaction time for **8** (■) no chain transfer agent, (●) 0.2 M $PhSiH_3$, (▲) 0.2 M $MePhSiH_2$

The initial Rp values were calculated from linear extrapolation of the initial rate values in the ascending part of the kinetic curves. It is seen that the initial rates are similar and are not affected by the nature of chain transfer agents.

6.3.3 Determination of chain transfer constants

The bis-phenoxy imine titanium catalyst **8** is reported to polymerize ethylene without any significant transfer reactions[8]. Based on this assumption and considering that chain transfer to silanes is the only operative chain transfer mechanism, chain transfer constants were estimated using a Mayo plot (**Fig. 6.10 - 6.13**, **eqns 6.3 and 6.4**).

$$1/\overline{DP}n = \frac{(1 + \Lambda) < k_t > [R^*]}{k_p [M]} + C_M + C_S \frac{[S]}{[M]} \qquad \textbf{(eqn 6.3)}$$

$\overline{DP_n}$ = no average degree of polymerization**,** $< k_t >$ = average termination rate coefficient

[R*] = total radical concentration, k_p= propagation rate coefficient

[M] = monomer concentration, [S] = chain transfer agent concentration

C_M = chain transfer to monomer constant, C_S = chain transfer to transfer agent const

Λ = fraction of chains undergoing disproportionation reactions

If the last term in the equation dominates, then, $1/DPn = C_S \frac{[S]}{M}$ **(eqn 6.4)**

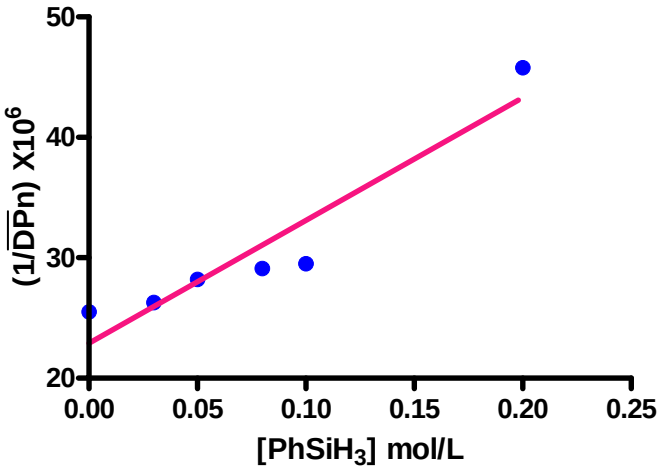

Figure 6.10: Number average degree of polymerization as a function of $PhSiH_3$ concentration at 25°C (Table 6.1, entries 1-6)

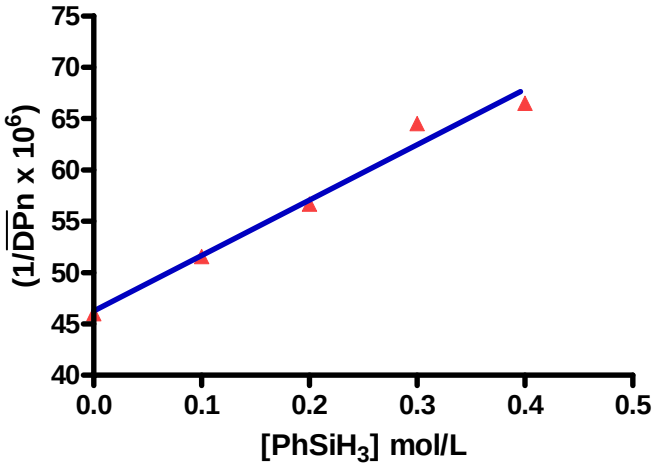

Figure 6.11: Number average degree of polymerization as a function of $PhSiH_3$ concentration at 0^oC (Table 6.1, entries 8-12)

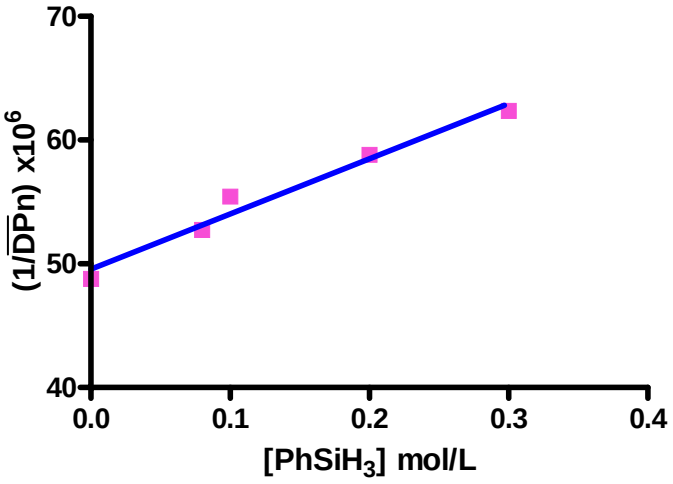

Figure 6.12: Number average degree of polymerization as a function of $PhSiH_3$ concentration at -10^oC (Table 6.1, entries 13-17)

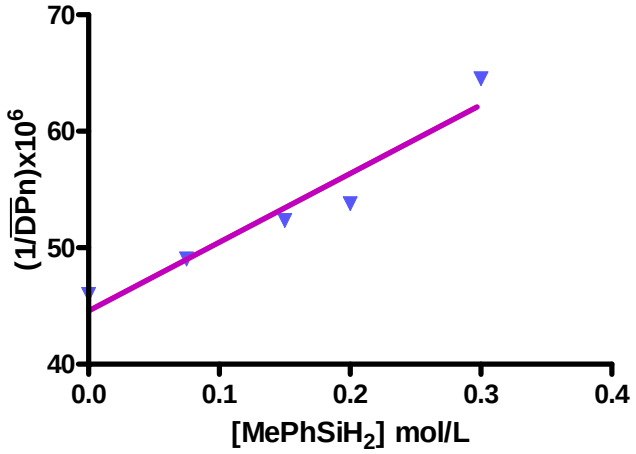

Figure 6.13: Number average degree of polymerization as a function of $MePhSiH_2$ concentration at 0^oC (Table 6.2, entries 1-5)

The chain transfer constants (Cs) obtained are shown in **Table 6.3**.

Table 6.3: Comparison of chain transfer constant values

Catalyst	Silane	Temp (^oC)	Cs
8	$PhSiH_3$	25	102
8	$PhSiH_3$	0	54
8	$PhSiH_3$	-10	45
8	$MePhSiH_2$	0	59
[a]$[Me_2Si(Me_4C_5)^tBuN]TiMe^+B(C_6F_5)_4^-$	$PhSiH_3$	25	35
[b]$Me_2Si(Me_4C_5)_2SmCH(SiMe_3)_2$	$PhSiH_3$	25	130

[a]propylene polymerization[2d]; [b]Ref 2b

The chain transfer constants for $PhSiH_3$/**8** are comparable to that reported for a Samarium based catalyst.

6.3.4 Polymer characterization

NMR spectroscopy

In order to detect silyl end groups in poly(ethylene)s by NMR spectroscopy, attempts were made to prepare low molecular weight poly(ethylene)s. Using a concentration of 20 μmol of **8**, [$PhSiH_3$] = 0.3 M, Al/Ti = 2500, temperature = 0^oC and reaction time of 20 seconds, a polymer with a $\overline{Mv}$ = 48, 300 was obtained. The ^1H NMR spectra of the above polymer (500 MHz, $C_2D_2Cl_4$, 130^oC) did not reveal the presence of silyl end groups. Further attempts to reduce the molecular weight were not fruitful.

From the foregoing study it is apparent that silanes are able to depress the molecular weight of the obtained poly(ethylene)s implying a silyl transfer reaction. However, since adequately low molecular weight poly(ethylene)s could not be prepared, no direct structural evidence could be obtained for a silyl end capped polyethylene. The Mayo plots were reasonably linear, implying that chain transfer to silicon is the most dominant chain transfer process. The value of Cs was also high and comparable to what has been observed earlier with Sm catalysts.

However, in the absence of structural evidence, the precise mechanism and the relative importance of silanolytic versus hydrogen transfer reactions under these conditions remain ambiguous.

Silanes also appear to diminish polymerization activity implying unfavorable interaction between silanes and the active chain end. However, at 0^o and -10^oC, and at 0.2 M concentration, silanes caused an increase in polymerization activity. The reason for this observation is not clear.

6.4 Conclusions

Phenyl silanes depress the molecular weight of poly(ethylene)s obtained using Bis[N(3-*tert*-butylsalicylidene)2,3,4,5,6-pentafluoroanilinato]Ti(IV) dichloride/ MAO catalyst systems. Number average degree of polymerization showed a linear

dependence on the concentration of the chain transfer agent implying that the silanolytic transfer was the dominant transfer process. However, direct structural evidence of the incorporation of silicon group in polymer could not be obtained.

6.5 References

1. Reviews of functionalized polymers: a) Ittel, S. D.; Johnson, L. K.; Brookhart, M. *Chem. Rev.* **2000**, 100, 1169-1204. b) Boffa, L. S.; Novak, B. M. *Chem. Rev.* **2000**, 100, 1479.
2. Chain transfer to silanes: a) Koo, K.; Marks, T. J. *CHEMTECH* **1999**, 13-19. b) Koo, K.; Fu, P.-F.; Marks, T. J. *Macromolecules* **1999**, 32, 981. c) Koo, K.; Fu, P. -F.; Marks, T. J. *J. Am. Chem. Soc.* **1999**, 121, 8791. d) Koo, K.; Fu, P. -F.; Marks, T. J. *J. Am. Chem. Soc.* **1998**, 120, 4019. e) Fu, P. -F.; Marks, T. J. *J. Am. Chem. Soc.* **1995**, 117, 10747.
3. Chain transfer to boranes: a) Xu, G.; Chung, T. C. *Macromolecules* **1999**, 32, 8689. b) Xu, G.; Chung, T. C. *J. Am. Chem. Soc.* **1999**, 121, 6763.
4. Fu, P. –F.; Brard, L.; Li, Y.; Marks, T. J. *Organometallics* **1995**, 117, 7157.
5. a) Yang, X.; Stern, C. L.; Marks, J. T. *J. Am. Chem. Soc.* **1994**, 116, 10015. (b) Jia, L.; Yang, X.; Stern, C. L.; Marks, T. J. *Organometallics* **1997**, 16, 842.
6. (a) Harrod, J. F.; Dioumaev, V. K. *J. Organomet. Chem.* **1996**, 521, 133. (b) Tilley, T. D. *Acc. Chem. Res.* **1993**, 26, 22 and references therein. (c) Corey, J.Y.; Huhmann, J. L.; Zhu, X.-H. *Organometallics* **1993**, 12, 1121 and references therein.
7. Makio, H.; Koo, K.; Marks, T. J. *Macromolecules* **2001**, 34, 4676.
8. Mitani, M.; Mohri, J.; Yoshida, Y.; Saito, J.; Ishii, S.; Tsuru, K.; Matsui, S.; Furuyama, R.; Nakano, T.; Tanaka, H.; Kojoh, S-i.; Matsugi, T.; Kashiwa, N.; Fujita, T. *J. Am. Chem. Soc.* **2002**, 124, 3327.

CHAPTER 7

POLYMERIZATION OF STYRENE WITH BIS-PHENOXYIMINE TITANIUM COMPLEXES

7.1 Introduction

Syndiotactic poly(styrene)s was first prepared in 1985[1]. Since then, many different titaniumcomplexes have been reported for the preparation of syndiotactic poly(styrene)s. Monocyclopentadienyltitanium (IV) complexes exhibit the highest catalyst activities and lead to poly(styrene)s with high degrees of syndiotacticity[2]. Non-metallocene complexes have also been reported for the syndio specific polymerization of styrene[3], e.g., bridged (bisphenolato)titanium dichloride complexes[4], β-diketonato, β-dinaphtholato, 8-hydroxyquinolatotitanium complexes[5] and titanium monoamidinate compounds[6].

Okuda and coworkers polymerized styrene using a series of MAO activated bis(phenolato)titanium complexes of the type $\{(OC_6H_2\text{-}4\text{-}Me\text{-}6\text{-}tBu)_2Z\}TiX_2$ (X = Cl, OiPr, η^5-C_5Me_5) (**1, 2**) to give syndiotactic poly(styrene)s[4].

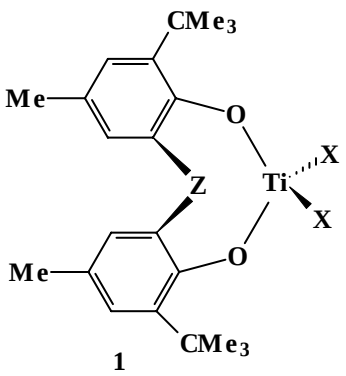

1

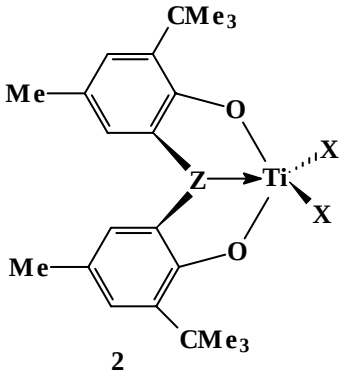

2

Z = CH_2 (mbmp) (a)
CH_2CH_2 (ebmp) (b)

X = Cl, O*i*Pr, n^5-C_5Me_5

Z = S (tbmp) (a)
S=O(sibmp) (b

A significant dependence on the nature of the titanium complex on activity was observed. Both the bis(phenolato)ligand and the ancillary ligands appear to influence the polymerization activity. Bridges other than methylene (Z = CH_2) or ethylene (Z = CH_2CH_2) for the phenolato units tend to form more active catalyst. The most active catalyst was (ebmp)Ti(Cl)(Cp*) (A = 3800 gPS $mmol^{-1}$ Ti^{-1} h^{-1}) which probably acted as a source for the [Cp*TiR]+ unit. The polystyrene obtained was > 95% syndiotactic.

Isotactic polystyrene, known for almost half a century and initially noted for its crystallinity, is still best produced by heterogeneous Ziegler–Natta catalysis. Isotactic polystyrene has a low crystallization rate. Examples of single-site organometallic catalysts for isotactic polystyrene are rare in the literature[7].

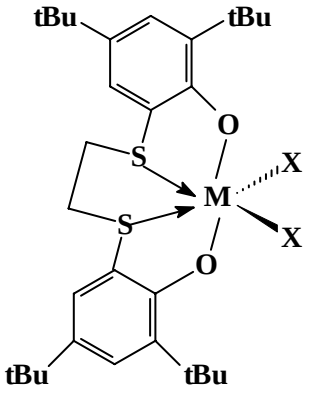

3a MX_2 = $TiCl_2$
3b MX_2 = $Ti(O^iPr_2)$

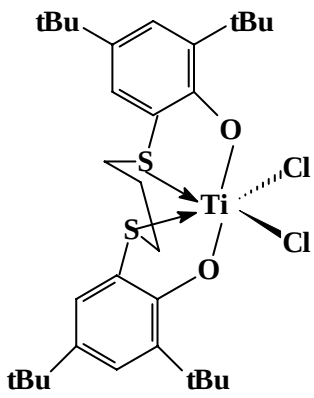

4

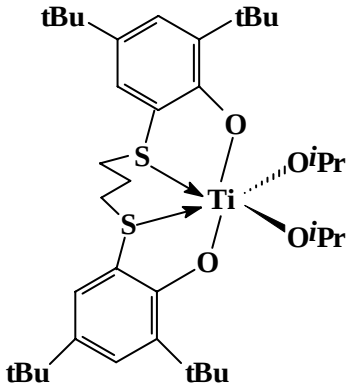

5

Upon activation with MAO, titanium, zirconium and hafnium complexes were found to be active for isospecific styrene polymerization. The 1,5-dithiapentane-bridged complexes **4** and **5** were one order of magnitude less active than the 1,4-dithiabutanebridged derivatives **3a** and **3b**. The highest activity observed was 1543 gPS $mmol^{-1}$ Ti^{-1} h^{-1} exhibited by the titanium dichloride complex **3a**.

Group 4 metal amidinates, in presence of MAO, provide homogeneous catalytic systems for the polymerization of a variety of hydrocarbon monomers, namely, ethylene, propylene, 1,3-butadiene, and styrene[8,9]. Titanium monoamidinate trihalides ($ATiX_3$) and MAO polymerize styrene to highly syndiotactic polymer. Zambelli and coworkers reported a series of titanium monoamidinate trihalides (**6a-f**), capable of syndiospecific polymerization of styrene[6].

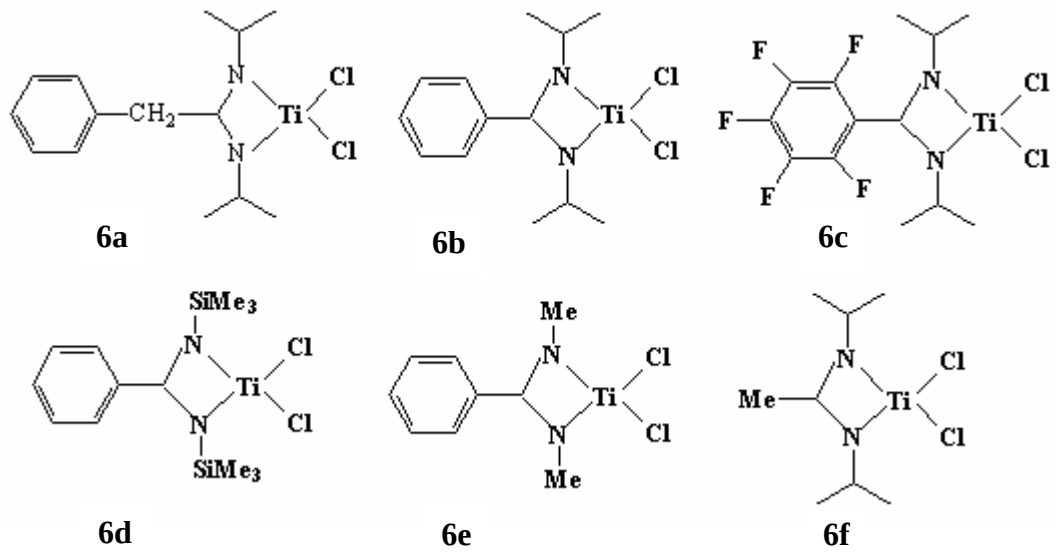

Schiff-base metal complexes have attracted attention on account of their ease of synthesis and the diversity of structures that can be accessed. The two reactive Ti–Cl bonds in a titanium salen-type [salen = N,N'-ethylenebis(salicylideneiminato)] complex can be easily alkylated, an important step in the formation of active species for polymerization. The first example of a titanium salen complex as catalyst precursor (**7a-e**) for the syndiospecific polymerization of styrene was reported only recently[10].

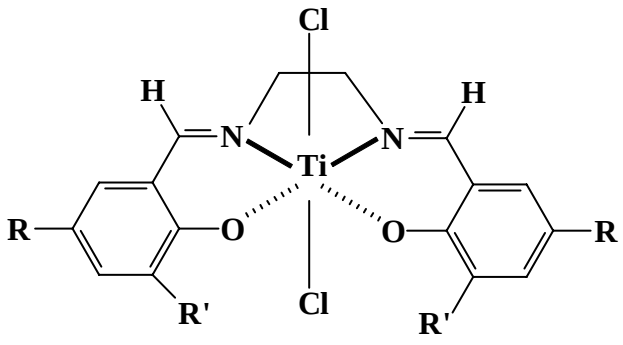

7

7a. R = R' = H
7b. R = H, R' = tBu
7c. R = R' = Me
7d. R = R' = tBu
7e. R = Me, R' = H

Change of the steric bulk of the substituents on the aryl ring had an influence on the degree of syndiospecificity. The catalytic activity was in the range of 10-20 gPS $mmol^{-1}$ Ti^{-1} h^{-1} using an [Al]/[Ti] ratio of 500 at 70°C. Compound **7d**, bearing an aryl group with bulky ^{t}Bu substituents, showed higher activity than the sterically less hindered complex

7a. All compounds bearing an alkyl substituent in the ortho position of the aryl ring showed high syndiospecificity. However, compound **7a** yielded low-molecular-weight atactic poly(styrene)s with no melting peak. Sterically more hindered complexes **7b** and **7d** yielded poly(styrene)s with higher syndiospecificity than complexes **7c** and **7e**. These results demonstrate that the presence of bulky substituents at the ortho position of the aryl ring in titanium salen is an important structural requirement that influences stereospecificity of styrene polymerization.

Organometallic Ni complexes (**8a-d**) are also reported to be active in the polymerization of styrene[11].

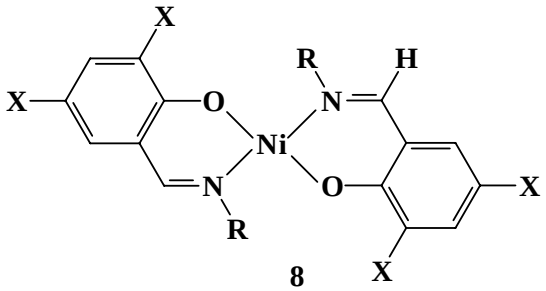

8

8a. X = H, R = iPr
8b. X = H, R = 2,6-(iPr $_2$)C$_6$H$_3$
8c. X = NO$_2$, R = 2,6-(iPr $_2$)C$_6$H$_3$
8d. X = NO$_2$, R = Ph

8a and **8b** in combination with MAO are active catalysts for styrene polymerization. However, they yield only low molecular weight poly(styrene)s. The higher activity of **8b (**39 gPS mmol^{-1} Ni^{-1} h^{-1}) than **8a** (17.5 gPS mmol^{-1} Ni^{-1} h^{-1}) can be ascribed to the nature of steric constraints at the metal center and the relative basicity of the aldimine nitrogen when, either, an alkyl group or a substituted phenyl ring is bound to nitrogen. Complexes **8c** and **8d** bearing a 2,4-dinitro substituent on the aryl ring showed higher catalytic activity (225 gPS mmol^{-1} Ni^{-1} h^{-1}). Complex **8d** led to poly(styrene)s with lower molecular weight than **8c**. Presumably, steric factors around the metal atom play a critical role in determining the relative rates of chain growth and transfer steps.

Group IV bis(phenoxyimine) complexes are examples of Group IV complexes bearing salicylaldiminato ligands capable of polymerizing ethylene with extremely high activity[12-16]. These complexes have also been employed for the polymerization of propylene, norbornene and higher α-olefins[17]. One of the notable features of the fluorinated Ti catalysts is the "living" syndiospecific polymerization of propylene. Isotactic propylene polymerization was observed with the zirconium and hafnium complexes.

Very recently, a preliminary study of the polymerization of styrene has been reported with Group IV bis(phenoxyimine) complexes[18]. The effect of ligand structure was investigated. The fluorinated complexes (viz, bis [N(3-*tert*-butyl salicylidene)2,3,4,5,6-pentafluoroanilinato]Ti (IV) and bis[N(3-trimethyl silyl salicylidene)2,3,4,5,6-pentafluoroanilinato]Ti (IV) in conjunction with dried MAO at 20^{o}C gave predominantly isotactic poly(styrene)s, whereas the non-fluorinated complexes gave mainly syndiotactic polymers. Interestingly, the fluorinated complex, bis[N(3-trimethyl silyl salicylidene)2,3,4,5,6-pentafluoroanilinato]Ti (IV), gave a mixture of syndio- and isotactic poly(styrene)s at a polymerization temperature of 40^{o}C and exclusively sydiotactic poly(styrene) when premixed with dried MAO at 40^{o}C. The reason behind different stereoregularities exhibited by these catalysts remains unclear.

The influence of the structure of bis(phenoxyimine) titanium (IV) complexes on the polymerization of styrene is examined in this chapter. The role of increasing fluorine atoms on the N-aryl ring on polymerization activity and stereoregularity was investigated. Accordingly, four different fluorinated and non-fluorinated bis(phenoxyimine) titanium complexes viz, bis[N(3-*tert*-butyl salicylidene)anilinato]Ti (IV) dichloride (**9a**), bis [N(3-*tert*-butyl salicylidene)2,6-difluoroanilinato]Ti (IV) dichloride (**9b**), bis[N(3-*tert*-butyl salicylidene)2,4,6-trifluoroanilinato]Ti (IV) dichloride (**9c**) and bis [N(3-*tert*-butyl salicylidene)2,3,4,5,6-pentafluoroanilinato]Ti (IV) (**9d**) were prepared. With increasing fluorine atoms, the electrophilic character of the titanium center is expected to increase in the order **9d** > **9c** > **9b** > **9a**. Of these, **9a** and **9d** have been recently investigated by

Fujita and coworkers[18]. The microstructure of poly(styrene)s formed was studied using high temperature ^{13}C NMR spectroscopy.

7.2 Experimental Methods

Materials used and their methods of purification has been described in Chapter 3 under Sections 3.2.4, 3.2.5 and 3.3

7.2.1 Synthesis of ligands and complexes

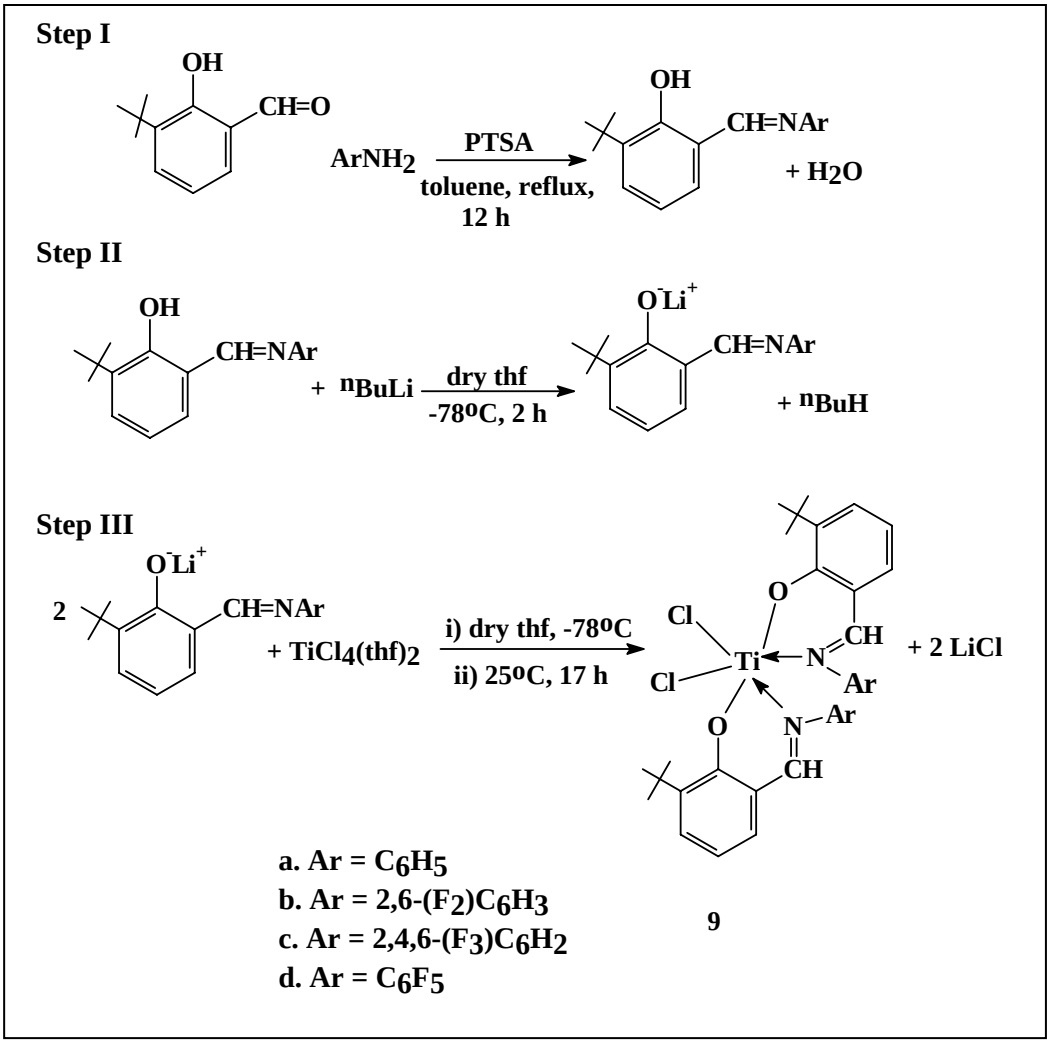

Scheme 7.1: Synthesis of ligands and titanium complexes (**9a-d**)

7.2.1.1 Preparation of Schiff's base of 3-tert-butyl salicylaldehyde and aniline (Scheme 7.1)

In a round bottom flask 3.1758 g (0.0178 mol) of 3- tertiary-butyl salicylaldehyde was placed along with 30 mL of toluene. Freshly distilled aniline, 4.06 mL (2.5 eqv) was added along with a pinch of *p*-toluene sulphonic acid. The mixture was refluxed for 12 h and the water of reaction separated using a Dean Stark apparatus. At the end of the reaction, toluene was evaporated in vacuo to obtain an orange colored oil. The crude product was purified by distillation using a Kugel Rohr apparatus (0.2 mbar). TLC of the resultant product showed a single spot. (yield: 3.83 g, 85%). ^{1}H NMR ($CDCl_3$, 200 MHz, 25°C): δ 1.40 (s, 9H, -C(CH_3)$_3$); 6.80, 7.17, 7.36, (m, 8H, aromatic H); 8.55 (s, 1H, CH=N); 13.83 (s, 1H, -OH) ppm.

7.2.1.2 Preparation of Schiff's base of 3-*tert*-butyl salicylaldehyde and 2,6-difluoroaniline (Scheme 7.1)

In a 100 mL round bottom flask, 3.005 g (0.0169 mol) of 3-tertiary butyl salicylaldehyde was placed along with 30 mL of toluene. 2,6-difluoroaniline, 2.7 mL (1.5 eqv) was added along with a pinch of p-toluene sulphonic acid. The mixture was refluxed for 12 h and the water of reaction separated using a Dean Stark apparatus. After the end of the reaction, toluene was evaporated in vacuo to obtain an orange colored oil. The crude product was purified by distillation using a Kugel Rohr apparatus (0.2 mbar). The ^{1}H NMR of the orange oil showed the presence of unreacted aldehyde. The compound was further purified by column chromatography (basic alumina, 100% petroleum ether). The pure compound was a crystalline orange-yellow solid (yield: 3.90 g, 80%). ^{1}H NMR ($CDCl_3$, 200 MHz, 25°C): δ 1.54 (s, 9H, -C(CH_3)$_3$); 6.95, 7.09, 7.33, 7.50 (m, 6H, aromatic H); 8.93 (s, 1H, CH=N); 13.58 (s, 1H, -OH) ppm.

7.2.1.3 Preparation of Schiff's base of 3-*tert*-butyl salicylaldehyde and 2,4,6-trifluoroaniline (Scheme 7.1)

In a 100 mL round bottom flask, 2.005 g (0.01125 mol) of 3-tertiary butyl salicylaldehyde was placed along with 30 mL of toluene. 2,4,6-trifluoroaniline, 2.33 g (1.5 eqv) was added along with a pinch of p-toluene sulphonic acid. The mixture was refluxed for 12 h and the water of reaction separated using a Dean Stark apparatus. After the end of the reaction, toluene was evaporated in vacuo to obtain an orange colored oil. The oil was washed with 5% $NaHCO_3$ solution to remove p-toluene sulphonic acid. The crude compound was then purified by column chromatography (basic alumina, 100% petroleum ether). The pure compound was a crystalline yellow solid (yield: 2.59 g, 75%). ^{1}H NMR ($CDCl_3$, 200 MHz, 25°C): δ 1.37 (s, 9H, -C(CH_3)$_3$); 6.68, 6.80, 7.14, 7.35 (m, 5H, aromatic H); 8.75 (s, 1H, CH=N); 13.28 (s, 1H, -OH) ppm.

7.2.1.4 Preparation of Schiff's base of 3-*tert*-butyl salicylaldehyde and 2,3,4,5,6-pentafluoroaniline (Scheme 7.1)

This has been described in Chapter 6, under section 6.2.1.1.

7.2.1.5 Preparation of bis [N(3-*tert*-butyl salicylidene)anilinato]Ti (IV) dichloride (9a, Scheme 7.1)

In a round bottom flask was placed 4.1209 g (16.29 mmol) of N(3-*tert*-butyl salicylidene)aniline and dissolved in 30 mL of dry tetrahydrofuran. n-BuLi (1.6 M in hexane) (16.29 mmol, 10.2 mL) was added dropwise over a period of 10 min at -78°C. The flask was slowly brought to room temperature and stirred for 2 h. $TiCl_4(thf)_2$ (0.5 eqv, 2.72 g) was placed in a round bottom flask and dissolved in 40 mL dry tetrahydrofuran. The lithiated aldimine solution was added dropwise over 30 min at –78°C to the THF solution of $TiCl_4(thf)_2$. The flask was warmed to 25^{o}C and allowed to stir for 17 h. A dark red colored turbid solution was obtained. A white precipitate of LiCl

settled down on storage. THF was evaporated in vacuo and the product redissolved in dichloromethane and allowed to stir for 1 h. Precipitated LiCl was filtered through a celite bed and the filtrate was concentrated in vacuo. Upon addition of hexane (4 times its volume) a solid precipitated out. The solid was separated and redissolved in 2-3 mL of dichloromethane and reprecipitated from hexane. The red-brown solid thus obtained was dried in vacuo to obtain the titanium complex **9a** (yield: 2.75 g, 55%). ^{1}H NMR ($CDCl_3$, 200 MHz, 25°C): δ 1.34 (s, 18H, -C$(CH_3)_3$); 6.75-7.64 (m, 16H, aromatic H); 7.92-8.07 (s, 2H, CH=N); ppm. Anal Calcd for $C_{34}H_{36}O_2N_2TiCl_2$: C, 65.29: H, 6.08; N, 4.48. Found: C, 65.77; H, 6.64; N, 4.52.

7.2.1.6 Preparation of bis [N(3-*tert*-butyl salicylidene)2,6-difluoroanilinato]Ti (IV) dichloride (9b, Scheme 7.1)

In a round bottom flask was placed 0.994 g (3.44 mmol) of N(3-*tert*-butyl salicylidene)2,6-difluoroaniline and dissolved in 30 mL of dry tetrahydrofuran. n-BuLi (1.6 M in hexane) (3.44 mmol, 2.15 mL) was added dropwise over a period of 10 min at –78°C. The flask was slowly brought to room temperature and stirred for 2 h. $TiCl_4(thf)_2$ (0.5 eqv, 0.574 g) was placed in a round bottom flask and dissolved in 40 mL dry tetrahydrofuran. The lithiated aldimine solution was added dropwise over 30 min at –78°C to the THF solution of $TiCl_4(thf)_2$. The flask was warmed to 25^{o}C and allowed to stir for 17 h. A dark red colored turbid solution was obtained. A white precipitate of LiCl settled down on storage. THF was evaporated in vacuo and the product redissolved in dichloromethane and allowed to stir for 1 h. Precipitated LiCl was filtered through a celite bed and the filtrate was concentrated in vacuo. Upon addition of hexane (4 times its volume) a solid precipitated out. The solid was separated and redissolved in 2-3 mL of dichloromethane and reprecipitated from hexane. The red-brown solid thus obtained was dried in vacuo to obtain the titanium complex **9b** (yield: 0.576 g, 48%). ^{1}H NMR ($CDCl_3$, 200 MHz, 25°C): δ 1.28 (s, 18H, -C$(CH_3)_3$); 6.52, 6.96, 7.25, 7.50 (m, 12H, aromatic H); 8.23 (s, 2H, CH=N) ppm. Anal Calcd for $C_{34}H_{32}O_2N_2F_4TiCl_2$: C, 58.72: H, 4.61; N, 4.03. Found: C, 58.16; H, 5.20; N, 3.78.

7.2.1.7 Preparation of bis [N(3-*tert*-butyl salicylidene)2,4,6-trifluoroanilinato]Ti (IV) dichloride (9c, Scheme 7.1)

In a round bottom flask was placed 1.5365 g (5.005 mmol) of N(3-*tert*-butyl salicylidene)2,4,6-trifluoroaniline and dissolved in 30 mL of dry tetrahydrofuran. n-BuLi (1.6 M in hexane) (5.005 mmol, 3.12 mL) was added dropwise over a period of 10 min at –78°C. The flask was slowly brought to room temperature and stirred for 2 h. $TiCl_4(thf)_2$ (0.5 eqv, 0.836 g) was placed in a round bottom flask and dissolved in 40 mL dry tetrahydrofuran. The lithiated aldimine solution was added dropwise over 30 min at –78°C to the THF solution of $TiCl_4(thf)_2$. The flask was warmed to 25^{o}C and allowed to stir for 17 h. A dark red colored turbid solution was obtained. A white precipitate of LiCl settled down on storage. THF was evaporated in vacuo and the product redissolved in dichloromethane and allowed to stir for 1 h. Precipitated LiCl was filtered through a celite bed and the filtrate was concentrated in vacuo. Upon addition of hexane (4 times its volume) a solid precipitated out. The solid was separated and redissolved in 2-3 mL of dichloromethane and reprecipitated from hexane. The red-brown solid thus obtained was dried in vacuo to obtain the titanium complex **9c** (yield: 0.730 g, 40%). ^{1}H NMR ($CDCl_3$, 200 MHz, 25°C): δ 1.49 (s, 18H, -C$(CH_3)_3$); 6.45, 6.87, 7.15, 7.43, 7.73 (m, 10H, aromatic H); 8.37 (s, 2H, CH=N) ppm. Anal Calcd for $C_{34}H_{30}O_2N_2F_6TiCl_2$: C, 55.83: H, 4.13; N, 3.83. Found: C, 54.99; H, 4.49; N, 3.20.

7.2.1.8 Preparation of bis [N(3-*tert*-butyl salicylidene)2,3,4,5,6-pentafluoroanilinato]Ti (IV) dichloride (9d, Scheme 7.1)

This has been described in Chapter 6, under section 6.2.1.2.

All the NMR spectral data of **9a-d** and their corresponding ligands agree with literature values[15a].

7.2.2 Polymerization of styrene

Polymerization of styrene was carried out in a Parr Multi Reactor System (Model No-5000) which has a provision for six polymerization runs at a time. The multi reactor system has the advantage of enabling six simultaneous runs with ability to vary temperature, pressure (in case of gaseous monomer), catalyst concentration and monomer concentration.

Figure 7.1: Parr Multi Reactor System

Six 75 mL capacity stainless steel reactors equipped with six magnetic stirring bars were kept in an oven at 180°C for 12 h. They were connected to the Multi Reactor system while hot and cooled to room temperature under a stream of nitrogen. The multi reactor heating system was switched on and the desired temperatures were set for each individual reactor. Dry toluene (5 mL) was added to each of the reactor followed by 5mL of styrene using a syringe. Desired quantity of MAO was added to each of the six reactors. Polymerization was initiated by adding the required amount of catalyst solution (in 5 mL toluene) into the reactor. All the additions were made under a flow of nitrogen. Polymerization was quenched by addition of acidified (10% HCl) methanol. The polymer samples were filtered and then repeatedly washed with methanol and dried in vacuo oven at 80°C for 10 h. The polymers, thus, obtained were a mixture of atactic and syndiotactic

poly(styrene)s. Polymer samples were dissolved in butan-2-one and refluxed for 6 h. The atactic polystyrene readily dissolved in the solvent, whereas, the syndiotactic part remained insoluble. The insoluble polymer was filtered, washed 2-3 times with butan-2-one and dried in vacuo at 80°C for 6 h.

7.2.3 Analysis and characterization

Methods of analysis by GPC, DSC and NMR are described in Chapter 3 under Section 3.4.1, 3.4.3 and 3.4.5 respectively.

Crystal structures of **9a**, **9b** and **9d** are reported in the literature. Attempts were made to crystallize **9c** in the laboratory, but single crystals suitable for X-Ray diffraction could not be obtained.

7.3 Results and discussion

7.3.1 Polymerization of styrene with titanium complexes 9(a-d)

7.3.1.1 Effect of catalyst structure

The effect of catalyst structure on catalyst performance is shown in **Table 7.1**.

Table 7.1: Polymerization of styrene with Ti complexes **9a-d**[a]

Entry	Catalyst	Yield (g)	Activity (gPS $mmol^{-1}$ Ti^{-1} h^{-1})
1	9a	0.145	2.9
2	9b	0.156	3.1
3	9c	0.206	4.1
4	9d	0.236	4.7

[a]Polymerization conditions: [cat] = 10 μmol, Al/Ti : 500, Temp = 70°C, Time = 5 h, Toluene = 10 mL, styrene = 5 mL

It is seen that increasing electrophilicity at the metal center (increase in the number of fluorine atoms on the phenyl ring attached to the imine nitrogen) marginally increases the catalyst activity.

7.3.1.2 Effect of catalyst concentration

The effect of catalyst concentration is shown in **Table 7.2**.

Table 7.2: Polymerization of styrene with titanium complexes **9a-d** as a function of catalyst concentration[a]

Entry	Catalyst	[M]x 10^6mol	Yield (g)	% MEK insoluble[b]	Tm[c] (°C)
1	9a	10	0.145	37	272
2	9a	25	0.200	33	271
3	9b	10	0.156	39	270
4	9b	25	0.264	30	269
5	9c	10	0.206	49	269
6	9c	25	0.291	41	269
7	9d	5	0.190	52	269
8	9d	10	0.236	54	271

[a]Polymerization conditions: Al/Ti : 500, Temp = 70°C, Time = 5 h, Toluene = 10 mL, styrene = 5 mL; [b](yield of MEK insoluble part/total yield) x 100; [c]MEK insoluble fraction, high melting transition.

The key observations are:

i) Yield increases with increase in catalyst concentration [M]

ii) No significant effect of catalyst concentration on % syndiotacticity

iii) % MEK insoluble fraction increases in the order **9d** > **9c** > **9b** ~ **9a**.

7.3.1.3 Effect of Al/Ti

Effect of Al/Ti is shown in **Table 7.3**.

Table 7.3: Polymerization of styrene with Ti complexes **9a-c** at different Al/Ti[a]

Entry	Catalyst	Al/Ti	Yield (g)	% MEK insoluble[b]	[c]Tm (°C)
1	9a	500	0.145	37	272
2	9a	1000	0.183	35	268
3	9b	500	0.156	39	270
4	9b	1000	0.211	36	269
5	9c	500	0.206	49	269
6	9c	1000	0.226	39	269

[a]Polymerization conditions: [cat] = 10 μmol, Temp = 70°C, Time = 5 h, Toluene = 10 mL, styrene = 5 mL; [b](yield of MEK insoluble part/total yield) x 100; [c]MEK insoluble fraction, high melting transition.

The key observations are:

i) Yield increases with increase in Al/Ti ratio.

ii) Marginal decrease in % syndiotacticity with increase in Al/Ti ratio.

7.3.1.4 Effect of temperature

The effect of temperature is shown in **Table 7.4**.

Table 7.4: Polymerization of styrene with Ti complexes **9a-c** at varying temperatures[a]

Entry	Catalyst	Temp (°C)	Yield (g)	[%] syndiotacticity[b]	[c]Tm (°C)
1	9c	70	0.206	49	269
2	9c	85	0.457	46	266
3	9b	70	0.156	39	270
4	9b	85	0.371	32	268
5	9a	70	0.145	37	272
6	9a	85	0.284	41	270

[a]Polymerization conditions: [cat] = 10 μmol, Al/Ti = 500, Time = 5 h, Toluene = 10 mL, styrene = 5mL; [b](yield of MEK insoluble part/total yield) x 100; [c]MEK insoluble fraction, high melting transition.

The key observations are:

i) Yield increases with temperature.

ii) No significant change in syndiotacticity with increase in temperature.

7.3.1.5 Effect of reaction time

The effect of reaction time on catalyst activity was studied (**Table 7.5**).

Table 7.5: Polymerization of styrene with Ti complex **9c**

Entry	Time (h)	Yield (g)	% syndiotacticity[b]	[c]Tm (°C)
1	1	0.072	29	271
2	2	0.102	32	271
3	3	0.140	49	269
4	5	0.206	49	269
5	7	0.297	64	269

[a]Polymerization conditions: [cat] = 10 μmol, Al/Ti = 500, Temp = 70°C, Toluene = 10 mL, styrene = 5mL; [b](yield of MEK insoluble part/total yield) x 100; [c]MEK insoluble fraction, high melting transition.

The key observations from this table are:

iii) Yield increases with increasing reaction time

iv) Syndiotacticity also increases with reaction time.

7.3.2 Polymer structure and properties

7.3.2.1 Polymer molecular weights

The molecular weight distributions of the poly(styrene) samples (MEK-insoluble fractions) prepared using **9(a-d)**, exhibited a bimodal shape (**Fig. 7.2** and **Fig. 7.3, Table 7.6**). Previous report showed that the poly(styrene)s synthesized using **9a** were mainly syndiotactic with monomodal distribution of molecular weights, at a polymerization temperature of 20°C[18].

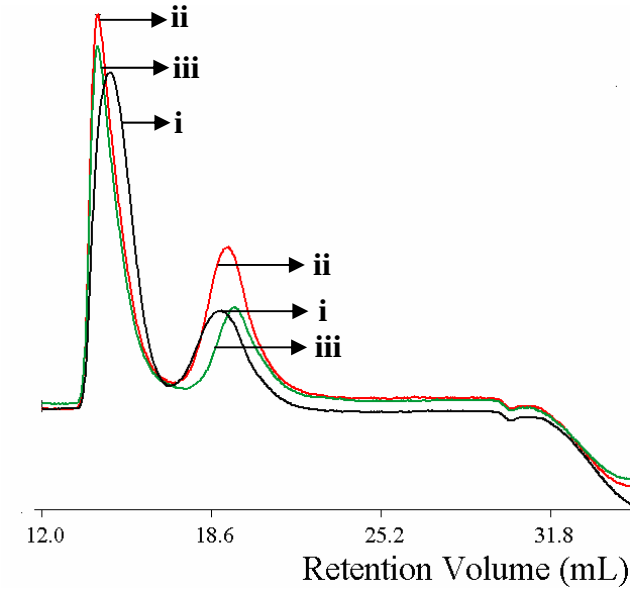

Figure 7.2: GPC of poly(styrene)s produced using **9c** i) cat = 10 µmol, Al/Ti = 500, Temp = 70°C, Time = 1 h (Table 7.5, entry 1) ii) cat = 10 µmol, Al/Ti = 500, Temp = 70°C, Time = 3 h (Table 7.5, entry 3) iii) cat = 10 µmol, Al/Ti = 1500, Temp = 70°C, Time = 5 h (Table 7.5, entry 4)

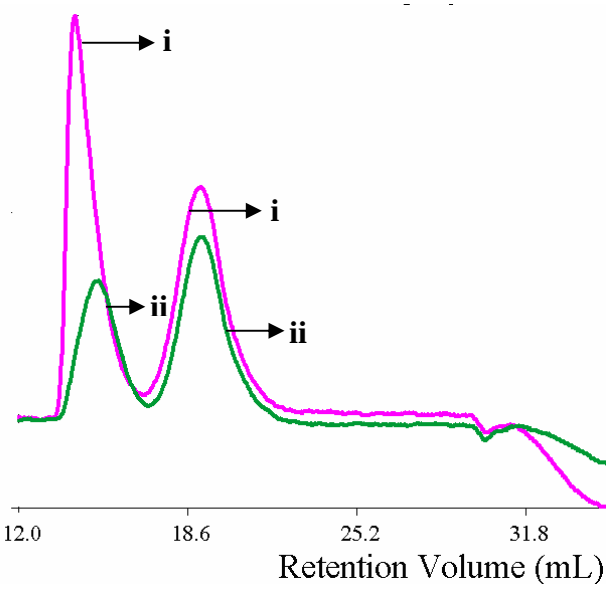

Figure 7.3: GPC of poly(styrene)s produced using **9a** i) cat = 10 µmol, Al/Ti = 1000, Temp = 70°C, Time = 5 h (Table 7.3, entry 2) ii) cat = 10 µmol, Al/Ti = 500, Temp = 70°C, Time = 5 h (Table 7.3, entry 1)

7.3.2.2 Thermal behavior of poly(styrene)s

Thermal properties of the polystyrene samples were investigated by Differential Scanning Calorimetry on a Perkin Elmer Q-10 instrument. DSC thermograms of a few polystyrene samples are shown below (**Fig. 7.4**):

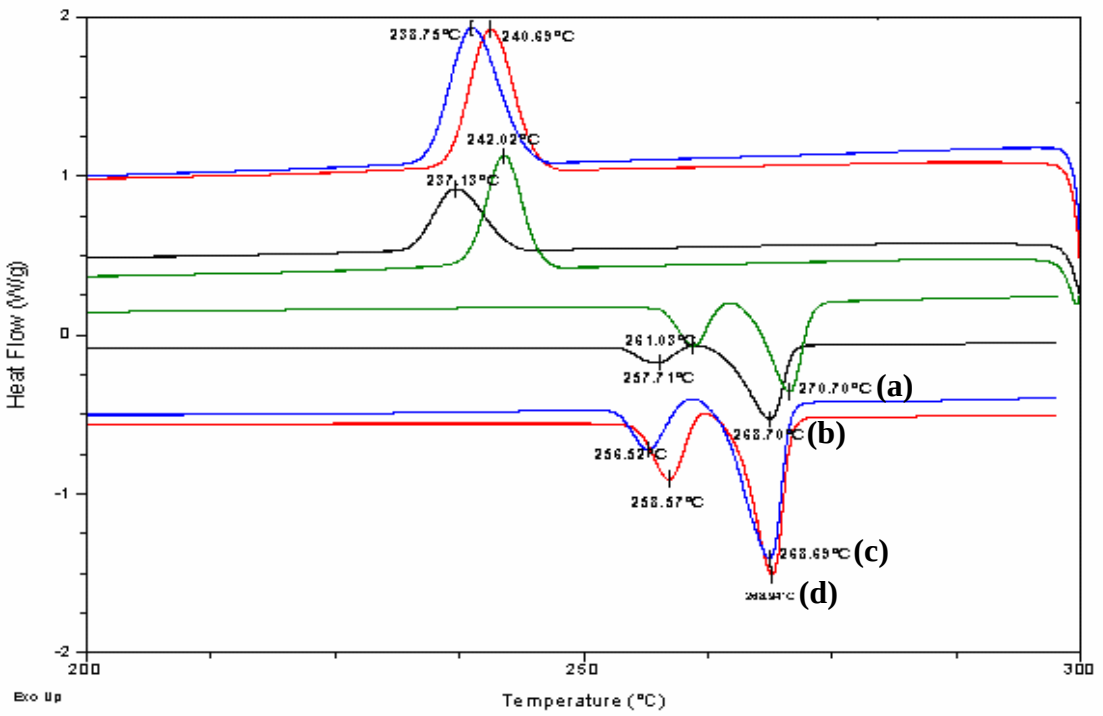

Figure 7.4: DSC thermograms of poly(styrene)s produced using: (a) **9a** (Table 7.6, entry 1); (b) **9c** (Table 7.6, entry 4); (c) **9c** (Table 7.6, entry 5). (d) **9c** (Table 7.6, entry 6)

The values of molecular weight and Tm of the obtained polymers are shown in **Table 7.6**. The polymers exhibited two distinct peaks and also two separate melting transitions.

Table 7.6: GPC and DSC data of poly(styrene)s synthesized using **9a** and **9c**

Catalyst	**[Ti] x 10^6 mol**	**Al/Ti**	**Time (h)**	**Mn_1 X 10^{-6}**	**Mw_1 X 10^{-6}**	**Mn_2 X 10^{-3}**	**Mw_2 X 10^{-3}**	**Tm (^oC)**
9a	25	500	5	8.6	9.6	42	69	271, 261
9a	10	1000	5	0.9	1.4	49	73	[b]nd
[a]9a	200	250	1	-	-	215	-	275
9c	10	500	1	2.0	3.6	35	88	269, 258
9c	10	500	3	3.6	6.0	7	79	269, 259
9c	10	1500	5	6.5	7.6	5	44	269, 256

[a]polystyrene synthesized using **9a** as reported in ref 18, Tp = 20^{o}C, PDI = 7.5 [b]not determined.

7.3.2.3 NMR spectroscopic studies

^{1}H and ^{13}C NMR spectra of syndiotactic poly(styrene)s (MEK insolubles) prepared using **9a** and **9b** are shown below. **(Fig. 7.5 - Fig. 7.8)**

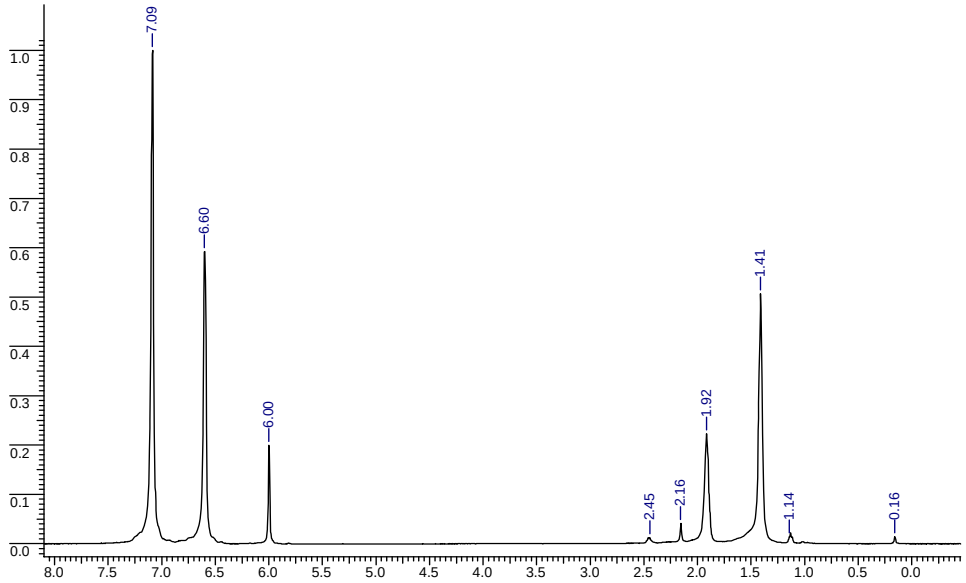

Figure 7.5: ^{1}H NMR spectrum (500 MHz, $C_2D_2Cl_4$, 135°C) of syndiotactic poly(styrene)s prepared using **9a** (Table 7.3, entry 2)

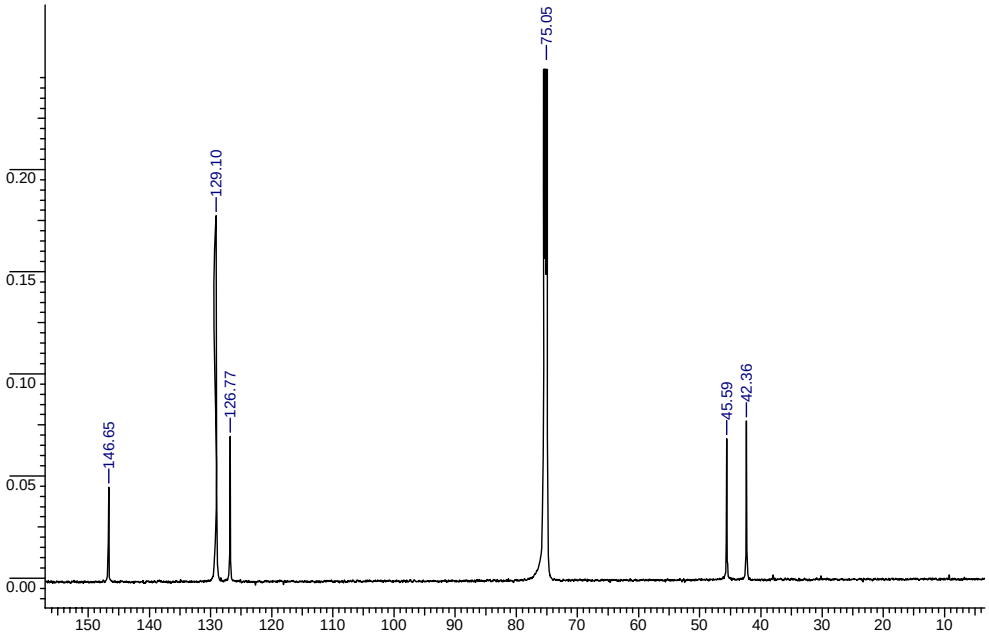

Figure 7.6: ^{13}C NMR spectrum (125.77 MHz, $C_2D_2Cl_4$, 135°C) of syndiotactic poly(styrene)s prepared using **9a** (Table 7.3, entry 2)

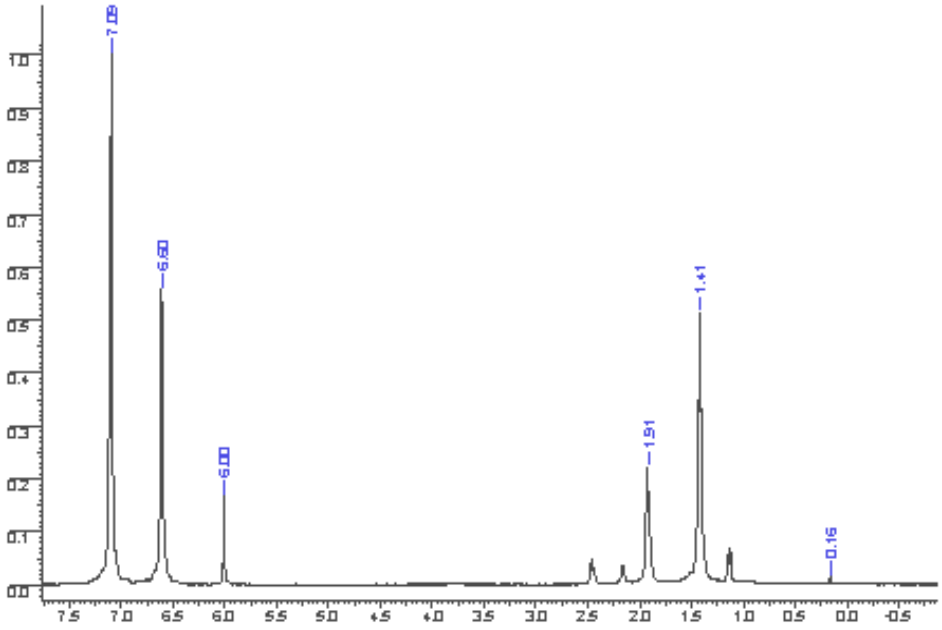

Figure 7.7: ^{1}H NMR spectrum (500 MHz, $C_2D_2Cl_4$, 135°C) of syndiotactic poly(styrene)s prepared using **9b** (Table 7.2, entry 4).

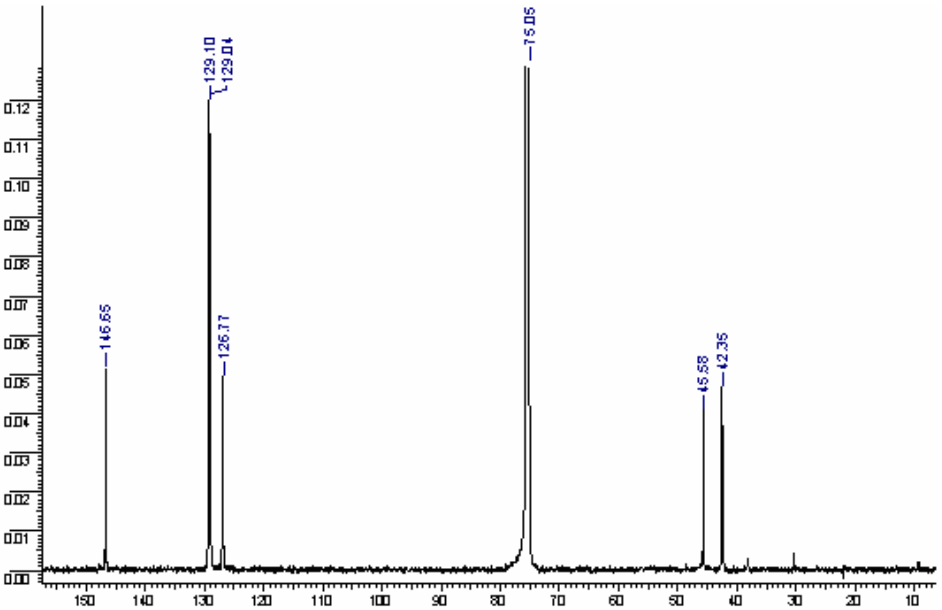

Figure 7.8: ^{13}C NMR spectrum (125.77 MHz, $C_2D_2Cl_4$, 135°C) of syndiotactic poly(styrene)s prepared using **9b** (Table 7.2, entry 4)

The peaks at δ 7.09 and 6.60 ppm in the ^{1}H NMR spectra (**Fig. 7.5** and **Fig. 7.7**) are characteristics of aromatic protons of the phenyl ring. The peak at δ 6.0 ppm is due to the solvent (1,1,2,2-tetrachloroethane-D2) resonance. The aliphatic resonances are observed at δ 1.41 (-CH_2-) ppm and 1.92 (-CH-) ppm. The small intensity peaks at 2.45, 2.16 and 1.14 ppm are due to traces of butan-2-one solvent present along with the polymer. In the ^{13}C NMR spectra (**Fig 7.6** and **Fig. 7.8**), peaks at δ 42.36 and 45.49 ppm refer to the -CH2- and -CH- resonances respectively. The aromatic resonances are observed from δ 126.77 to 146.65 ppm.

7.3.2.4 Microstructure of poly(styrene)s

Representative ^{13}C NMR spectra of syndiotactic, isotactic, isotactic-rich and atactic samples of poly(styrene)s are shown in **Fig. 7.9**[19]. C1 region of the spectrum is sensitive to the tacticity of the polymer. For atactic polystyrene (A-PS), Sato and Tanaka[20] assigned C-1 peaks 2 and 3 to *mm*-centred pentads, peaks 4 and 5 to *mr*-centred pentads and peak 6 to rr triads.

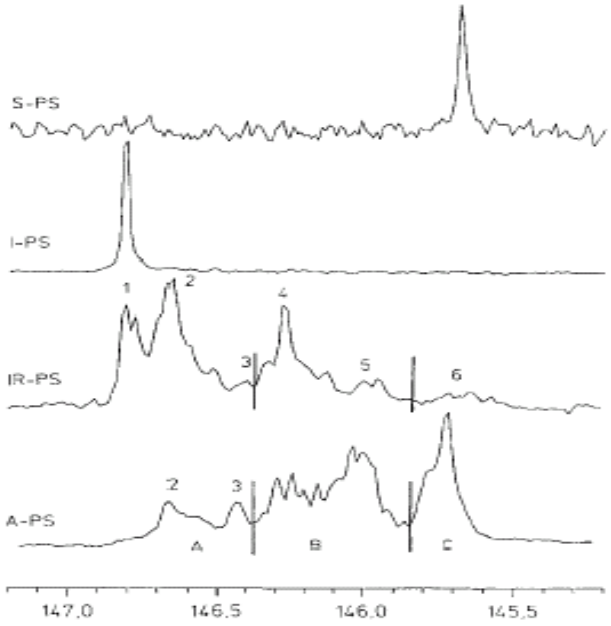

Figure 7.9: ^{13}C NMR spectra of aromatic C-1 region of poly(styrene)s determined in o-dichlorobenzene at 150°C (S-PS: syndiotactic; I-PS: isotactic; IR-PS: isotactic-rich; A-PS: atactic)[19] (from ref 19).

Therefore the spectra can be divided into three main parts (A-C) as shown in (**Fig. 7.9**) namely, *mm*, *mr* and *rr* triads respectively in the order of increasing field. If pentad sequences are considered, peak A includes *mmmm*, *mmmr*, *rmmr* and *mrmm*, peak B includes *rmrm*, *rrmm* and *mrrm*, and peak C includes *rrmr*, *rrrm* and *rrrr*.

^{13}C NMR spectra of unfractionated poly(styrene)s obtained during the present study are shown in **Figures 7.10, 7.12, 7.14 and 7.16**. The signals in the region of δ 145.7 to δ 148.0 ppm were deconvoluted using a Dimfit (Dm 2006-20060706) software program. The deconvoluted spectra are shown in **Figures 7.11, 7.13, 7.15 and 7.17**.

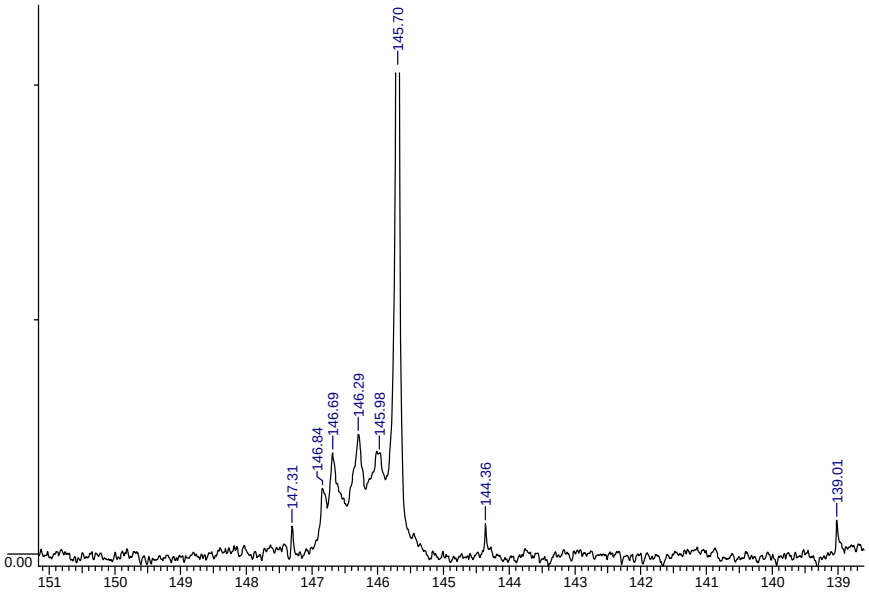

Figure 7.10: ^{13}C NMR Spectrum (125.7 MHz, $C_2D_2Cl_4$, 135^{o}C) of the aromatic-C1 carbon of a polystyrene sample (whole polymer) prepared using **9a** (Table 7.4, entry 6)

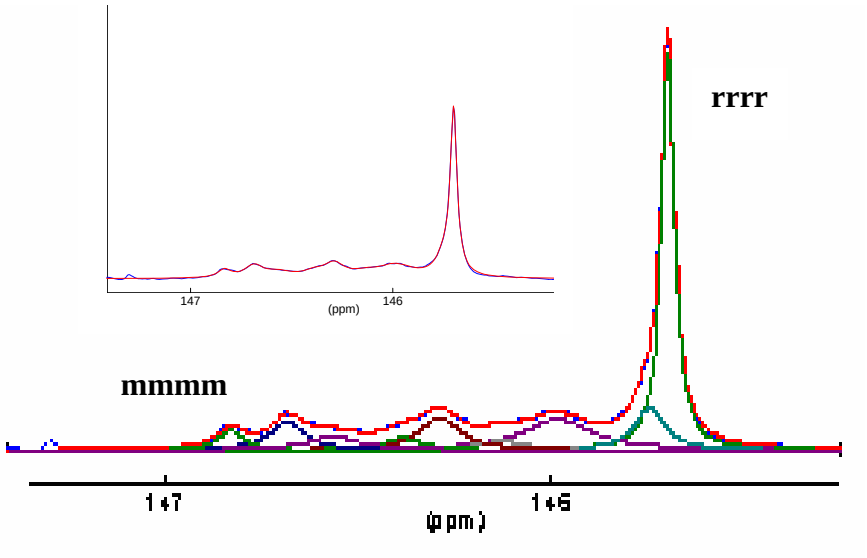

Figure 7.11: Deconvoluted spectrum of the region of δ 145.7 to δ 148.0 ppm in Fig. 7.10

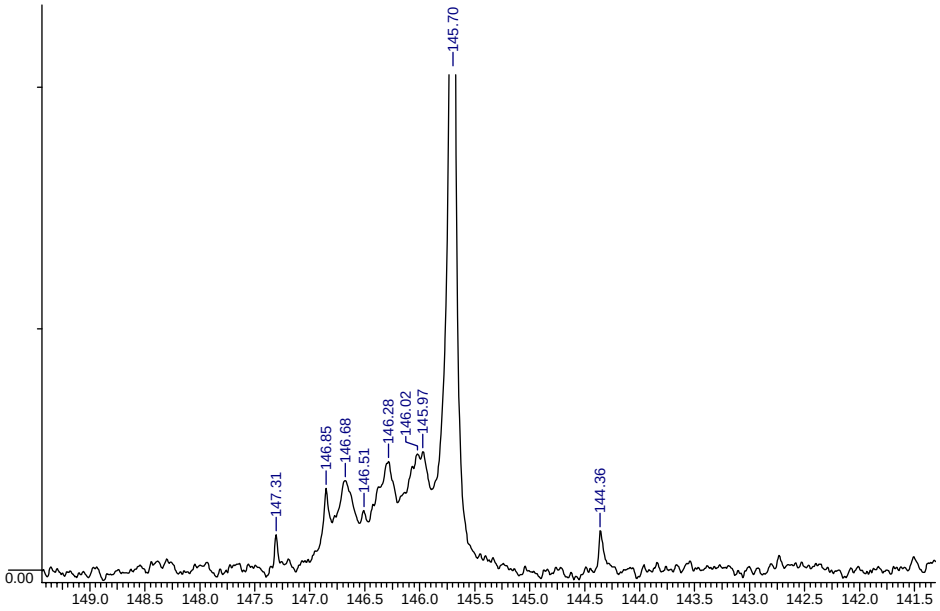

Figure 7.12: ^{13}C NMR Spectrum (125.7 MHz, $C_2D_2Cl_4$, 135°C) of the aromatic-C1 carbon of a polystyrene sample (whole polymer) prepared using **9b** (Table 7.1, entry 2)

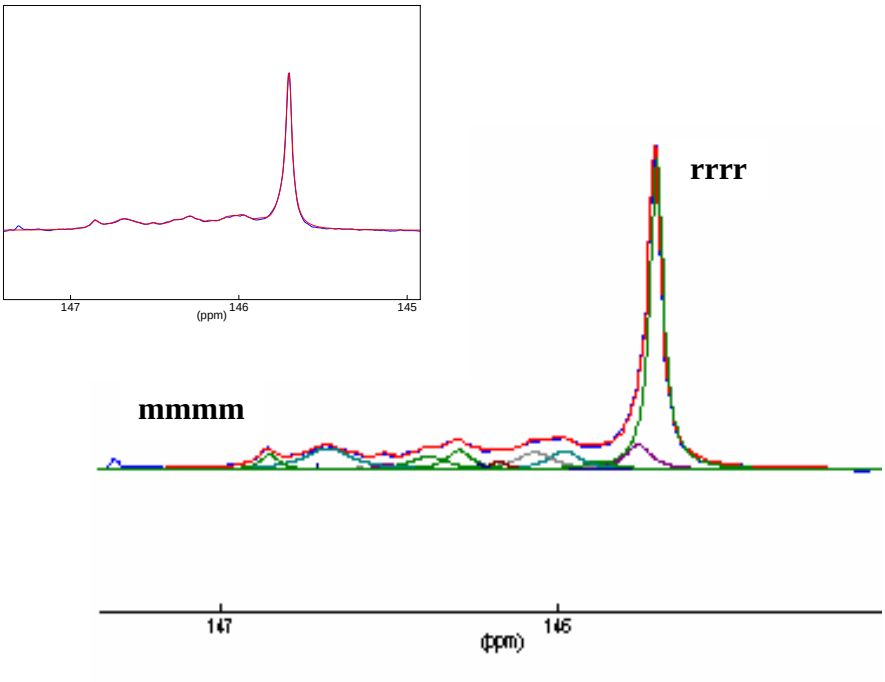

Figure 7.13: Deconvoluted spectrum of the region of δ 145.7 to δ 148.0 ppm in Fig. 7.12

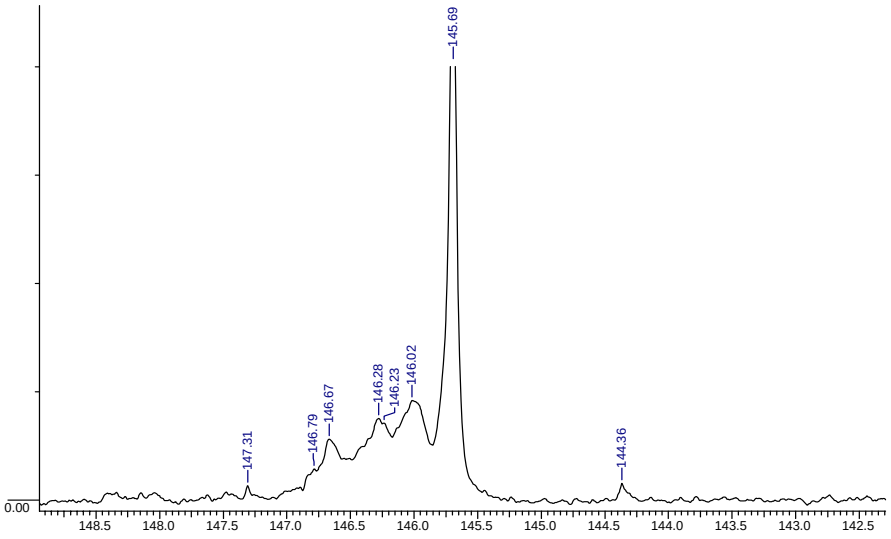

Figure 7.14: ^{13}C NMR Spectrum (125.7 MHz, $C_2D_2Cl_4$, 135°C) of the aromatic-C1 carbon of a polystyrene sample (whole polymer) prepared using **9c** (Table 7.1, entry 3)

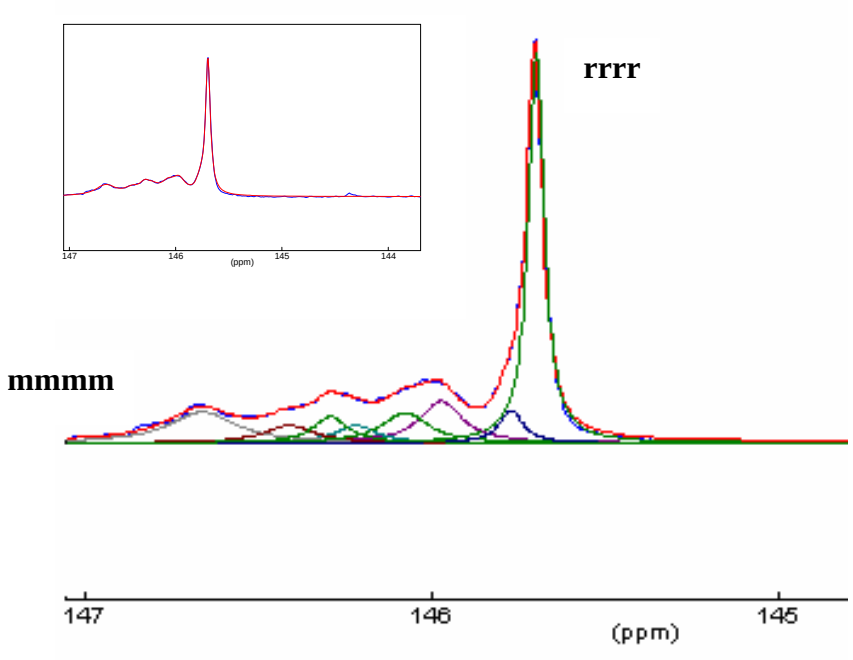

Figure 7.15: Deconvoluted spectrum of the region of δ 145.7 to δ 148.0 ppm in Fig. 7.14

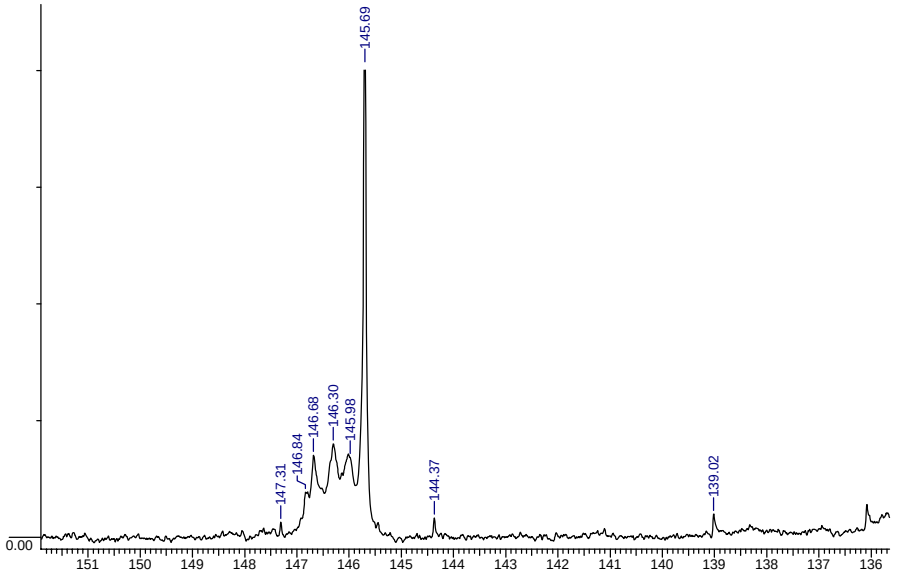

Figure 7.16: ^{13}C NMR Spectrum (125.7 MHz, $C_2D_2Cl_4$, 135°C) of the aromatic-C1 carbon of a polystyrene sample (whole polymer) prepared using **9d** (Table 7.1, entry 4)

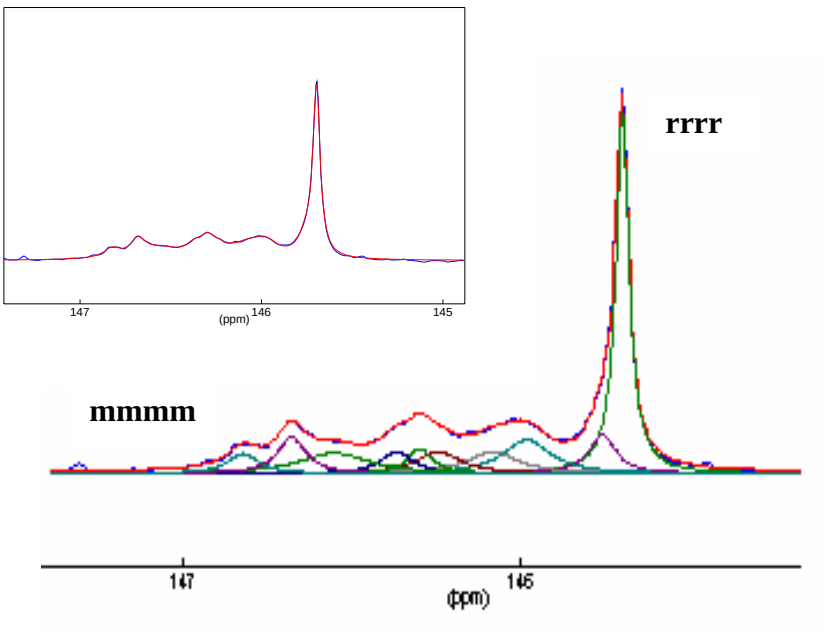

Figure 7.17: Deconvoluted spectrum of the region of δ 145.7 to δ 148.0 ppm in Fig. 7.16

The stereochemistry of poly(styrene)s obtained from catalyst **9a-d** is shown in **Table 7.7**.

Table 7.7: Stereochemistry of poly(styrene)s

Entry	Catalyst	Tp (^{o}C)	(mmmm, mmmr, rmmr, mrmm) %	(rmrm, rrmm, mrrm) %	(rrmr, rrrm, rrrr) %	% MEK insoluble
1	9a	85	17	34	49	41
2	9b	70	17	29	58	39
3	9c	70	14	39	47	49
4	9d	70	22	36	42	54

The values of % syndiotacticity (% rrrr) established from NMR do not agree with the value estimated by fractionation in MEK. This is attributed to the fact that the former was estimated using whole, unfractionated poly(styrene)s.

The three key observations made from the foregoing study are:

The syndiotacticity of poly(styrene)s obtained using **9a-d** is dependent on the number of fluorine atoms attached to the N-aryl ring. Increase in the number of fluorine atoms increases the % syndiotacticity of the poly(styrene)s formed.

9d with pentafluoro substituted phenyl ring, exhibits a syndiotacticity of 54% at 70^{o}C. This observation is contrary to previous reports wherein, predominantly isotactic poly(styrene)s were obtained using **9d** at a polymerization temperature of 20^{o}C[18].

MEK insoluble poly(styrene)s show two distinct molecular weight fractions. DSC also shows the presence of two peaks, one of a high melting and another, a low melting transition.

The X-ray of complexes **9b** and **9d** reveal a distorted octahedral structure in which the titanium is bound to two *cis*-coordinated [O, N] chelating ligands (the oxygen atoms situated in the *trans*-position) and to two chlorine atoms (situated in the *cis*-position)[15a]. Therefore, the spatial arrangement of complexes **9b** and **9d** is the same as that of complex **9a**. Complexes **9d** and **9b** have narrower Cl-Ti-Cl (96.42^{o} and 98.09^{o} respectively) angles than **9a** (103.11^{o}). O-Ti-O angles in **9d** and **9b** are narrower (163.61^{o} and 166.99^{o} respectively) compared to that in **9a** (171.6^{o}) and N-Ti-N (86.94^{o} and 86.18^{o} respectively) angles are relatively wider to that for complex **9a** (76.4^{o} respectively). In addition, complexes **9d** and **9b** possess wider Ti-N-C-C torsion angles involving the phenyl on the imine nitrogen than complex **9a**. These differences in the angles are due to the steric repulsion between the fluorine atoms in the 2 and 6 positions of the substituted phenyl ring attached to the imine nitrogen and the *tert*-butyl group in the phenoxy benzene rings and electronic repulsion between the fluorine atoms and the chlorine atoms bound to the titanium metal. Since the fluorine atoms are situated near chlorine atoms, they are expected to influence the olefin polymerization process.

Insertion of a styrene monomer to the Ti-CH_3 bond proceeds via a secondary insertion (2,1 addition) and the syndiospecific polymer chain grows via a chain-end control

mechanism[21]. Syndiotactic configuration arises from the phenyl–phenyl repulsive interaction between the last inserted monomer and the incoming styrene unit.

As a result of the interaction between the ortho-F and a β-H, a polymer chain is forced to be oriented in one direction and be fixed firmly in one conformation. The rigid conformation of the polymer chain will help the stereochemical information of the α-carbon of the last inserted styrene unit to transfer to the incoming monomer, thus resulting in higher syndiotacticity. Similar observations were also made with polymerization of propylene using **9d**[22, 23]. High syndioregularity via chain-end control mechanism and with a 2,1 insertion mode was observed at room temperature. Based on QM/MM calculations, a site inversion mechanism has been proposed to explain the ligand-directed stereo control. A fluxional isomerization exists in bis-phenoxy imine Ti complexes, which is controlled by the *trans*-O and *cis*-N configuration. This fluxional isomerisim in turn is controlled by the steric repulsion of the growing polymer chain and the substituent on the imine nitrogen. If site inversion mechanism is operative, the steric bulk of the *ortho* substituent of the phenoxy group also influences the stereoregularity. It has been found that a *tert*-butyl group at the ortho position of the phenoxy ligand improves the syndiotacticity for propylene polymerization. Complex **9d** satisfies both the steric demands (a *tert*-butyl substituted phenoxy group and a pentafluoro substituted N-aryl ring). In light of above, the observation that **9d** results in isotactic polymerization at 20^{o}C appears anomalous. Poly(styrene)s obtained with the above catalysts exhibit multiple molecular weight and melting peaks. We hypothesize that the low molecular weight fractions may arise as a result of the presence of residual TMA in MAO. Commercial MAO has 30-35% residual TMA. TMA in MAO has been previously reported to reduce polymer molecular weights[24].

7.4 Conclusions

Bis(phenoxyimine) titanium (IV) complexes result in a mixture of atactic and syndiotactic poly(styrene)s with moderate degree of syndiotacticity. Steric bulk influences both catalyst activity and degree of syndiotacticity. Increase in the number of fluorine atoms increases the % syndiotacticity of the polymer formed.

7.5 References

1. JP [1a] 62187708, **1985**, Idemitsu Kosan Co. Ltd, invs.: Ishihara, N.; Kuramoto, M.; Uoi, M. [1b] EP 210615, **1986**, Idemitsu Kosan Co. Ltd, invs.: Ishihara, N.; Kuramoto, M.; Uoi, M. *Chem. Abstr.* 106(22)177084P.
2. a) Kaminsky, W.; Lenk, S.; Scholz, V.; Roesky, H. W.; Herzog, A. *Macromolecules*, **1997,** 30, 25, 7647. b) Grassi, A.; Lamberti, C.; Zambelli, A.; Mingozzi, I. *Macromolecules*, **1997**, 30, 7, 1884. c) Grassi, A.; Saccheo, S.; Zambelli, A. *Macromolecules*, **1998**, 31, 17, 5588.
3. Schellenberg, J.; Tomotsu, N. *Prog. Polym. Sci.* **2002**, 27, 1925.
4. Okuda, J.; Masoud, E. *Macromol. Chem. Phys.* **1998,** 199, 543.
5. a) Yan, W.; Zhou, N.; Feng, R.; He, D.; Hu, Y.; *Gaofenzi Xuebao* **1999**, 20, 671. b) Zhou, N.; Yan, W.; Xie, G.; Hu, Y. *Chem. Res. Chin. Univ.* **1999**, 15, 200. c) Xie, G.; Xu, X.; Zhou, N.; Yan, W.; Hu, Y.; Li, Y.; Chen, X.; Chang, W. *Hecheng Shuzhi Ji Suliao* **1997**, 14, 8. d) Xu, X.; Xie, G.; *Gaofenzi Xuebao* **1997**, 2, 253. e) Xu, X.; Zhou, N.; Xie, G. *Gaofenzi Xuebao* **1997**, 6, 746. f) Yan, W.; Zhou, N.; Hong, H.; Xie, G.; Hu, Y.; *Shiyou Huagong* **1998**, 27, 653.
6. Liguori, D.; Centore, R.; Tuzi, A.; Grissi, F.; Sessa, I.; Zambelli, A. *Macromolecules*, **2003**, 36, 5451.
7. Capacchione, C.; Proto, A.; Ebeling, H.; Mülhaupt, R.; Möller, K.; Manivannan, R.; Spaniol, T. P.; Okuda, J. *J. Mol. Catal. A: Chem.* **2004**, 213, 137.

8. a) Flores, J. C.; Chien, J. C. W.; Rausch, M. D. *Organometallics* **1995**, 14, 4,1827. b) Flores, J. C.; Chien, J. C. W.; Rausch, M. D. *Organometallics* **1995**, 14, 4, 2106. c) Herskovics-Korine, D.; Eisen, M. S. *J. Organomet. Chem.* **1995**, 503, 307.
9. a) Liguori, D.; Grisi, F.; Sessa, I.; Zambelli, A. *Macromol. Chem. Phys.* **2003**, 204, 164. b) Volkis, V.; Nelkenbaum, E.; Lisovskii, A.; Hasson, G.; Semiat, R.; Kapon, M.; Botoshansky, M.; Eishen, Y.; Eisen, M. S. *J. Am. Chem. Soc.* **2003**, *125*, 2179.
10. Kim, IL.; Ha, Y. S.; Zhang, D. F.; Ha, C-S.; Lee, UK. *Macromol. Rapid Commun.* **2004**, 25, 1319.
11. Carlini, C.; Macinai, A.; Galletti, A. M. R.; Sbrana, G. *Macromol. Symp.* **2004**, 213, 209.
12. a) Fujita, T. *Chem. Lett.* **1999**, 1263. b) Matsui, S.; Tohi, Y.; Mitani, M.; Saito, J.; Makio, H.; Tanaka, H.; Nitabaru, M.; Nakano, T.; Fujita, T. *Chem. Lett.* **1999,** 1065. b) Matsui, S.; Tohi, Y.; Mitani, M.; Saito, J.; Makio, H.; Tanaka, H.; Nitabaru, M.; Nakano, T.; Matsukawa, N.; Takagi, Y.; Tsuru, K.; Kashiwa, N.; Fujita, T. *J. Am. Chem. Soc.* **2001**, 123, 6847. c) Matsui, S.; Fujita, T. *Catal. Today*, **2001**, 66, 63.
13. a) Matsui, S.; Inoue, Y.; Fujita, T. *J. Synth. Org. Chem. Jpn.* **2001**, 59, 232. b) Matsui, S.; Mitani, M.; Saito, J.; Matsukawa, N.; Tanaka, H.; Nakano, T.; Fujita, T. *Chem. Lett.* **2000**, 554.
14. a) Kojoh, S.; Matsugi, T.; Saito, J.; Mitani, M.; Fujita, T. *Chem. Lett.* **2001,** 822**.** b) Matsukawa, N.; Matsui, S.; Mitani, M.; Saito, J.; Tsuru, K.; Kashiwa, N.; Fujita, T. *J. Mol. Catal. A: Chem.* **2001**, 169, 99. c) Matsui, S.; Mitani, M.; Saito, J.; Tsuru, K.; Kashiwa, N.; Mohri, J.; Fujita, T. *Angew. Chem., Int. Ed. Engl.* **2001**, 40, 2918.
15. a) Mitani, M.; Mohri, J.; Yoshida, Y.; Saito, J.; Ishii, S.; Tsuru, K.; Matsui, S.; Furuyama, R.; Nakano, T.; Tanaka, H.; Kojoh, S.; Kashiwa, N.; Fujita, T. *J Am. Chem. Soc.* **2002**, 124, 3327. b) Saito, J.; Mitani, M.; Onda, M.; Mohri, J.; Ishi, J. I.; Yoshida, Y.; Nakano, T.; Tanaka, H.; Matsugi, T.; Kojoh, S.; Kashiwa, N.; Fujita, T. *Macromol. Rapid. Commun.* **2001**, 22, 1072.
16. a) Saito, J.; Mitani, M.; Mohri, J.; Matsui, S.; Tohi, Y.; Makio, H.; Nakano, T.; Tanaka, H.; Kashiwa, N.; Fujita, T. *Macromol. Chem. Phys.* **2002**, 203, 59. b) Ishii, S.; Saito, J.; Mitani, M.; Matsuura, S.; Kojoh, S.; Kashiwa, N.; Fujita, T. *J. Mol.*

Catal. A:Chem **2002**, 179, 11. c) Ishii, S.; Saito, J.; Mitani, M.; Matsuura, S.; Kojoh, S.; Kashiwa, N.; Fujita, T. *Chem. Lett.* **2002,** 740.

17. a) Saito, J.; Mitani, M.; Matsui, S.; Kashiwa, N.; Fujita, T. *Macromol. Rapid. Commun.* **2000**, 21, 1333. b) Saito, J.; Mitani, M.; Mohri, J.; Ishii, S.; Yoshida, Y.; Matsugi, T.; Kojoh, S.; Kashiwa, N.; Fujita, T. *Chem. Lett.* **2001**, 576. c) Mitani, M.; Furuyama, R.; Mohri, J.; Saito, J.; Ishii, S.; Terao, H.; Kashiwa, N.; Fujita, T. *J. Am. Chem. Soc.* **2002,** 124, 7888. d) Tian, J.; Hustad, P. D.; Coates, G. W. *J. Am. Chem. Soc.* **2001**, 123, 5134.
18. Michiue, K.; Onda, M.; Tanaka, H.; Mitani, M.; Fujita, T. *Polymeric Materials: Science & Engineering* **2006,** 94, 236.
19. Kawamura, T.; Toshima, N. *Macromol. Rapid. Commun.* **1994**, 479.
20. Sato, H.; Tanaka, Y. NMR Spectra of Styrene Oligomers and Polymers, pp.181, in: *NMR and Macromolecules*, Randall, Jr., R. C.; Ed: *ACS. Symp. Ser.* **1984**, 247, 181.
21. a) Pellecchia, C.: Longo, P.; Grassi, A.; Ammendola, P.; Zambelli, A. *Makromol Chem Rapid Commun* **1987**, 8, 277. b) Ammendola, P.; Pellecchia, C.; Longo, P.; Zambelli, *Gazz Chim Ital* **1987**,117, 65. c) Po, R.; Cardi, N. *Prog Polym Sci* **1996**, 21, 47. d) Pellecchia, C.; Grassi, A. *Top Catal* **1999**, 7, 125.
22. Nakayama, Y.; Saito, J.; Bando, H.; Fujita, T. *Macromol. Chem. Phys.* **2005**, 206, 1847.
23. Furuyama, R.; Saito, J.; Ishii, S.; Makio, H.; Mitani, M.; Tanaka, H.; Fujita, T. *J. Organomet. Chem.* **2005**, 690, 4398.
24. Wu, Q.; Gao, Q.; Lin, S. *J. Appl. Polym. Sci.* **1998**, 70, 765.

CHAPTER 8

SUMMARY AND CONCLUSIONS

Summary and conclusions

Ni (II) and Pd (II) complexes of novel bis-phosphine ligands were synthesized and their efficacy for the polymerization of ethylene and norbornene was studied. Nickel (II) and palladium (II) complexes of bis [*N,N* (diphenylphosphinomethyl)] alkyl/aryl amines were characterized by X-Ray crystallography. The crystallographic data reveals that the square planar complexes with a *tert*-butyl substituent on nitrogen are more sterically crowded than those with a 3,5-dimethyl phenyl substituent. The orientation of the meta-substituted phenyl ring is such that, the incoming monomer can easily approach the metal activation site. The complexes with a 2,6-diisopropyl phenyl substituent on nitrogen are the most sterically encumbered. The nature of the steric bulk had an influence on oligomerization/polymerization activity. The N-3,5-dimethyl phenyl substituted complexes exhibit the highest activity in the oligomerization of ethylene. Due to smaller bite angles and consequent openness of the structures, β-hydride elimination is the predominant chain transfer pathway. The rate of β-hydride elimination is faster than the rate of propagation. Consequently, dimers and trimers of ethylene are the exclusive products of oligomerization. At higher ethylene pressures, use of N-*tert*-butyl substituted complexes led to the formation of poly(ethylene)s with 2 ethyl branches per 1000 carbon atoms. However, the N-3,5-dimethyl phenyl substituted complexes led to the formation of poly(ethylene)s containing about 6 ethyl branches per 1000 carbon atoms. Furthermore, the catalyst activity for polymerization was very low. The N-2,6-diisopropyl phenyl substituted complexes, which are the most hindered, exhibit the lowest activities for oligomerization and polymerization of ethylene.

The pattern of reactivity for the polymerization of norbornene with the Ni (II) and Pd (II) complexes of bis [*N,N* (diphenylphosphinomethyl)] alkyl/aryl amines were similar to polymerization of ethylene. The N-3,5-dimethyl phenyl substituted complexes were the most active and the N-2,6-diisopropyl phenyl substituted ones, the least. The nickel bromide complexes exhibit marginally higher activity than the nickel chloride complexes since alkylation of a Ni-Br bond is more facile. The bisphosphine palladium (II) complexes exhibit lower activity and produce poly(norbornene)s which are insoluble in aromatic organic solvents. The insolubility arises due to cross-linked structures. The

stereochemistry of poly(norbornene)s obtained using the palladium complexes is mostly erythrodiisotactic. The soluble polymers prepared using the nickel (II) complexes are amorphous and possess erythrodisyndiotactic microstructures.

Nickel (II) and palladium (II) complexes of bis-phosphine ligands with a C-N-C ligand backbone exhibit higher activity in ethylene and norbornene polymerization when compared to bis-phosphines having a C-C-C framework. The geometry around the metal center in the former enables easy access of the monomer to the metal coordination site. The bite angle in a $NiCl_2$(dppp) complex (C-C-C) has a value of 91^o. The bite angles in the nickel chloride C-N-C systems have values of 89^o, 96^o and 97^o for N-3,5- dimethyl phenyl substituted, N-2,6-diisopropyl phenyl substituted and N-*tert*-butyl substituted complexes, respectively. In view of the above, it is surprising that earlier work has reported no activity for the polymerization of ethylene using $NiCl_2$(dppp) complexes.

Bis-phenoxyimine titanium (IV) complexes exhibit extremely high activity in the polymerization of ethylene and α-olefins. The fluorinated bis-phenoxyimine titanium (IV) complexes are reported to exhibit characteristics of "living" (transfer free) polymerization. However, there is no report on the use of external chain transfer agents like silanes, with such catalysts. Silanes have been reported to be useful chain transfer agents with certain Ti (IV) and Sm (II) complexes. Consequently, the ability of silanes as chain transfer agents with bis-phenoxyimine Ti (IV) catalyst was explored.

Phenyl silanes depress the molecular weight of poly(ethylene)s obtained using Bis[N(3-*tert*-butylsalicylidene)2,3,4,5,6-pentafluoroanilinato]Ti(IV) dichloride/ MAO catalyst systems. Number average degree of polymerization showed a linear dependence on the concentration of the chain transfer agent implying that the silanolytic transfer was the dominant transfer process. However, direct structural evidence of the incorporation of silicon group in polymer could not be obtained.

Bis- phenoxyimine titanium (IV) complexes with phenyl, 2,6-difluoro, 2,4,6-trifluoro and 2,3,4,5,6-pentafluoro phenyl substitutent on imine nitrogen were synthesized and explored for the polymerization of styrene in conjunction with MAO. All the catalysts led to a mixture of atactic and syndiotactic poly(styrene)s with

moderate degree of syndiotacticity. The number of fluorine atoms attached to the imine nitrogen influences both the degree of syndiotacticity as well as activity. Increase in the number of fluorine atoms increases the % syndiotacticity of the poly(styrene)s formed.

APPENDIX 1

Table 1. Crystal data and structure refinement for **15a**.

Identification code	15a
Empirical formula	C31 H35 Cl4 N Ni P2
Formula weight	684.05
Temperature	293(2) K
Wavelength	0.71073 Å
Crystal system, space group	Orthorhombic, *P*nma
Unit cell dimensions	a = 21.518(5) Å α = 90°. b = 17.608(4) Å β = 90°. c = 8.6453(18) Å γ = 90°.
Volume	3275.5(12) $Å^3$
Z, Calculated density	4, 1.387 Mg/m^3
Absorption coefficient	1.038 mm^{-1}
F(000)	1416
Crystal size	0.54 x 0.24 x 0.04 mm
Theta range for data collection	1.89 to 26.00 deg.
Limiting indices	-26<=h<=26, -21<=k<=20, -10<=l<=10
Reflections collected / unique	24057 / 3329 [R(int) = 0.0448]
Completeness to theta = 26.00	99.8 %
Max. and min. transmission	0.9597 and 0.6061
Refinement method	Full-matrix least-squares on F^2
Data / restraints / parameters	3329 / 0 / 195
Goodness-of-fit on F^2	1.164
Final R indices [I>2sigma(I)]	R1 = 0.0539, wR2 = 0.1169
R indices (all data)	R1 = 0.0601, wR2 = 0.1202
Largest diff. peak and hole	0.940 and -0.732 e. $Å^{-3}$

Table 2. Bond lengths [Å] and angles [deg] for **15a.**

Cl(3)-C(17)	1.714(9)
C(17)-Cl(2)	1.718(9)
Ni(1)-P(1)#1	2.1716(9)
Ni(1)-P(1)	2.1716(9)
Ni(1)-Cl(1)#1	2.2098(9)
Ni(1)-Cl(1)	2.2099(9)
P(1)-C(11)	1.825(3)
P(1)-C(5)	1.828(3)
P(1)-C(1)	1.855(3)
N(1)-C(1)	1.462(4)
N(1)-C(1)#1	1.462(4)
N(1)-C(2)	1.510(6)
C(5)-C(6)	1.385(5)
C(5)-C(10)	1.398(4)
C(10)-C(9)	1.386(5)
C(7)-C(8)	1.378(6)
C(7)-C(6)	1.387(5)
C(2)-C(4)	1.516(8)
C(2)-C(3)#1	1.524(5)
C(2)-C(3)	1.524(5)
C(11)-C(16)	1.389(5)
C(11)-C(12)	1.390(5)
C(12)-C(13)	1.384(6)
C(16)-C(15)	1.397(5)
C(8)-C(9)	1.380(6)
C(15)-C(14)	1.370(7)
C(14)-C(13)	1.362(7)
Cl(3)-C(17)-Cl(2)	116.7(4)
P(1)#1-Ni(1)-P(1)	95.94(5)
P(1)#1-Ni(1)-Cl(1)#1	85.45(4)
P(1)-Ni(1)-Cl(1)#1	177.37(4)
P(1)#1-Ni(1)-Cl(1)	177.38(4)
P(1)-Ni(1)-Cl(1)	85.45(4)
Cl(1)#1-Ni(1)-Cl(1)	93.07(5)
C(11)-P(1)-C(5)	108.45(15)
C(11)-P(1)-C(1)	102.41(15)
C(5)-P(1)-C(1)	99.73(15)
C(11)-P(1)-Ni(1)	113.66(11)
C(5)-P(1)-Ni(1)	112.55(11)
C(1)-P(1)-Ni(1)	118.62(11)
C(1)-N(1)-C(1)#1	108.2(4)
C(1)-N(1)-C(2)	116.3(2)
C(1)#1-N(1)-C(2)	116.3(2)
C(6)-C(5)-C(10)	119.1(3)
C(6)-C(5)-P(1)	119.9(2)
C(10)-C(5)-P(1)	120.6(3)
C(9)-C(10)-C(5)	120.2(3)
C(8)-C(7)-C(6)	120.3(4)
C(5)-C(6)-C(7)	120.3(3)
N(1)-C(2)-C(4)	111.3(5)
N(1)-C(2)-C(3)#1	108.3(3)
C(4)-C(2)-C(3)#1	110.8(3)
N(1)-C(2)-C(3)	108.3(3)

C(4)-C(2)-C(3)	110.8(3)
C(3)#1-C(2)-C(3)	107.2(5)
C(16)-C(11)-C(12)	118.5(3)
C(16)-C(11)-P(1)	123.5(3)
C(12)-C(11)-P(1)	118.0(3)
C(13)-C(12)-C(11)	120.7(4)
C(11)-C(16)-C(15)	119.8(4)
C(7)-C(8)-C(9)	120.0(3)
C(8)-C(9)-C(10)	120.1(3)
C(14)-C(15)-C(16)	120.7(4)
C(13)-C(14)-C(15)	119.7(4)
C(14)-C(13)-C(12)	120.6(5)
N(1)-C(1)-P(1)	108.3(2)

Symmetry transformations used to generate equivalent atoms:
#1 x,-y+1/2,z

Table 3. Torsion angles [deg] for **15a**.

P(1)#1-Ni(1)-P(1)-C(11)	-123.60(13)
Cl(1)#1-Ni(1)-P(1)-C(11)	114.5(9)
Cl(1)-Ni(1)-P(1)-C(11)	58.63(13)
P(1)#1-Ni(1)-P(1)-C(5)	112.61(11)
Cl(1)#1-Ni(1)-P(1)-C(5)	-9.3(9)
Cl(1)-Ni(1)-P(1)-C(5)	-65.16(11)
P(1)#1-Ni(1)-P(1)-C(1)	-3.18(13)
Cl(1)#1-Ni(1)-P(1)-C(1)	-125.0(9)
Cl(1)-Ni(1)-P(1)-C(1)	179.06(12)
C(11)-P(1)-C(5)-C(6)	-142.4(3)
C(1)-P(1)-C(5)-C(6)	110.9(3)
Ni(1)-P(1)-C(5)-C(6)	-15.8(3)
C(11)-P(1)-C(5)-C(10)	45.5(3)
C(1)-P(1)-C(5)-C(10)	-61.2(3)
Ni(1)-P(1)-C(5)-C(10)	172.2(2)
C(6)-C(5)-C(10)-C(9)	-0.3(5)
P(1)-C(5)-C(10)-C(9)	171.8(3)
C(10)-C(5)-C(6)-C(7)	1.0(5)
P(1)-C(5)-C(6)-C(7)	-171.2(3)
C(8)-C(7)-C(6)-C(5)	-1.1(5)
C(1)-N(1)-C(2)-C(4)	64.7(3)
C(1)#1-N(1)-C(2)-C(4)	-64.7(3)
C(1)-N(1)-C(2)-C(3)#1	-173.3(3)
C(1)#1-N(1)-C(2)-C(3)#1	57.4(5)
C(1)-N(1)-C(2)-C(3)	-57.4(5)
C(1)#1-N(1)-C(2)-C(3)	173.3(3)
C(5)-P(1)-C(11)-C(16)	20.5(3)
C(1)-P(1)-C(11)-C(16)	125.3(3)
Ni(1)-P(1)-C(11)-C(16)	-105.5(3)
C(5)-P(1)-C(11)-C(12)	-159.7(3)
C(1)-P(1)-C(11)-C(12)	-54.9(3)
Ni(1)-P(1)-C(11)-C(12)	74.3(3)
C(16)-C(11)-C(12)-C(13)	-1.2(6)
P(1)-C(11)-C(12)-C(13)	178.9(4)
C(12)-C(11)-C(16)-C(15)	1.6(5)
P(1)-C(11)-C(16)-C(15)	-178.6(3)
C(6)-C(7)-C(8)-C(9)	0.5(6)
C(7)-C(8)-C(9)-C(10)	0.2(6)
C(5)-C(10)-C(9)-C(8)	-0.3(6)
C(11)-C(16)-C(15)-C(14)	-0.1(6)
C(16)-C(15)-C(14)-C(13)	-1.8(7)
C(15)-C(14)-C(13)-C(12)	2.2(8)
C(11)-C(12)-C(13)-C(14)	-0.7(7)
C(1)#1-N(1)-C(1)-P(1)	-87.6(3)
C(2)-N(1)-C(1)-P(1)	139.4(3)
C(11)-P(1)-C(1)-N(1)	165.2(2)
C(5)-P(1)-C(1)-N(1)	-83.3(2)
Ni(1)-P(1)-C(1)-N(1)	39.2(3)

Symmetry transformations used to generate equivalent atoms:
#1 x,-y+1/2,z

Table 4. Crystal data and structure refinement for **15b**.

Identification code	15b
Empirical formula	C34.50 H34 Cl3 N Ni P2
Formula weight	689.63
Temperature	293(2) K
Wavelength	0.71073 Å
Crystal system, space group	Monoclinic, C2/c
Unit cell dimensions	a = 11.392(3) Å α = 90°. b = 19.927(5) Å β = 100.277(4)°. c = 16.001(4) Å γ = 90°.
Volume	3574.1(16) $Å^3$
Z, Calculated density	4, 1.282 Mg/m^3
Absorption coefficient	0.880 mm^{-1}
F(000)	1428
Crystal size	0.73 x 0.22 x 0.11 mm
Theta range for data collection	2.28 to 26.00°.
Limiting indices	-14<=h<=14, -20<=k<=24, -19<=l<=19
Reflections collected / unique	11925 / 3454 [R(int) = 0.0494]
Completeness to theta = 26.00	98.3 %
Max. and min. transmission	0.9133 and 0.5660
Refinement method	Full-matrix least-squares on F^2
Data / restraints / parameters	3454 / 0 / 198
Goodness-of-fit on F^2	1.127
Final R indices [I>2sigma(I)]	R1 = 0.0537, wR2 = 0.1561
R indices (all data)	R1 = 0.0589, wR2 = 0.1608
Largest diff. peak and hole	0.948 and -0.421 e.$Å^{-3}$

Table 5. Bond lengths [Å] and angles [deg] for **15b.**

Ni(1)-P(1)#1	2.1523(9)
Ni(1)-P(1)	2.1523(9)
Ni(1)-Cl(1)#1	2.1967(9)
Ni(1)-Cl(1)	2.1967(9)
P(1)-C(7)	1.816(3)
P(1)-C(13)	1.816(3)
P(1)-C(1)	1.848(3)
N(1)-C(2)	1.417(5)
N(1)-C(1)#1	1.444(3)
N(1)-C(1)	1.444(3)
C(3)-C(4)	1.389(5)
C(3)-C(2)	1.396(4)
C(7)-C(8)	1.387(5)
C(7)-C(12)	1.391(5)
C(2)-C(3)#1	1.396(4)
C(4)-C(5)	1.387(4)
C(4)-C(6)	1.504(5)
C(13)-C(18)	1.386(5)
C(13)-C(14)	1.389(5)
C(8)-C(9)	1.381(6)
C(12)-C(11)	1.367(6)
C(14)-C(15)	1.384(5)
C(11)-C(10)	1.394(7)
C(9)-C(10)	1.371(7)
C(15)-C(16)	1.370(7)
C(18)-C(17)	1.402(5)
C(16)-C(17)	1.357(7)
C(5)-C(4)#1	1.387(4)
C(19)-Cl(3)	1.783(7)
C(19)-Cl(3)#1	1.783(7)
P(1)#1-Ni(1)-P(1)	89.72(5)
P(1)#1-Ni(1)-Cl(1)#1	88.67(4)
P(1)-Ni(1)-Cl(1)#1	177.12(3)
P(1)#1-Ni(1)-Cl(1)	177.12(3)
P(1)-Ni(1)-Cl(1)	88.67(4)
Cl(1)#1-Ni(1)-Cl(1)	93.04(5)
C(7)-P(1)-C(13)	108.46(14)
C(7)-P(1)-C(1)	104.92(15)
C(13)-P(1)-C(1)	98.01(13)
C(7)-P(1)-Ni(1)	112.27(10)
C(13)-P(1)-Ni(1)	115.64(10)
C(1)-P(1)-Ni(1)	116.16(11)
C(2)-N(1)-C(1)#1	119.59(17)
C(2)-N(1)-C(1)	119.59(17)
C(1)#1-N(1)-C(1)	120.8(3)
N(1)-C(1)-P(1)	115.6(2)
C(4)-C(3)-C(2)	121.2(3)
C(8)-C(7)-C(12)	118.8(3)
C(8)-C(7)-P(1)	119.0(3)
C(12)-C(7)-P(1)	122.3(3)
C(3)-C(2)-C(3)#1	118.5(4)
C(3)-C(2)-N(1)	120.77(19)
C(3)#1-C(2)-N(1)	120.77(19)

C(5)-C(4)-C(3)	118.9(3)
C(5)-C(4)-C(6)	120.8(3)
C(3)-C(4)-C(6)	120.2(3)
C(18)-C(13)-C(14)	119.7(3)
C(18)-C(13)-P(1)	121.7(3)
C(14)-C(13)-P(1)	118.6(2)
C(9)-C(8)-C(7)	121.0(4)
C(11)-C(12)-C(7)	120.3(4)
C(15)-C(14)-C(13)	119.8(4)
C(12)-C(11)-C(10)	120.4(4)
C(10)-C(9)-C(8)	119.7(4)
C(9)-C(10)-C(11)	119.8(4)
C(16)-C(15)-C(14)	120.3(4)
C(13)-C(18)-C(17)	119.1(4)
C(17)-C(16)-C(15)	120.4(4)
C(4)-C(5)-C(4)#1	121.3(4)
C(16)-C(17)-C(18)	120.6(4)
Cl(3)-C(19)-Cl(3)#1	116.7(8)

Symmetry transformations used to generate equivalent atoms:
#1 -x,y,-z+3/2

Table 6. Torsion angles [deg] for **15b**.

P(1)#1-Ni(1)-P(1)-C(7)	95.19(11)
Cl(1)#1-Ni(1)-P(1)-C(7)	151.1(6)
Cl(1)-Ni(1)-P(1)-C(7)	-82.42(12)
P(1)#1-Ni(1)-P(1)-C(13)	-139.63(12)
Cl(1)#1-Ni(1)-P(1)-C(13)	-83.7(6)
Cl(1)-Ni(1)-P(1)-C(13)	42.76(12)
P(1)#1-Ni(1)-P(1)-C(1)	-25.55(10)
Cl(1)#1-Ni(1)-P(1)-C(1)	30.4(6)
Cl(1)-Ni(1)-P(1)-C(1)	156.83(11)
C(2)-N(1)-C(1)-P(1)	148.72(12)
C(1)#1-N(1)-C(1)-P(1)	-31.28(12)
C(7)-P(1)-C(1)-N(1)	-59.8(2)
C(13)-P(1)-C(1)-N(1)	-171.4(2)
Ni(1)-P(1)-C(1)-N(1)	64.8(2)
C(13)-P(1)-C(7)-C(8)	-100.2(3)
C(1)-P(1)-C(7)-C(8)	155.9(3)
Ni(1)-P(1)-C(7)-C(8)	28.8(3)
C(13)-P(1)-C(7)-C(12)	81.3(3)
C(1)-P(1)-C(7)-C(12)	-22.7(3)
Ni(1)-P(1)-C(7)-C(12)	-149.7(3)
C(4)-C(3)-C(2)-C(3)#1	0.7(2)
C(4)-C(3)-C(2)-N(1)	-179.3(2)
C(1)#1-N(1)-C(2)-C(3)	-168.5(2)
C(1)-N(1)-C(2)-C(3)	11.5(2)
C(1)#1-N(1)-C(2)-C(3)#1	11.5(2)
C(1)-N(1)-C(2)-C(3)#1	-168.5(2)
C(2)-C(3)-C(4)-C(5)	-1.4(5)
C(2)-C(3)-C(4)-C(6)	179.0(3)
C(7)-P(1)-C(13)-C(18)	6.1(3)
C(1)-P(1)-C(13)-C(18)	114.9(3)
Ni(1)-P(1)-C(13)-C(18)	-121.0(3)
C(7)-P(1)-C(13)-C(14)	-172.5(3)
C(1)-P(1)-C(13)-C(14)	-63.7(3)
Ni(1)-P(1)-C(13)-C(14)	60.4(3)
C(12)-C(7)-C(8)-C(9)	0.2(6)
P(1)-C(7)-C(8)-C(9)	-178.4(3)
C(8)-C(7)-C(12)-C(11)	-0.2(6)
P(1)-C(7)-C(12)-C(11)	178.3(4)
C(18)-C(13)-C(14)-C(15)	-0.2(6)
P(1)-C(13)-C(14)-C(15)	178.4(3)
C(7)-C(12)-C(11)-C(10)	-1.0(8)
C(7)-C(8)-C(9)-C(10)	1.0(7)
C(8)-C(9)-C(10)-C(11)	-2.2(8)
C(12)-C(11)-C(10)-C(9)	2.2(9)
C(13)-C(14)-C(15)-C(16)	0.7(7)
C(14)-C(13)-C(18)-C(17)	0.2(5)
P(1)-C(13)-C(18)-C(17)	-178.4(3)
C(14)-C(15)-C(16)-C(17)	-1.1(7)
C(3)-C(4)-C(5)-C(4)#1	0.7(2)
C(6)-C(4)-C(5)-C(4)#1	-179.7(4)
C(15)-C(16)-C(17)-C(18)	1.1(7)
C(13)-C(18)-C(17)-C(16)	-0.6(6)

Symmetry transformations used to generate equivalent atoms:
#1 -x,y,-z+3/2

Table 7. Crystal data and structure refinement for **15c**.

Identification code	15c
Empirical formula	C38 H41 Cl2 N Ni P2
Formula weight	703.27
Temperature	293(2) K
Wavelength	0.71073 A
Crystal system, space group	Monoclinic, P2(1)/m
Unit cell dimensions	a = 10.971(4) A α = 90°. b = 16.817(7) A β = 118.351(7)°. c = 10.971(4) A γ = 90°.
Volume	1781.4(12) A^3
Z, Calculated density	2, 1.311 Mg/m^3
Absorption coefficient	0.812 mm^-1
F(000)	736
Crystal size	0.68 x 0.22 x 0.02 mm
Theta range for data collection	2.11 to 23.00 deg.
Limiting indices	-12<=h<=11, -18<=k<=18, -12<=l<=9
Reflections collected / unique	7474 / 2573 [R(int) = 0.1240]
Completeness to theta = 23.00	99.7 %
Absorption correction	Semi-empirical from equivalents
Max. and min. transmission	0.9863 and 0.6072
Refinement method	Full-matrix least-squares on F^2
Data / restraints / parameters	2573 / 0 / 216
Goodness-of-fit on F^2	1.080
Final R indices [I>2sigma(I)]	R1 = 0.0763, wR2 = 0.1697
R indices (all data)	R1 = 0.1259, wR2 = 0.1864
Largest diff. peak and hole	1.123 and -0.789 e.A^-3

Table 8. Bond lengths [A] and angles [deg] for **15c**.

Ni(1)-P(1)	2.163(2)
Ni(1)-P(1)#1	2.163(2)
Ni(1)-Cl(1)	2.188(2)
Ni(1)-Cl(1)#1	2.188(2)
P(1)-C(7)	1.808(7)
P(1)-C(4)	1.812(7)
P(1)-C(2)	1.836(7)
N(1)-C(2)#1	1.450(8)
N(1)-C(2)	1.450(8)
N(1)-C(5)	1.473(12)
C(2)-H(2A)	0.9700
C(2)-H(2B)	0.9700
C(4)-C(11)	1.376(10)
C(4)-C(21)	1.388(10)
C(5)-C(8)	1.377(13)
C(5)-C(14)	1.387(14)
C(7)-C(9)	1.355(10)
C(7)-C(20)	1.393(10)
C(8)-C(18)	1.409(14)
C(8)-C(15)	1.481(14)
C(9)-C(24)	1.389(11)
C(9)-H(9)	0.9300
C(11)-C(23)	1.372(11)
C(11)-H(11)	0.9300
C(14)-C(16)	1.367(14)
C(14)-C(17)	1.509(15)
C(15)-C(36)	1.527(10)
C(15)-C(36)#1	1.527(10)
C(15)-H(15)	0.9800
C(16)-C(19)	1.363(15)
C(16)-H(16)	0.9300
C(17)-C(37)	1.530(10)
C(17)-C(37)#1	1.530(10)
C(17)-H(17)	0.9800
C(18)-C(19)	1.371(16)
C(18)-H(18)	0.9300
C(19)-H(19)	0.9300
C(20)-C(32)	1.388(11)
C(20)-H(20)	0.9300
C(21)-C(27)	1.380(11)
C(21)-H(21)	0.9300
C(23)-C(25)	1.384(13)
C(23)-H(23)	0.9300
C(24)-C(34)	1.374(12)
C(24)-H(24)	0.9300
C(25)-C(27)	1.332(13)
C(25)-H(25)	0.9300
C(27)-H(27)	0.9300
C(32)-C(34)	1.335(12)
C(32)-H(32)	0.9300
C(34)-H(34)	0.9300

C(36)-H(36A)	0.9600
C(36)-H(36B)	0.9600
C(36)-H(36C)	0.9600
C(37)-H(37A)	0.9600
C(37)-H(37B)	0.9600
C(37)-H(37C)	0.9600

P(1)-Ni(1)-P(1)#1	97.16(11)
P(1)-Ni(1)-Cl(1)	85.14(7)
P(1)#1-Ni(1)-Cl(1)	177.31(9)
P(1)-Ni(1)-Cl(1)#1	177.31(9)
P(1)#1-Ni(1)-Cl(1)#1	85.14(7)
Cl(1)-Ni(1)-Cl(1)#1	92.52(11)
C(7)-P(1)-C(4)	106.6(3)
C(7)-P(1)-C(2)	104.1(3)
C(4)-P(1)-C(2)	100.4(3)
C(7)-P(1)-Ni(1)	115.6(2)
C(4)-P(1)-Ni(1)	110.7(2)
C(2)-P(1)-Ni(1)	117.9(2)
C(2)#1-N(1)-C(2)	112.2(8)
C(2)#1-N(1)-C(5)	116.4(5)
C(2)-N(1)-C(5)	116.4(5)
N(1)-C(2)-P(1)	111.8(5)
N(1)-C(2)-H(2A)	109.3
P(1)-C(2)-H(2A)	109.3
N(1)-C(2)-H(2B)	109.3
P(1)-C(2)-H(2B)	109.3
H(2A)-C(2)-H(2B)	107.9
C(11)-C(4)-C(21)	117.9(7)
C(11)-C(4)-P(1)	119.3(6)
C(21)-C(4)-P(1)	122.8(6)
C(8)-C(5)-C(14)	123.4(9)
C(8)-C(5)-N(1)	120.5(9)
C(14)-C(5)-N(1)	116.1(9)
C(9)-C(7)-C(20)	117.5(7)
C(9)-C(7)-P(1)	122.0(6)
C(20)-C(7)-P(1)	120.4(6)
C(5)-C(8)-C(18)	116.6(10)
C(5)-C(8)-C(15)	125.8(9)
C(18)-C(8)-C(15)	117.6(10)
C(7)-C(9)-C(24)	122.0(8)
C(7)-C(9)-H(9)	119.0
C(24)-C(9)-H(9)	119.0
C(23)-C(11)-C(4)	121.4(8)
C(23)-C(11)-H(11)	119.3
C(4)-C(11)-H(11)	119.3
C(16)-C(14)-C(5)	116.9(10)
C(16)-C(14)-C(17)	119.3(10)
C(5)-C(14)-C(17)	123.8(9)
C(8)-C(15)-C(36)	113.6(6)
C(8)-C(15)-C(36)#1	113.6(6)
C(36)-C(15)-C(36)#1	109.1(10)
C(8)-C(15)-H(15)	106.7
C(36)-C(15)-H(15)	106.7
C(36)#1-C(15)-H(15)	106.7
C(19)-C(16)-C(14)	122.7(11)
C(19)-C(16)-H(16)	118.6

C(14)-C(16)-H(16)	118.6
C(14)-C(17)-C(37)	111.6(7)
C(14)-C(17)-C(37)#1	111.6(7)
C(37)-C(17)-C(37)#1	107.0(10)
C(14)-C(17)-H(17)	108.9
C(37)-C(17)-H(17)	108.9
C(37)#1-C(17)-H(17)	108.9
C(19)-C(18)-C(8)	121.0(11)
C(19)-C(18)-H(18)	119.5
C(8)-C(18)-H(18)	119.5
C(16)-C(19)-C(18)	119.4(10)
C(16)-C(19)-H(19)	120.3
C(18)-C(19)-H(19)	120.3
C(32)-C(20)-C(7)	120.3(8)
C(32)-C(20)-H(20)	119.9
C(7)-C(20)-H(20)	119.9
C(27)-C(21)-C(4)	119.5(9)
C(27)-C(21)-H(21)	120.2
C(4)-C(21)-H(21)	120.2
C(11)-C(23)-C(25)	119.9(9)
C(11)-C(23)-H(23)	120.1
C(25)-C(23)-H(23)	120.1
C(34)-C(24)-C(9)	119.3(9)
C(34)-C(24)-H(24)	120.4
C(9)-C(24)-H(24)	120.4
C(27)-C(25)-C(23)	118.9(9)
C(27)-C(25)-H(25)	120.5
C(23)-C(25)-H(25)	120.5
C(25)-C(27)-C(21)	122.4(9)
C(25)-C(27)-H(27)	118.8
C(21)-C(27)-H(27)	118.8
C(34)-C(32)-C(20)	121.1(9)
C(34)-C(32)-H(32)	119.5
C(20)-C(32)-H(32)	119.5
C(32)-C(34)-C(24)	119.9(9)
C(32)-C(34)-H(34)	120.1
C(24)-C(34)-H(34)	120.1
C(15)-C(36)-H(36A)	109.5
C(15)-C(36)-H(36B)	109.5
H(36A)-C(36)-H(36B)	109.5
C(15)-C(36)-H(36C)	109.5
H(36A)-C(36)-H(36C)	109.5
H(36B)-C(36)-H(36C)	109.5
C(17)-C(37)-H(37A)	109.5
C(17)-C(37)-H(37B)	109.5
H(37A)-C(37)-H(37B)	109.5
C(17)-C(37)-H(37C)	109.5
H(37A)-C(37)-H(37C)	109.5
H(37B)-C(37)-H(37C)	109.5

Symmetry transformations used to generate equivalent atoms:
#1 x,-y+1/2,z

Table 9. Torsion angles [deg] for **15c**.

P(1)#1-Ni(1)-P(1)-C(7)	115.9(3)
Cl(1)-Ni(1)-P(1)-C(7)	-65.5(3)
Cl(1)#1-Ni(1)-P(1)-C(7)	-95(2)
P(1)#1-Ni(1)-P(1)-C(4)	-122.7(3)
Cl(1)-Ni(1)-P(1)-C(4)	55.9(3)
Cl(1)#1-Ni(1)-P(1)-C(4)	26(2)
P(1)#1-Ni(1)-P(1)-C(2)	-8.1(3)
Cl(1)-Ni(1)-P(1)-C(2)	170.5(3)
Cl(1)#1-Ni(1)-P(1)-C(2)	141(2)
C(2)#1-N(1)-C(2)-P(1)	-81.1(8)
C(5)-N(1)-C(2)-P(1)	141.2(6)
C(7)-P(1)-C(2)-N(1)	-89.7(6)
C(4)-P(1)-C(2)-N(1)	160.1(5)
Ni(1)-P(1)-C(2)-N(1)	39.9(6)
C(7)-P(1)-C(4)-C(11)	-174.3(6)
C(2)-P(1)-C(4)-C(11)	-66.1(7)
Ni(1)-P(1)-C(4)-C(11)	59.2(6)
C(7)-P(1)-C(4)-C(21)	8.1(7)
C(2)-P(1)-C(4)-C(21)	116.3(6)
Ni(1)-P(1)-C(4)-C(21)	-118.4(6)
C(2)#1-N(1)-C(5)-C(8)	-68.0(6)
C(2)-N(1)-C(5)-C(8)	68.0(6)
C(2)#1-N(1)-C(5)-C(14)	112.0(6)
C(2)-N(1)-C(5)-C(14)	-112.0(6)
C(4)-P(1)-C(7)-C(9)	-114.1(7)
C(2)-P(1)-C(7)-C(9)	140.4(6)
Ni(1)-P(1)-C(7)-C(9)	9.4(7)
C(4)-P(1)-C(7)-C(20)	63.7(7)
C(2)-P(1)-C(7)-C(20)	-41.8(7)
Ni(1)-P(1)-C(7)-C(20)	-172.8(5)
C(14)-C(5)-C(8)-C(18)	0.000(1)
N(1)-C(5)-C(8)-C(18)	180.0
C(14)-C(5)-C(8)-C(15)	180.000(2)
N(1)-C(5)-C(8)-C(15)	0.000(1)
C(20)-C(7)-C(9)-C(24)	-1.6(12)
P(1)-C(7)-C(9)-C(24)	176.2(7)
C(21)-C(4)-C(11)-C(23)	-0.2(12)
P(1)-C(4)-C(11)-C(23)	-178.0(7)
C(8)-C(5)-C(14)-C(16)	0.000(1)
N(1)-C(5)-C(14)-C(16)	180.000(1)
C(8)-C(5)-C(14)-C(17)	180.000(2)
N(1)-C(5)-C(14)-C(17)	0.000(1)
C(5)-C(8)-C(15)-C(36)	117.3(7)
C(18)-C(8)-C(15)-C(36)	-62.7(7)
C(5)-C(8)-C(15)-C(36)#1	-117.3(7)
C(18)-C(8)-C(15)-C(36)#1	62.7(7)
C(5)-C(14)-C(16)-C(19)	0.000(2)
C(17)-C(14)-C(16)-C(19)	180.000(2)
C(16)-C(14)-C(17)-C(37)	-59.8(7)
C(5)-C(14)-C(17)-C(37)	120.2(7)
C(16)-C(14)-C(17)-C(37)#1	59.8(7)
C(5)-C(14)-C(17)-C(37)#1	-120.2(7)

C(5)-C(8)-C(18)-C(19)	0.000(2)
C(15)-C(8)-C(18)-C(19)	180.000(1)
C(14)-C(16)-C(19)-C(18)	0.000(1)
C(8)-C(18)-C(19)-C(16)	0.0
C(9)-C(7)-C(20)-C(32)	0.8(12)
P(1)-C(7)-C(20)-C(32)	-177.1(7)
C(11)-C(4)-C(21)-C(27)	1.0(12)
P(1)-C(4)-C(21)-C(27)	178.7(6)
C(4)-C(11)-C(23)-C(25)	-0.2(14)
C(7)-C(9)-C(24)-C(34)	1.5(14)
C(11)-C(23)-C(25)-C(27)	-0.1(15)
C(23)-C(25)-C(27)-C(21)	0.9(16)
C(4)-C(21)-C(27)-C(25)	-1.4(14)
C(7)-C(20)-C(32)-C(34)	0.2(14)
C(20)-C(32)-C(34)-C(24)	-0.3(14)
C(9)-C(24)-C(34)-C(32)	-0.5(14)

Symmetry transformations used to generate equivalent atoms:
#1 x,-y+1/2,z

Table 10. Crystal data and structure refinement for **16a**.

Identification code	16a
Empirical formula	C31 H35 Br2 Cl2 N Ni P2
Formula weight	772.97
Temperature	293(2) K
Wavelength	0.71073 Å
Crystal system, space group	Orthorhombic, Pnma
Unit cell dimensions	a = 21.823(6) Å α = 90°. b = 17.833(5) Å β = 90°. c = 8.521(2) Å γ = 90°.
Volume	3316.2(15) $Å^3$
Z, Calculated density	4, 1.548 Mg/m^3
Absorption coefficient	3.274 mm^{-1}
F(000)	1560
Crystal size	0.62 x 0.13 x 0.08 mm
Theta range for data collection	1.87 to 26.00 deg.
Limiting indices	-15<=h<=26, -21<=k<=21, -10<=l<=10
Reflections collected / unique	16964 / 3374 [R(int) = 0.0459]
Completeness to theta = 26.00	100.0 %
Max. and min. transmission	0.7797 and 0.2360
Refinement method	Full-matrix least-squares on F^2
Data / restraints / parameters	3374 / 0 / 195
Goodness-of-fit on F^2	1.038
Final R indices [I>2sigma(I)]	R1 = 0.0443, wR2 = 0.1094
R indices (all data)	R1 = 0.0686, wR2 = 0.1204
Largest diff. peak and hole	0.846 and -0.622 e. $Å^{-3}$

Table 11. Bond lengths [Å] and angles [deg] for **16**a.

Br(1)-Ni	2.3333(7)
Cl(1)-C(23)	1.692(12)
Cl(2)-C(23)	1.690(12)
N(1)-C(1)#1	1.458(5)
N(1)-C(1)	1.458(5)
N(1)-C(2)	1.507(7)
Ni-P(1)	2.1678(11)
Ni-P(1)#1	2.1678(11)
Ni-Br(1)#1	2.3333(7)
P(1)-C(5)	1.815(4)
P(1)-C(11)	1.820(4)
P(1)-C(1)	1.836(4)
C(2)-C(4)	1.505(9)
C(2)-C(3)#1	1.505(6)
C(2)-C(3)	1.505(6)
C(5)-C(6)	1.373(6)
C(5)-C(10)	1.382(5)
C(6)-C(7)	1.379(6)
C(7)-C(8)	1.375(7)
C(8)-C(9)	1.359(7)
C(9)-C(10)	1.378(6)
C(11)-C(12)	1.380(7)
C(11)-C(16)	1.383(6)
C(12)-C(13)	1.370(7)
C(13)-C(14)	1.368(9)
C(14)-C(15)	1.336(8)
C(15)-C(16)	1.386(7)

C(1)#1-N(1)-C(1)	107.6(4)
C(1)#1-N(1)-C(2)	116.7(3)
C(1)-N(1)-C(2)	116.7(3)
P(1)-Ni-P(1)#1	96.01(6)
P(1)-Ni-Br(1)#1	177.03(4)
P(1)#1-Ni-Br(1)#1	86.00(4)
P(1)-Ni-Br(1)	86.00(4)
P(1)#1-Ni-Br(1)	177.03(4)
Br(1)#1-Ni-Br(1)	91.91(4)
C(5)-P(1)-C(11)	108.24(19)
C(5)-P(1)-C(1)	99.56(18)
C(11)-P(1)-C(1)	102.21(19)
C(5)-P(1)-Ni	113.15(13)
C(11)-P(1)-Ni	113.89(14)
C(1)-P(1)-Ni	118.25(13)
N(1)-C(1)-P(1)	108.7(3)
C(4)-C(2)-C(3)#1	111.0(4)
C(4)-C(2)-C(3)	111.0(4)
C(3)#1-C(2)-C(3)	106.6(6)
C(4)-C(2)-N(1)	110.3(6)
C(3)#1-C(2)-N(1)	108.9(3)
C(3)-C(2)-N(1)	108.9(3)
C(6)-C(5)-C(10)	118.2(4)
C(6)-C(5)-P(1)	120.2(3)
C(10)-C(5)-P(1)	121.0(3)

C(5)-C(6)-C(7)	121.1(4)
C(8)-C(7)-C(6)	119.9(4)
C(9)-C(8)-C(7)	119.6(4)
C(8)-C(9)-C(10)	120.5(4)
C(9)-C(10)-C(5)	120.7(4)
C(12)-C(11)-C(16)	118.3(4)
C(12)-C(11)-P(1)	118.3(3)
C(16)-C(11)-P(1)	123.4(4)
C(13)-C(12)-C(11)	120.5(5)
C(14)-C(13)-C(12)	120.3(6)
C(15)-C(14)-C(13)	120.0(5)
C(14)-C(15)-C(16)	120.9(5)
C(11)-C(16)-C(15)	119.9(5)
Cl(2)-C(23)-Cl(1)	117.8(6)

Symmetry transformations used to generate equivalent atoms:
#1 x,-y+1/2,z

Table 12. Torsion angles [deg] for **16a**.

P(1)#1-Ni-P(1)-C(5)	-112.42(14)
Br(1)#1-Ni-P(1)-C(5)	19.9(8)
Br(1)-Ni-P(1)-C(5)	65.37(14)
P(1)#1-Ni-P(1)-C(11)	123.40(16)
Br(1)#1-Ni-P(1)-C(11)	-104.3(8)
Br(1)-Ni-P(1)-C(11)	-58.81(16)
P(1)#1-Ni-P(1)-C(1)	3.36(17)
Br(1)#1-Ni-P(1)-C(1)	135.7(8)
Br(1)-Ni-P(1)-C(1)	-178.84(16)
C(1)#1-N(1)-C(1)-P(1)	87.7(4)
C(2)-N(1)-C(1)-P(1)	-139.0(3)
C(5)-P(1)-C(1)-N(1)	83.2(3)
C(11)-P(1)-C(1)-N(1)	-165.6(3)
Ni-P(1)-C(1)-N(1)	-39.7(3)
C(1)#1-N(1)-C(2)-C(4)	64.5(3)
C(1)-N(1)-C(2)-C(4)	-64.5(3)
C(1)#1-N(1)-C(2)-C(3)#1	-57.5(6)
C(1)-N(1)-C(2)-C(3)#1	173.5(4)
C(1)#1-N(1)-C(2)-C(3)	-173.5(4)
C(1)-N(1)-C(2)-C(3)	57.5(6)
C(11)-P(1)-C(5)-C(6)	144.6(3)
C(1)-P(1)-C(5)-C(6)	-109.0(3)
Ni-P(1)-C(5)-C(6)	17.4(4)
C(11)-P(1)-C(5)-C(10)	-44.9(4)
C(1)-P(1)-C(5)-C(10)	61.4(4)
Ni-P(1)-C(5)-C(10)	-172.1(3)
C(10)-C(5)-C(6)-C(7)	0.5(6)
P(1)-C(5)-C(6)-C(7)	171.2(3)
C(5)-C(6)-C(7)-C(8)	0.0(7)
C(6)-C(7)-C(8)-C(9)	0.1(7)
C(7)-C(8)-C(9)-C(10)	-0.7(7)
C(8)-C(9)-C(10)-C(5)	1.2(7)
C(6)-C(5)-C(10)-C(9)	-1.1(6)
P(1)-C(5)-C(10)-C(9)	-171.7(3)
C(5)-P(1)-C(11)-C(12)	158.6(4)
C(1)-P(1)-C(11)-C(12)	54.1(4)
Ni-P(1)-C(11)-C(12)	-74.6(4)
C(5)-P(1)-C(11)-C(16)	-21.7(4)
C(1)-P(1)-C(11)-C(16)	-126.2(4)
Ni-P(1)-C(11)-C(16)	105.0(4)
C(16)-C(11)-C(12)-C(13)	0.3(8)
P(1)-C(11)-C(12)-C(13)	180.0(4)
C(11)-C(12)-C(13)-C(14)	1.1(9)
C(12)-C(13)-C(14)-C(15)	-2.0(10)
C(13)-C(14)-C(15)-C(16)	1.5(9)
C(12)-C(11)-C(16)-C(15)	-0.8(7)
P(1)-C(11)-C(16)-C(15)	179.5(4)
C(14)-C(15)-C(16)-C(11)	-0.1(8)

Symmetry transformations used to generate equivalent atoms:
#1 x,-y+1/2,z

APPENDIX 2

Table 1. Crystal data and structure refinement for **35**.

Identification code	**35**
Empirical formula	C35 H35 Cl4 N P2 Pd
Formula weight	779.78
Temperature	293(2) K
Wavelength	0.71073 Å
Crystal system, space group	Monoclinic, C2/c
Unit cell dimensions	a = 11.3666(15) Å α = 90°. b = 19.894(3) Å β = 100.236(2)°. c = 16.239(2) Å γ = 90°.
Volume	3613.6(8) $Å^3$
Z, Calculated density	4, 1.433 Mg/m^3
Absorption coefficient	0.923 mm^{-1}
F(000)	1584
Crystal size	0.84 x 0.19 x 0.17 mm
Theta range for data collection	2.05 to 26.00 deg.
Limiting indices	-8<=h<=14, -24<=k<=24, -19<=l<=20
Reflections collected / unique	9742 / 3541 [R(int) = 0.0191]
Completeness to theta = 26.00	99.7 %
Max. and min. transmission	0.8582 and 0.5122
Refinement method	Full-matrix least-squares on F^2
Data / restraints / parameters	3541 / 0 / 198
Goodness-of-fit on F^2	1.028
Final R indices [I>2sigma(I)]	R1 = 0.0283, wR2 = 0.0823
R indices (all data)	R1 = 0.0315, wR2 = 0.0852
Largest diff. peak and hole	0.658 and -0.448 e. $Å^{-3}$

Table 2. Bond lengths [Å] and angles [deg] for **35.**

Pd(4)-P(4)#1	2.2299(6)
Pd(4)-P(4)	2.2299(6)
Pd(4)-Cl(1)	2.3413(6)
Pd(4)-Cl(1)#1	2.3413(6)
P(4)-C(7)	1.805(2)
P(4)-C(13)	1.810(2)
P(4)-C(1)	1.843(2)
N(1)-C(2)	1.405(4)
N(1)-C(1)#1	1.441(2)
N(1)-C(1)	1.441(2)
C(13)-C(18)	1.382(3)
C(13)-C(14)	1.383(4)
C(3)-C(4)	1.389(3)
C(3)-C(2)	1.399(3)
C(2)-C(3)#1	1.399(3)
C(18)-C(17)	1.388(4)
C(4)-C(5)	1.381(3)
C(4)-C(6)	1.512(4)
C(7)-C(12)	1.382(4)
C(7)-C(8)	1.386(4)
C(14)-C(15)	1.385(4)
C(8)-C(9)	1.377(4)
C(15)-C(16)	1.370(5)
C(17)-C(16)	1.363(5)
C(9)-C(10)	1.366(5)
C(10)-C(11)	1.375(5)
C(12)-C(11)	1.383(5)
C(5)-C(4)#1	1.381(3)
Cl(3)-C(19)	1.723(5)
C(19)-Cl(3)#1	1.723(5)
P(4)#1-Pd(4)-P(4)	89.05(3)
P(4)#1-Pd(4)-Cl(1)	89.76(2)
P(4)-Pd(4)-Cl(1)	178.25(2)
P(4)#1-Pd(4)-Cl(1)#1	178.25(2)
P(4)-Pd(4)-Cl(1)#1	89.76(2)
Cl(1)-Pd(4)-Cl(1)#1	91.46(3)
C(7)-P(4)-C(13)	108.50(11)
C(7)-P(4)-C(1)	105.85(11)
C(13)-P(4)-C(1)	99.27(10)
C(7)-P(4)-Pd(4)	112.62(8)
C(13)-P(4)-Pd(4)	114.29(7)
C(1)-P(4)-Pd(4)	115.19(8)
C(2)-N(1)-C(1)#1	119.22(12)
C(2)-N(1)-C(1)	119.22(12)
C(1)#1-N(1)-C(1)	121.6(2)
C(18)-C(13)-C(14)	119.5(2)
C(18)-C(13)-P(4)	121.9(2)
C(14)-C(13)-P(4)	118.53(18)
C(4)-C(3)-C(2)	120.8(2)
N(1)-C(1)-P(4)	116.36(15)
C(3)#1-C(2)-C(3)	118.4(3)
C(3)#1-C(2)-N(1)	120.80(14)

C(3)-C(2)-N(1)	120.80(14)
C(13)-C(18)-C(17)	119.6(3)
C(5)-C(4)-C(3)	119.4(2)
C(5)-C(4)-C(6)	121.1(2)
C(3)-C(4)-C(6)	119.5(2)
C(12)-C(7)-C(8)	119.0(2)
C(12)-C(7)-P(4)	122.5(2)
C(8)-C(7)-P(4)	118.49(19)
C(13)-C(14)-C(15)	120.0(3)
C(9)-C(8)-C(7)	120.4(3)
C(16)-C(15)-C(14)	120.2(3)
C(16)-C(17)-C(18)	120.6(3)
C(10)-C(9)-C(8)	120.4(3)
C(9)-C(10)-C(11)	119.9(3)
C(7)-C(12)-C(11)	120.2(3)
C(10)-C(11)-C(12)	120.2(3)
C(17)-C(16)-C(15)	120.1(3)
C(4)-C(5)-C(4)#1	121.1(3)
Cl(3)-C(19)-Cl(3)#1	117.9(5)

Symmetry transformations used to generate equivalent atoms:
#1 -x,y,-z+1/2

Table 3. Torsion angles [deg] for **35.**

P(4)#1-Pd(4)-P(4)-C(7)	96.34(8)
Cl(1)-Pd(4)-P(4)-C(7)	143.6(7)
Cl(1)#1-Pd(4)-P(4)-C(7)	-82.38(8)
P(4)#1-Pd(4)-P(4)-C(13)	-139.26(9)
Cl(1)-Pd(4)-P(4)-C(13)	-92.0(7)
Cl(1)#1-Pd(4)-P(4)-C(13)	42.03(9)
P(4)#1-Pd(4)-P(4)-C(1)	-25.20(8)
Cl(1)-Pd(4)-P(4)-C(1)	22.1(7)
Cl(1)#1-Pd(4)-P(4)-C(1)	156.09(8)
C(7)-P(4)-C(13)-C(18)	5.0(2)
C(1)-P(4)-C(13)-C(18)	115.2(2)
Pd(4)-P(4)-C(13)-C(18)	-121.61(19)
C(7)-P(4)-C(13)-C(14)	-174.5(2)
C(1)-P(4)-C(13)-C(14)	-64.3(2)
Pd(4)-P(4)-C(13)-C(14)	58.9(2)
C(2)-N(1)-C(1)-P(4)	147.68(9)
C(1)#1-N(1)-C(1)-P(4)	-32.32(9)
C(7)-P(4)-C(1)-N(1)	-60.40(18)
C(13)-P(4)-C(1)-N(1)	-172.76(16)
Pd(4)-P(4)-C(1)-N(1)	64.73(17)
C(4)-C(3)-C(2)-C(3)#1	0.47(17)
C(4)-C(3)-C(2)-N(1)	-179.53(17)
C(1)#1-N(1)-C(2)-C(3)#1	13.59(15)
C(1)-N(1)-C(2)-C(3)#1	-166.41(15)
C(1)#1-N(1)-C(2)-C(3)	-166.41(15)
C(1)-N(1)-C(2)-C(3)	13.59(15)
C(14)-C(13)-C(18)-C(17)	0.6(4)
P(4)-C(13)-C(18)-C(17)	-178.9(2)
C(2)-C(3)-C(4)-C(5)	-0.9(3)
C(2)-C(3)-C(4)-C(6)	179.0(2)
C(13)-P(4)-C(7)-C(12)	83.9(3)
C(1)-P(4)-C(7)-C(12)	-21.9(3)
Pd(4)-P(4)-C(7)-C(12)	-148.6(2)
C(13)-P(4)-C(7)-C(8)	-96.4(2)
C(1)-P(4)-C(7)-C(8)	157.9(2)
Pd(4)-P(4)-C(7)-C(8)	31.1(2)
C(18)-C(13)-C(14)-C(15)	-0.8(4)
P(4)-C(13)-C(14)-C(15)	178.7(2)
C(12)-C(7)-C(8)-C(9)	0.5(5)
P(4)-C(7)-C(8)-C(9)	-179.2(3)
C(13)-C(14)-C(15)-C(16)	0.6(5)
C(13)-C(18)-C(17)-C(16)	-0.2(5)
C(7)-C(8)-C(9)-C(10)	-0.5(6)
C(8)-C(9)-C(10)-C(11)	0.1(6)
C(8)-C(7)-C(12)-C(11)	-0.2(5)
P(4)-C(7)-C(12)-C(11)	179.5(3)
C(9)-C(10)-C(11)-C(12)	0.2(7)
C(7)-C(12)-C(11)-C(10)	-0.1(6)
C(18)-C(17)-C(16)-C(15)	0.0(5)
C(14)-C(15)-C(16)-C(17)	-0.2(5)
C(3)-C(4)-C(5)-C(4)#1	0.46(16)
C(6)-C(4)-C(5)-C(4)#1	-179.4(3)

Symmetry transformations used to generate equivalent atoms:
#1 -x,y,-z+1/2

Publications:

1. Synthesis and characterization of nickel complexes containing bis-phosphine donors and their use as catalysts for ethylene oligomerization and polymerization. **Chaki**, **Amrita**.; Sivaram, S. (*Manuscript under preparation*)

2. Vinyl type polymerization of norbornene with Ni (II) and Pd (II) complexes of bis-[N,N(diphenylphosphinomethyl)]alkyl/aryl amines with $B(C_6F_5)_3/Et_3Al$ and methylaluminoxane as cocatalysts. **Chaki**, **Amrita**.; Sivaram, S. (*Manuscript under preparation*)

Conference papers:

1. Synthesis and characterization of nickel complexes containing phosphorous and nitrogen donor atoms as potential catalysts for olefin polymerizations.
   Chaki, **Amrita**.; Sivaram, S. *Internal seminar on Frontiers of Polymer Science and Engineering* (*Macro 2002*), 9-11 December, **2002**, Organized by Indian Institute of Technology, Kharagpur (**Poster presentation**).

2.. Synthesis and characterization of non-metallocene complexes containing bis-phosphine donor ligands and their use as catalysts for olefin polymerization. **Chaki**, **Amrita**; Sivaram, S. MACRO 2004, International Conference on Polymers for Advanced Technologies, Thiruvananthapuram, India, Dec. 15-17, **2004**, CAN 144:108645 AN 2005:708793.